Recovery of Platinum Group Metals from Spent Furnace Linings and Used Automotive Catalysts

By

Angela Janet Murray

A thesis submitted to the University of Birmingham for the degree of
DOCTOR OF PHILOSOPHY

School of Chemical Engineering
College of Engineering and Physical Sciences
The University of Birmingham

October 2011

UNIVERSITY OF
BIRMINGHAM

University of Birmingham Research Archive

e-theses repository

This unpublished thesis/dissertation is copyright of the author and/or third parties. The intellectual property rights of the author or third parties in respect of this work are as defined by The Copyright Designs and Patents Act 1988 or as modified by any successor legislation.

Any use made of information contained in this thesis/dissertation must be in accordance with that legislation and must be properly acknowledged. Further distribution or reproduction in any format is prohibited without the permission of the copyright holder.

Abstract

The availability of finite resources is uncertain due to the worldwide increase in population growth and global industrialisation. Consequently, there is a pressing need for substitutive replacements and methods of replenishing stocks by recycling. The platinum group metals (PGMs) are rare, expensive elements with an unpredictable supply chain and a wide range of industrial applications for which there are often no substitutes. Mining from primary ores is environmentally damaging; hence recycling is vital to minimise losses and maintain stock at sustainable levels.

This work investigates the feasibility of recovering PGMs from secondary waste sources and bioconverting them into new catalysts, circumventing the current environmentally polluting and energy expensive pyrometallurgical processing. Two secondary sources of PGMs were examined: scrap automotive catalysts and spent furnace refractory lining.

Spent furnace lining is a high grade PGM waste material that is currently recycled by re-smelting in the newly relined furnace. However this process is energy intensive, time consuming and inefficient as large areas of brick are minimally contaminated. This work applied a number of physical processing techniques (comminution, magnetic, eddy current and electrostatic separations, air table) to 'end of life' lining to produce a 'fast track' metal concentrate that could be smelted for rapid PGM recovery. Such physical concentration recovered 69%, 57% and 80% of the Pt, Pd and Rh respectively in ~17% of the starting mass,

allowing rapid metal recovery in a lower mass fraction and hence significantly improving the efficiency of the current recycling process.

Spent furnace lining (SFL) and automotive catalyst (AC) were subjected to leaching using concentrated *aqua regia* in a MARS 5 microwave reactor to solubilise the PGMs. Conditions of 109˚C for 15 minutes with a liquid to solid ratio of 5:1 provided recovery of >87% of all PGMs present. Less concentrated acid (50%) could be used if rhodium was not present.

Example leachates of SFL and AC were subjected to a bacterial biorecovery process, producing nanoscale PGM clusters tethered on micron sized carrier particles (dead bacterial cells; bio-PGMs). Full recovery of PGMs was achieved from AC leachate but not from SFL leachate, attributable to potentially inhibitory base metal cations present in this material. The bio-PGMs produced from both leachates were tested for catalytic activity in the reduction of Cr(VI) against bio-PGMs made from 'clean' model solutions. The 'bio-PGMs' from AC reduced 0.5 mM CrO_4^{2-} at half the rate of the 'model' material. The poorer quality of the AC leachate-derived catalyst was attributed to the Si and Al components in the source material. In all cases this activity was lower than a commercially available palladium catalyst used for comparison. Pre-depositing Pd on the cells before exposing them to leachate produced superior catalysts than pre-depositing Pt, discussed in terms of the possible ability of the cells to 'recognise' and 'traffic' Pd(II) as an analogue of Ni(II), an essential metal.

In conclusion, this study shows a route to improve PGM recycling from secondary waste sources and, further, the potential to produce a catalytically active end product without the need for traditional refining.

Acknowledgements

Financial support provided by the Engineering and Physical Sciences Research Council (EPSRC), the Royal Society and Johnson Matthey is gratefully acknowledged.

I would like to thank my supervisors, Professor Lynne Macaskie and Professor Stuart Blackburn, for their support and guidance over the duration of the project. I would also like to thank Dr Neil Rowson for his supervisory input in the early stages of the research. Acknowledgement is also due to past and present members of the Unit of Functional Bionanomaterials – their humour and encouragement proved invaluable.

Thanks to Simon Collard and Mike Wright at Johnson Matthey for their industrial supervision, John Setchfield and Ben Hillary at Engelhard for their extensive analytical expertise, Camborne School of Mines for use of QEM-SCAN facilities and both Master Magnets and Eriez Magnetics for access to their magnetic processing laboratories.

Finally I would like to thank my family for their kindness and unfaltering support while this thesis was written. It wouldn't have happened without your encouragement and belief.

CONTENTS

LIST OF FIGURES

LIST OF TABLES

1. Introduction

1.1 The Importance of Platinum Group Metals

The six platinum group metals (platinum, palladium, rhodium, ruthenium, iridium and osmium; PGMs) are considered to be "precious" metals due to their high demand coupled with low abundance. PGMs have high technological importance; their major uses are found in the chemical, electrical, electronic, glass and automotive industries.

South Africa is currently the largest producer of PGMs, accounting for 76% of the world's platinum, 33% of its palladium and 82% of its rhodium. The three largest mining houses – Anglo Platinum, Impala and Lonmin – have all recorded lower output in recent years due to bad weather, safety shutdowns, industrial unrest and skills shortages. As a result the supply chain for over three quarters of the global supply of platinum and rhodium is insecure, with one nation holding a virtual monopoly. It is also significant that Europe has no primary reserves of these metals and relies solely on imports.

Over most of the past decade demand for platinum (Pt), palladium (Pd) and rhodium (Rh) has exceeded supply, resulting in large price increases; in particular all three metals experienced significant price increases from 2005 to 2008. The global economic crisis that started in the latter part of 2008 meant a significant drop in PGM demand and this caused the prices of all three metals to drop greatly. Thus during the course of the project (2006 to 2010) the price of rhodium has fluctuated by 8.5 times its lowest value and platinum and palladium by 2.5 times their lowest values. This has been important in relation to funding

for analysis, required recovery levels and acceptable losses during recycling, as these all fluctuated in line with prices.

Although figures for proven and probable reserves suggest they are sufficient for the next 40 years at current rate of production it has been estimated that if all the 500 million vehicles in use today were re-equipped with fuel cells, operating losses would mean that all the world's sources of platinum would be exhausted within 15 years. Thus if countries are going to move away from a fossil fuel based economy it will be vital to conserve stocks of these metals by increasing recycling technologies.

In 2008 the Resource Efficiency Knowledge Transfer Network (KTN) estimated that worldwide mining activities (of all minerals) were responsible for around 5% of global carbon dioxide emissions. As an example, mining 1kg of rhodium releases over ten thousand times as much CO_2 as mining 1kg of copper and around 10 tonnes of ore is extracted per troy ounce of PGM produced, resulting in large spoil heaps and high energy consumption. In fact 65 – 75% of the total cost of producing pure PGMs is accrued at the mining stage due to the large energy demand. Water and air pollution are also both serious problems associated with PGM mining.

In most of its industrial applications, platinum is either irreplaceable or can only be substituted with significant compromises in performance. In most cases, the only feasible substitutes for platinum are other PGMs but these are no more abundant than platinum. PGMs currently have low substitutability due to their high activity for catalysis. “Thrifting”

has been studied extensively over the past decade in the field of car catalyst production but reduction of PGM content can only be taken so far without impairing catalyst performance. The upcoming Euro VI vehicle emissions legislation means that further reductions in PGM loadings are unlikely.

1.2 The Environmental Paradox

A large number of new "environmentally-friendly" technologies now rely on materials for which demand was previously low. Frequently, the materials in demand are rare in the earth's crust or concentrated in regions subject to political instability. The most obvious example is the large increase in demand for PGMs in catalytic converters in response to tightening worldwide vehicle emissions standards.

Hence a paradox exists that greater environmental performance or efficiency is often achieved through the use of materials with greater environmental impacts and with less material security.

Therefore improving recycling from secondary occurrences is important because it not only preserves a finite resource by preventing it being dispersed into the environment, but also dramatically reduces PGM related CO_2 emissions and energy usage during primary mining. It also provides an increased secure source of PGM within Europe, thereby helping to minimise price fluctuations. Strategies for minimisation of dispersal need to take a whole life-cycle approach and factor in the environmental impacts of the collection and reprocessing steps.

1.3 Background to this Research

In 2005 Professor Lynne Macaskie was awarded the Royal Society Brian Mercer Senior Award for innovation. The objective of the award was to establish and commercialise "clean" processes to recover energy from waste in the urban environment. The Mercer project was highly interdisciplinary and had a number of parallel strands (clean hydrogen production, biocatalysis production, waste processing etc.) and a sub-project investigated the concept of "mining" the urban environment i.e. treating secondary wastes as an ore body analogue for the recovery of valuable components. The aim was to assess a number of precious metal containing wastes and upgrade suitable ones before converting them into catalytically active added value products, using technology previously developed (but not yet optimised) at Birmingham.

In parallel Johnson Matthey (JM) approached the University as they wished to collaborate on a project to improve their reprocessing route for spent precious metal smelting furnace linings. JM had a zero loss recycling chain for these furnace linings but the process was both energy and time consuming and so significantly reduced overall operational capacity. As a result JM formally sponsored 50% of the PhD and the two projects proceeded in parallel, providing both a low grade, commercially available PGM waste (autocatalyst) and a high grade PGM waste with an inefficient recycling process (furnace lining).

1.4 Aims of the Thesis

The purpose of this thesis is to evaluate the amenability of two PGM containing wastes (spent furnace linings and used automotive catalysts) to physical concentration and upgrading, in order to recover the valuable metal component. These wastes will then be leached using microwave technology in order to solubilise the metals prior to biorecovery. This technique utilises bacterial enzymatic activity to produce precious metal nanoparticles which, in turn, catalyse recovery of metals from non-physiological and aggressive solutions by chemical catalysis. These "biocatalysts" have catalytic activity and therefore the valuable metal is not only recovered but converted into an added value product, with a range of uses and worth far in excess of value of the metal present.

The methods used for concentration are standard minerals processing techniques that were traditionally applied to primary ores. They are now being adapted for use on secondary waste materials and thus they are reliable, scalable and inexpensive; all key considerations when dealing with low grade metal sources. However the mineralogy of secondary occurrences is completely different to that of primary ores and so substantial development work is required to make them commercially effective.

Previous work at Birmingham proved that biocatalysts produced from model solutions exhibit catalytic activity in a number of key industrial reactions (e.g. "clean chemistry" syntheses, hydrogenations, decontamination of toxic agents and fuel cells). However, in order to reduce the cost of production to become more comparable with current chemical

catalysts made by traditional routes using “virgin” metals, significant savings have to be made. Using waste metal sources is one potential way to make these catalysts more commercially attractive and at the same time reduce reliance on imports and hence strengthen materials security.

2. Literature Review

2.1 The Platinum Group Elements – An Overview

The six platinum group metals (PGMs) are platinum, palladium, ruthenium, rhodium, iridium and osmium. These, together with gold and silver, are considered to be "precious" metals due to their high demand coupled with relative scarcity, resulting in high prices.

The platinum group metals are extremely scarce by comparison to the other precious metals (such as gold and silver) due to both their low natural abundance and the complex processes required for their extraction and refining (Bernardis *et al.*, 2005).

Relative to the other precious metals PGMs have high technological importance. Valuable for their resistance to corrosion and oxidation, high melting points, electrical conductivity and catalytic activity, these elements have wide industrial applications (Xiao and Laplante, 2004). The major uses are found in the chemical, electrical, electronic, glass and automotive industries. For example their high catalytic activity for a wide range of substrates has resulted in their use in many industrial synthetic processes; reforming reactions in the petroleum refining industry, hydrogenation and dehydrogenation reactions in the pharmaceutical industry, and both organic and inorganic oxidation reactions (Bernardis *et al.*, 2005) to name but a few. The catalytic properties of PGM are also having a positive impact on the environment through the

development of automotive emission control catalysts (Whiteley and Murray, 2003; Ek *et al.*, 2004; Wiseman and Zereini, 2009).

All six PGMs are silvery white lustrous metals. They are sufficiently ductile and malleable to be drawn into wire, rolled into sheet or formed by spinning and stamping (Xiao and Laplante, 2004). They can be classified into two groups when compared to the specific gravity of gold. Ruthenium, rhodium and palladium are lighter than gold (specific gravities around 12 to 12.4), whereas osmium, iridium and platinum are heavier than gold (specific gravities in the range 21 to 22.5) (Xiao and Laplante, 2004).

2.2 Background Levels of Platinum Group Metals

PGMs are present in the Earth's crust at very low concentrations. According to Taylor and McLennan (1985) and Rauch *et al.* (2000) background concentrations of these elements are in the range 0.06-0.40 mg/kg (60-400 ppb). Greenwood and Earnshaw (1989) proposed an average palladium concentration in the Upper Continental Crust of 0.015 mg/kg (15 ppb). Going further back, Crustal data support values of around 5 ppb for platinum and 10 ppb for palladium (Mason, 1958).

Recently the platinum concentration in 24 oceanic sediments was found to average 3.8 ppb (Goldberg *et al.*, 1986), close to the crustal abundance. In summary these elements occur naturally at very low background levels.

2.3 Mineralogy of PGM Ores (Primary Production)

Unlike gold, which occurs in a fairly small number of minerals, there are 109 platinum group mineral species recognised by the International Mineralogical Association (IMA) (Xiao and Laplante, 2004; Xiao *et al.*, 2009). They range from sulphides e.g. braggite, to tellurides, antimonides, arsenides, alloys e.g. ferroplatinum and native species i.e. nuggets. Natural PGM deposits are usually related to basic igneous rocks and are closely associated with copper, nickel and iron sulphides (Bernardis *et al.*, 2005).

The extremely low concentration of PGMs in typical ore bodies along with their fine size distribution, the difficulty of accurate detection and ensuring sample representativity are typical problems when working with primary sources of PGM (Xiao and Laplante, 2004).

Historically little information about the mining and processing of PGM ores can be obtained due to geographic and academic isolation of the worlds primary producers but this is gradually beginning to change due to the stronger demand for these metals.

2.3.1 Classification of Primary Ores

According to Cole and Ferron (2002) PGM ores can be grouped into three primary classes:

1) **PGM dominant ores** – exploited primarily for their PGM content (e.g. Merensky or chromite ores). Other associated metals (e.g. nickel and copper) are produced as by-products. The economic value of the PGMs are high in comparison to the by-product values.

2) **Nickel – copper (Ni-Cu) dominant ores** – mined primarily for the value of Ni and Cu. The PGMs are produced as by-products. Usually the economic importance of PGMs in these ores is minor; however they can sometimes be important factors for overall project economics. For example, Canada's PGMs are a by-product of nickel-copper mining (Brynard *et al.*, 1976).

3) **Miscellaneous ores** – these ores contain very low PGM concentration compared to the previous two types of ores. The value of the PGMs has little or no economic advantage compared to the primary product. Much less is known about these ores than the other two types.

Table 2.1 shows the main constituents of these three groupings graphically.

Table 2.1 Ore type classification (Cole and Ferron, 2002), reproduced from Xiao and Laplante (2004).

PGM Ores		
PGM Dominant	**Ni-Cu Dominant**	**Miscellaneous Ore**
Merensky Type	Class I Ni-Cu Ore	Porphyry Cu Ore
Chromite Type	Class II Ni-Cu Ore	Cu-Mo Ore
Placer Type	Class III Ni-Cu Ore	Carbonatite Ore
Dunite Pipes	Class IV Ni-Cu Ore	Ni Laterites
	Other Ni-Cu Ore	Black Shales

2.3.2 South African Ores

South Africa currently accounts for the majority of worldwide PGM supply. South African PGM production centres on a geographical area known as the **Bushveld complex** and falls into category one above i.e. the PGM bearing ores are mined primarily for the recovery of these metals.

There are two main types of deposit in the Bushveld complex in South Africa (the world's largest known reserves):

Merensky Type - The PGMs in the Merensky Reef in the Bushveld complex are strongly associated with the base metal sulphide (BMS) minerals present in the reef, either as discrete platinum group minerals included or attached to the sulphides, or in solid solution with these sulphides (Ballhaus and Sylvester, 2000). A solid solution is a solid state solution of one or more solutes in a solvent. Such a mixture is considered a solution rather than a compound when the crystal structure of the solvent remains unchanged by addition of the solutes and when the mixture remains in a single homogenous phase. Solid solutions often occur when the two elements (generally metals) involved are close together on the periodic table. A compound is usually formed with two non-proximity elements (Callister, 2006). In general the BMS content of the reef is in the region of 1% (Wiese *et al.*, 2006) however the PGM content is typically less than 10 parts per million (ppm)[1] (Bernardis *et al.*, 2005). The Merensky reef has been the principal source of PGM since it was first worked in 1925.

Chromite Type (UG2) – There is a correlation between chromite and PGMs mineralisation but the precise relationship depends on the geological environment. Stratiform chromite deposits occur in the Bushveld complex UG2 reef. A large portion of the PGMs are in the form of PGM minerals (laurite and alloys, a portion of which are associated with chromium). One of the most detrimental constituents of this ore is the clay-like slimes, which interfere with flotation methods used for separation and contribute to high reagent consumption (Bulatovic, 2003).

[1] Parts per million (ppm) and grams per tonne (g/t) are equivalent and are used interchangeably.

Extraction methods for the Bushveld complex can be broken down into four parts, namely mining, processing, smelting and refining and each stage is technically challenging (Pincock, 2008). Figure 2.1 shows a brief outline of the typical process that is used to concentrate PGM from South African ores.

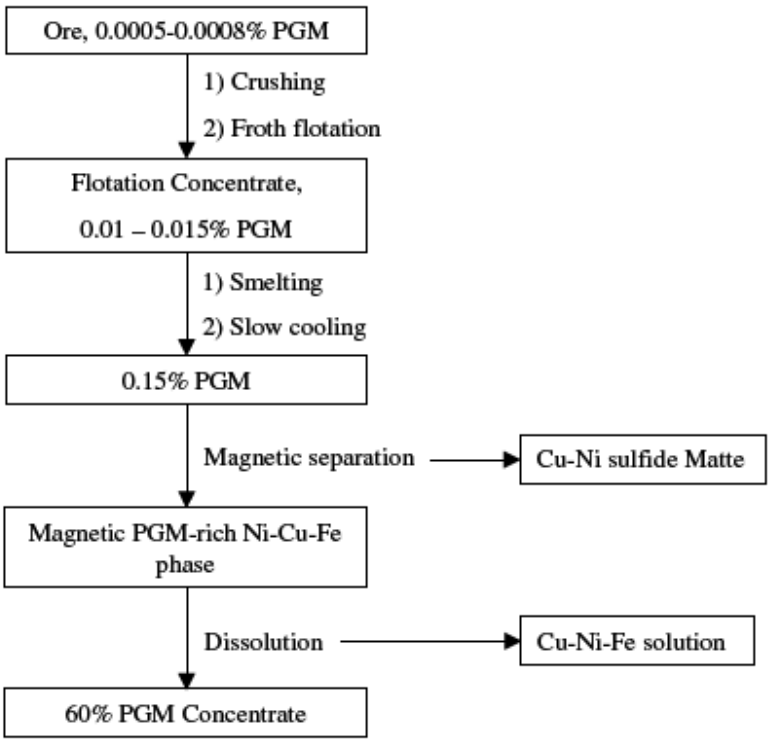

Fig. 2.1 The concentration process for PGM from sulphide ores such as those in South Africa's Merensky Reef (reproduced from Bernardis *et al.*, 2005).

Table 2.2 contains a summary of the key features of the PGM extraction process, including costs, PGM concentrations and processing time for each stage (Pincock, 2008). Each stage is discussed in more depth in sections 2.3.2.1 to 2.3.2.3.

Table 2.2 The key features of the PGM extraction business relating to mining, processing, smelting and refining (reproduced from Pincock, 2008).

Parameter	Mining	Comminution and Flotation	Smelting and Converting	Base Metal Refining	PGM Refining	Total
% Total Cost	65 – 75	9 – 12	6	7	4 - 5	100
PGM Grade	4 -6 g/t	100 – 600 g/t	640–6000 g/t	30 – 65%	>99.8%	-
PGM Recovery %	-	80 - 90	95 - 98	>99	98 - 99	75 – 85
Concentration Ratio	-	30 - 80	20	75	2	200,000
Processing Time (Days)	-	2	7	14	30 - 150	Up to 170

2.3.2.1 Comminution and Flotation

The mined ore is crushed and milled to reduce the size of the rock particles and to expose the minerals which contain the PGM. The particles are mixed with water and specialised chemical reagents (collectors) after which air is pumped through the liquid, creating bubbles to which the PGM containing particles adhere. These float to the surface and are removed as a soapy froth. The PGM content of this flotation concentrate varies between 100 and 1,000 grams per tonne (g/t or ppm) (Bulatovic, 2003). Most of the operating plants from the Merensky Reef use

xanthate as the primary PGM collector, with dithiophosphate as a secondary collector. In a number of operating plants, the collector consumption is in excess of 200 g/t, specifically in plants that treat tarnished sulphides (Bulatovic, 2003).

2.3.2.2 Smelting

Following flotation, the froth is dried and the resulting concentrate is smelted in an electric furnace at temperatures which can exceed 1,500 ˚C. During this process, a matte containing the valuable metals is separated from the unwanted minerals, which form a slag and are discarded. The matte is transferred to converters, where air is blown through it in order to remove iron and sulphur. The PGM content of the "converter matte" now exceeds 1,400 g/t (Johnson Matthey Platinum Today http://www.platinum.matthey.com/production/africa.html).

2.3.2.3 Refining

Following concentration the PGMs need to be separated from the base metals. The result is the separation and purification of the six PGMs, plus small amounts of gold and silver from the concentrate. In practice for the purposes of refining Pt and Pd are referred to as “soluble PGMs.” Ir, Ru, Rh and Os are referred to as “insoluble PGMs” as they dissolve more slowly than either platinum or palladium, which, under controlled conditions enables a partial separation between these groups (Bernardis *et al.*, 2005).

The refined PGMs have a purity of over 99.95%, and can be produced in a number of forms: ingot, grain or a fine powder known as "sponge". The time between mining of the ore and production of pure metal typically ranges from around 6 weeks for palladium to up to 20 weeks for rhodium.

2.3.2.3.1 Classical Precipitation Methods

Up until the late 1970s the separation of PGM was achieved using a series of precipitation reactions. An initial leach under oxidising conditions typically dissolved over 90% of the Pt, 70 to 80% of the Pd and between 10 and 20% of the insoluble metals (Edwards *et al.*, 1986). This gave a coarse separation between the “soluble PGMs” and “insoluble PGMs.” However due to significant amounts of contaminant PGM in both streams, many recycling and intermediate steps were required to produce high purity individual metals (Bernardis *et al.*, 2005).

2.3.2.3.2 Solvent Extraction methods

A number of solvent extractants were introduced in commercial PGM refineries in the 1980s and are still used today. The solvent extraction process comprises three basic steps: 1) an extraction step, to selectively extract a given metal; 2) a scrubbing step, to remove co-extracted metals and 3) a stripping step, to remove the extracted metal from the organic phase (Bernardis *et al.*, 2005).

Solvent extraction offers a number of advantages over classical precipitation methods; higher selectivity can be obtained, the use of scrubbing techniques means high purity metal is produced and more complete removal of metals is also possible through the use of multi-stage extraction (Bernardis *et al.*, 2005). These have reduced the need for excessive recycling, shortened refining times significantly and lowered production costs (Barnes and Edwards, 1982). Bernardis *et al.* (2005) note that research and development in the field of PGM refining will always be fuelled by potential economic gains, arising from faster, simpler and more efficient refining methods. Of increasing importance however is the need for processes which reduce harm to the environment.

2.3.3 Russian Ores

Russia currently accounts for over 50% of the global annual mine production of palladium and approximately 15% of platinum. Despite the importance of the Russian PGM mining industry to global PGM markets, hard facts on reserves, production and sales have historically been difficult to come by, as all data was confidential under Russian state secrecy law (Johnson Matthey, 2004).

However in 2004 a bill was passed by the Russian parliament to declassify PGM information and so some limited data has now been published, based primarily upon Johnson Matthey visiting and liaising with the mines (Johnson Matthey, 2004).

The Urals deposits - PGM production in Russia has a history stretching back to the early nineteenth century. Large alluvial platinum deposits were discovered in the Ural Mountains in 1823, and have been exploited continuously since. Once far richer than any known underground sources, these deposits have long since been stripped of the highest grade ore and now account for <1% of Russian platinum production (Johnson Matthey, 2004).

The Noril'sk-Talnakh mines - These are currently the most important of Russia's known PGM reserves. The first to be discovered and exploited was the Noril'sk deposit. In 1960, high grade copper-nickel deposits were discovered at Talnakh, a short distance north of Noril'sk. Four mines were developed between the 1960s and 1980s, all of which are still in operation. The first, and shallowest at a maximum depth of around 400 metres, was the Mayak mine; production here started in 1965. It was followed by the Komsomolsky mine in around 1970, and the Oktyabrsky mine about five years later. The last named is the largest of the Talnakh operations, mining at a depth of around 1,100 metres, and accessing the richest ores. The Taimyrsky mine entered production during the 1980s and is worked to depths of around 1,500 metres (Johnson Matthey, 2004).

It is estimated that head grades at Noril'sk-Talnakh mines average between 10 and 11 ppm PGM, more than twice the typical grade of ore mined in South Africa. This is in addition to high base metal values of around 1.8% nickel and over 3% copper (Johnson Matthey, 2004).

However the majority of these reserves are palladium rather than platinum, thus South African deposits have a much larger economic value due to their higher platinum content and size.

Concentrating, smelting and base metal refining are carried out in facilities at the Noril'sk-Talnakh complex. They operate two "enrichment plants" (concentrators) and three metallurgical plants (incorporating smelting, base metal refining and the upgrading of PGM residues). PGM slimes are recovered from the electrolytic refining of nickel and copper and are sent outside NNC to specialist precious metals refineries for additional extraction of PGM (Johnson Matthey 2004).

2.3.4 Canadian Ores

Canadian ores are typically nickel-copper dominant ores and as such fall into category 2 of table 2.1 i.e. the PGMs are mined as by-products of Ni-Cu mining. The metals in these ore types occur as discrete PGMs and in solid solution with metal sulphides and to a lesser extent with gangue minerals. PGM recovery is not the prime driving force behind the flowsheet development and optimisation (Xiao and Laplante, 2004).

The Sudbury Basin in central Ontario has the largest number of PGM-producing mines. PGMs are also extracted from the Raglan nickel mine in northern Quebec and from a nickel complex in Manitoba. In all of these ore bodies, palladium is the predominant platinum group metal. Palladium typically accounts for 55-60% of the PGM while the remainder is mainly platinum; the

rhodium content is small. The average overall grade is less than 2 ppm (Johnson Matthey, 2001). Both Russian and Canadian deposits are processed in a similar way to South African ores i.e. by comminution, flotation and smelting (as discussed previously in section 2.3).

2.4 Primary Occurrences of Platinum Group Metals

2.4.1 Worldwide Supply of PGMs

South Africa is currently the largest producer of PGMs, followed by Russia and North America. Figure 2.2 shows the total PGM production worldwide in 2008 and illustrates that South Africa supplied 76% of the world's platinum, 33% of its palladium and 82% of its rhodium. Russia supplied more palladium than South Africa (51%) but its contribution of the other two metals was much smaller.

Johnson Matthey's Platinum Review 2009 stated that the platinum market was in deficit to demand by 375,000 oz in 2008. Global platinum supplies fell heavily to 5.97 million ounces (from 6.60 million ounces in 2007) however net demand for platinum also decreased by 5% to 6.35 million ounces, as a number of sectors were affected by the global economic slowdown.

Significantly, South Africa, the largest miner of platinum supplies gave disappointing results in 2008, with output falling by 540,000 oz to only 4.53 million ounces. The three largest mining

houses – Anglo Platinum, Impala and Lonmin – all recorded lower output than in 2007 due to bad weather, safety shutdowns, industrial unrest and skills shortages (Johnson Matthey, 2009).

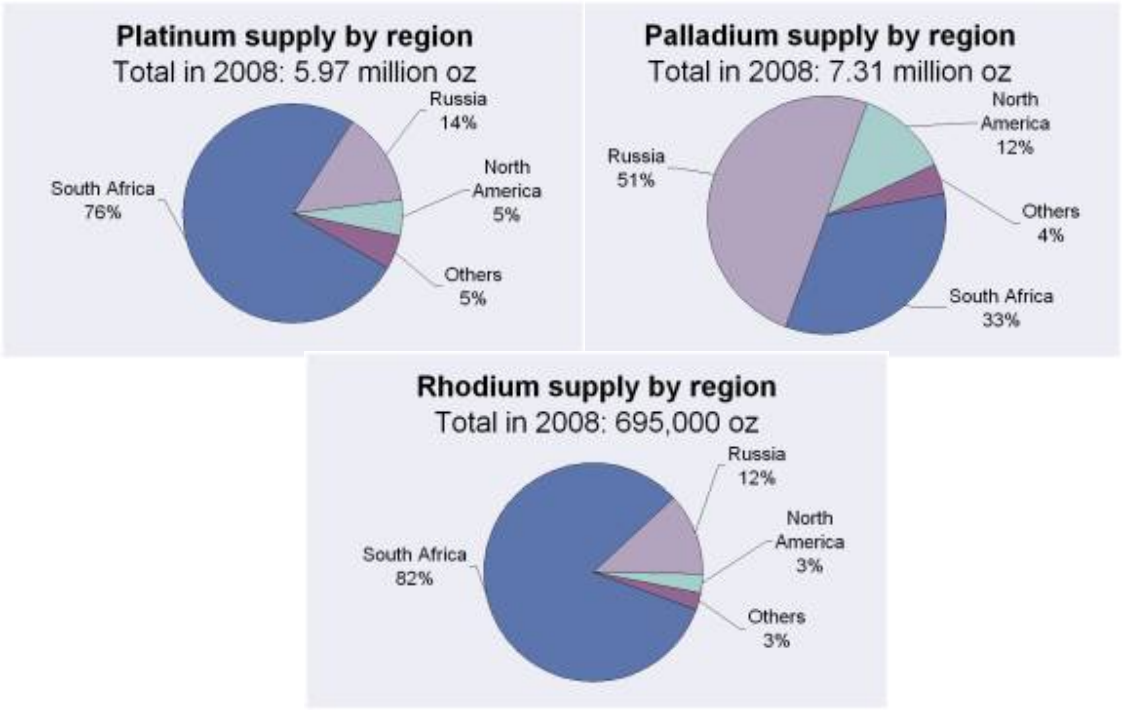

Fig. 2.2 Total PGM production worldwide in 2008 (from Johnson Matthey http://www.platinum.matthey.com/market_data/1147696813.html)

2.4.2 Worldwide Demand for PGMs

Figure 2.3 shows the demand for PGMs by application in 2008. It shows that the majority (46% of platinum, 48% of palladium and 84% of rhodium) were used in the manufacture of autocatalysts for the reduction of vehicle exhaust emissions, however significant quantities were also used in the chemical, glass, electronics and jewellery sectors. These applications are discussed in more detail in section 2.7.

Gross autocatalyst demand for platinum fell by over 8% in 2008. European car manufacturers purchased less platinum for use in catalytic converters than in 2007 due to lower light duty vehicle production, despite the greater use of platinum-containing diesel particulate filters. Platinum use in other regions fell, reflecting lower vehicle output and continuing efforts to replace any remaining platinum in petrol catalyst formulations with palladium for cost reasons (Johnson Matthey, 2009).

Jewellery demand for platinum also declined by 6% in 2008. Manufacturing volumes and retail sales were depressed by the high metal prices in the first half of the year in every region, but recovered later in China and Japan once the platinum price declined (Johnson Matthey, 2009).

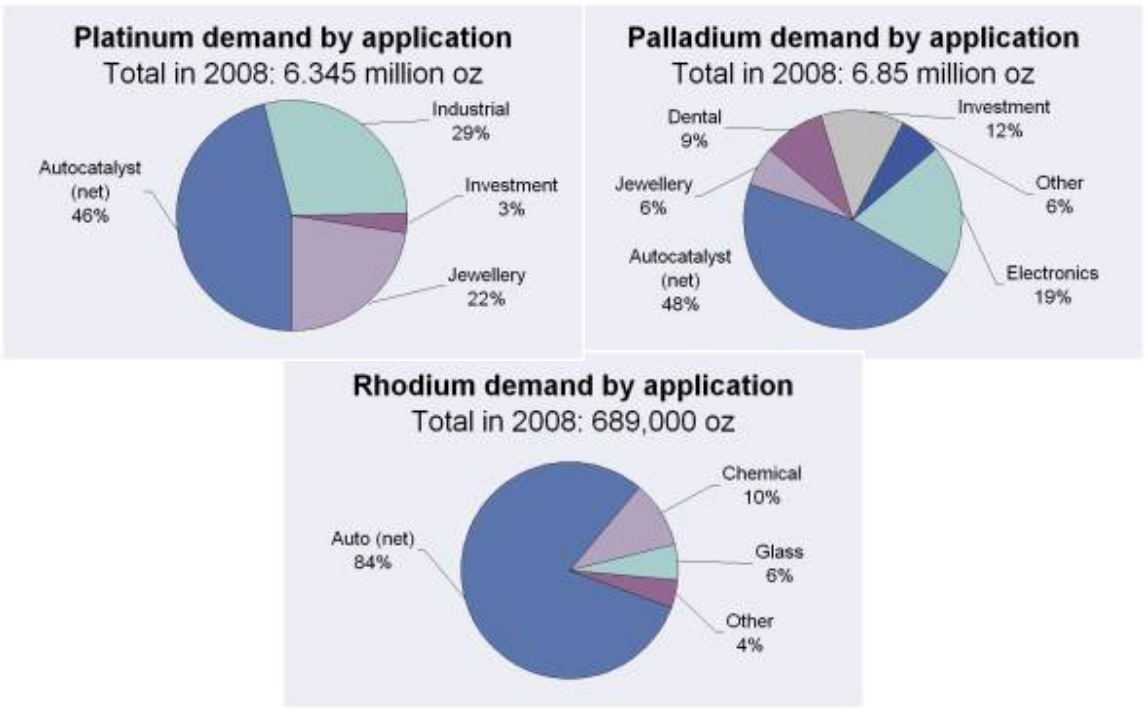

Fig. 2.3 Total PGM demand worldwide in 2008 (from Johnson Matthey http://www.platinum.matthey.com/market_data/1147696813.html)

2.4.3 The Relationship Between Supply and Demand

Figure 2.4 shows the worldwide supply and demand of platinum, palladium and rhodium during the ten year period 1999 – 2008. For platinum, with the exception of 2006, demand has constantly exceeded supply, resulting in large price increases within the industry. The disparity in 2006 is thought (by Johnson Matthey, 2009) to have been caused by significantly lower platinum usage in jewellery compared with previous years (in fact the lowest usage since 1993). In addition, the recycling of old platinum jewellery stock in China increased, resulting in a reduction in demand for newly mined metal.

As a comparison with platinum, palladium supply has constantly exceeded demand (even if only slightly) from 2002 onwards. For rhodium, demand has outstripped supply every year for the same ten year period with the exception of 2001-2003.

In the past (up to 2008) many large organizations kept a PGM inventory “in-house” in order to cover periods of undersupply. However the present financial climate has caused companies to reduce these inventories (as they are effectively “dead money”), meaning they are now even more exposed to price fluctuations as they cannot wait and choose when to buy to the same degree (personal communications with Dr. Mike Wright at Johnson Matthey, Dr. Ben Hillary at Engelhard and Dr. David Deagan at Platinum Recoveries Ltd., 2009).

Fig. 2.4 Worldwide platinum, palladium and rhodium supply and demand from 1999 to 2008 (from Johnson Matthey http://www.platinum.matthey.com/market_data/1147696813.html)

2.5 Current and Historical Price Data

Figures 2.5 and 2.6 show the fluctuation in platinum, palladium and rhodium prices from 1992 to 2009[2]. For platinum and palladium the prices remained constant throughout most of the nineties when supply matched demand. From 2000 the effect of demand exceeding supply (due to increased use of both metals in autocatalysts) is noticeable as prices start to rise dramatically.

Throughout the 17 year period documented (Johnson Matthey, 2009) platinum has always had a significantly higher value than palladium with one exception during the period 1999 to 2001 where palladium equalled and then exceeded the price of platinum. This was due to an announcement by the Russian State Treasury, Gokhran, that no PGM would be sold in 2001. As previously discussed the majority (51%) of palladium is mined in Russia and therefore the price of this metal was inflated as vehicle manufacturers and other users moved to ensure they would have adequate stocks. Following the price peak, supply of palladium expanded from other producers and industry began seeking alternatives to this now very expensive metal, resulting in a steep price drop at the end of 2001 (http://www.stillwaterpalladium.com/priceJM.html). Platinum continued to see a steady rise in both demand and price during this time.

[2] This section relies heavily on figures from Johnson Matthey. They produce an annual market report entitled "Platinum" which the industry recognises as the definitive record of PGM supply and demand in the preceding year. It incorporates short-term market outlooks and platinum and palladium price forecasts. No other refiner places this level of information in the public domain.

Rhodium prices experienced a slight drop at the beginning of the nineties, followed by a period of stability similar to the trend observed for platinum and palladium. It also experienced a similar rise and then fall of price during 2000 and 2001 due to the interruptions to Russian supplies at that time.

All three metals experienced large price increases from 2005 to 2008[3]. The global economic crisis that started in the latter part of 2008 and is still ongoing has meant a significant drop in PGM demand for car catalysts and other applications and this has caused the prices of all three metals to drop greatly. Figures 2.7 and 2.8 show the prices of all three metals over the duration of this study from October 2005 to August 2009 and allows a more in depth discussion of the recent fluctuations.

[3] Prices are all quoted in dollars per troy ounce ($ / Tr Oz) as this is the international standard for precious metals. One troy ounce is 31.1 g.

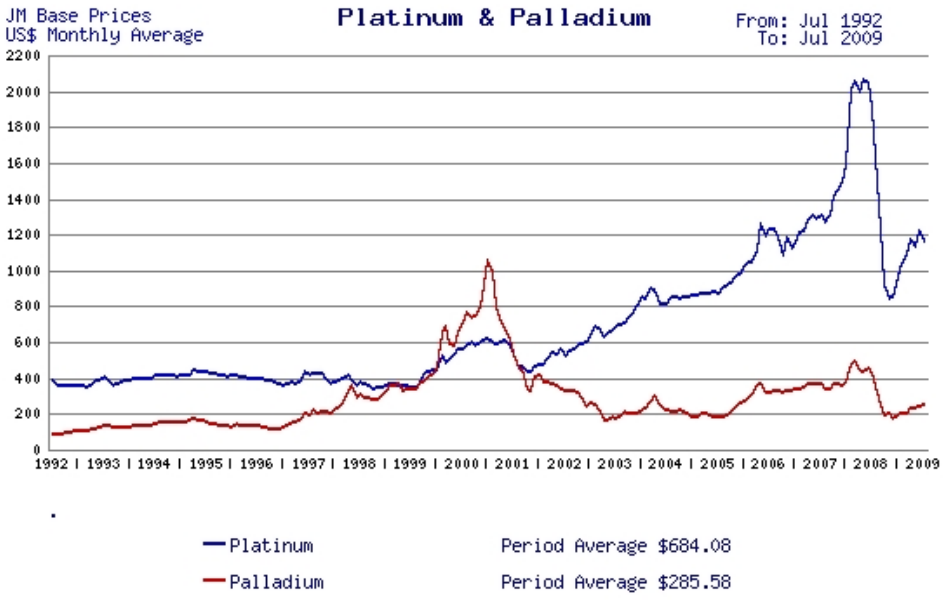

Fig. 2.5 Monthly platinum and palladium prices from 1992 to 2009 (from Johnson Matthey http://www.platinum.matthey.com/prices/price_charts.html)

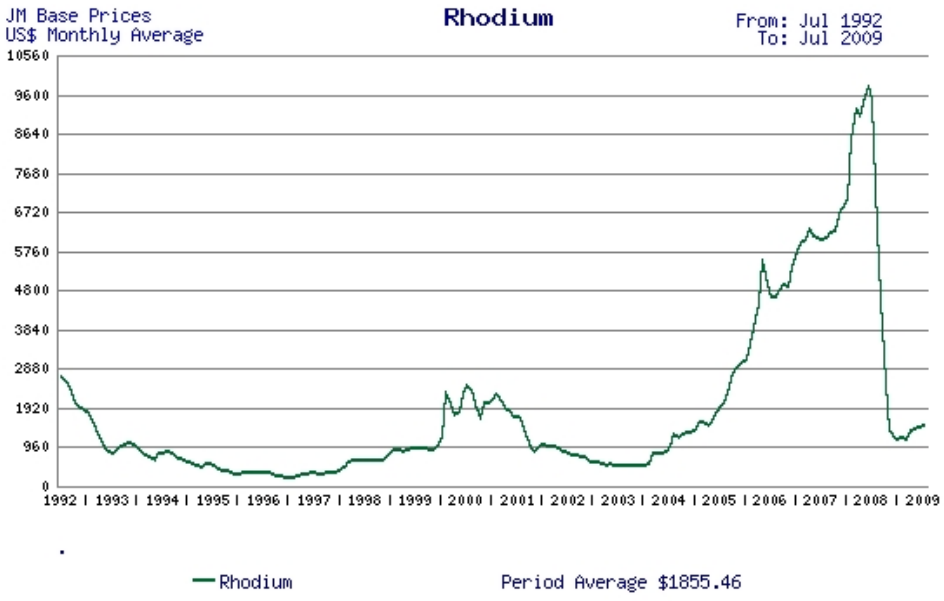

Fig. 2.6 Monthly rhodium price from 1992 to 2009 (from Johnson Matthey http://www.platinum.matthey.com/prices/price_charts.html)

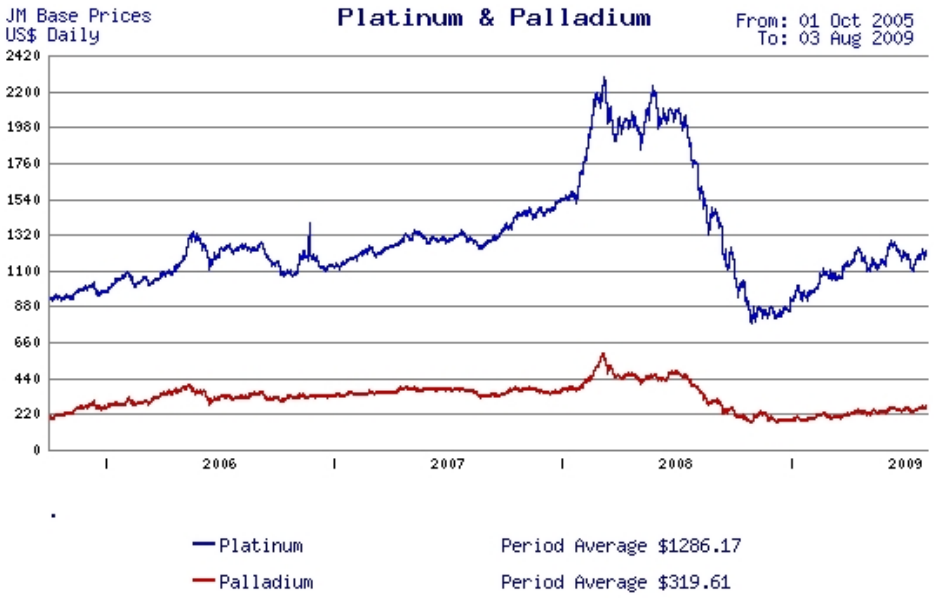

Fig. 2.7 Monthly platinum and palladium prices from 1st October 2005 to 3rd August 2009 (from Johnson Matthey http://www.platinum.matthey.com/prices/price_charts.html)

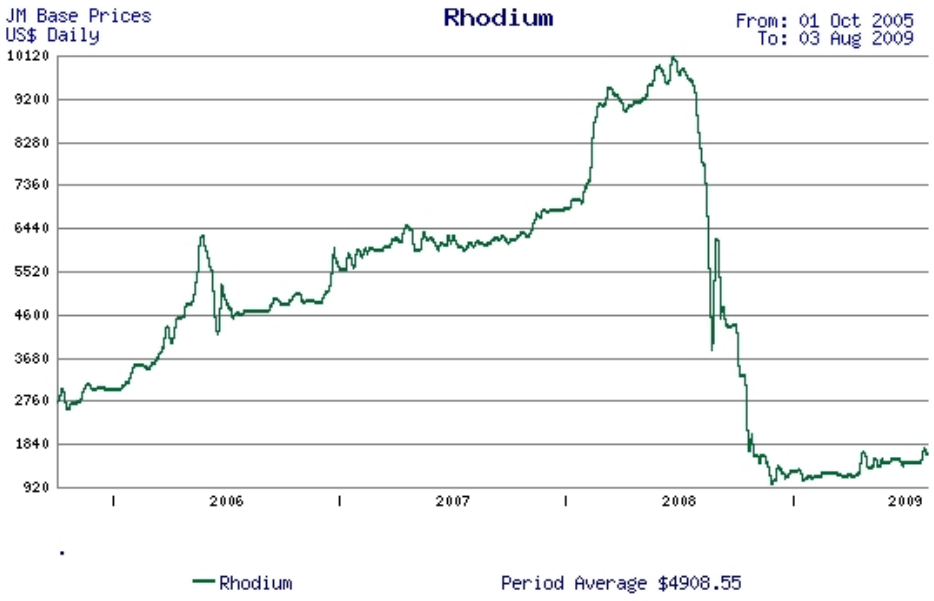

Fig. 2.8 Monthly rhodium price from 1st October 2005 to 3rd August 2009 (from Johnson Matthey http://www.platinum.matthey.com/prices/price_charts.html)

In October 2005 when this study commenced platinum was trading at $933 per troy oz, palladium was $209 per troy oz and rhodium was $2,753 per troy oz (monthly average figures). For all three metals these prices would rise almost continuously between October 2005 and May 2008 when record prices for platinum and rhodium were reached. In May 2008 platinum was $2,060, palladium was $490 and rhodium was $9,776 per troy oz. Using an exchange rate of $1 = £0.51 (the conversion rate for the 30th May 2008) this equates to a platinum price of £34 per gram, a palladium price of £8 per gram and a rhodium price of £160 per gram. These price increases indicate why recycling technologies are becoming more attractive within the precious metals industry.

Many of the economic decisions made during the project were based upon these increasing prices as there was little or no indication that things would change significantly. However, the banking crisis of August 2008 and the accompanying global recession caused prices to plummet between August 2008 and January 2009. In January 2009 platinum was trading at only $844 per troy oz, palladium at $189 and rhodium at $1152. This has been attributed to lower car production (America's light vehicle market dropped by 20% between the middle and the end of 2008 and Europe's by 6%) and also to the fact that the purchasing of metal over recent years for investment had helped drive the price to record levels but much of this metal (several million ounces) – in the form of forward purchases, futures positions and physical metal – was sold in the second half of 2008, hence prices fell sharply due to sudden oversupply (Johnson Matthey, 2009).

In effect this means that during the course of the project the price of rhodium has fluctuated by 8.5 times its lowest value and platinum and palladium by 2.5 times their lowest values. This has been important in relation to what analysis costs could be justified, what recovery levels were required and what could be discarded during different phases of the project. Prices have recovered a little from their lowest point but due to the ongoing uncertain economic situation they are much lower than the record values of 2008.

2.6 Predicted Reserves of PGMs

The last 75 years have seen the overall consumption and uses of platinum expand dramatically. Demand (and hence price) and uses are impossible to predict far into the future, but the resources and potential supply of platinum and palladium can be calculated with some degree of confidence.

The Bushveld Complex in South Africa is well-known for its large proportion of the world's platinum and palladium resources. Their global importance has justified several resource calculations in the past (Gruenewaldt, 1977; Vermaak, 1995). For resource calculations mining company reports include only proven and probable reserves, where sufficient information is available to justify such a classification. However, the continuity of layers within the Bushveld Complex justifies qualitative extrapolation to adjacent areas (Cawthorn, 1999).

Cawthorn's calculations indicate about 204 and 116 million ounces of proven and probable reserves of platinum and palladium, respectively, and 939 and 711 million ounces of inferred resources, down to a depth of 2 km. These figures represent about 75 and 50% of the world's platinum and palladium resources, respectively. These figures for proven and probable reserves in the Bushveld Complex alone are sufficient for the next 40 years at current rate of production.

Although the Bushveld Complex dominates world platinum production and resources, there are other deposits which produce platinum and palladium, or may do so in the future, depending upon economic forces. Cawthorn (1999) estimated that world resources, excluding the Bushveld, could be 387 million ounces of platinum. Total reserves and resources of platinum amount to 1140 million ounces in the Bushveld and a further 387 million ounces worldwide. Allowing for a demand increasing at 6% per year, those existing resources would supply all needs for over 50 years.

However, it has been estimated that if all the 500 million vehicles in use today were re-equipped with fuel cells, operating losses would mean that all the world's sources of platinum would be exhausted within 15 years (Gordon *et al.*, 2006). Thus if we are going to move away from a fossil fuel based economy it will be vital to conserve stocks of these metals by increasing recycling technologies.

2.7 Current Applications for the Platinum Group Metals

2.7.1 Vehicle Catalytic Converters

In 2008 the majority of PGMs (46% of platinum, 48% of palladium and 84% of rhodium) were used in the manufacture of automotive catalysts for the reduction of vehicle exhaust emissions (Johnson Matthey, 2009). As this application is central to this project it is discussed in greater detail in section 2.10.

2.7.2 Catalysts

PGMs are used extensively in the fine chemicals sector as catalysts. The largest application for platinum catalysts is in the production of silicones which are used primarily by the automotive and construction industries (Bernardis *et al.*, 2005). Palladium is used as a catalyst in purified terephthalic-acid production and unsaturated C-C bond hydrogenation (Clipsham and Claes, 2010). Palladium-gold catalysts are used in the production of vinyl acetate monomer, which is an extremely important intermediate product in the manufacture of polymers used in products such as paints, adhesives and textiles. They are also used in the selective oxidation of alcohols and in glycerol oxidation (Clipsham and Claes, 2010). Platinum and palladium gauzes are also well known in the production of nitric acid. Rhodium catalysts are used in the manufacturing of oxo-alcohols and acetic acid, the latter also using ruthenium and iridium as catalysts (Acres, 1987).

2.7.3 Jewellery

Platinum and palladium jewellery is popular, particularly in Asian markets. These white-metal jewellery items are hallmarked with purities of 990 and 950 fineness (i.e. 950 parts per 1000 of PGM or 95% PGM by mass), which contain significantly higher PGM content compared to white-gold alloys (white gold is an alloy of gold and at least one white metal, usually palladium). An advantage of palladium over platinum is the density, with a difference of almost 50%, making palladium jewellery lighter and, therefore more comfortable to wear (Creamer *et al*., 2006).

2.7.4 Electronics

The quantity of electronic equipment produced in the 21st century is very high and has been constantly increasing due to the growth in the consumption of these goods as well as the relatively short lifetime of this equipment (Veit *et al.*, 2005). Hard disks for computers, video recorders and MP3 music players are all important consumers of platinum. The single largest application for palladium in the electronics sector is in multilayer ceramic capacitors (MLCC) for personal computers and mobile phones, as well as in automotive electronic components (Creamer *et al.*, 2006).

2.7.5 Fuel Cells

A currently small but growing use for platinum in the future is in fuel-cell technology. Fuel cells generate electricity by means of an electrochemical reaction where hydrogen is split anodically

to form current and protons, electrons and oxygen combine to form water at the cathode. Since water is the only by-product of the fuel-cell reaction, the technology is extremely environmentally friendly (Department for Transport, 2006; Yang, 2009). If large-scale commercialisation becomes a reality, as the technology develops larger amounts of platinum will be required for use in fuel cells for automotive, electronic and stationary power applications.

2.7.6 Glass

Platinum, with its excellent resistance to corrosion and wear at high temperatures, is the material of choice in specialty glass production, in which some 355,000 ounces are consumed annually. Major applications include the production of liquid crystal displays for flat-screen computer monitors and televisions and in the production of glass fibre in the US.

Additionally, the glass industry consumes approximately 55,000 ounces per year of rhodium. The addition of rhodium (typically 10 wt%) to platinum produces a much stronger alloy which can be used under more highly stressed conditions, and with some gain in maximum operating temperature. However, the high initial cost of rhodium tends to limit its use as a platinum strengthener to about 20% (Stokes, 1987).

2.7.7 Medical

In the past three decades the use of platinum based drugs to treat, amongst others cancer, has increased with the result of improved patient survival. Platinum is radio-opaque and thus visible under X-rays. This property also makes it an ideal choice in the diagnosis of constricted arteries as it can be used to make guide wires for stent positioning. Pt - Au alloys are also used in dental bridges and crowns. The platinum imparts increased strength to high gold alloy, which typically contain 75% to 99% gold, 1% to 20% platinum and small amounts of palladium, silver and base metals (Johnson Matthey, 2009).

2.8 Environmental Impact of Primary Mining of PGMs

2.8.1 Principal Environmental Impacts

The environmental impact of mining, extraction and primary production is uncertain but likely to be large. The Resource Efficiency KTN (2008) estimated that worldwide mining activities (of all minerals) were responsible for around 5% of global carbon dioxide emissions. A 2004 report by Earthworks calculated a larger figure, stating that the metals mining industry was responsible for 7-10% of global energy consumption. Either figure demonstrates that the overall environmental impact of the extractive industries is extremely large.

According to research commissioned by the UK Department for Transport (2006) 12.7 tonnes of ore is extracted per troy ounce of platinum produced. The resource efficiency KTN (2008) put this figure at approximately 10 tonnes per ounce, depending on ore concentration and mining

depth. This results in large spoil heaps and high energy consumption. In fact 65 – 75% of the total cost of producing pure PGMs is accrued at the mining stage due to the large energy demand (Pincock, 2008).

In the long-term carbon intensities will increase, as more energy is required to process lower grades of ore, unless technological improvements can offset the impact. Table 2.3 shows the estimated carbon impacts from the initial extraction of various materials from the earth (data summarised from the Resource Efficiency KTN, 2008). These figures were compiled from data on the average ore grade at major mines, along with annual production and energy consumption for each location. Crucially these figures do not take into account what happens to the materials once they have been extracted from the ground i.e. they do not include processing and refining, merely extraction.

Table 2.3 The estimated carbon impacts (in kg CO_2 equivalents) from the initial extraction of selected PGMs, copper and iron. This table does not include processing and refining.

Material	**CO_2 Emissions per kg of material mined (kg CO_2 Equiv)**
Rhodium	32,208
Platinum	14,704
Palladium	9,912
Copper	3
Iron	0.005

Water and air pollution are also both serious problems associated with the mining and processing of PGMs. Flotation plants recycle water through several processes before releasing back into the groundwater system. Pollutants then become concentrated in a very small volume of water. Smelting of ores releases sulphur dioxide into the atmosphere and ammonia, chlorine and hydrogen chloride gases are all released as process emissions. Most significantly, residual effluent remains at the end of the process. This is the base metal liquor containing iron and zinc, which is removed and the residue metals are precipitated and then landfilled. The presence of the base metal precipitate in landfill can cause groundwater contamination and add to landfill leachate problems (International Centre for Science and High Technology, 2002).

So in summary the main environmental impacts of primary mining of the platinum group metals are as follows:

- High (and increasing) energy usage
- Large amounts of waste or “spoil” from mines
- Significant CO_2 emissions (many times higher than base metals)
- Water and air pollution
- Toxic effluents

The resulting external costs to society are not fully accounted for, presenting challenges to governments and regulators, particularly in less developed countries where mining companies increasingly operate and where environmental legislation is often less rigorous.

2.8.2 Strategies to Reduce Environmental Damage

In general resource efficiency measures can help reduce demand for primary materials. This usually involves one of the following strategies (Resource Efficiency KTN, 2008):

- **Substitution** – The use of an alternative metal or alloy with a higher abundance and / or lower impact

- **Minimisation or "thrifting"** – Using technological advances to reduce the amount of a material that is required for a certain purpose

- **Recycling** – Increasing the reuse and recovery rates for metals often have positive cost implications as well as environmental benefits. It also reduces the dispersion of critical materials into the environment. Most natural resources which are not chemically transformed are ultimately non-depletable. However, most elements are located and mined at places where they occur in substantial excess of their average concentration in the earth's crust and depletion occurs due to dispersion into the biosphere during extraction, production, use and disposal.

However the PGMs are an unusual case due to their low abundance and high technical importance (Bernardis *et al.*, 2005) and the first two measures i.e. substitution and thrifting have limited applicability. In most of its industrial applications, platinum is either irreplaceable or can only be substituted with significant compromises in performance. In most cases, the only feasible substitutes for platinum are other PGMs, including palladium, rhodium, ruthenium, iridium, or osmium, but these are no more abundant than platinum (Yang, 2009). PGMs currently have low substitutability due to their high activity for catalysis. Thrifting has been studied extensively over the past decade in the field of car catalyst production but reduction of PGM content can only be taken so far without impairing catalyst performance (Johnson Matthey, 2003). The upcoming Euro VI emissions legislation means that further reductions in PGM loadings are unlikely (Bloxham, 2009).

Thus recycling from secondary occurrences (such as road dust, electronic scrap, sewage sludge etc.) is important because it not only preserves a finite resource by preventing it being dispersed into the environment, but also dramatically reduces PGM related CO_2 emissions. Strategies for minimisation of dispersal need to take a whole life-cycle approach and factor in the environmental impacts of the collection and reprocessing steps (Resource Efficiency KTN, 2008).

2.8.3 Material Security

Although not directly linked to environmental concerns, material security is worthy of consideration here as it forms part of the sustainability issue surrounding PGMs. The concept of material security concerns the access to raw materials to ensure military and economic sufficiency. Recently, its importance has increased due to limited short term availability of some raw materials, widespread large increases in raw material prices and dependence on a limited number of sometimes politically unstable countries as sources of key materials. Materials are most insecure when lack of substitutability in critical applications is combined with the above factors (Resource Efficiency KTN, 2008).

As previously stated PGM production is concentrated in only three countries and 76% of platinum and 82% of rhodium come from just one country, South Africa. Energy shortages have disrupted metal supply several times since 2008 and will continue to do so for the foreseeable future until new power generating stations come online in 2018 (Yang, 2009). As a result in 2008 rhodium was classified as the second most insecure metal in the UK and platinum was ranked fourth (using supply, demand, production and environmental impact as key indicators). The Resource Efficiency KTN suggested that research should be focused on improving recycling technologies (with the environmental benefits they bring) in order to improve security of these metals within the UK. They stated that technologies to enable “mining” of waste streams for insecure metals are especially worthy of consideration.

2.8.4 Material Security and the Environmental Paradox

The report by the Resource Efficiency KTN also noted that the imperative to achieve more sustainable consumption of resources is having unexpected repercussions in the area of material security.

A large number of new 'environmentally-friendly' technologies now rely on materials for which demand was previously low. Frequently, the materials in demand are rare in the earth's crust or concentrated in regions subject to political instability. The most obvious example is the large increase in demand for PGMs in catalytic converters in response to tightening worldwide vehicle emissions standards.

Hence a paradox exists that greater environmental performance or efficiency is often achieved through the use of materials with greater environmental impacts and with less material security. The paradox may be substantially avoided by developing new material processing techniques that give more secure or common materials exceptional performance characteristics (i.e. substitution). The paradox may also be successfully managed by the application of life-cycle assessment tools. Whichever approach is taken, a key strategy is that the cost of sourcing metals and minerals should more closely reflect impacts on the global environment and climate change (Resource Efficiency KTN, 2008).

2.9 Recycling of Platinum Group Metals

Recycling is ecologically advantageous as it reduces the large CO_2 burden associated with primary mining and potentially helps to manage PGMs in a sustainable way. Efficient recycling technologies for PGM bearing materials have been established for many years and have been used successfully. However, the recycled PGM quantities are often substantially below the original PGM input for the various applications (Hageluken *et al.*, 2006).

2.9.1 Current Recycling Technology

There are a number of facilities that recycle PGMs in Europe but almost all rely on high temperature, energy intense, pyrometallurgical processes. Johnson Matthey for instance operates three reverberatory furnaces and two arc furnaces in the UK for the reprocessing of PGM containing scrap such as autocatalysts, spent industrial catalysts, high end electrical components etc. (Wright, 2008). Platinum Recoveries Limited (PRL) focus solely on autocatalysts and use a furnace with a plasma torch (Deagan, 2009) but again this is a pyrometallurgical route (smelting) and is similar to that used in primary concentration from ores. Thus PGM recovery from primary ores and secondary "wastes" both rely on smelting followed by refining as the main recovery mechanism.

In these pyrometallurgical methods, PGM containing scrap is mixed with fluxes and a collector metal such as iron or copper and is heated to a high temperature (1500 – 1600 ˚C). The PGMs

are recovered in the collector metal and the unwanted material such as catalyst support is removed via the slag layer (Benson *et al.*, 2000; Brumby *et al.*, 2005). The collector metal is then separated from the slag (tapped off) and the PGM recovered from this by conventional refining techniques. The method is widely employed as it is well established and can handle many different pollutants in the scrap, such as carbon, sulphur and hydrocarbons (Brumby *et al.*, 2005). The recovery rate is usually >98% of the PGM content of the feedstock (Sibley *et al.*, 1995, Wright, 2008). Recovery rates >95% can still be achieved even when the PGM content of the feedstock is extremely low (<0.1%) (Benson *et al.*, 2000).

Pyrometallurgical processes for recycling also generate their own PGM containing wastes that require reprocessing (such as PGM containing slag and end of life furnace linings). Spent furnace linings form part of this study and are discussed in greater depth in chapter 4.

2.10 The Use of PGMs in Vehicle Catalytic Converters

The three-way catalytic converter (autocatalyst) for the reduction of exhaust emissions was introduced into Europe in the late 1980's. By January 1993 it was compulsory for all new cars sold within the European Union to be fitted with an autocatalyst (Zereini *et al.*, 1998; Jarvis *et al.*, 2001; Lesniewska *et al.*, 2004). Modern catalytic converters reduce the emission of nitrous oxides, carbon monoxide and hydrocarbons from motor vehicles. The environmental benefit of this reduction has been obvious with the removal of approximately 90% of carbon monoxide,

unburned hydrocarbons and nitrous oxides from the exhaust (Barefoot, 1997; Whiteley and Murray, 2003).

Substantial benefits are gained through atmospheric emissions reduction at the exhaust pipe. On average over the 160,000 km life of a catalytic converter, about 1500 kg of carbon monoxide, 290 kg of nitrogen oxides, 140 kg of hydrocarbons and 11 kg of methane are reduced from the exhaust emissions (Amatayakul and Ramnas, 2001).

2.10.1 The Necessity of PGMs

Lui and Dettling (1993) and Shelef and McCabe (2000) stated that the choice of PGMs as the active catalytic materials in autocatalysts was the result of three factors:

a) Only PGMs had the required activity needed for the removal of the pollutants in the very short residence times dictated by the large volumetric flows of the exhaust in relation to the size of catalyst which could be accommodated in the available space.

b) PGMs were the only catalytic materials with the requisite resistance to poisoning by residual amounts of sulfur oxides in the exhaust gases.

c) PGMs were less prone (but not entirely immune) to deactivation by high-temperature interaction with the insulator oxides of Al, Ce, Zr, etc., which constitute the high surface area "washcoat" on which the active catalytic components are dispersed.

Platinum and palladium are responsible for the oxidation of carbon monoxide to carbon dioxide and hydrocarbons to carbon dioxide and water (CO to CO_2 and HCs to CO_2 and H_2O). Rhodium is responsible for the reduction of nitrous oxides to nitrogen and oxygen (NOx to N_2 and O_2) (Shelef and McCabe, 2000; Ek *et al.*, 2004).

Currently three-way formulations containing Pt/Rh, Pt/Pd/Rh (trimetal) and Pd/Rh metal combinations are all in commercial use. Issues of fuel quality (residual lead levels and sulfur concentration) still play an important role in the choice of catalyst formulation for a particular market. As formulations have improved over time, however, decisions regarding the choice and loading of particular PGM combinations are becoming increasingly based on cost factors. Indeed, with fluctuations in PGM prices likely to persist into the future, one strategy for vehicle producers may be to have a number of available formulations "on the shelf" that can be deployed in response to changing market conditions (Shelef and McCabe, 2000).

However a market report by Johnson Matthey (2003) countered this opinion. They stated that dual certification (having two formulations for the same vehicle model) would in theory allow manufacturers to have more control over PGM costs. However in practice the characteristics of

different formulations (such as reactivity, pollutant conversion efficiency and durability) are not identical and a recalibration of the engine management systems and on-board diagnostics will normally be required. This in turn is impractical as it usually means that the entire engine system has to be recertified and the costs associated with this are likely to offset any metal savings made.

2.10.2 Projected Life of Catalytic Converters

Amatayakul and Ramnas (2001) stated that the guaranteed service life of a catalytic converter from Swedish manufacturers was 160,000 km (99,400 miles) assuming the catalyst is not broken due to accidental impacts or engine misfires. Shelef and McCabe (2000) discussed US legislation and noted that governmental regulations require proper functionality of emissions systems for 100,000 miles of use (120,000 for trucks).

The Automobile Association (AA) in the UK (2010) noted that it is not unusual for catalysts to last 10 years, though actual life depends on mileage and engine tune. 50,000 miles is perhaps a more reasonable benchmark. If failure occurs early, it is important that the reason for failure is identified and the cause rectified before fitting a new catalyst, otherwise the replacement can be expected to fail prematurely too. The AA also state that there are three main failure modes:

1) **Melt down** - unburned fuel entering the catalyst ignites on contact and the extreme heat melts the ceramic matrix. Poor ignition timing, a faulty oxygen sensor, worn or defective

spark plugs, incorrect fuel mixture and other ignition/fuel injection related faults could lead to this failure.

2) **Carbon deposits** - oil or antifreeze entering the combustion chamber/exhaust system can lead to a build-up of carbon on the matrix, which increases back pressure leading to overheating and poor performance.

3) **Catalyst fracture** - the ceramic matrix is fragile and can break-up as a result of excessive vibration or external impact. As the matrix breaks up back-pressure increases and overheating can result.

2.10.3 Platinum Group Metal Loadings on Catalytic Converters

2.10.3.1 Current and Historical PGM Loadings

Mouza *et al.* (1995) stated that the size and shape of catalytic converters, along with their PGM catalyst loading, may vary according to the size of the vehicles engine. They summarised that an average catalytic converter contains 1.8 g of active constituent, consisting of 1.5 g platinum and 0.3 g rhodium. The content of the ceramic substrate is 0.14 to 0.28 wt% platinum and 0.03 to 0.05 wt% rhodium. The weight of a ceramic catalytic converter depends on the vehicle type and ranges from 600 to 4500 g (average weight 900 g).

Although the composition and relative proportion of platinum, rhodium and palladium varies, Coombes (1992) noted that catalysts produced during the 1990's (now nearing the end of their useful life) contained a platinum to rhodium ratio of approximately five to one. The size of the catalyst depends on the engine size, but a typical catalytic converter for a family car would contain a total of about 1.75 g of PGM (Coombes, 1992). Xiao and Laplante, 2004 stated that newer catalytic converters contain approximately 2.4 g of PGM.

Tollefson (2007) noted that the platinum loading in a catalytic converter depends on engine type and size and emission standards, ranging from 1 – 2 g for a small car in a lightly regulated environment to 12 – 15 g for a large truck with stringent regulations.

2.10.3.2 Pending Legislation and Future PGM Loadings

It is estimated that emissions from road transport contribute 17% of total anthropogenic carbon dioxide (CO_2) emissions (International Energy Agency, 2007). Regulations coming into force in Europe and in the U.S.A. are seeking to change this. In December 2008, the European Parliament approved a directive (Euro VI legislation) to reduce the average CO_2 emissions of new passenger cars to 120 g km^{-1} by 2015, with a three-year phase-in period. Overall, the 120 g km^{-1} target represents an improvement in fuel economy of about 25% from current levels (European Commission, 2009 www.ec.europa.eu/environmentair/transport/co2).

The technologies in question are (1) diesel engines, (2) downsized turbocharged petrol engines combined with direct injection, and (3) hybrid petrol - or diesel-electric vehicles (Bloxham, 2009). Each of these will have a different impact on PGM use. Given the considerably higher amount of PGM used in diesel after treatment as compared with petrol, any increase in the share of diesel engines will lead to greater demand for PGMs. Downsized petrol engines (such as turbo and super-charged engines) provide similar, or improved performance at reduced engine size and hence the potential for greater fuel economy. In recently developed vehicles, the catalyst size tends to be smaller, but the PGM loading may be higher. In the coming years, assuming that vehicles are manufactured to meet the same regional emissions standards, the current view is that a switch to hybrid vehicles from conventional gasoline or diesel vehicles will have little impact on overall uptake of PGM (Bloxham, 2009).

Overall, Bloxham (2009) predicted that it is unlikely that tighter CO_2 emissions limits will strongly affect PGM demand from the automotive sector in either direction within the foreseeable future i.e. there will continue to be similar amount of PGM used in the production of autocatalysts. However, Yang (2009) believed that in order to meet stringent emission standards, automobiles must be equipped with advanced catalytic converters, which require higher loadings of platinum.

2.10.3.3 The Proportion of Worldwide PGM Production Used in Catalytic Converters

In 1997, 64,550 kg of platinum was utilized worldwide for the production of autocatalysts. Of that total just over 16,000 kg was used in Europe (Jarvis *et al.*, 2001). In 2008, over 118,500 kg of platinum was used (Johnson Matthey, 2009) i.e. in just over ten years the amount of platinum used for this application almost doubled.

In the year 2000, 146,000 kg of palladium was used by autocatalysts (Stuben and Kupper, 2006). This has stayed fairly constant with 140,000 kg being used in 2008. The strong demand for palladium, particularly in Europe is largely in response to the introduction of European emissions legislation (Euro stages III to VI from January 2000 to January 2015). Palladium-rich catalysts can meet stricter emission limits for petrol-fuelled vehicles, resulting in a divergence from platinum-based technology (Johnson Matthey, 2001).

In addition in 2008 just over 23,500 kg of rhodium was used in the manufacture of automotive catalysts (Johnson Matthey, 2009). Although this is a much lower figure than either platinum or palladium in percentage terms it represents the major worldwide use of rhodium.

The 2008 figures for autocatalyst PGM use represent 46% of the worldwide supply of platinum, 48% of palladium and 84% of rhodium (Johnson Matthey, 2009).

Although autocatalysts are recycled, typical recovery is only around 20 – 30% and so over the lifetime of a catalyst up to 70% of the platinum used in production could be released into the environment (Jarvis *et al.*, 2001).

During fuel combustion the catalysts are physically and chemically stressed by fast changing oxidative / reductive conditions, high temperatures and mechanical abrasion, thus releasing PGM containing particles from their surface (Palacios *et al.*, 2000a). The quantity of platinum emitted depends on different factors such as the age of the catalyst, driving conditions (e.g. urban or motorway), duration and speed of driving and the temperature of the exhaust gases (Palacios *et al.*, 2000a).

2.11 Spent Refractory Lining and PGM Recovery

Refractories are chemical compounds that are used as structural materials forming insulation linings in high temperature and corrosive environments in many industrial processes (Velez, 2000). The mineral chromite is the only ore of chromium and around fifteen percent of the total world chromite consumption is in the refractories industry (Kim *et al.*, 1992). Its usefulness is based on its high melting point (2,180°C), moderate thermal expansion, neutral chemical behaviour and relatively high corrosion resistance. Refractory bricks of 100% chromium ore have largely been replaced by bricks composed of mixtures of chromite and added oxides (e.g. magnesia) for greater volume stability and resistance to spalling (cracking / rupturing of a refractory shape).

Johnson Matthey's precious metal refinery in Enfield, UK operates three rotary furnaces lined with a magnesia-chromite refractory brick. Each furnace is lined with just over thirty tonnes of brick which has an operational life of six months. Therefore every six months around one hundred tonnes of refractory is produced for disposal.

Due to the high temperatures reached during normal operation of the furnace, molten precious metal can permeate the exposed side of the brick i.e. the furnace lining absorbs precious metals throughout its operational life. At present the spent lining is removed from the furnace and is itself reprocessed by smelting in order to recover the significant amounts of precious metal present. For these reasons precious metal refiners such as Johnson Matthey are keen to develop alternative processing solutions for their refractory linings.

2.12 Losses of Platinum Group Metals into the Environment

As a result of "open loop" recycling (discussed in section 2.9) PGMs are being dispersed into the environment. If these metals are not to be permanently lost from the recycling chain then new methods will need to be devised to process these "secondary" occurrences, also known as "urban wastes."

2.12.1 Concentration of Platinum Group Elements in Road Dust

The distribution of platinum, rhodium and palladium adjacent to two major UK roads shows a rapid decrease (more than one order of magnitude) away from the road and reflects patterns shown by other traffic-derived elements such as lead and zinc. A temporal study over a twelve month period, of road dust and surface samples, revealed elevated concentrations above background levels, with maximum values of platinum in excess of 500 ppb, rhodium 70 ppb and palladium 70 ppb. Since the introduction of autocatalysts in Europe in the 1980's there has been a clear link between their use and increasing concentrations of PGMs in the environment resulting in enhanced levels of these elements occurring in road dust and soils, particularly in urban areas and around major roads (Jarvis *et al.*, 2001).

The authors of an American report on the platinum group metals, published in 1977, estimated that it would take over 1000 years for platinum metal concentrations in roadside topsoil to reach the concentration observed in the rich ores in South African mines (4-10 ppm). However, less than 10 years later dust analysed from the leaves of roadside plants in San Diego, California were found to contain concentrations of platinum as high as 0.7 ppm and palladium as high as 0.3 ppm (Hodge and Stallard, 1986). The concentrations of both metals in the dust samples are once again much higher than the reported natural abundances of these elements. Thus it appears that widespread use of the catalytic converter makes it possible for these rare metals to enter the environment in a dispersive manner.

Whiteley and Murray (2003) measured platinum, palladium and rhodium concentrations in road dusts in Perth, Western Australia. All samples analysed show significant enrichment relative to background soil samples. Platinum concentration ranged from 30-420 ppb and rhodium concentration from 3.5-91 ppb. These are within the range of values reported from road dusts in European studies.

Konig *et al.* (1992) stated that although the particle size of PGM on a fresh catalyst is only 1.6 nm, research has shown that the average diameter of an emitted platinum particle is around 7 µm. These larger particles may be generated simply by mechanical abrasion or due to vaporisation of platinum oxides which are then reduced to metal, depositing on aluminium oxide particles in the exhaust. Artelt *et al.* (1999) demonstrated that between 43% and 71% of these larger particles are greater than 10 µm in diameter.

The dependence of PGM concentrations in environmental materials on traffic density and number of cars equipped with catalysts has been confirmed by a number of authors (Farago *et al.*, 1996; Barefoot, 1997; Zereini *et al.*, 2000). Farago *et al.* (1996) demonstrated differences between platinum concentrations in road dust samples taken from areas of high and low traffic density. It is also known that emission of platinum from cars driving under full load conditions and at frequently changing speed or with repeated stops (e.g. at roundabouts and traffic lights) is much higher than from cars moving at a constant average speed of 80 km/h (Artelt *et al.*, 2000).

Tunnel dust is a also a good indicator of pollution since it is less influenced by different atmospheric conditions such as rain and wind and therefore more realistically reflects the level of emission from car catalytic converters (Lesniewska *et al.*, 2004).

Zereini *et al.* (1997) and Lesniewska *et al*. (2004) both found that the highest content of metals was observed in the smallest size classification of dust (< 75 µm), suggesting that PGMs are bound to the smallest particles of soil, dust and sludge. However in contrast to this Jarvis *et al.* (2001) found that platinum, palladium and rhodium are preferentially found in the larger 63-250 µm size fraction.

In summary, in contradiction to earlier projections, the levels of PGMs being reported in road dust are comparable to low grade ores. Platinum is mined South Africa where the ores have concentrations of 4-10 ppm, the richest in the world, while in Sudbury Canada platinum is a by-product from processing ores with less than 1ppm precious metal content (Hodge and Stallard, 1986).

Road sweeping in the UK is the responsibility of each Local Authority (who may sub-contract collection). At present road sweepers collect then store the dust before sending it for expensive landfill disposal. Millions of pounds of valuable PGMs are literally being thrown away.

2.12.2 Concentration of Platinum Group Elements in Sewage Sludge and Incinerator Ash

As previously discussed platinum group elements are released into the environment via abrasion from autocatalysts. This however is not their only source of emission - other sources include dental alloys, cancer drugs and jewellery production and wearing (Stuben and Kupper, 2006). These other sources also accumulate extensively and form part of the total contamination in sewage sludge, along with the run-off from roads during rainfall.

In Switzerland, the palladium content in sewage sludge is in general lower than 100 ppb (Stuben and Kupper, 2006). In the USA it has been documented up to two orders of magnitude higher, with palladium concentrations of more than 10 ppm (Furr *et al.*, 1976). Lottermoser (1994) reported data of sludges sampled in more than thirty German cities. Concentrations ranged from 38 ppb to 1 ppm for palladium and 10-130 ppb for platinum.

Variability of sample as well as analytical issues can be a big issue when trying to calculate PGM content of sewage sludge. An unusually high discharge from local industry into the wastewater system may result in a large volume of sludge at the treatment plant. This in turn can dilute the concentration of metal present. For this reason, careful thought must be given to experimental design, for recovery of PGM from this source ensuring sufficient replicates are taken over a set period.

At present the sludge is typically drained by gravity thickener, centrifuged and thermally dried to reduce the water content by around 50% (Boch and Schuster, 2006). It is then burned in a fluidised bed incinerator at around 950 °C to create an ash that is currently sent to landfill or used as a filler material in the construction industry. This incinerator ash is therefore another potential “urban mine” for PGMs.

3. Experimental Techniques

"As mined" ores consist of valuable minerals and gangue (commercially worthless mineral matter). Mineral processing, also known as *ore dressing*, *mineral dressing* or *milling*, follows mining and prepares the ore for extraction of the valuable component(s) and produces a commercial end product (Wills, 2008). The purpose of this project was to extract valuable metals from secondary composite waste sources. These waste sources were analogous to primary ores, with components of varying value, and so the methods used to process them were similar.

For a number of the techniques discussed in this chapter (magnetic separation, electrostatic separation, eddy current separation and specific gravity separation) efficient segregation depends on adjusting experimental parameters by visual inspection of the particle streams. Thus a sacrificial sample of each size fraction (for each test material) was used to optimise the key variables such as belt speed, feed rate, field strength / current, splitter plate location, gap width etc. This sacrificial sample was often separated and then recombined 5 to 10 times during optimisation. A second (representative) sample was then separated using the optimal machine settings deduced for that sample and the sub-fractions generated sent for analysis.

Due to the number of combinations of machine parameters used on different size fractions for each test material in many cases the details of specific separations are listed in the relevant experimental chapters.

3.1 Liberation of Particles

An essential prerequisite for the separation of an ore into valuable and waste fractions is the liberation of the valuable mineral grains from the waste mineral grains. The degree of liberation is the percentage of a given component that exists as free particles i.e. particles containing only that material (Kelly and Spottiswood, 1982). Particles containing both valuable and waste particles are called *middling particles*. A large proportion of the difficulties experienced in mineral separations are associated with the treatment of these particles.

Comminution is employed to fracture mineral aggregates and thus induce or increase liberation. One of the major objectives is the release of the valuable minerals from the associated gangue minerals at the coarsest possible particle size (Wills, 2008). As a result of fracture two types of liberation can be distinguished (Kelly and Spottiswood, 1982).

- **Intergranular Liberation** – If the interface between mineral grains is weak then intergranular fracture occurs. Here the fracture is at grain boundaries rather than across the grains. Pure intergranular fracture is comparatively rare.

- **Transgranular Liberation** – Fracture occurs across the grains instead of at the grain boundaries. By applying sufficient size reduction a high degree of liberation can be achieved, although complete liberation is improbable.

3.2 Comminution

Liberation of the valuable minerals from the gangue is accomplished by comminution which involves crushing, and, if necessary, grinding to such a particle size that the product is a relatively clean mixture of mineral and gangue. Kelly and Spottiswood (1982) stated that crushing is usually a dry process and is often performed in several stages (primary, secondary, tertiary and sometimes even quaternary stages).

3.2.1 Crushing

When an irregular particle is broken by crushing the products fall into two distinct size ranges; coarse particles resulting from the induced tensile failure and fines from compressive failure near the points of loading or by shear at projections. The amount of fines produced can be reduced by minimising the area of loading and this is often done in compressive crushing machines by using corrugated crushing surfaces (Wills, 2008).

3.2.1.1 Jaw Crushing

Jaw crushers are reciprocating-pressure breakers and consist of two crushing surfaces set at a small angle convergent downward, one fixed, the other movable and caused to approach and recede alternately from the fixed surface (Taggart, 1954). The aperture between the plates can be adjusted in order to alter the size of the particles produced. A schematic of a jaw crusher is shown in figure 3.1.

The jaw crusher used for this research was a Sturtevant 150 mm jaw crusher with corrugated jaw plates. For the spent refractory lining (chapter 4) in order to reduce the occurrence of fine particles (which cannot be processed effectively in an industrial setting) several passes were made using the jaw crusher with progressively smaller crushing plate gaps (22 mm, 16 mm and 14 mm) until at least 98% of the material passed a 16 mm wire mesh. Before each pass the material was screened so that only particles greater than 16000 µm passed through the crusher again. Particles greater than 16000 µm were undesirable due to difficulties with sampling and assaying high value non-homogeneous materials.

For spent autocatalyst the jaw crusher gap was set to the minimum value of 14 mm in order to prepare material suitable for secondary rolls crushing as 100% of material was required to pass a 1 mm wire mesh prior to leaching trials.

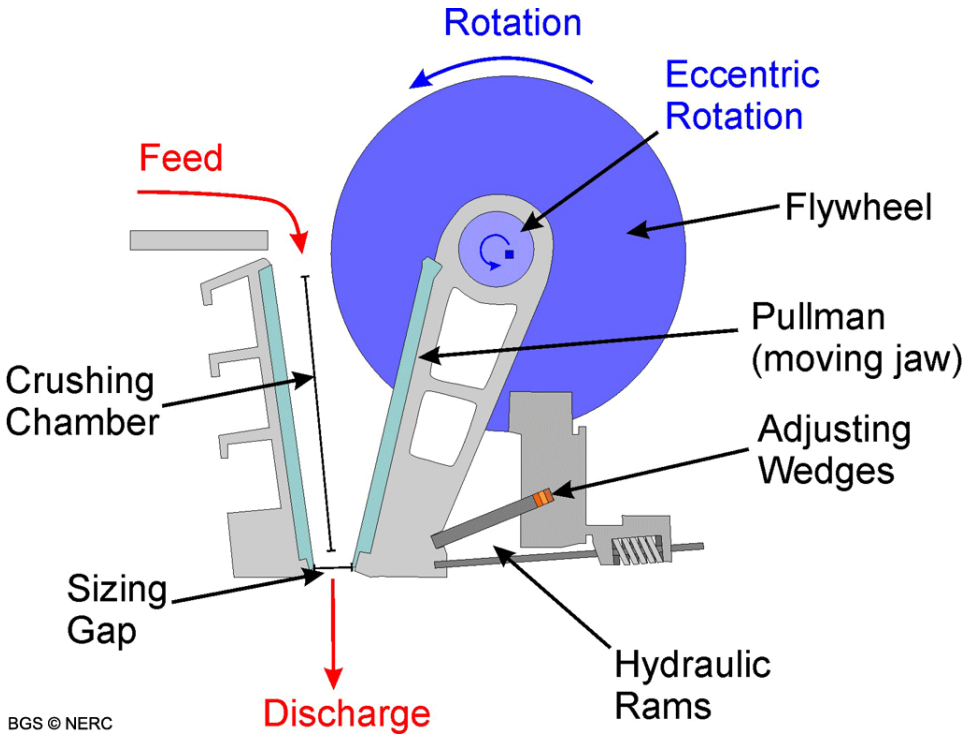

Fig. 3.1 Schematic of a jaw crusher showing the adjustable gap between the plates (from http://www.goodquarry.com/images/productiontechnology/PPT_photo8_large.gif)

3.2.1.2 Roll Crushing

Roll crushers are continuous breakers in which, in the crushing zone, there is a continuous approach of the crushing surfaces with a fixed predetermined minimum spacing, whereas jaw crushers are reciprocating breakers (Taggart, 1954). In general jaw crushers are suited to breaking hard, tough, abrasive materials. Roll crushers have high wear rate with such materials but are useful with relatively soft, friable materials such as autocatalyst and refractory linings.

A roll crusher (figure 3.2) crushes using compression, with two rolls rotating towards the gap between the rolls. The gap between the rolls is set to the size of product desired, with the

limitation that the largest feed particle can only be 4 times the gap dimension (www.mine-engineer.com/mining/rollcrush.htm). The particles are drawn into the gap between the rolls by their rotating motion and a friction angle formed between the rolls and the particle, called the nip angle. The two rolls force the particle between their rotating surface into the ever smaller gap area, and it fractures from the compressive forces presented by the rotating rolls. Some major advantages of roll crushers are that they give a very fine product size distribution and they produce very little dust or fines (Pryor, 1965).

The roll crusher used in this research was a Sturtevant 150 mm Roll Crusher. Secondary crushing of spent refractory lining and autocatalyst was conducted after jaw crushing. For the spent refractory lining the gap between the rolls was controlled via the addition of two spacers and the material was passed through the rolls twice until all material passed a 1180 µm wire mesh. For the spent autocatalyst the gap was reduced by using only one spacer in order to ensure that 100% of material was less than 1 mm.

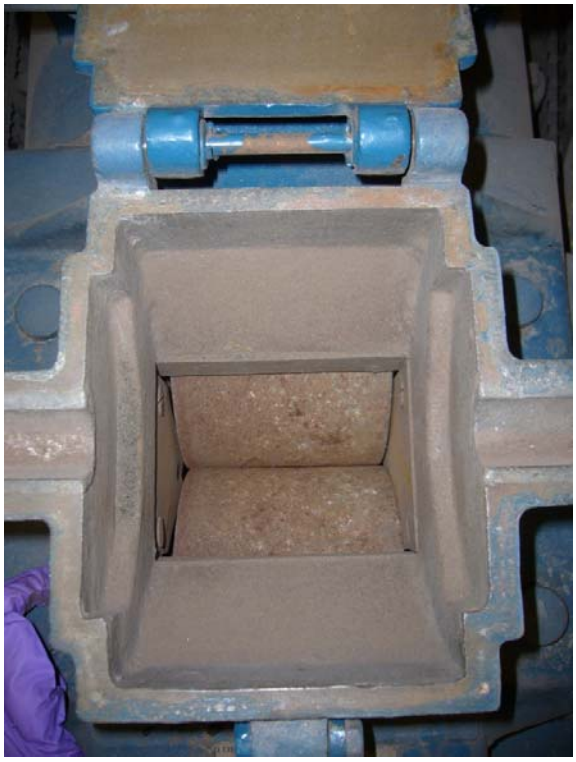

Fig. 3.2 View into the Sturtevant 150 mm roll crusher. Both rotating rolls are visible through the feed hopper. One roller is fixed and one is sprung and so gap adjustment is achieved by adding spacers to move the sprung roller.

3.2.2 Grinding

For some experiments, or analysis, it was necessary to reduce the size of the material to a fine powder. When required, samples of 20 to 100 g were placed in a concentric steel ring tema mill (figure 3.3) and milled for increasing amounts of time depending on the experimental requirements.

The tema mill used for grinding should be employed after large particles have been crushed to less than 10 mm, so that the particles fit between the rings of the mill. The material to be milled

is evenly distributed in the bowl between the removable rings. The unbalanced motor induces the parts within the mill bowl to move and impart force upon the particles.

Fig. 3.3 A tema mill, including detailed view of the concentric steel rings in the head.

In this research test material was milled for between 30 s and 120 s depending on nature of the material and the final particle size required.

3.3 Representative Sampling

When smaller samples are required to be taken from a large amount of material it is important that the smaller sample is fully representative of the whole. To achieve this samples are taken by riffling down to the required quantity.

Research by Gerlach *et al.* (2002) showed that riffle splitting was the most accurate method of practically producing representative subsamples. They established 99% confidence levels of less

than 2% variability for this technique. They compared several methods of subsampling including riffle splitting, paper cone riffle splitting, coning and quartering, fractional shoveling and common grab sampling using synthetic samples in order to test Gy's sampling theory (Gy, 1979). It should be noted that their synthetic samples were closely controlled and so the results obtained in an industrial setting are likely to be more variable, depending on feedstock. However riffle splitting is still accepted to be the most accurate method of gaining representative samples under these conditions. Gerlach *et al.* (2002) also noted that the error in sampling is often two orders of magnitude greater than the error in assaying.

Two types of riffling devices were utilised during this research - a box riffle and a spinning riffle (both designed to subsample dry, free flowing material). Both types of device take theoretically identical smaller samples from a larger whole.

3.4 Particle Size Analysis

There are many methods to determine the particle size distribution of a given sample. For the purposes of this research sieving was the main method used.

3.4.1 Test Sieving

Sieving is a mechanical separation of particles on the basis of size. A laboratory sieve consists of a screening surface, normally of woven wire, which results in square apertures with small

tolerances. Ideally particles larger than the apertures are retained on the surface, while particles smaller pass through (Kelly and Spottiswood, 1982).

In each of the standard sieve series the apertures of consecutive sieves bear a constant relationship to each other. It has been found that a useful sieve scale is one in which the ratio of the aperture widths of adjacent sieves is the square root of 2 ($\sqrt{2} = 1.414$). The advantage of such a scale is that the aperture areas double at each sieve, making graphical presentation of results easier (Wills, 2008; Pryor, 1965). Many modern sieve series are based on a fourth root of 2 ratio ($\sqrt[4]{2} = 1.189$) which makes much closer sizing possible.

Screening is commonly used as the first stage of physical separation as it can reduce the volume of material for further processing and all other physical separation techniques are more efficient when presented with a narrower size distribution.

Once the test materials (autocatalyst and spent refractory brick) material had been crushed it was put through a series of sieves. Depending on the material being processed the sieves ranged from +16000 µm to +38µm in a $\sqrt{2}$ or $\sqrt[4]{2}$ progression. All sieving was carried out in accordance with BS 1796-1: *Methods using Test Sieves of Woven Wire Cloth and Perforated Metal Plate (1989)*. The nest of sieves was placed on a receiver pan and the sample was placed on the top sieve of the nest and sealed with a tight fitting lid. The sealed nest was then placed on a Retsch VS1000 automatic sieve shaker and left for 20 minutes. Afterwards the mass of

sample retained on each of the sieves, and the mass of the sample passing the final sieve in the nest, was recorded. From the recorded masses it is possible to determine the particles size distribution (PSD) of the material under test – PSD can be expressed as a "range" analysis, in which the amount in each size range is listed in order, or it may be presented in "cumulative" form, in which the total of all sizes retained by a single notional sieve is given for a range of sizes. Range analysis is suitable when a particular particle size is being sought, while cumulative analysis is used where the amount of undersize or oversize must be controlled.

3.5 Magnetic Separation

Magnetic separators exploit the difference in magnetic properties between ore minerals and are used to separate either valuable minerals from the non-magnetic gangue or valuable minerals from the non-magnetic values (Wills, 2008). All materials are affected in some way when placed in a magnetic field. The property of the material that determines its response to a magnetic field is the *magnetic susceptibility*. Based on this susceptibility materials may be divided into three groups:

- **Diamagnetic Materials –** are repelled along the lines of magnetic force to a point where the field gradient is smaller. The forces involved are very small and diamagnetic substances cannot be concentrated magnetically.

- **Paramagnetic Materials –** are attracted along the lines of magnetic force to points of greater field gradient. These materials can be concentrated in high-intensity magnetic separators. All the platinum group metals are weakly paramagnetic.

- **Ferromagnetic Materials –** can be regarded as a special case of paramagnetism involving very high forces. These materials have a very high susceptibility to magnetic forces and retain some magnetism when removed from the field (remanence). They can be concentrated in low-intensity magnetic separators.

3.5.1 Dry High Intensity Magnetic Separation

Very weakly paramagnetic materials can only be effectively separated if they are allowed to come into direct contact with the magnet pole tip. Dry high-intensity magnetic separation has been used commercially for over one hundred years and presently handles considerable tonnage (Pryor, 1965). The roll on to which the test material is fed is composed of steel laminates compressed together on a non-magnetic stainless steel shaft. By using two sizes of lamination the roll is given a serrated profile which promotes the high field intensity and gradient required (Wills, 2008). Non-magnetic particles are thrown off the roll into the tailings compartment, whereas magnetic particles are gripped and brushed off the roll into a separate compartment.

Dry magnetic separation is generally only effective down to a particle size of around 150 µm, due to dust issues during laboratory scale testing (Rowson, personal communication, 2006).

3.5.1.1 Induced Roll Magnetic Separation

Figure 3.4 is a schematic diagram of a dry, high-intensity, induced roll magnetic separator. The test material (ideally with a narrow particle size distribution) is placed in the feed hopper and the current is switched on. The feed hopper is opened so that the test material exits as a monolayer. Magnetic particles are attracted to the roll and are removed with a brush into the right hand tray. Non-magnetic particles are not attracted to the roll and are therefore thrown off by centrifugal force and collect in the left hand tray.

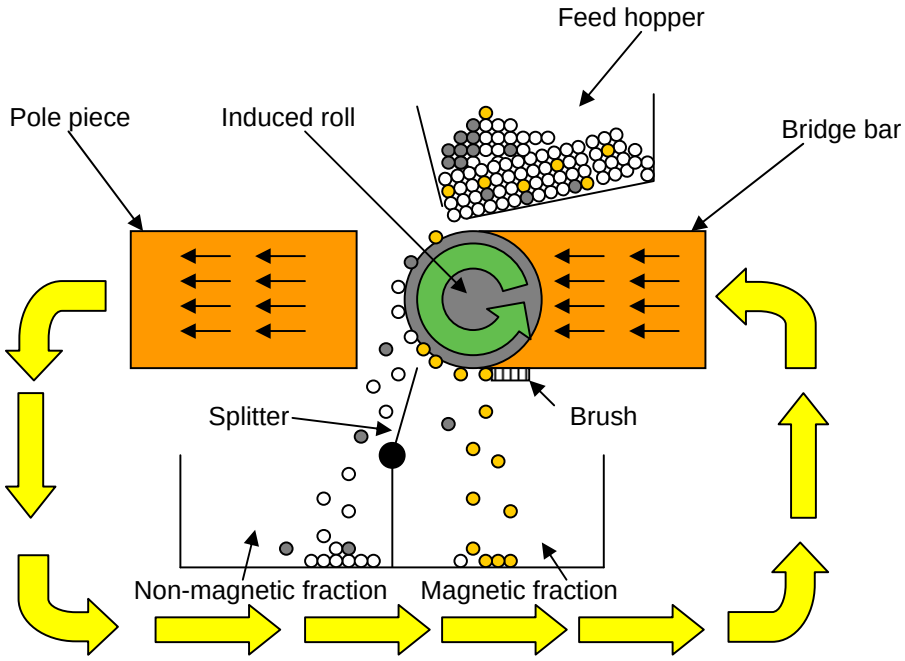

Fig. 3.4 Schematic of a high-intensity induced roll magnetic separator (Buckley 2008)

After crushing and screening suitably sized fractions of spent refractory brick were processed via induced roll magnetic separation. The test material was processed at successively higher magnetic field strengths (from 0.04 T to 1.6 T), with the magnetic fraction at each field strength retained and the non-magnetic material reprocessed. Any material still reporting to the non-magnetic fraction at maximum field strength was classified as "non-magnetic" for analysis. This technique where material undergoes multiple passes through a separator is known as "magnetic profiling."

3.5.1.2 Disc Separation

The laboratory scale disc separator (also known as an ore-grade separator) is widely used to ensure an accurate separation of materials that have varied magnetic susceptibilities. A thin layer of material is continuously transported beneath the rotating disc where magnetic particles are attracted upwards to the high gradient magnetic zones on the disc. The rotating discs then carry these captured particles to the discharge chutes where they are released. Scrapers mounted on chutes ensure the total discharge of magnetic particles.

The field strength can be adjusted so that successive passes of material allow magnetic fractions to be produced from 0.1 T to 1.2 T. Figure 3.5 shows a schematic of the disc separator and the fractions generated. Figure 3.6 is a photograph of the disc separator (Master Magnets, Redditch) in use. The test material is fed (via a vibratory feeder) as a monolayer onto the

moving belt of the separator. This belt passes underneath the magnetic disc which is rotating. Magnetic particles are attracted to the disc and are thus lifted out of the moving stream. Non-magnetic particles continue unimpeded along the conveyer and are discharged from the end of the belt. The field strength is controlled via adjusting the current and the gap between the disc and the belt. The relationship between field strength (magnetic flux density), belt-disc gap and current is shown in figure 3.7.

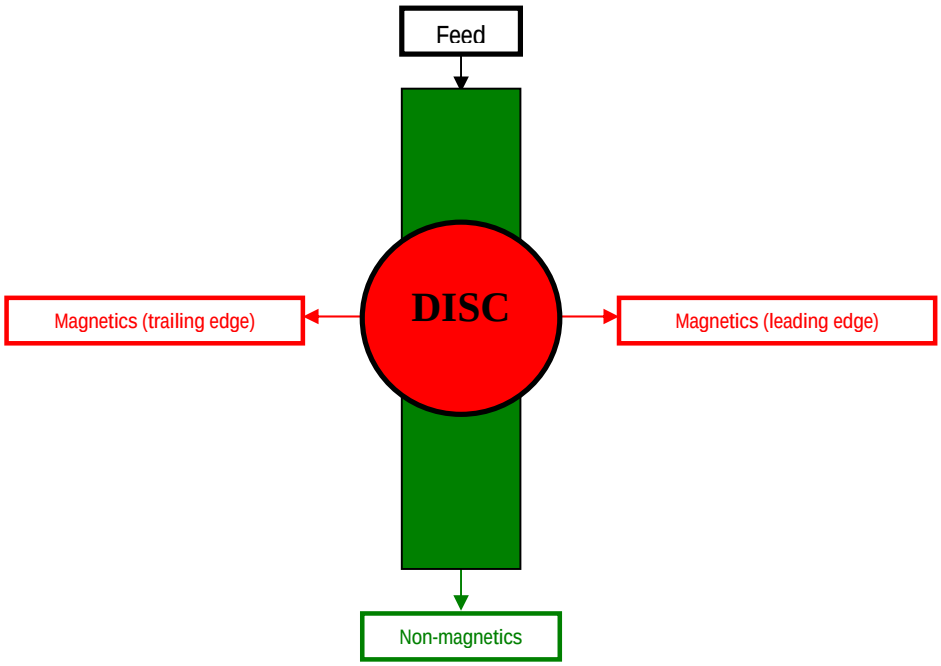

Fig. 3.5 Schematic of a disc separator and the fractions generated during magnetic separation. The leading edge and trailing edge magnetics are usually combined for analysis (diagram courtesy of Iain Wells, 2009)

Fig. 3.6 – The disc separator at Master Magnets, Redditch, with feed hopper visible on the right. The green belt that carries the material beneath the rotating disc is also visible.

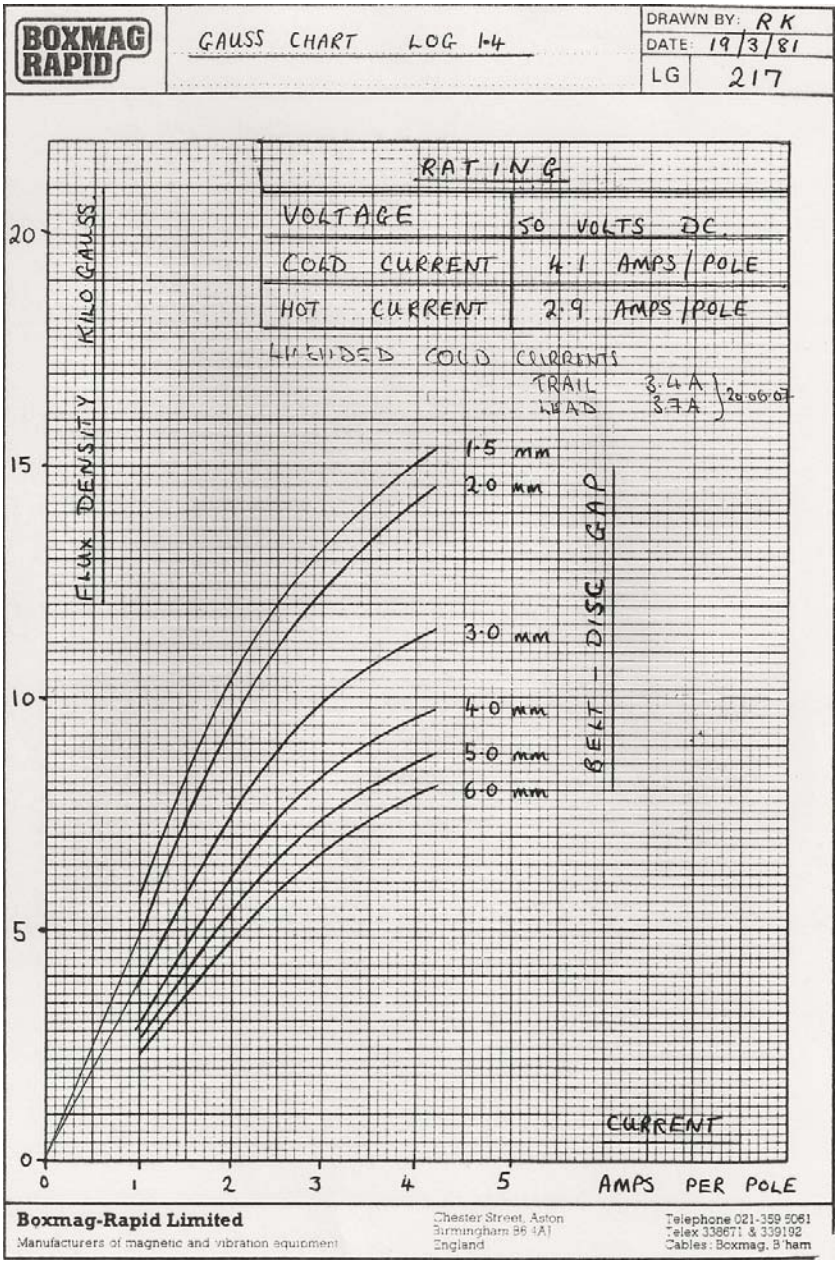

Fig 3.7 Calibration chart for the laboratory disc separator, showing the relationship between current, belt-disc gap and field strength (diagram courtesy of Iain Wells, 2009)

Samples of crushed and sized refractory brick were processed via the disc separator. The test material was processed at successively higher magnetic field strengths, with the magnetic

fraction at each field strength retained and the non-magnetic material reprocessed. Any material still reporting to the non-magnetic fraction at maximum field strength was classified as "non-magnetic" for analysis.

A laboratory scale machine was used for characterisation of the test materials but the technology is scalable (a number of units are used industrially in several applications). This type of magnetic separator is more suitable for profiling than others (e.g. the induced roll separator) as it lifts particles in order to separate them and so less non-magnetic particles become entrained in the magnetic fraction. Separations were performed from 0.1 T to 1.0 T at 0.1 T increments, producing 10 magnetic and one non-magnetic fractions for analysis (the two magnetic fractions generated from the leading and trailing edge of the disc were combined to create a single magnetic fraction for analysis on each run). The disc separator was used on refractory brick samples of 2 mm and smaller.

3.5.1.3 Pilot Scale Magnetic Drums

Due to the industrial nature of this project some samples were generated that exceeded the size limits for laboratory scale equipment. The induced roll and disc magnetic separators were unsuitable for material above 2000 µm and so larger scale, commercial magnetic drums were used for magnetic profiling of larger size fractions (2000 to 16000 µm). These drums operate in a similar manner to the induced roll separator as magnetic particles (for a given field strength) are attracted to the drum and are collected separately from non-magnetic particles. However,

the induced roll separator uses an electromagnet and so field strength (T) is varied by altering current (A), whereas commercial drums often use permanent magnets and so the field strength is fixed. Permanent magnet drums are normally preferred industrially due to their lower energy requirements. The disadvantage is the lack of flexibility they offer.

In order to conduct magnetic profiling on the coarser material four magnetic drums of increasing field strength were used sequentially in order to generate five fractions for analysis. The four magnetic drums and associated field strengths are listed below (all supplied by Eriez Magnetics, Caerphilly, UK):

- Ferrite Drum (FD) = approx 0.1T
- Standard RE* Drum (RED) = approx 0.4T
- RS Special drum (RSD) = approx 0.6T
- RE* Roll (RER) = approx 1.0T

*RE = Rare earth – a type of permanent magnet capable of generating high field strengths. **Rare-earth magnets** are strong permanent magnets made from alloys of rare earth elements. They are the strongest type of permanent magnets made, producing significantly stronger magnetic fields than other types such as ferrite magnets.

Any material that was not separated by the 1.0T rare earth roll was classified as “non-magnetic” for analysis.

These drums were large enough to be suitable for pilot scale trials (hundreds of kilograms per day), thus 5 to 10 kgs of material were employed for each test in order to get an accurate indication of separation efficiency while still allowing analysis of complete (and therefore representative) samples. Figure 3.8 is a photograph of the ferrite drum, however all drums were similar in appearance, with a vibratory feed hopper, a rotating drum and a “splitter plate” (divider) to ensure the non-magnetic particle stream is kept separate from the magnetic stream.

Fig. 3.8 The barium ferrite magnetic drum separator at Eriez Magnetics

3.5.2 Wet High Intensity Magnetic Separation

This type of separator passes the test material (in suspension) through a ferromagnetic matrix that allows a very high magnetic gradient to be achieved. Non-magnetic particles pass through the matrix and are collected below it. The matrix is then washed through to dislodge any entrained particles with the field turned on. The current is switched off and the magnetic particles are liberated and collected below. Once again the matrix is washed through to remove any entrained material (Kelly and Spottiswood, 1982). Both dry and wet magnetic separations are processes which are most effective on particles with a narrow size distribution (Wills, 2008). Figure 3.9 is a schematic of a wet high-intensity magnetic separator.

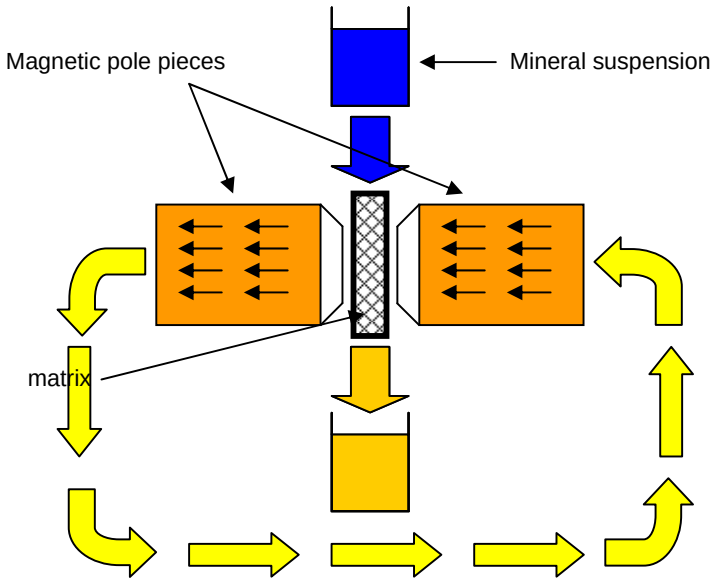

Fig. 3.9 Schematic of a wet high-intensity magnetic separator (Buckley, 2008)

After crushing and screening sized fractions of test material were made into suspensions with water (25% w/v), with an appropriate surfactant (Calgon powder; sodium hexametaphosphate, 0.1% by mass) used to reduce the surface tension and facilitate thorough mixing. These suspensions were passed through the separator. The test material was processed at successively higher magnetic field strengths, with the magnetic fraction at each field strength retained and the non-magnetic material reprocessed. Any material still reporting to the non-magnetic fraction at maximum field strength was classified as "non-magnetic" for analysis. All fractions were then filtered (10cm Buchner funnel fitted with Whatman grade 3 filter discs) and dried at 60 ˚C for 4 hours before being sent for analysis. The suspension formulation and drying protocols were developed specifically for this research as these conditions gave a suspension that did not block the matrix of the separator and produced dry granular powders for analysis.

3.6 Eddy Current Separation

Eddy current separation is a technique used for segregating metallic particles from non-metallic ones. It is most effective in the particle size range 1-10 mm, but efficiency can vary dependent on the density and shape of the feed material (Paul Fears, managing director of Eriez Europe, personal communication, 2008). The principle is that an electrical charge is induced into a conductor by changes in the magnetic flux cutting through it. Such changes in magnetic flux can be achieved by moving permanent magnets past a conductor. The effect of these currents is to induce a secondary magnetic field around the particle. This field reacts with the magnetic field of the rotor, resulting in a combined driving and repelling force which literally ejects the

conducting particle from the product stream (Star Trace, 2011 www.magneticseparator.in/eddy_current_separator.php).

In the Eriez Eddy Current Separators, a high speed concentrically mounted magnetic rotor is fitted within a non-metallic drum which travels much more slowly than the rotor so as to produce flux variations at the surface of the drum. As the conducting particles (any metallic objects) are carried by the conveyor over the drum, the magnetic field passing through the particles induces currents into them. Since these particles are of random shapes, it is difficult for the induced current to flow within them in an orderly manner and the currents therefore tend to swirl around within the particles; hence Eddy Current (Paul Fears, managing director of Eriez Europe, personal communication, 2008).

Figure 3.10 is a schematic of a typical eddy current separator. The red and green blocks illustrate the arrangement of magnets used to construct the rotor, with alternating north and south poles forming a ring. Although it is typical to run the rotor in the same direction as the drum and conveyor, the author has found that reversing the direction of the rotor for smaller particles enhances the separation achieved.

During the pilot study samples of five size fractions (from >850 µm to >9500 µm) were processed using an eddy current separator (Eriez Magnetics “SR 2010” Model ECS) in order to

examine PGM recovery in the resulting, magnetic, metallic and non-metallic fractions. Belt speed varied from 30 to 70 m/min and rotor speed varied from 1500 to 3500 rpm. The rotor was operated in both the forward and backward directions dependent on the size fraction being separated. The "SR 2010" separator had 8 magnets around the rotor. These were 6.5cm wide with a 1 cm gap between them. They produced a field strength of 1.6 T on the surface of the belt.

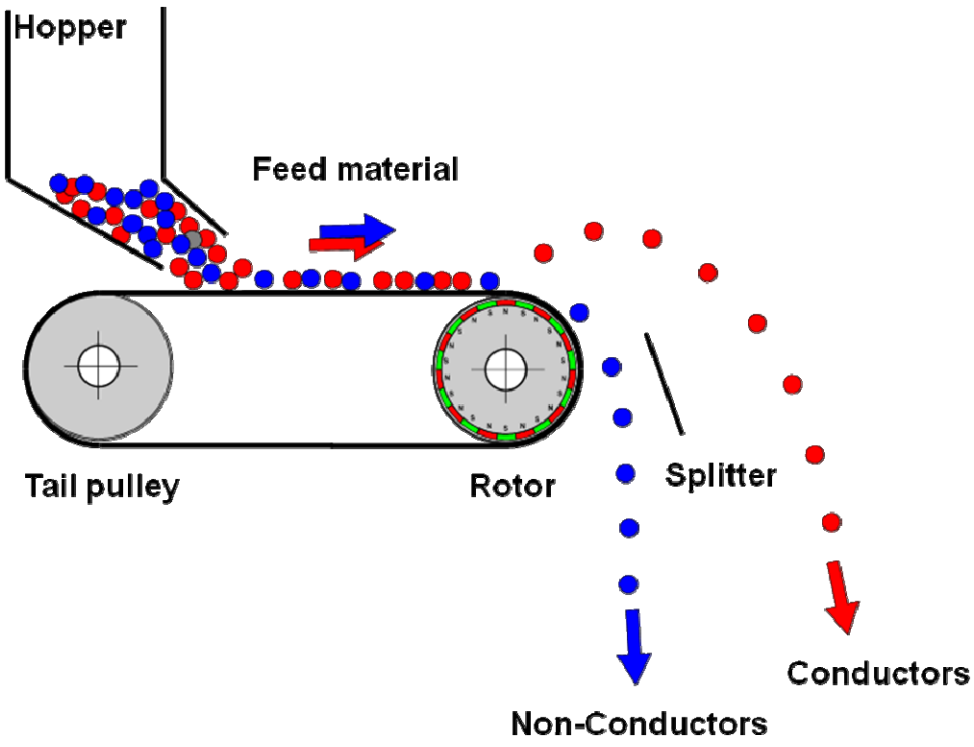

Fig. 3.10 Schematic of a typical belted eddy current separator

3.7 Electrostatic Separation

Electrostatic separation is the separation of particles that differ in electrical conductivity (Wills 2008). It utilises the force of an electric field, co-acting with another force (e.g. gravity) to produce differential movement of mineral grains (Taggart, 1954). The electrostatic forces are generated by the action of an electric field on a charged particle. In general the material is either a mixture of particles in which the various components are chemically pure, or a mixture of particles in which some of the particles contain several elements to be separated (Inculet, 1984). In the second case the material must be comminuted to a sufficiently small size such that the particles in the mixture become practically pure for a successful physical separation process. Should the comminution process fail to produce particles of an acceptable chemical purity, any electrostatic separation process becomes ineffective (Inculet, 1984).

In any electrostatic mineral separation process, the separation forces results from the interaction of electric fields with the electric charges which are more or less bound to the particles to be separated (Inculet, 1984). Regardless of the material the particle is made of, the electrostatic separation force is given by the formula:

$$F = E\,q \qquad (1)$$

where F is the force on the particle, E is the electric field intensity at the particle, and q is the charge of the particle -which is assumed to be a point charge. If a number of point charges q_n

are to be considered that each contribute to the field intensity then the net force imposed on the total charge *Q* is the vectoral sum of all the forces given by

$$F = E\,Q \qquad (2)$$

In a high tension separator the feed material is carried by the grounded rotor into the field of a charged ionising electrode. The feed particles accept a charge by ion bombardment. The conductor particles lose their charge to the grounded rotor and are thrown from the surface by centrifugal force. They then come under the influence of the non-ionising electrode and are further attracted from the rotor surface. The non-conductor particles are unable to dissipate their charge rapidly to the rotor and so are held to the surface by their own image forces. As the rotor carries the non-conductor particles on its surface, their charge is slowly lost and they drop from the rotor, middlings particles losing their charge faster and dropping first. The residual non-conductors are removed from the rotor by a brush (Kelly and Spottiswood, 1982). Figure 3.11 is a schematic of the principle of a high tension separator.

To cater for an extensive range of materials, all the parameters of separation can be readily adjusted during operation. These variables include the roll speed, the position of the electrode wire, variation of the DC voltage, the splitter plate position and the feed rate (Wills, 2008).

In theory high tension separators operate on feeds containing particles of between 75 and 500 µm in diameter (Pryor, 1965), however in practice separation is often problematic below 150 µm due to dust issues. This type of separation works best with a narrow size range of feed particles as particle size influences separation behaviour.

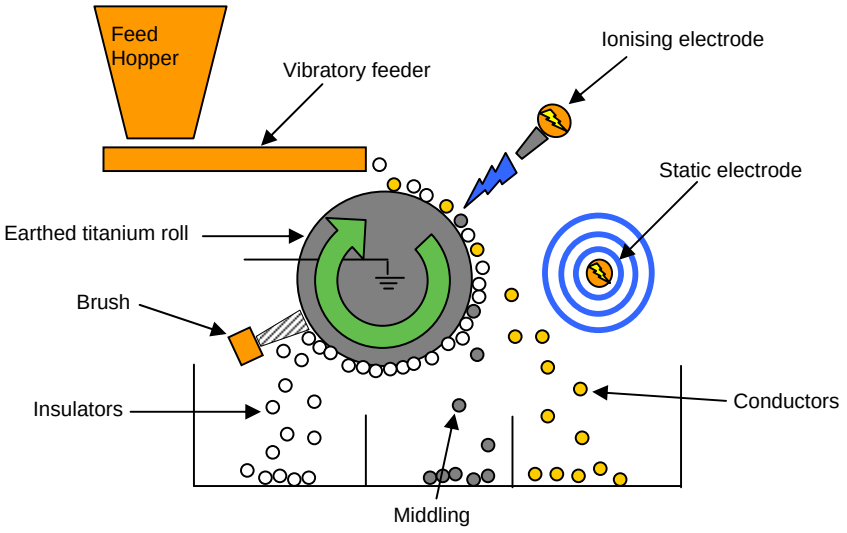

Fig. 3.11 Schematic of a high tension electrostatic separator (Buckley, 2008).

Electrostatic separations of spent refractory brick (maximum particle diameter 2000 µm) were completed on a HT model electrostatic separator manufactured by Boxmag Rapid Ltd. Representative samples were fed into the separator at a constant rate to allow the formation of a monolayer. The position of the ionising electrode remained fixed throughout the experiment as did the applied charge (20keV) and the speed of the roll (53 rpm). The samples are collected in trays underneath the separator with any highly charged "pinned" non-conducting particles

being removed by a brush. Due to analytical constraints the sample dividers were set so that only conducting and non-conducting fractions were produced i.e. there was no middling fraction. This reduced the overall efficiency of the separations but allowed a larger number of exploratory tests to be carried out.

3.8 Specific Gravity Separation

3.8.1 Pneumatic Concentration using an Air Table

Pneumatic concentrators are those in which a gas, usually air, is used to effect differential movement of particles of different specific gravities. They are used to separate dry, granular, free-flowing material according to particle density (Taggart, 1954). Although pneumatic devices have value in arid regions or where water cannot be tolerated in the feed, product or process, they suffer from two major impediments; a poor equal settling ratio and the difficulty and expense of dust containment (Aplan, 2003). Relatively few air flow jigs survive in the minerals industry today due to increasingly stringent dust control standards, but one device that is still in common use is the air table (also known as an air-float table).

An air table (figure 3.12) separates particles by a combination of the throwing action of a shaking deck and a continuous stream of air upward through holes in the deck. It comprises a trapezoidal riffled deck, forming the top of a shallow air box, tiltably mounted on inclined spring supports, reciprocated longitudinally by an eccentric motor and connected by an air pipe to a

blower located in the box support (Taggart, 1954). Air admitted below the porous deck fluidizes the particles and concentrate, middlings and tailings are produced. To achieve a good separation, close sizing of the feed is necessary. Feed sizing by √2 screens is common and sometimes even $^{4}\sqrt{2}$ sizing is employed (Aplan, 2003). Manufacturers' representatives state that the air table will make separations between minerals when the specific gravity difference is greater than or equal to 10% (Jarman, 1941). The denser material moves up the slope of the table and is discharged on the right hand side of the deck. The lighter (less dense) particles will be discharged on the left hand side of the table (figure 3.13).

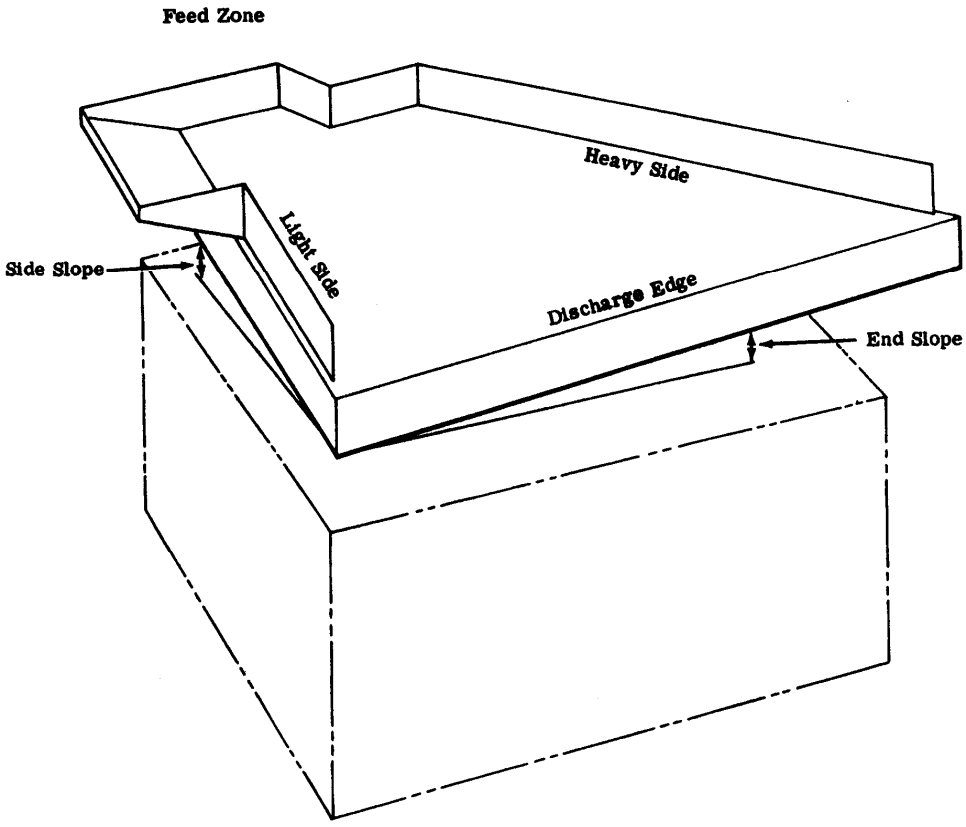

Fig. 3.12 Schematic of an air table (reproduced from http://www.mine-engineer.com/mining/minproc/air-table2.htm)

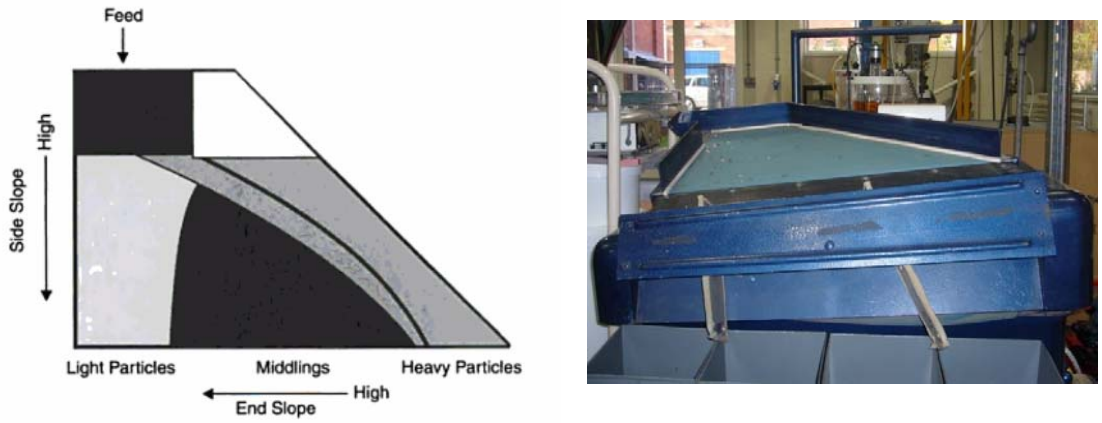

Fig. 3.13 (Left) Plan view of the deck of an air table showing the position of feed conveyor and the zones of the deck for light, middling and heavy particle discharge (reproduced from Aplan, 2003). (Right) a photo of the laboratory air table in use.

Unused refractory bricks from all three lining layers were used to produce test samples for the air table. These were crushed and then screened to the same range of particle sizes as the spent lining used in this study (maximum particle diameter 16000 µm). The 9.5 mm ≥ d > 5.6 mm size fraction was used for testing and the three brick types were recombined in a 1:1:1 ratio by mass. 1 kg of this mixed material was then passed across the air table at maximum inclination and maximum airflow and the resulting fractions photographed and visually examined for colour concentration of any of the brick types.

3.8.2 Vertical Vibration Separation

The vertical vibration separator or "vib sep" is an experimental device developed by the Granular Dynamics Group at the University of Nottingham. It works by using an acoustic signal to vibrate a cell and separate materials of different densities. It is often suitable on particle sizes too fine for other dry separation techniques.

It is well known that when granular materials are subjected to vibration segregation occurs. This phenomenon has been studied by a number of researchers but the mechanisms are not yet fully understood (Mohabuth and Miles, 2005). The most common segregation is size segregation, which is known as the "Brazil Nut Effect" (BNE), where the larger size particles appear on top of smaller ones when subjected to vibration (Mohabuth and Miles, 2005).

The experimental apparatus consisted of two acoustic speakers vertically mounted in a wooden framework, which was connected to a pair of accelerometers and an amplifier in order to control the vibration. The whole assembly is attached to a large concrete block to prevent horizontal motion during vibration. The experiments were carried out in a rectangular vessel or "cell" of thickness 10 mm, height 40mm and width 40 mm. The glass cell was fixed by screws to the bottom of the metal frame in between the two loud speakers and could be detached easily between experiments. The glass cell is shown in figure 3.14.

The experiments were conducted under atmospheric pressure with vibrational frequency ranging from 10 to 120 Hz and the dimensionless vibrational acceleration, Γ ($\Gamma = a\omega 2/g$, where a is the amplitude of the oscillation, g the acceleration due to gravity and $\omega = 2\pi f$, is the angular frequency) in the range 2–10.

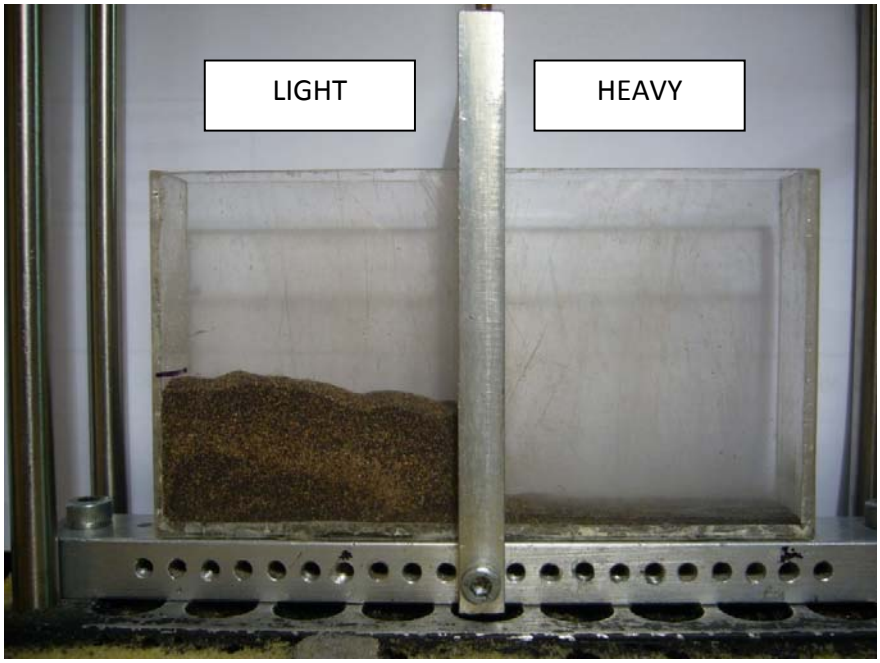

Fig. 3.14 The glass separation chamber of the vertical vibration separator (vib sep)

Samples of spent refractory lining ranging from 212 µm to 63 µm were evaluated for PGM segregation in the vib sep. For each size fraction the material to be separated was put into the left hand side of the cell which was then screwed into position. The frequency and gamma values were set and the machine was turned on and allowed to run until equilibrium was reached and the RHS of the cell was no longer filling. The dark (heavy) fraction was removed from the RHS of the cell and retained. The material remaining in the LHS was then run again in order to "polish" it. After this polishing run both sides of the cell were emptied and retained for analysis. The cell being used could only hold a small amount of material per run and so several runs were required in order to get the required 15 g of heavy fraction for analysis.

3.9 Sensor Based Sorting

Classical sorting machines (e.g. magnetic separators, eddy current separators etc.) are based on an interaction of a force field and specific attributes of the particle itself. There are sorting criteria which do not involve interaction with a force field e.g. colour, texture or shape; the only way to separate these from a mass flow is hand picking or sensor based sorting.

For successful sorting, every particle in the mass flow has to be considered. The feed must be in a monolayer with enough free space around the particles to allow classification, but not too much space as this will reduce throughput.

Optical sorting (one type of sensor based sorting) is already well established in the glass recycling industry. High resolution colour cameras can detect up to one million glass fragments per minute and sort them into colour classes. Optical sorting is also used to increase the value of seeds by removing contaminants such as small stones, sticks, mud balls and immature seeds.

Near infrared sorting allows material to be analysed and separated on the basis of composition rather than colour. An interesting use of NIR spectroscopy is in the food industry where it is used to grade fruit (e.g. apples and kiwi fruits). The amount of reflectance can be converted into a measure of how “juicy” a fruit is. Low quality fruit can then be removed from the mass flow without good quality fruit being mechanically examined and possibly damaged.

The equipment used for this research was a “Mikrosort” sorting control system based at Camborne School of Mines in Falmouth. The sorter was equipped with four different types of sensor to classify particles:

- High Resolution Colour Camera
- Monochromatic Camera
- Infrared Spectrometer
- Conductivity Sensor

Depending on the test material, different sensors / combinations of sensors can be selected. Rejection behaviour is material dependant – i.e. it is possible to remove materials with special value very reliably without causing excessive sorting of other low value materials. Figure 3.15 summarises the principles of sensor based sorting.

The Mikrosort was used to evaluate the amenability of refractory lining to concentration by sensor based sorting. Crushed and sized samples of unused refractory bricks were separated on the basis of both colour identification and infrared spectroscopy and samples of spent lining were separated on the basis of differences in conductivity. For all test work the conveyor speed was 3 m/s.

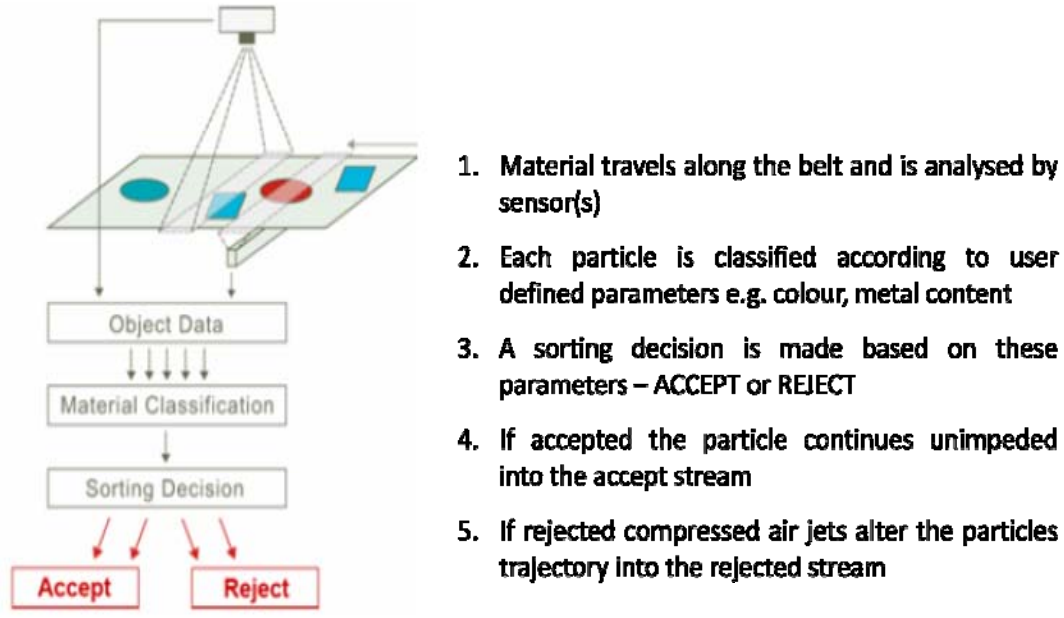

Fig. 3.15 Summary of the principles of sensor based sorting.

3.10 Leaching / Acid Extraction Using a MARS 5 Microwave Reactor

The microwave accelerated reaction system (MARS 5) is designed for digesting, dissolving and hydrolysing a wide variety of materials. The system uses microwave energy to heat samples in polar or ionic solutions rapidly and at elevated pressures. Its main purpose is for preparing samples for analysis by atomic absorption (AA), inductively coupled plasma emission spectroscopy (ICP), gas or liquid chromatography (CEM, 1999).

Each reaction vessel is made of Teflon and fits within a microwave-transparent sleeve made of Kevlar. Twelve 100 ml reaction vessels can be monitored simultaneously in the reactor. In

order to produce liquid leachates for biorecovery experiments milled spent refractory lining and crushed spent autocatalyst were leached in *aqua regia* (a mixture of concentrated HCl and HNO_3 in varying proportions) in a MARS 5. In order to assess PGM leaching efficiency the reaction time, temperature, liquid to solid ratio and concentration of *aqua regia* were all varied as per the individual experiment parameters.

For each sample the test substrate was placed in an open vessel, *aqua regia* was added and the vessel was stirred for one minute. The vessel was then left to stand uncovered in a fume hood for 30 minutes before being sealed and then microwaved (power, time and temperature depended on the specific experiment and each set of conditions is noted in chapter 5). Each vessel was left to cool to room temperature before the solid and liquid phases were separated by Buchner funnel and retained for analysis.

3.11 Electron Microscopy

A Philips XL-30 Environmental Scanning Electron Microscope (ESEM) (Philips, UK) fitted with an Inca 300 EDS analysis system (Oxford Instruments, UK) was used for characterisation of the solid PGM containing wastes.

A Jeol 7000F SEM (JEOL Ltd, UK) fitted with an Oxford Wave WDS analysis system was used for elemental mapping of PGMs on the surface of samples of spent autocatalyst, as EDS analysis lacked the necessary accuracy and resolution for these metals.

A Jeol 1200CX2 (JEOL Ltd, UK) Transmission Electron Microscope (TEM) was used for examining cut sections of biological samples. Metal-loaded bacteria were fixed in 2.5% (wt/vol) glutaraldehyde, stained in 1% osmium tetroxide in 0.1M phosphate buffer, pH 7.0 and embedded in epoxy resin.

A Jeol JXA-8500F field emission electron probe microanalyzer (EPMA) was used to identify and measure the concentration of PGMs within particles of spent refractory lining. Samples were set in resin and polished to a high shine in order to produce compositional X-ray maps for each particle.

3.12 Microbiology Methods

3.12.1 Growth of Organisms

Escherichia coli MC4100 cells were cultured in nutrient broth in 200 ml serum bottles under anaerobic conditions (Deplanche *et al.*, 2008). Cells were grown to the mid-logarithmic phase and harvested by centrifugation, washed three times in 20 mM MOPS-NaOH buffer pH 7.0 and resuspended in a known volume of buffer. The cell density was checked by measuring OD_{600} (optical density at 600 nm) which was then converted to bacterial dry weight by a previously determined calibration (an OD_{600} value of 1.0 ≡ 0.482 mg / ml cell dry weight for *E. coli* MC4100), (Lloyd *et al.*, 1998). With a dry weight of cells of between 20-30 mg/ml the cell suspensions were then split into aliquots in preparation for pre-metallisation.

3.12.2 Preparation of Pre-Metallised Cells and PGM Removal

The cells were resuspended in MOPS-NaOH buffer pH 7.0 and transferred anaerobically to 100 ml of 2 mM Na_2PtCl_6 or Na_2PdCl_4in 0.01 M HNO_3 (final suspension pH 2.2) and pre-equilibrated with N_2. The dry biomass to mass of Pd(II) or Pt(IV) ratio was 19:1 i.e. a 5% metal loading on the cells. The suspension was left for 1 hour at 30 ^oC to form nucleation sites on the biomass. The electron donor for bioreduction was H_2 (bubbled; 20 min). After complete of Pd(II) or Pt(IV) reduction the cells were removed by centrifugation. The pellet was washed with distilled water and acetone and dried in air. PGM removal from model solutions and wastes followed the same procedure using 19 parts dry weight of biomass, (fresh, pre-palladied or pre-platinised with 5% Pt loading) to 1 part of metal weight in test solution (2 mM of each PGM) or leachate.

3.12.3 Preparation of Metal Solutions

For initial investigation of Pd(II), Pt(IV) and Rh(III) bioaccumulation on fresh and pre-platinised biomass 2 mM solutions of Na_2PdCl_4, Na_2PtCl_6 and $RhCl_3$ (supplied by Aldrich Chemical Company) in 0.01 M HNO_3, pH 2.2 were used.

3.12.4 Preparation of Leachate from Waste

The spent refractory bricks (provided by Johnson Matthey and described in chapter 4) were processed by jaw crushing, ground using a roll crusher and sieved to ≤212µm. *Aqua regia* (30 ml; 3 parts 37 % HCl to 1 part 70 % HNO_3) was added to 6 g of milled refractory lining and allowed to

stand in an open vessel (30 min). The vessel was then sealed and placed in a microwave (CEM Microwave Accelerated Reaction System 5) set to ramp to 106 ˚C in one min using a power of 600W, maintain that temperature (15 min), then undergo a cooling cycle (5 min). The contents of the vessel were centrifuged (4000 rpm; 10 min) and the supernatant was retained for biomass metallisation tests. Commercial analysis of leachate gave 4.1 mM Pt, 6.6 mM Pd, 0.4 mM Ir, 2.2 mM Rh and 1.5 mM Ru). The leachate was diluted to 1% original concentration to bring the pH to a level suitable for bio-reduction (pH 1.6).

3.12.5 Spectrophotometric Assay of PGM

Removal of PGM from test solution was monitored by a spectrophotometric method using $SnCl_2$ (Charlot, 1978). The reagent solution contained 5.98 g of $SnCl_2$/100 ml in concentrated HCl. For PGM determination 200 µl of test sample was added to 800 µl $SnCl_2$ solution and A_{463} for Pd(II) and A_{401} for Pt(IV) was determined after one hour. It was not possible to estimate accurately the concentrations of metals in mixed metal solutions due to cross-interferences, but the assay was a convenient indicator of the presence of residual non-reduced metal in solution.

3.12.6 Transmission Electron Microscopy (TEM), Energy Dispersive X-ray Analysis (EDX) and X-ray Powder Diffraction Analysis (XRD)

Metal-loaded bacteria were fixed in 2.5% (wt/vol) glutaraldehyde, stained in 1% osmium tetroxide in 0.1M phosphate buffer, pH 7.0 and embedded in epoxy resin. Cut sections were viewed with a

JEOL 1200CX2 transmission electron microscope (TEM) (Yong *et al.*, 2002). Electron-opaque deposits were examined by energy-dispersive X-ray microanalysis (Yong *et al.*, 2002). The identity of the deposited material was checked by X-ray powder diffraction using dried ground samples.

3.12.7 Catalytic Activity Measurement

A Cr(VI) reduction test (Mabbett *et al.*, 2004) was used to evaluate the catalytic activity of the Bio-PGMs under oxygen free nitrogen. Bio-PGM was added to 10 ml of 0.5 mM Na_2CrO_4 in 20 mM MOPS-NaOH buffer at pH 7.0 (1 mg PGM to 10 ml of Cr(VI) solution). The bottle was then sealed and degassed under vacuum, sparged with oxygen free nitrogen and placed onto a rotary shaker (180 rpm; 10 min) to ensure mixing and distribution of catalyst. The reaction was initiated by addition of sodium formate (electron donor; final concentration 25 mM). Samples were withdrawn and centrifuged (13000 rpm, 3 min). The supernatant was analysed for residual Cr(VI) using diphenylcarbazide (Mabbett *et al.*, 2004). The catalytic activity was expressed as the percentage of Cr(VI) reduced. Commercial palladium catalyst (5%Pd/C) was used as a control.

4. Processing and Concentration of Spent Furnace Refractory Lining

4.1 Glossary of terms used by JM for Refractory Linings

- **Barrel**: The cylindrical area along the axis of a reverberatory (rev) furnace
- **Brick:** A general term used to describe any preformed refractory shape used in the rev furnaces
- **Brick, bricking, rebricking**: The action of installing the refractory bricks into the furnace
- **Cement**: Various jointing materials for the safety linings and the working linings
- **Concrete:** A general term used by the bricklayers for castable products that are used for filling in gaps or casting specific shapes from wood or steel formers e.g. slip rings for arc furnace electrodes
- **Debrick, debricking , wrecking**: The removal of a used brick lining
- **Dome end:** The 2 dished ends of the furnace (front and rear); a “dome end” can refer to the set of bricks of particular specification required to brick this part of the furnace
- **Drop out box (tower):** the partially brick lined steel tower at the rear of the slice, connecting the furnace to the main extraction ducting
- **Lip, launder:** The spout or pouring chute down which molten products flow into a pot, mould etc.
- **Magchrome**: General designation of refractories made from chromium oxide and magnesium oxide and suitable for use in the non-ferrous sector

- **Number of Melts:** The number of completed Rev charges in any one barrel or dome end lining
- **Slice:** The removable exhaust section at the rear of the furnace, attached to the drop out box tower and housing the burner block
- **Spalling**: Falling off of face of brick due to differential thermal expansion
- **Taphole, tapping port:** The opening in the furnace body through which molten materials are removed from the furnace

4.2 Definition of a Furnace

A furnace is an apparatus for conducting reactions at high temperature. These elevated temperatures are necessary for the processing of non-ferrous scrap and a number of technologies are applied at different scales of operation. Furnace designs are influenced by different operating parameters such as heat input, melt rate, mixing and temperature uniformity (Rao, 2006).

4.3 The Rotary Reverberatory Furnace

A rotary reverberatory furnace ("rev") is a metallurgical furnace used for smelting or refining, in which the fuel is not in direct contact with the material being processed (known as the "charge"), but heats it via a flame blown over it from another chamber. It consists of a horizontal, refractory-lined cylinder, which is rotated during processing. The energy is supplied by an air-fuel flame entering at one end and the exhaust gases leave through a duct at the opposite end of the furnace. The large volume of the flame leads to contact between

the flame and the charge and to mass transfer between the flame flue gases and the charge (Rao, 2006).

Rev furnaces are less energy efficient than blast furnaces (in which fuel and material are mixed in a single chamber) but are suited to specialist applications where contact with the products of combustion may add undesirable elements to the material being processed. Control of the fuel / air balance can alter the exhaust gas chemistry toward either an oxidising or a reducing mixture, and thus alter the chemistry of the material being processed. Johnson Matthey utilise this oxidising and reducing (converting) capability regularly during furnace operation.

4.4 Refractory Materials

Refractories are chemical compounds that are used as structural materials forming insulation linings in high temperature and corrosive environments in many industrial processes (Velez, 2000).

The American Society for Testing and Materials (ASTM) defines refractories as non-metallic materials having chemical and physical properties that make them applicable as components of systems that are exposed to environments above 1,000 °F (538 °C). They are used in linings for furnaces, kilns, incinerators and reactors and are also used to make crucibles.

Refractory materials are used to line smelting furnaces. The most usual lining configuration in North America is a thin layer of insulation castable protected from the liquid metal by a monolithic material with non-wetting additives. European practice is to use fired blocks and bricks. These bricks are often easier to bring into service and form a more durable lining (allowing repair of individual brick sections over the operational lifetime of a lining). They can be manufactured within very tight dimensional tolerances giving 1-2 mm average joint thickness (Rao, 2006).

Refractories can be classified on the basis of chemical composition as neutral, acidic or basic. Neutral refractories are used in areas where slags can be either acidic or basic and are chemically stable to both acids and bases. The main raw materials belong to, but are not confined to, the R_2O_3 group; common examples of these materials are alumina (Al_2O_3) and chromia (Cr_2O_3). Neutral refractories are often used when scrap is being refined as it is an extremely variable feedstock and linings must withstand a wide range of conditions (Johnson Matthey, 2009).

4.5 Processing Precious Metal-Containing Wastes

There are two important PGM recyclers in Europe; Johnson Matthey in the UK and Umicore in Belgium. Recycling and refining precious metals involves complex pyrometallurgical and hydrometallurgical processes. The specific flow sheet varies between producers; however the core process is generally to collect the precious metals in base metal bullion (Saurat, 2006). This base metal collection technique is known as “secondary smelting” (as the term

primary smelting is reserved for newly mined ores) (Rao, 2006). Possible collector metals include lead, copper, silver, iron and nickel (Johnson Matthey, 2009).

4.5.1 Smelting

The term "smelting" is used for a variety of processes to mean melting of an ore or a concentrate. In this chapter it is used to describe processes where the furnace charge (consisting of the secondary materials instead of ore) is melted for precious metal recovery.

Precious metal bearing scraps are mechanically reduced (usually by crushing or shredding) to forms suitable for handling, sampling and minimisation of loss. The sized metal is then mixed with fluxes and smelted in the presence of the collector metal. The function of the fluxes are to facilitate the melting process by combining with and neutralising the gangue (e.g. autocatalyst monolith supports, casing materials etc.) and products of decomposition, making a product that is fusible and easy to handle and separate from the metal at the furnace operating temperature (Rao, 2006). After melting the flux forms a slag that floats on top of the molten metal and can be "poured-off" easily when the furnace is tapped. The output of the smelter thus consists of a slag phase and bullion of impure collector metal containing the PGMs.

4.6 The Johnson Matthey UK Precious Metal Refinery (Enfield)

The Johnson Matthey precious metal refinery in Enfield operates a number of rotary reverberatory furnaces ("revs"), coreless induction furnaces and a DC arc furnace. The three

rev furnaces are used for the secondary smelting of precious metal containing scrap. The metal concentrate produced is fed into the induction furnace circuit and finally into the arc furnace in order to progressively increase the purity prior to hydrometallurgical separation of the individual precious metal components.

This study focuses on the rev furnaces as they deal with large quantities of chemically diverse material, operate under a wide range of conditions and generate large quantities of spent lining for reprocessing.

The collector metals used by JM in the revs are silver and copper, known as silver with assisted copper. Both are fed into each charge simultaneously as different PGMs have solubility in (and therefore affinity for) different collector metals. As the scrap invariably contains a lot of iron (from component casings etc.) this effectively produces an environment with three different collector metals, one being magnetic and two being non-magnetic

4.6.1 Types of Scrap Processed

Precious metal refineries cater to a large number of customers with a wide variety of waste streams and so in theory almost anything that contains PGM could potentially enter the rev furnaces. However JM have several large long term contracts for PGM recovery and so typical types of scrap present are as follows:

- Spent industrial catalysts (both from their own catalysis division and external customers)
- Autocatalysts
- Sludges and residues from gold plating
- Early printed circuit boards (PCBs)
- PGM coated wires (e.g. gold and platinum plated wires)
- Aircraft parts
- Scrap jewellery
- Medical waste (dental scrap, angioplasty guide wires, electrophysiology catheters etc.)
- Platinum thermocouple wire

4.6.2 The Challenges of Recycling Precious Metals from Scrap

The recovery and recycling of precious metals is challenging for a number of reasons:

1) In relative terms only a very small percentage of waste and scrap is precious metal. The majority is composed of base metals, plastics, ceramics etc. When primary ores are smelted they have usually been upgraded by flotation or magnetic separation and so are pre-enriched before entering the smelter.

2) The mixed nature of precious metals in these products can be problematic; a single metal is seldom present. Again ore bodies usually only have one or two precious elements present and so separation is more straightforward.

3) The wide variety of chemical and physical properties of the PGM bearing scrap, ranging from metallic to non-metallic and from solids to solutions, can cause complications for refiners (Rao, 2006). In addition the type of fluxes used in the smelting process has an effect on the life of the furnace lining.

4) The high value of the precious metals combined with their dilute and mixed nature requires extensive and accurate assay techniques, leading to additional costs and processing times (Rao, 2006).

4.6.3 Type and Number of Linings Used per Reverberatory Furnace

Smelting and converting reactions are carried out in the revs at temperatures of 1300-1350°C for normal melts and up to 1600°C for oxidation / converter reactions. The mild steel shell of the furnaces must be protected by a lining of suitable refractory material that can withstand temperatures up to 1700°C.

A variety of refractory bricks, cements and castables are used as lining materials. These furnaces follow the European refractory trend and use preformed, fired bricks for the majority of the components. The lining usually consists of a “working” or “hot face” lining and a number of “backing” or “safety” linings. Currently two safety linings are installed in the barrel area of the furnaces as additional safety precaution during converting reactions. Hence there are a total of three linings in the cylindrical section of the furnace that has maximum contact with molten metal and a minimum of two linings in other areas.

4.6.3.1 Selection of Brick Grades

The selection of refractory brick grade is determined by the chemical composition of the slag produced in a smelting process, the nature of the metal i.e. bullion in the process and the operating temperature range. Alumina ($Al_2O_{3)}$, magnesia (MgO) and chromium (III) oxide (Cr_2O_3) are all refractory solids with melting points in the range 2000 to 2800 ˚C. As refractory bricks are slightly porous the molten smelting products will enter the pores in the brickwork.

In the slag system used at JM Enfield the iron oxide and silica present will attack any MgO. This chemical attack will lead to crack formation in the refractory behind the hot or working face. The chemical reaction also leads to spalling caused by differential thermal expansion. This reaction is accelerated above 1300 ˚C.

Addition of Cr_2O_3 to the refractory mix is a very effective way of protecting the MgO and therefore extending the operational life of the lining. However the high chromium oxide content of these materials has always been an issue as JM recycles all used refractory in order to recover the PGM content. The three specific linings used are as follows:

4.6.3.1.1 Hot face Lining – "Radex FG" Magchrome Brick

The hot face lining is "Radex FG" manufactured by RHI Refractories, Austria. It is used for bricking the front dome end, the barrel and the rear dome end i.e. anywhere there will be regular contact with molten metal.

Radex FG is the trade name for a family of magnesia chrome "magchrome" bricks. It is supplied as both sintered and fused grain grades containing 19.5% to 23% Cr_2O_3 and is more expensive than any other refractory material used in the revs. Grades based on fused grain are more expensive than sintered grain as the fused grain material has to be produced at very high temperatures in an arc furnace as part of the manufacturing process. The fused grain material is called "Radex FG Compact" and is reserved for the barrel bricks where wear rate is the greatest. The other major constituent of the magchrome bricks is MgO at around 60%. The hot face lining is brown in colour and wears from approximately 300 mm in width to 50 mm in width during the 100 cycle life of the refractory.

4.6.3.1.2 Intermediate Safety Lining – "Resistal RA13" Magchrome Brick

The intermediate safety lining is "Resistal RA13" made by RHI Refractories, Austria. It is supplied in a wide variety of shapes and thicknesses and is used for creating a backing lining behind high wear areas of the hot face lining. These are also sintered grain magchrome bricks but have a lower density and a lower cost than the hot face magchrome bricks. The intermediate safety layer directly behind this is purple and is approximately 50 mm in thickness.

4.6.3.1.3 Outer (Fail Safe) Safety Layer – Alumina firebrick

The outer safety lining is a 42% alumina (Al_2O_3) firebrick. It is low cost and has no specific manufacturer. It is known as a "fail safe" lining as it should never be exposed during normal operation of the furnace and is only there to protect the mild steel shell if something goes

wrong during a melt. It is pale yellow / white in colour so that it is highly visible. A visual inspection is carried out after each heating and cooling cycle and if any light coloured brick is showing then the furnace is immediately taken offline for wrecking and rebricking. The outer safety layer sits behind the intermediate layer and is also approximately 50 mm in thickness.

4.6.3.2 Summary of JM Refractory Brick Use in Rev Furnaces

Table 4.1 summarises the type of brick used to line each furnace, along with the density and the percentage of the lining they comprise. The outer safety layer has a lower density and significantly different colour to both the intermediate safety and the hot face layers. Around 80% of the total mass is hot face lining, which is similar in colour to the intermediate safety lining. 12% of the mass is lighter coloured, lower density outer safety layer and cement. Figure 4.1 is a bricking diagram for the rev furnaces used by JM showing the dimensions and positions of each brick type.

Table 4.1 A summary of the proportions of each type of brick in the furnace along with the colour and density before use.

Type of Lining	Brick Grade	% of Total Mass	Colour	Density (g/cm^3)
Hot Face	Radex FG	80.0	Dark Brown	3.35
Intermediate Safety	Resistal RA-13	8.0	Purple	3.12
Outer safety	42% Alumina	7.1	Yellow / White	2.25
Cement	Radexplast AO	4.9	Yellow / White	2.00

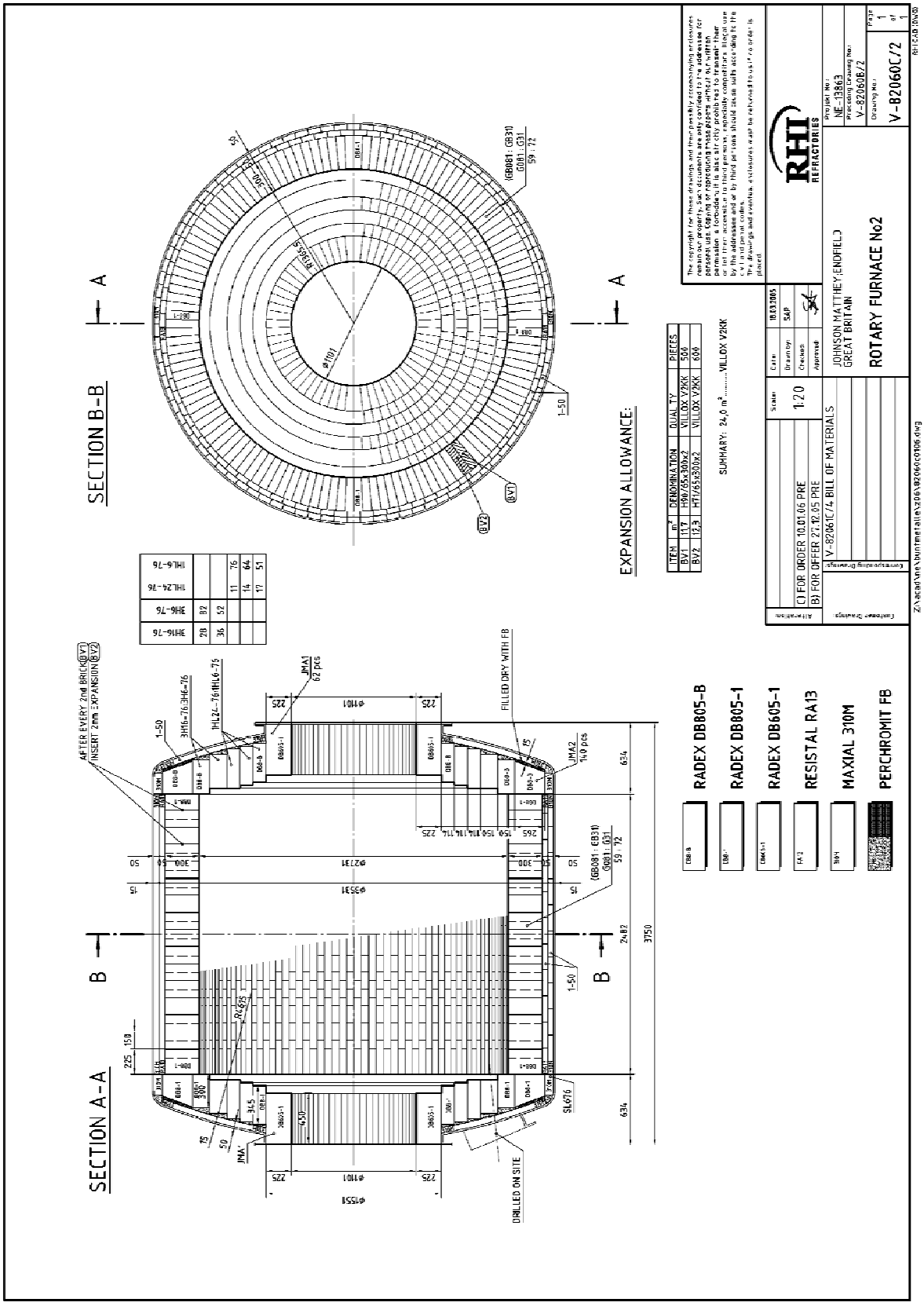

Fig. 4.1 A bricking diagram for the JM rev furnaces, showing brick type and position.

4.6.4 The Reason Spent Lining is a Problem for JM

As refractory bricks are slightly porous the molten smelting products will enter the pores in the brickwork. This occurs during each melting and cooling cycle and so the lining absorbs precious metals throughout its operational life. JM must recover this "lost" metal and so all the spent lining must be reprocessed.

Each lining has an operational life of 5-6 months depending on the specific types of scrap processed and the number of melts conducted, but the average is approximately 100 melt cycles per lining. After this time, (or earlier if the fail safe lining is visible) it has to be removed and replaced. JM operate three revs and each one requires between 30 and 40 tonnes of brick per re-lining and so around 200 tonnes of spent lining are produced per annum.

Wrecking and relining of the furnaces is still done manually and skilled crews are employed specifically for this task. Once removed the entire lining is roughly jaw crushed into pieces of 10 x 10 x 10 cm or smaller and is then stored until there is spare capacity in the arc furnace circuit to reprocess it and recover the PGMs. The arc furnaces operate at higher temperatures, suitable for processing the refractory lining. This reprocessing is further complicated by the fact that a furnace charge should not exceed 10% chromium and so it takes a long time to reprocess an entire 40 tonne lining and recover the precious metal value. When spent brick forms part of an arc furnace charge the resultant slag needs a second pass through the arc furnace before it is "clean enough" (i.e. <2 ppm PGM content)

to be released from site. Thus during peak times it can take almost six months to reprocess an entire lining and the additional arc furnace slag generated.

Each batch of brick varies considerably and its composition will depend on what material has been smelted, the number of oxidations carried out and the residual weight of the spent refractory. In addition the Ir and Ru content will be altered depending on the success rate at removing these physically from the furnace on wrecking as "ball-up metallics." These are high concentration pebbles of insoluble PGM that have dropped out of solution with copper and deposited in the base of the furnace and where possible they are recovered and immediately fast tracked into the arc furnace circuit.

In addition in every October JM Enfield closes to customers in order to conduct an annual stock take. All PGM in the refinery must be inventoried and all three rev furnace linings are removed, crushed and assayed, regardless of wear level. As a result of these annual assays there is a historical record of average lining PGM concentrations. JM state that the 200 tonnes of spent lining generated every year contains £23 to £50 million of precious metal (PGMs, gold and silver), before taking into consideration the additional value of base metals.

JM are a "toll" refiner i.e. they charge a fee for processing waste and recovering the metals. The amount paid back to the customer is based upon assaying the waste as it enters the plant, not on smelter output (as this will be the combined concentrate from a number of customers scrap) and so they are effectively losing revenue while metal is trapped in the

spent lining as they cannot sell it or earn interest on the value, despite having already paid the customer.

In the past JM minimised these losses by employing people to manually sort through the lining and separate out the heavily impregnated brick by eye so it could be fast tracked and the metal recovered but this is no longer economic with rising labour costs.

JM therefore approached the University of Birmingham to collaborate in a feasibility study to investigate whether a “fast track” concentrate could be produced using mechanised processes in order to recover the majority of the metal rapidly while avoiding overloading the smelters with chromium from large tonnages of brick.

4.7 Initial Feasibility Study on Spent Refractory Lining

None of the information in section 4.6 (brick grades, densities, tonnages, collector metals etc.) was available at the time of the pilot work, which was a short feasibility study in order to provide basic proof of principle i.e. whether any PGM concentration was possible. The precious metals of interest to JM were Pd, Pt, Rh, Ru and Ag. Within the context of this thesis the purpose of the feasibility study was to evaluate the efficacy of various PGM enrichment methods with a sample of high PGM content before embarking on a more complex waste with PGMs at ppm / ppb levels.

4.7.1 Spent Refractory Lining Sample 1 – Milled Brick

A 25 kg sample of lining was provided that had been ball milled until 100% passed a 12 mesh sieve i.e. had a particle size of d ≤ 1.4mm. An assay of the initial precious metal content was also supplied, however nothing was revealed about the sampling procedure and brick composition prior to ball milling. Table 4.2 lists the concentrations of key elements from the supplied assay.

Table 4.2 The concentrations (in %) of key elements in refractory lining sample 1. Data supplied by Johnson Matthey.

Element	Concentration (%)
Pd	0.248
Pt	0.254
Rh	0.166
Ru	1.055
Ag	6.725
Cr	8.895

4.7.1.1 Screening

A 4 kg subsample of milled lining was taken for this project and screened to produce seven different size fractions, with particle sizes ranging from 1400 µm to ≤38 µm. Each of these fractions were analysed at JM by XRF of the loose (i.e. non-pelleted) powder. As it was a pilot study no replicates were provided and the error level associated with the analysis was not provided. The results of analysis of each size fraction is given in figure 4.2, along with the mass of that fraction as a percentage of the total input mass for screening.

Figure 4.2 shows that there was a significant enrichment of PGMs in the 1400≥d > 212 µm size fraction. This fraction was also the most abundant, accounting for 37.6% of the total input mass. All other size fractions contained less PGM than the reference material. Hence a single size fractionation is a beneficial "upgrading" step.

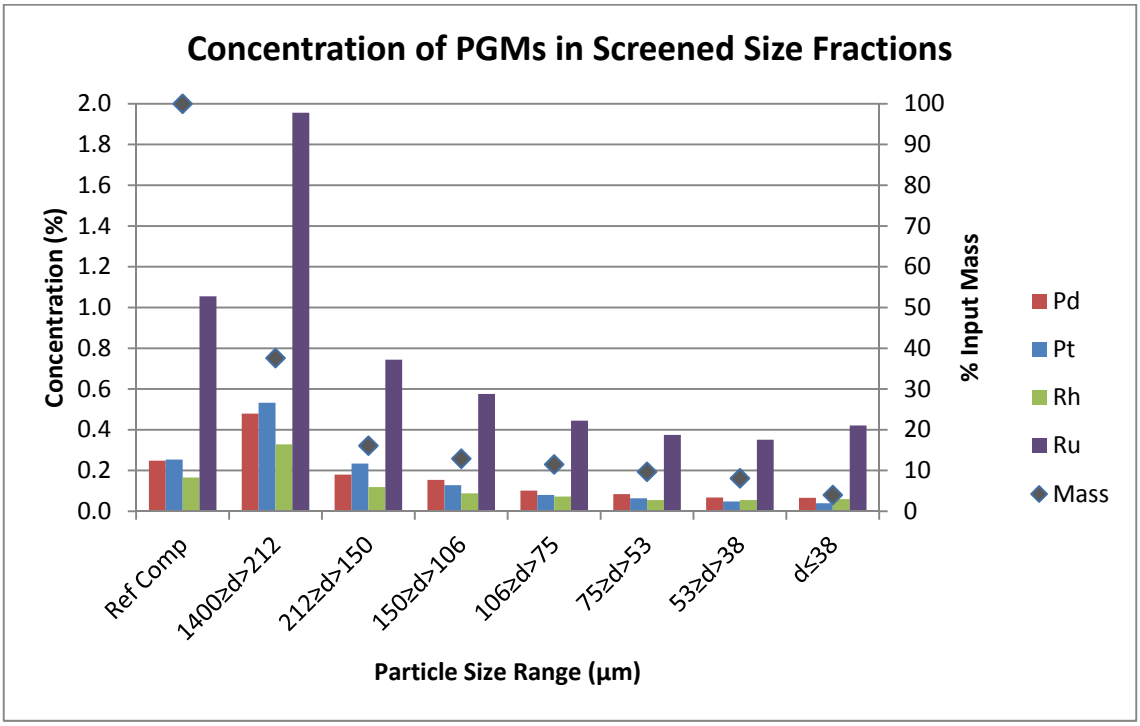

Fig. 4.2 The PGM concentration of the seven size fractions of milled refractory brick, compared against the reference composition before subdivision by screening. The % mass of each fraction is given on the secondary y-axis, with the reference material "ref comp" being 100% of the input mass. Analysis was by Johnson Matthey.

Figure 4.3 illustrates the Ag and Cr content for each of the size fractions in figure 4.2. These metals were shown separately as they are much more abundant than any of the PGMs. Once again the % mass of the fraction is shown for reference. It shows that the largest size fraction (1400≥d > 212 µm) had significantly more silver and less chromium than the reference material. Chromium was in fact reduced by 34% in this fraction. All other

fractions had less silver than the original milled brick but the chromium was elevated above the reference composition in all but the largest and smallest size fractions.

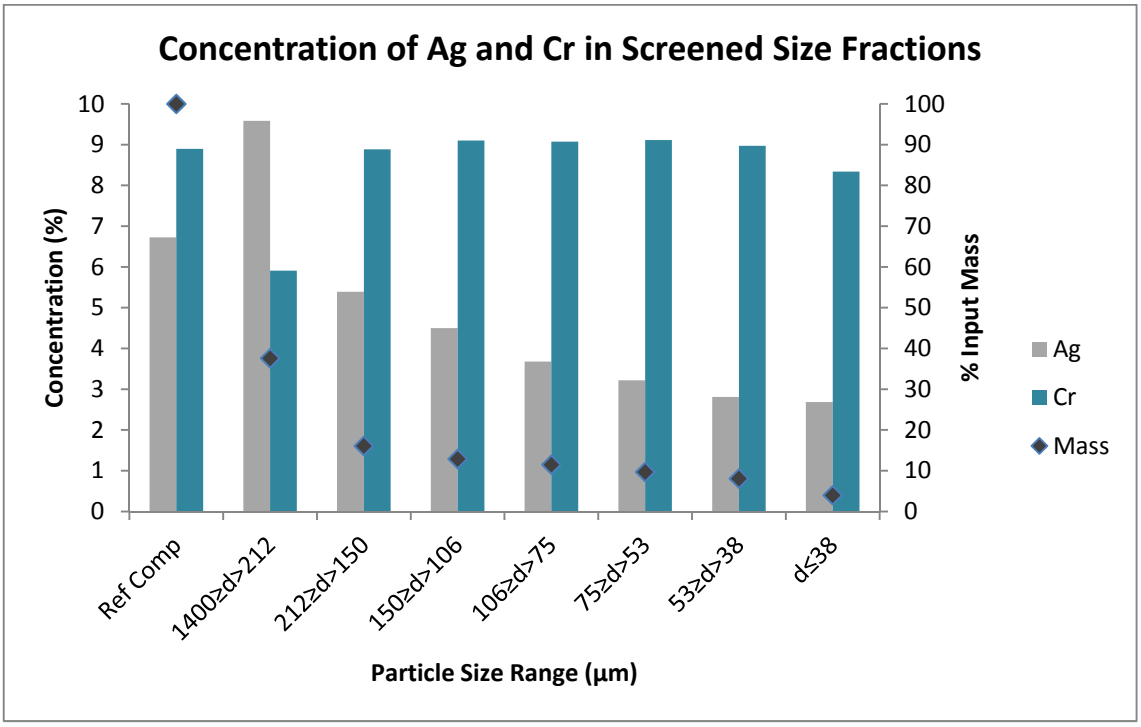

Fig. 4.3 Ag and Cr concentration (in %) of each of the seven size fractions of milled refractory brick, compared against the reference composition. The % mass of each fraction is given on the secondary y-axis, with the reference material being 100% of the input mass.

The key data from figures 4.2 and 4.3 are summarised in table 4.3, which converts PGM concentrations for the largest (1400≥d > 212 µm) size fraction into the percentage of metal recovered from the original feedstock. It shows that 70-80% of the total PGM content could be concentrated in less than 40% of the original starting mass by screening. This fraction also had lower chromium content and increased silver content with respect to reference composition. It was not known at the time but has subsequently been established that the elevated PGM content of this fraction was due to silver being used as one of the smelting

collector metals (and therefore it follows that any size fraction with elevated silver content should also be PGM enriched).

Table 4.3 Summarising the percentage of PGM that could be recovered in 37.6% of the starting mass by screening and retaining the largest fraction (1400≥d> 212 µm) for potential fast tracking by JM.

Element	% Metal Recovered from Original Feedstock	% of Total Input Mass (1400≥d > 212 µm)
Palladium	72.0	37.6
Platinum	78.7	37.6
Rhodium	72.3	37.6
Ruthenium	70.1	37.6

4.7.1.2 Dry Magnetic Separation

A representative sample of the largest fraction from screening (1400≥d> 212 µm) was separated on an induced roll magnetic separator (Boxmag Lab Scale Induced Roll) to investigate possible further metal enrichment and create a basic magnetic profile. The sample was first processed using a 400 gauss hand magnet and was then passed through the separator at successively higher field strengths from 1 A to 4.25 A (the maximum current and therefore field strength achievable on the unit)[1], with the magnetic fraction being retained

[1] The data shown here are relative and machine specific as the boxmag separator is controlled using a dial labelled in amps (A). The accurate conversion from amps to gauss is not possible without access to factory data on the heating rate of the magnetic coils etc., however the higher the current, the higher the magnetic field strength. A hand held gauss meter provides inaccurate reading in a separator with a large gap between poles and so using the amps value was considered the most reproducible way of operating the separator. Dr. Iain Wells (previously employed by Boxmag Ltd.) had records indicating that the maximum current of 4.25 A was

from each pass and sent for analysis along with the final non-magnetic fraction. Figure 4.4 illustrates the test schedule and the five fractions produced.

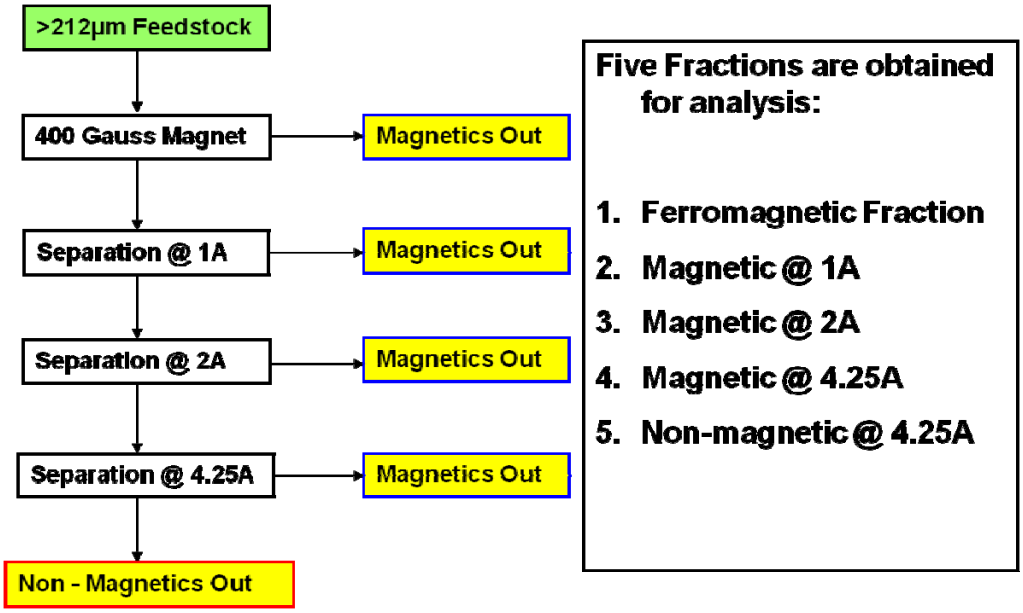

Fig. 4.4 Magnetic profiling of 1400≥d> 212 µm using an induced roll separator

Cumulative metal recovery in the sub-fractions of 1400≥d> 212 µm produced by induced roll magnetic separation is shown in figure 4.5. (A) shows PGM recovery and (B) shows Ag and Cr recovery. The % mass of each sub-fraction is also shown.

Figure 4.5 (A) shows that there was significant concentration of PGMs in the 0.04 T, 1 A and 2 A magnetic fractions, as the % mass of the sample is lower than the % recovery for each

equivalent to a field strength of 1.6 T. The separator used at Birmingham dated from the 1960's and the company ceased trading in the 1980's and so little additional information remains available.

metal. The 4.25 A (1.6 T) sub-fraction offers a small increase in PGM recovery but at the expense of a proportionally larger increase in % mass, thus making it unattractive as a candidate for fast tracking. In all sub-fractions Pd recovery was much lower than the recovery of other PGMs, with more Pd reporting in the final non-magnetic fraction than any other metal. Figure 4.5 (B) shows that there was also significant Ag concentration in the 0.04 T, 1 A and 2 A magnetic fractions. These fractions all have reduced Cr content.

Combining the 0.04 T, 1 A and 2 A magnetic fractions gives a PGM recovery of 60-81% from the 1400≥d>212 µm fraction. This equates to a PGM recovery of 43-58% recovery from the original milled brick sample. The specific values for each metal are given in Table 4.4. The mass balance for magnetic separation was relatively accurate, with the recombined fractions matching the feed material to within 6% for PGMs, 10% for Cr and 20% for silver. Silver was present in concentrations of up to 15% and so it is likely that the high concentration was affecting the accuracy of the XRF assay.

Due to the small particle size of the supplied milled brick only one size fraction was suitable for dry magnetic separation and the six smaller fractions were not tested. The smaller size fractions created a dust hazard and so were considered impractical for this separation technique.

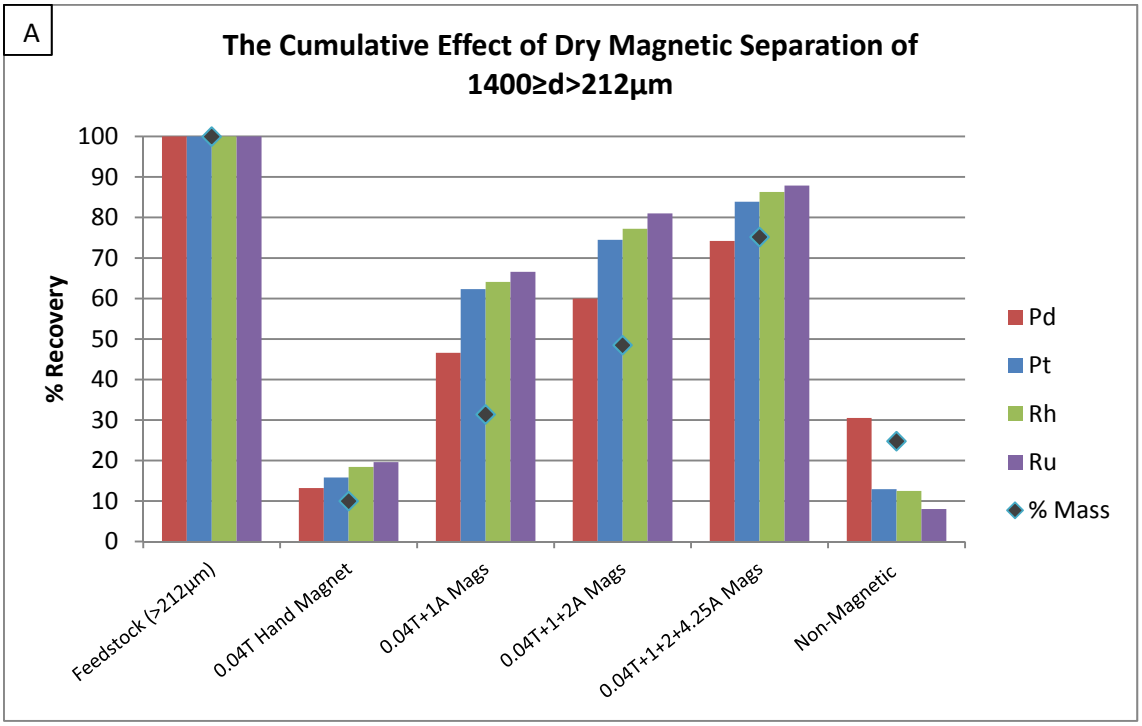

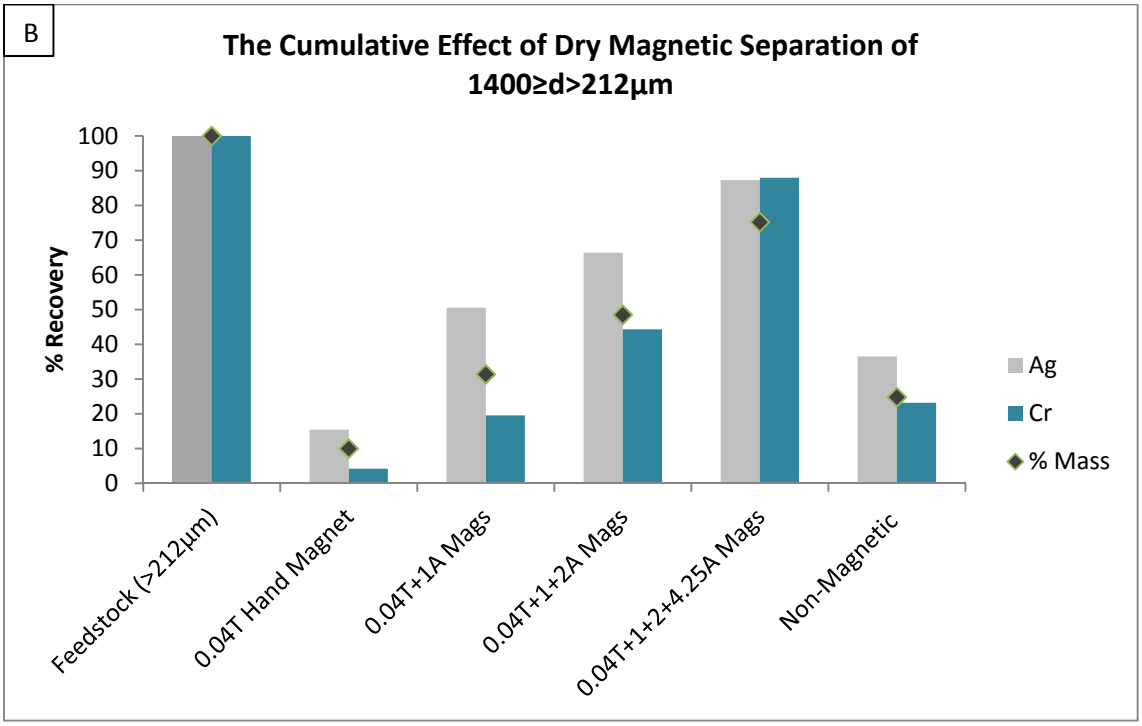

Fig. 4.5 Cumulative metal recovery in the sub-fractions of 1400≥d> 212 µm produced by induced roll magnetic separation

Table 4.4 Recovery of PGMs using induced roll magnetic separation. 43-59% of the total PGM content of the milled brick has been concentrated in only 18.2% of the starting mass.

Element	% Recovery from 1400≥d>212 µm Fraction	% Recovery from Milled Brick
Palladium	60.0	43.2
Platinum	74.5	58.6
Rhodium	77.2	55.8
Ruthenium	81.0	56.8

4.7.1.3 Electrostatic Separation

The largest size fraction (1400≥d > 212 µm) was also subjected to electrostatic separation at two different operating voltages i.e. 20 keV and 30 keV. This produced two fractions for analysis; conductors and non-conductors. Unfortunately there was a problem with the JM XRF analysis for these tests and the mass balance gave poor agreement between the sum of the fractions and the input feed material. However there was an obvious concentration of PGM in the conducting fraction, suggesting that electrostatic separation is a potentially successful concentration technique for this material. No other fractions could be separated in this way due to the dust produced from dry processing small particles.

4.7.1.4 Wet High Intensity Magnetic Separation

Due to the degree of ball milling that the brick had undergone, only the largest size fraction was suitable for dry processing; the remainder were too fine and presented a dust hazard. Therefore further magnetic tests using a wet high intensity magnetic separator were carried

out on the smaller size fractions in order to see if concentration could be achieved. The material was made into a 20% w/w suspension with water and was passed through the separator at increasing field strengths, with the magnetic fraction at each field strength being retained for analysis (as per 4.7.1.2). The field strength ranged from 0.04 T to 1.6 T (the amps to gauss conversion chart for this separator was provided by Dr Iain Wells) and a total of four magnetic fractions and one non-magnetic fraction were produced.

Unfortunately once again there was a problem with the JM XRF analysis for these tests (see section 4.7.1.3) and the mass balance gave extremely poor agreement between the sum of the fractions and the input feed material. This mass balance differed by up to 60% for platinum, however it was more accurate for palladium, with less than 10% difference between the assayed and inferred values.

Due to the large inaccuracies the data have not been presented here but in all cases each of the magnetic fractions contained significantly higher metal concentrations than the non-magnetic fractions and so preliminary studies indicate that wet high intensity magnetic separation has the potential to produce a metal “fast track” from smaller brick particles. JM expressed concern that wet processing may leach toxic chromium from the test material and so samples of water from each magnetic separation test were sent for analysis. No chromium was found and so this hazard can be discounted.

4.7.1.5 Summary of Spent Refractory Lining Sample 1

The characterisation of refractory lining sample 1 indicated that concentration of precious metals was possible using common, established physical processing techniques. However the limitations of the analysis technique (and the lack of replicates to highlight outlying values) caused poor reproducibility and resulted discrepancies of up to 60% in the mass balance. Furthermore it was established that the sample was not representative of the lining routinely produced onsite as it had been ball milled for assaying, resulting in the majority of the particles being too small for dry concentration techniques. At present the best PGM concentration results come from a combination of screening and dry magnetic separation (around 65% recovery with a 73% reduction in mass), but these figures have to be viewed in relation to the varying error levels discussed previously.

4.7.2 Spent Refractory Lining Sample 2 – Partially Crushed Brick

The initial results from brick sample 1 were encouraging with enrichment being achieved via screening, magnetic separation and electrostatic separation. However there were two main research issues:

1. The sample was ball milled to a small particle size and the majority of it was too small for dry processing techniques to be effective.

2. The adopted XRF technique led to significant error on some samples / batches.

The milled brick (sample 1) had been provided as it was a well characterised sample with an accurate PGM assay, having been taken from a furnace lining and ball milled for JM's internal PGM accounting during the annual stock take. However it would not be feasible to ball mill an entire 40 tonne lining before physically processing it to enrich the PGM content, as the energy requirement would be prohibitive and would negate any financial benefits of a fast track concentrate. Hence, a second lining sample was provided for further tests that was more typical of the material produced onsite. This had been lightly crushed after removal from the furnace so that the brick pieces were approximately 10 x 10 x 5 cm and would undergo further comminution at Birmingham. The aim was to prevent over generation of fine particles that were not amenable to dry processing techniques.

Further details of the XRF analytical method were also provided. The samples were placed into a sample cup, the cup was tapped to pack it to a more consistent density and the powder surface was scanned by XRF. However no pressing of the samples occurred and hence the bulk density may not be consistent; grain size variation can cause results to vary and finer grains can be forced to the surface during tap packing; because of these problems this method works best with homogenous material that has been dried and ground to a uniform grain size. This XRF assay is generally not used when accurate results are required, under those circumstances full PGM bead dissolution and ICP of resultant solutions is undertaken. However for investigative work where high sample throughput was necessary XRF was used as it is more cost and time effective.

The fire assay method is expensive and labour intensive and so could not be justified for a feasibility study, however an alternative method was proposed, based upon improving the XRF scanning technique. It was known that PGMs are usually associated with other metals and that several samples had small visible metal prills in them; these samples were inherently non-homogeneous with distinct metal and brick phases. The surface XRF scanning method could therefore misreport metal concentrations depending on particle orientation and density. Homogeneity was likely to get progressively poorer as particle size increased and the JM equipment was only suited to sample sizes of 10-20 g, making representative sampling difficult when 100-500 g of material was generally used per test.

In order to provide suitable samples for future analysis tema milling was carried out to d ≤38 µm, thus improving homogeneity and metal liberation and allowing for small representative sub-samples to be taken. In order to overcome concerns that the metal could smear in the tema mill, causing contamination between samples, SiO_2 sand (produced from milling colourless quartz) was used as an abrasive cleaning agent between samples. The suitability of this milling methodology was verified by tema milling a small number of samples and analysing them initially. SiO_2 cleaning samples were also provided for XRF analysis in order to establish PGM levels. All PGMs occurred at a concentration of <10 ppm in the $SiO_2$and so the method was considered suitable for sample preparation. Highly metallic fractions were likely to be inaccurately analysed by this method and so they were jaw crushed and the metallics were screened out and analysed by a basic NiS fire assay. The remaining brick was then milled and analysed by XRF, providing two analyses to underpin mass balance calculations of final metal concentration.

A second 25 kg sample of lining was provided for further testing. Figure 4.6 illustrates some of the visual differences between samples 1 and 2. (A) and (B) compare the milled and lightly crushed material as received. (C) is a close-up view of a single brick showing metal permeation through it. (D) is a flattened metal fragment found within sample 2. These appear to be found on the front face of some of the darker bricks. Lighter safety lining bricks are also visible in this sample.

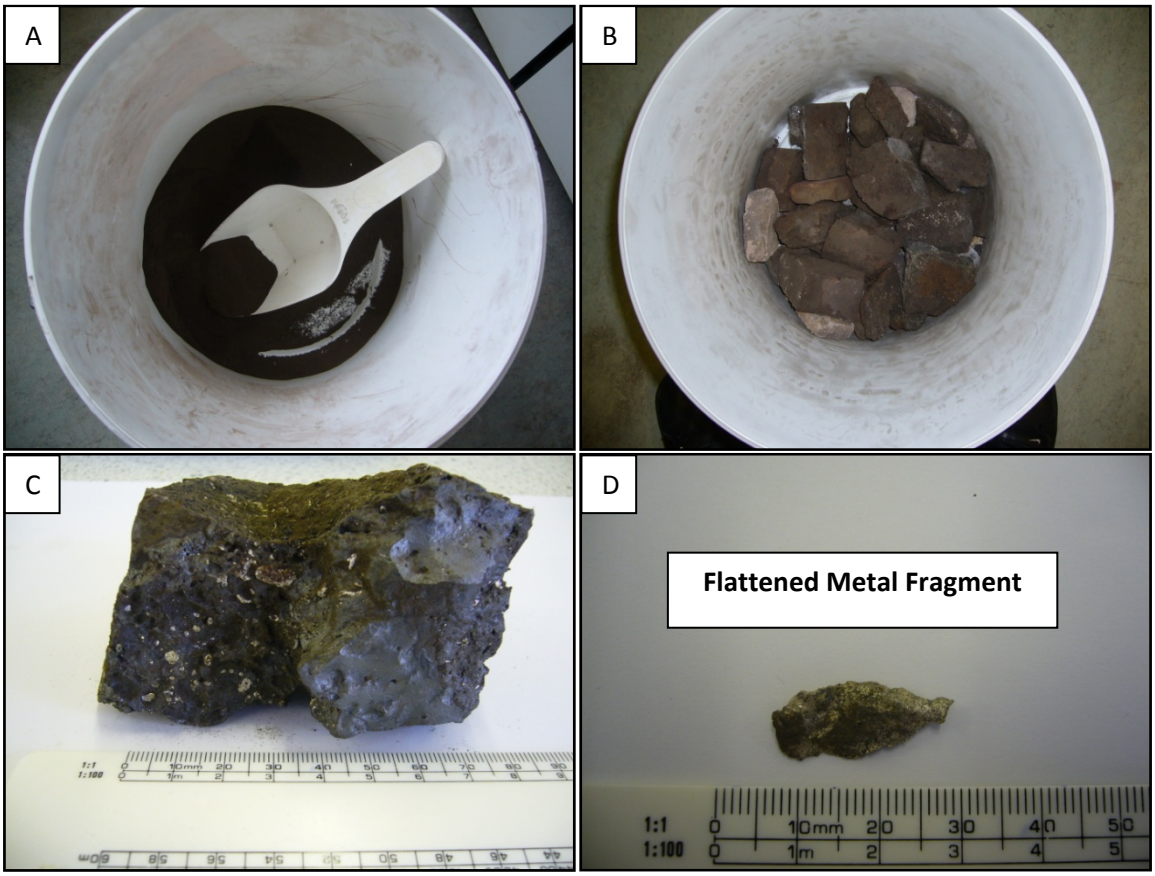

Fig. 4.6 (A) Milled refractory lining sample 1. (B) Lightly crushed refractory lining sample 2. (C) Close-up of a single brick from sample 2 showing metal prills dispersed throughout the material. (D) Large flattened metal fragment found within sample 2.

Figure 4.7 is a flow sheet of the processing techniques applied during material characterisation. Each of the techniques and the results generated will be discussed in subsequent sections of this chapter.

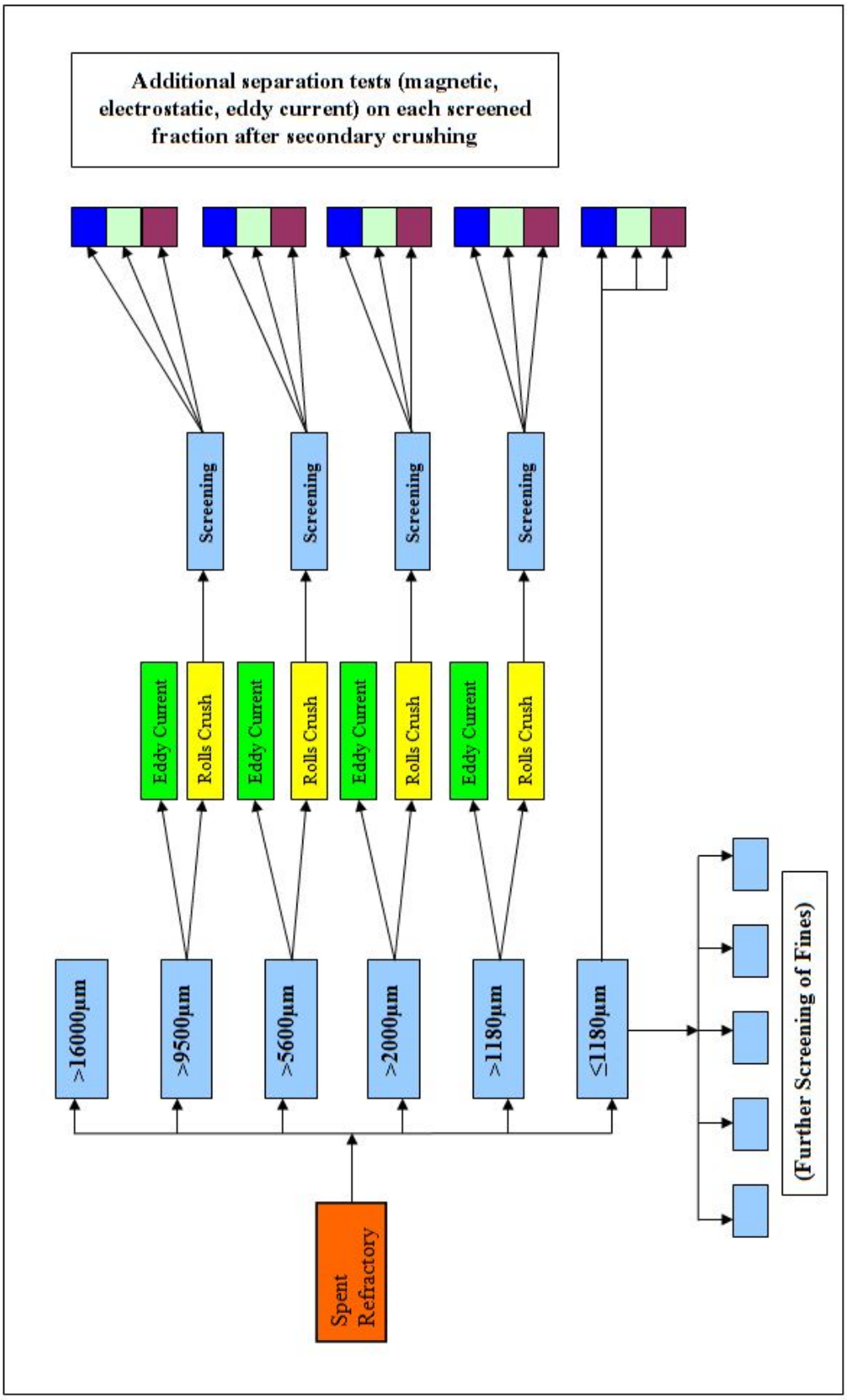

Fig. 4.7 An overview of the characterisation and physical processing of refractory lining sample 2

4.7.2.1 Crushing and Primary Screening

A jaw crusher was used for initial processing of the brick sample (Sturtevant 150 mm jaw crusher with a maximum gap of 22 mm between the plates). Three passes were required to produce particles with the desired size range for physical processing; approximately 1-20 mm. The crushed material was then screened into closely sized fractions to produce feed material for further test work. Table 4.5 shows the particle size ranges produced and the percentage mass of the original sample they comprised. It shows that the largest fraction (d > 16 mm) is less than 2 % of the entire sample and that over 70% is between 2 – 9.5 mm.

Table 4.5 The particle size ranges produced from primary jaw crushing of refractory lining sample 2.

Particle Diameter, d (µm)	% Reporting
d > 16000	1.4
16000 ≥ d > 9500	30.7
9500 ≥ d > 5600	22.0
5600 ≥ d > 2000	22.0
2000 ≥ d > 1180	6.9
d ≤ 1180	17.1

Figure 4.8 shows the Pt, Pd and Rh concentration in each of the size fractions, along with the percentage mass of that fraction. An initial reference composition could not be supplied for this sample as it was comprised of large heterogeneous bricks for crushing at Birmingham and could not be effectively sub-sampled and assayed in this form. Thus the reference

composition bars differ from section 4.7.1 as they are inferred from performing a weighted average on each size fraction as opposed to being experimentally assayed. Figure 4.8 indicates that there is no palladium or rhodium in the largest size fraction, which is less than 2% of the total sample mass. Palladium occurs in varying quantities in all size fractions, but appears to be most concentrated in the two finest fractions. Rhodium was found only in the two smallest size fractions.

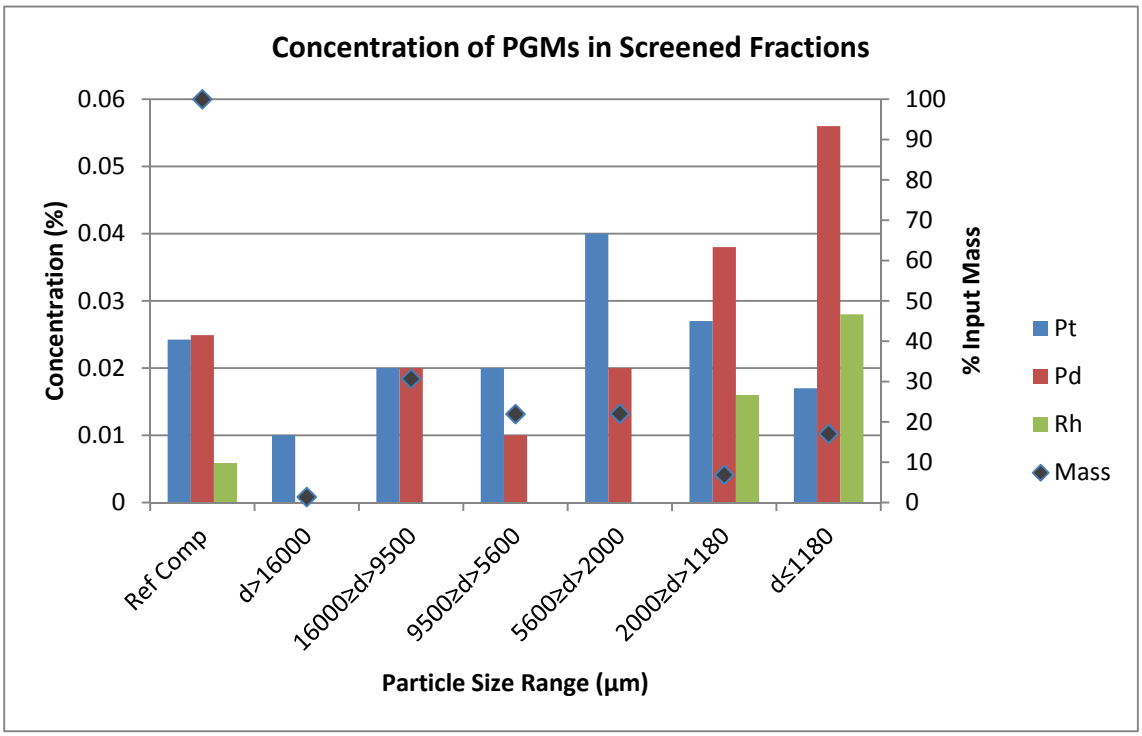

Fig. 4.8 The PGM concentration of the six size fractions of crushed refractory brick, compared against the reference composition (which is a weighted average of the PGM content of all fractions).

Figure 4.9 shows PGM recovery in each of the primary size fractions. Recovery takes account of the both concentration and mass of fraction in order to help determine which fractions contained the most value. This figure indicates that over 80% of the rhodium

reported in the finest fraction, which is only 17% of the starting mass and 100% of the rhodium occurred in less than 25% of the starting mass. Platinum and palladium are spread throughout the size range and so for this reason testing was undertaken on all fractions but the largest (d ≥ 16 mm which had negligible metal content). However, it is important to note that there could be no mass balance verification of these results as no reference composition was produced and no replicates were analysed.

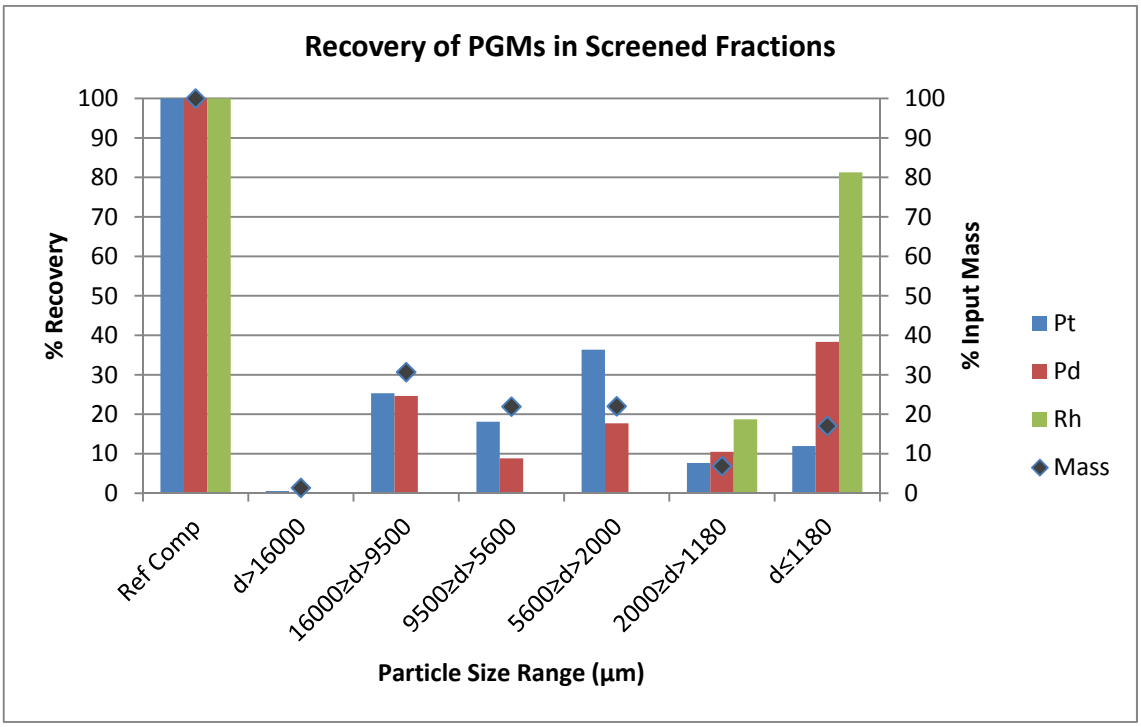

Fig. 4.9 PGM recovery (expressed as a % of the total PGM in the sample) in the 6 fractions produced from jaw crushing refractory lining sample 2.

Table 4.6 compares the measured starting composition of lining sample 1 (section 4.7.1) with the inferred starting composition of lining sample 2 (determined by a mass balance of assays from sub-samples of each size fraction). According to the data sample 1 (the finely milled sample) contained at least ten times as much PGM as sample 2 (the lump brick

sample). As previously discussed the level of metal contamination can vary depending on type of scrap processed in the furnace and the number of melts before failure. However most linings complete approximately 100 cycles and so it is unusual to see such variation between batches of lining. This could indicate a potential analytical issue with regard to accurately assaying larger particles band further tests are required before this can be fully determined.

Table 4.6 Comparison of the PGM concentration in refractory lining samples 1 and 2.

Element	Concentration (%) in Sample 1	Concentration (%) in Sample 2
Pt	0.248	0.024
Pd	0.254	0.025
Rh	0.166	0.006
Ru	1.055	0.023

As the analytical data indicated that the smallest fraction (d ≤ 1180 µm) was PGM enriched (with respect to the starting material) it was further sub-divided by screening to produce five additional size fractions. These are shown in figure 4.10. Although all three PGMs were present in each sub-fraction two (850 ≥ d > 300 and d ≤ 90 µm) contained approximately 70% of the total PGM from the d ≤ 1180 µm feed material.

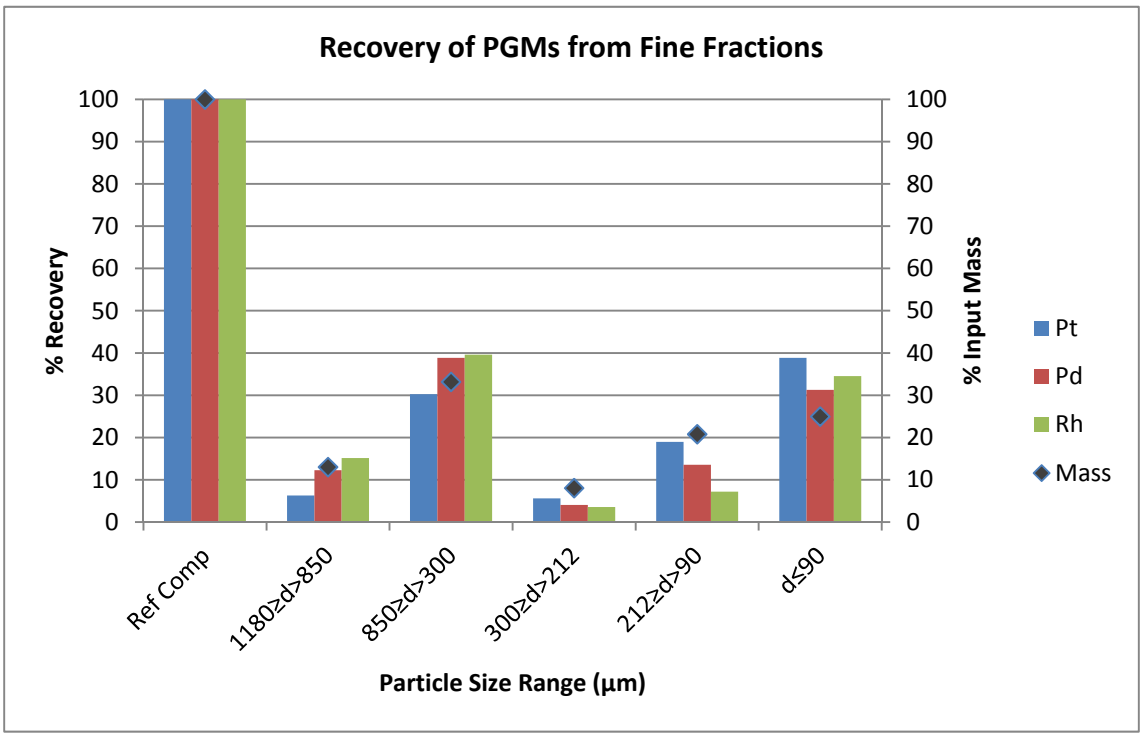

Fig. 4.10 PGM recovery (expressed as a % of the total PGM in the sample) in the 5 sub-fractions produced from further screening the d ≤ 1180 µm size fraction.

Analysis of the five sub-fractions produced from additional screening of d ≤ 1180 µm provided the first opportunity to cross validate the analytical accuracy for this material. A weighted average of the PGM content of the five sub-fractions was performed and compared against the directly assayed PGM content in the d ≤ 1180 µm feed material. This comparison is shown in table 4.7. The results vary by 10 to 13% and show the new assay method is relatively accurate for finer material. However this error will accumulate through additive process steps and may increase for larger particles with less PGM liberation.

Table 4.7 Comparison of implied (via weighted average) and measured PGM content in d ≤ 1180 µm fraction.

Element	Concentration (%) measured in d ≤ 1180 µm fraction	Concentration (%) inferred from mass balance of five d ≤ 1180 µm sub-fractions	% Difference
Pt	0.017	0.019	11.1
Pd	0.056	0.062	10.2
Rh	0.028	0.032	13.3

Primary crushing and screening therefore produced ten size fractions, ranging d > 16000 µm to d ≤ 90 µm for further testing.

4.7.2.2 Secondary Crushing and Screening

The >9.5 mm, >5.6 mm and >2.0 mm fractions were divided into two representative samples by riffling. One sample of each was retained for testing on an eddy current separator (section 4.7.2.3) and the other was recrushed and screened (into five smaller particle size ranges as per the d ≤ 1180 µm undersize material in section 4.7.2.1) prior to undergoing physical concentration in order to investigate whether reduced particle size had an effect on PGM liberation (and therefore recovery). The recrushed material was tested via eddy current, magnetic and electrostatic separation techniques. Figure 4.11 summarises the results of screening each size fraction after rolls crushing.

Fig. 4.11 PGM recovery in sub-fractions of 5600 ≥ d > 2000, 9500 ≥ d > 5600 and 16000 ≥ d > 9500 µm size fractions after secondary crushing and screening.

Figure 4.11 indicates that rhodium was present in all sub-fractions. This is surprising as primary screening (figure 4.9) indicated that all three fractions contained no rhodium and suggests either a sampling or an analysis issue (or both). There are few similarities in the PGM behaviour in the three size fractions as the maximum percentage recovery occurs in a different fraction for each size range. The ratio of Pt:Pd:Rh was also not constant between size fractions.

Due to the expense and difficulty of analysis, replicates were not usually assayed, however the detailed characterisation of lining sample 2 by screening allowed comparison of three separate assays for >9.5 mm, >5.6 mm and >2.0 mm. These samples were:

1. The material produced from primary screening
2. The rolls crushed material before secondary screening
3. A weighted average of the 5 sub-fractions from secondary screening

Figure 4.12 shows the PGM concentrations in each of the three samples for all three size fractions. Overall agreement between the three samples is poor and is particularly pronounced in the +9.5 mm material, where one sample is more than double either of the others.

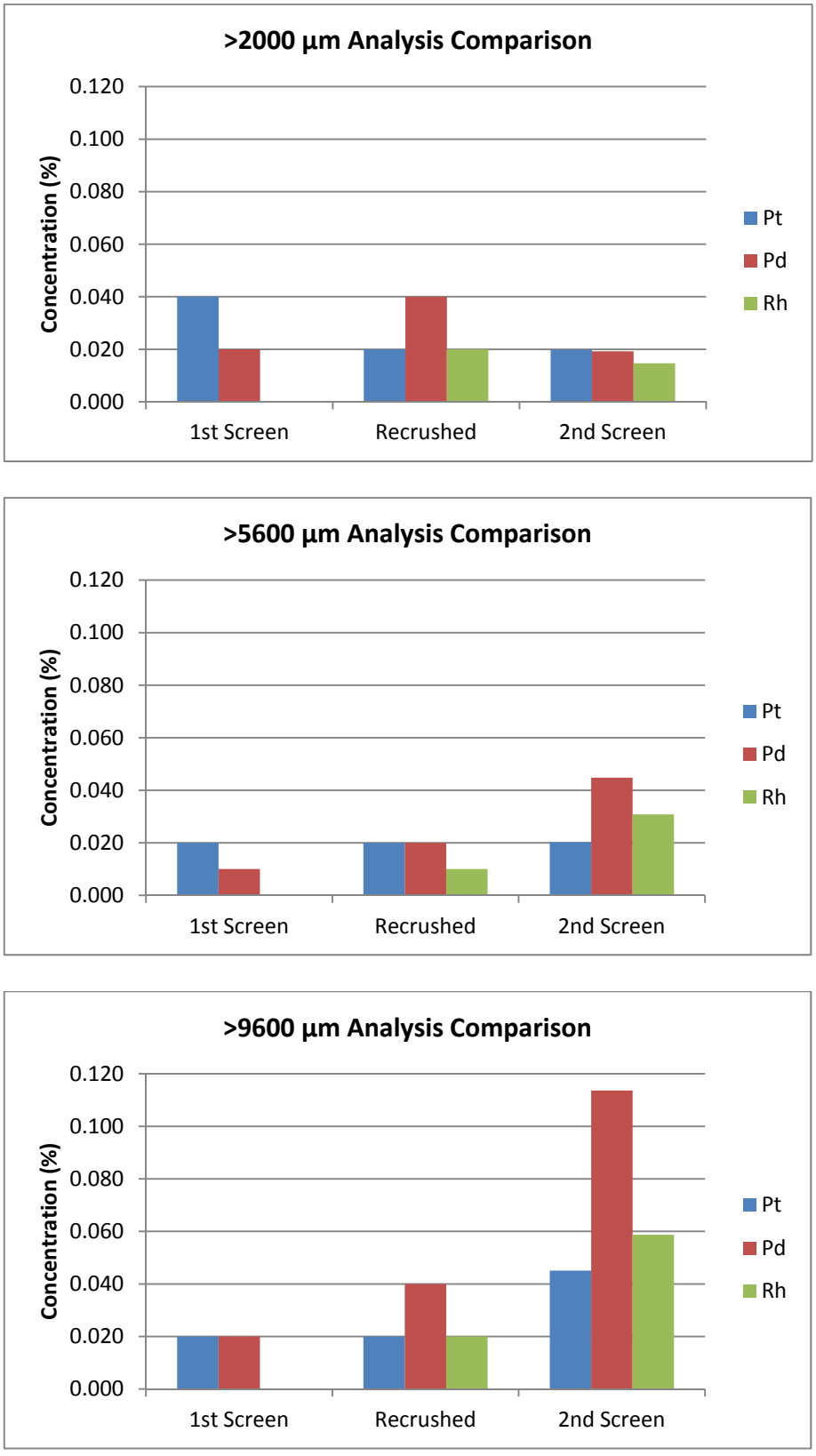

Fig. 4.12 Comparison of PGM concentration in three equivalent samples assayed after primary screening, secondary crushing and secondary screening.

In order to summarise these results and give a better idea of accuracy the mean and the standard error of the mean were calculated for each size fraction. These are shown in figure 4.13 and indicate that analytical error increases with increasing particle size.

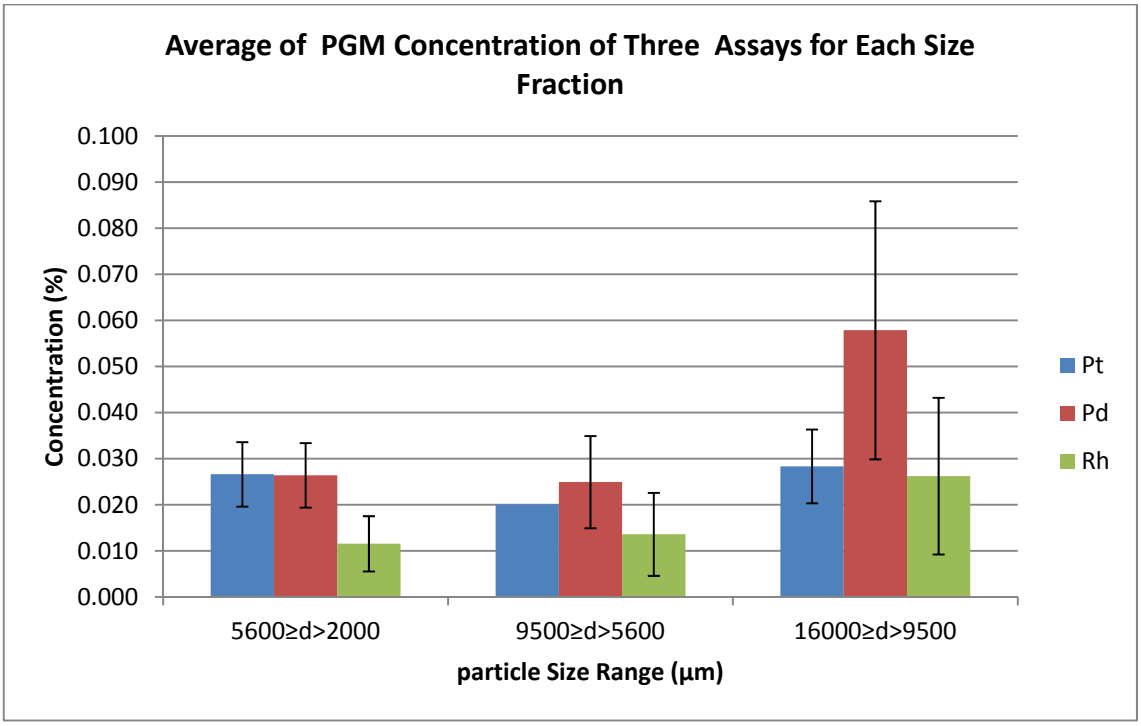

Fig. 4.13 Mean PGM concentration +/- standard error of the mean (no. of replicates = 3) for each particle size range tested. Error increases with increasing particle size.

The results in section 4.7.2 indicate major analysis and / or sampling deficiencies relating to JM sample 2 (the lump brick sample). The crushing protocol worked well to reduce the generation of fine particles that were less amenable to dry processing. Only 17% of the crushed material was less than 1180 µm. However larger particles (specifically those in the region 2000 to 16000 µm) presented challenges in terms of representative sampling for both the experimental protocol and the analytical protocol. As only 25 kg of material was available in total these test samples were limited to 100-500 g. Thus the inclusion of one of

the numerous metal fragments (shown in figure 4.6) could significantly change the composition of a small sample, making it non-representative of the bulk material. In addition correspondence with JM showed that due to a backlog of customer analysis (and a resultant pressure on equipment such as the tema mills) they had been sub-sampling 10-20 g of material for analysis prior to milling instead of after milling. This is likely to be exacerbating the sampling issue as any metal fragments will have a much larger proportional effect as the sample mass decreases. The lack of replicates meant that these outlying values could not be identified and removed from the dataset.

4.7.2.3 Eddy Current Separation

During the pilot study samples of five size fractions (from >850 µm to >9500 µm) were processed using an eddy current separator (Eriez Magnetics "SR" Model ECS) in order to examine PGM recovery in the resulting, magnetic, metallic and non-metallic fractions. Figure 4.14 shows the processing method used to divide the feed sample into four sub-samples based upon the magnetism and conductivity of each particle (in turn dependent on level and type of metal ingress during furnace use). Ferromagnetic particles are attracted to the magnets located in the rotating eddy current roller. These remain on the belt and interfere with the trajectory of following particles and so a 0.8 T sheathed hand magnet was used to remove ferromagentic particles prior to separation. Metallic particles were ejected from the main particle stream and collected separately for analysis. The feed was passed across the separator twice in order to ensure that all metallic particles segregated. Any remaining material not classified as "magnetic" or "metallic" after two passes through the separator was classed as "non-metallic."

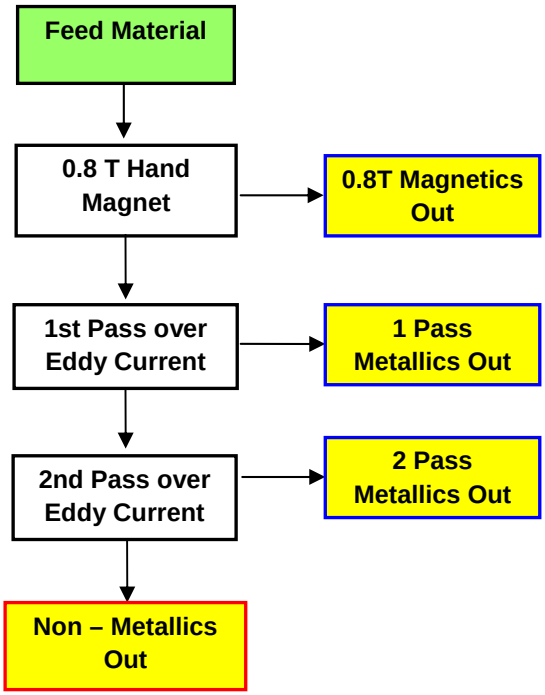

Fig. 4.14 Processing of spent lining via eddy current separation to produce 4 sub-fractions for PGM analysis.

Figure 4.15 shows examples of the metallic concentrates produced during eddy current separation. The majority of the particles in these samples are plates of metal and very little brick material is present. The metal plates were up to 30 mm long in the largest size fractions and are presumed to be silver as that is the collector metal used in the rev furnaces. Although PGMs will also collect in iron (which is present in PGM bearing scrap) any ferromagnetic material is removed by the hand magnet prior to separation and should not be present in the metallic concentrates.

Fig. 4.15 Examples of the metallic concentrates produced from eddy current separation of spent refractory lining. Very few brick particles are present.

Figure 4.16 illustrates the results of eddy current separation of the 9500 ≥ d > 5600 µm size fraction. It shows concentration of PGMs in the magnetic fraction and both metallic fractions as the % mass of the sample is lower than the % recovery for each metal. For this fraction over 50% of each PGM was concentrated into approximately 20% of the initial mass when the magnetic and two metallic fractions were combined. The non-magnetic, non-metallic material was metal depleted with respect to mass. Figure 4.17 gives the results of eddy current separation of the smaller size fraction 5600 ≥ d > 2000 µm. The metal segregation trends are very similar to those in the larger size fraction, with PGM

concentration occurring in the magnetic and metallic sub-fractions. Rhodium extraction was very high (compared to platinum and palladium) in the magnetic fraction and did not increase much upon addition of the metallic fractions suggesting that the majority of the rhodium in the brick is mainly associated with iron. Platinum and palladium recovery increased upon addition of the metallic fractions to the magnetic one suggesting that these metals were associated with both iron and silver. The majority of ruthenium extraction occurs in the magnetic fraction, suggesting it is also associated with iron, however as no screening analysis results were provided no error can be associated with this observation. All five size fractions tested gave similar results and so figures 4.16 and 4.17 have been presented as typical of all samples.

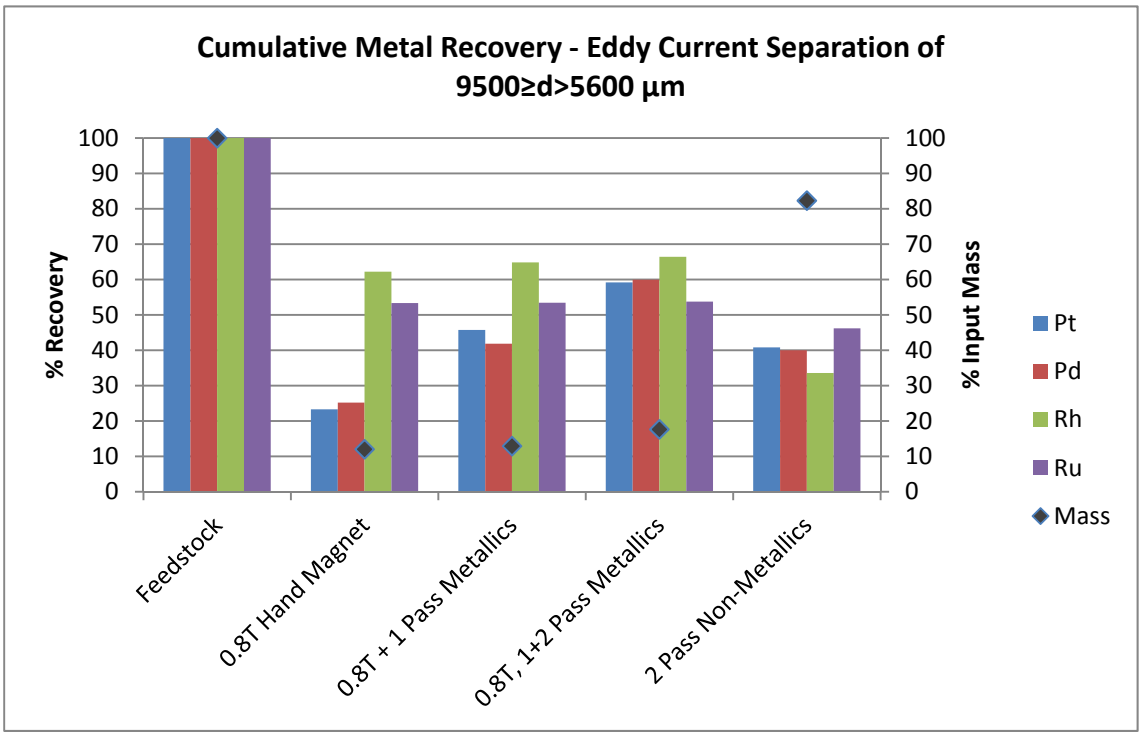

Fig. 4.16 Cumulative metal recovery in the sub-fractions of 9500 ≥ d >5600 µm produced by eddy current separation (no. of replicates = 1).

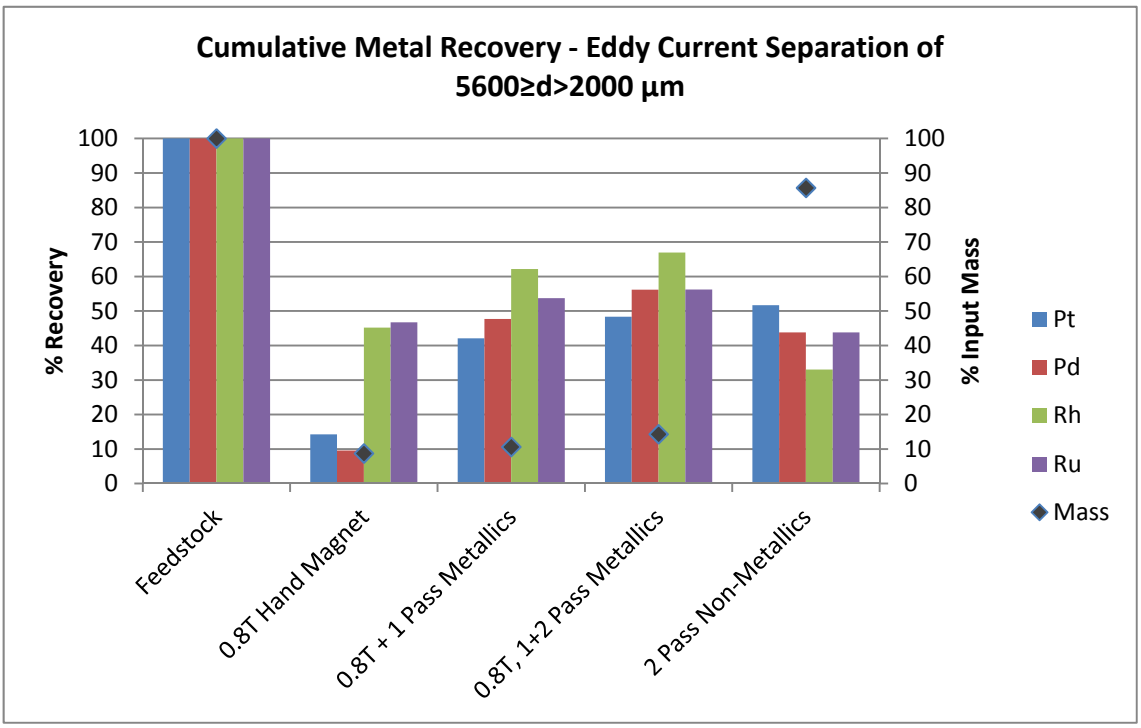

Fig. 4.17 Cumulative metal recovery in the sub-fractions of 5600 ≥ d > 2000 µm produced by eddy current separation (no. of replicates = 1).

Both figures 4.16 and 4.17 show the % recovery of PGMs from the sized brick fractions but neither gives an indication of PGM concentration after eddy current processing. Figure 4.18 compares the PGM concentration of the 1st pass metallics from the 1180 ≥ d > 850 µm size fraction with the PGM concentration of the initial spent brick (calculated from the mass balance of the primary screened fractions). This figure shows that concentration factors of up to 22 x initial concentration for Pt, 126 x for Pd, and 81 x for Rh were achievable via eddy current separation. This metallic fraction was also over 72% silver by mass as the majority of the iron had been removed using a hand magnet. Figure 4.13 indicated quite large errors in some analytical results for this material but such large concentration factors show that the technique has the capability to concentrate PGMs. Although these metallic fractions are only a small mass of each size fraction, the high PGM (and silver) content suggests the

technique may be suitable for producing a “fast track” concentrate for rapid metal recovery in a vastly reduced mass fraction.

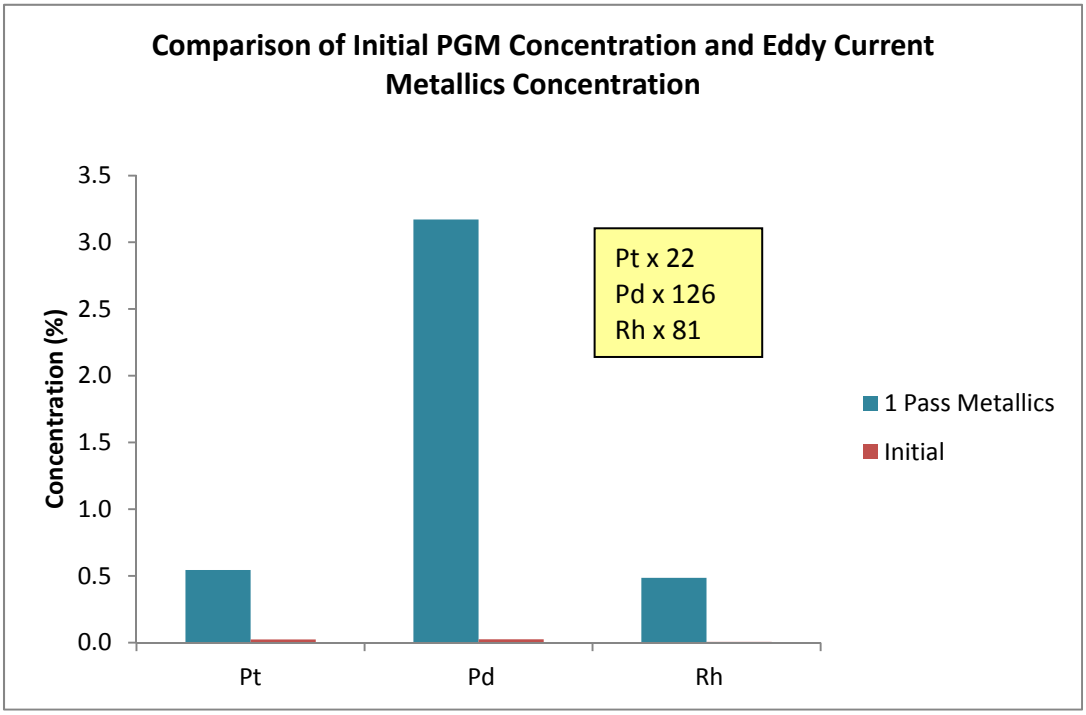

Fig. 4.18 Comparison of the PGM concentration of the 1st pass metallics from the 1180 ≥ d > 850 µm size fraction with the PGM concentration of the initial spent brick (calculated from the mass balance of the primary screened fractions).

Table 4.8 lists the % total mass and % recovery of PGMs for each of the eddy current fractions derived from the 9500 ≥ d > 5600 µm size fraction. It shows that by combining the magnetic and two metallic fractions it is possible to concentrate approximately 60% of the Pt, 60% of the Pd, 66% of the Rh and 54% of the Ru in less than 18% of the initial mass.

Table 4.8 % total mass and % recovery of PGMs for each of the eddy current fractions derived from the 9500 ≥ d > 5600 µm size fraction.

	% Total Mass	Pt%	Pd%	Rh%	Ru%
Feedstock (9.5≥d>5.6 mm)	**100**	**100.0**	**100.0**	**100.0**	**100.0**
0.8T Hand Magnet	12.0	23.3	25.2	62.2	53.4
0.8T + 1 Pass Metallics	12.9	45.7	41.9	64.9	53.5
0.8T, 1+2 Pass Metallics	17.7	59.2	60.0	66.4	53.8
2 Pass Non-Metallics	82.3	40.8	40.0	33.6	46.2

By combining the magnetic and metallic data for the five fractions subjected to eddy current separation and factoring in the metal segregation and masses of each of the primary screened fractions (used as the feed for eddy current testing) it is possible to estimate the likely achievable recovery of metal from the initial lining sample. Calculations showed that it is possible to recover 50-70% of the initial precious metal content in less than 20% of the original brick mass. As JM stated that between £23 and £50 million of PGM is contained within the 200 tonnes of lining produced per annum this equates to being able to rapidly recover PGM worth £11.5 to £35 million, instead of storing it for long periods until furnace capacity becomes available.

4.7.2.4 Electrostatic Separation

Electrostatic separation was carried out on the finer screened size fractions of spent refractory lining (d ≤ 2000 µm). Figure 4.19 shows the results for electrostatic separation of the 2000 ≥ d > 1180 µm and d ≤ 1180 µm size fractions at 20 keV with a roll speed of 53 rpm. Figure 4.19 indicates that there was no enrichment of PGMs in either the conducting or non-conducting fractions under these conditions. Electrostatic separation is highly dependent on the feed material having a narrow particle size distribution. Both of these feeds have a wide range of particle diameters within their upper and lower bounds and so it is likely that differences in particle mass may be overriding and / or masking the charge based separation of conductors and non-conductors.

Figure 4.20 shows the results of electrostatic separation on the two largest size fractions after they were recrushed and further screened into finer sub-fractions. For both size fractions there is a concentration of PGMs in the conducing sub-fraction. For the >5.6 mm material around 70% of the PGM was concentrated into 15% of the input mass and for >2.0 mm over 50% of the PGM content was concentrated into 20% of the input mass. Thus it appears that samples with a narrower particle size distribution and a greater degree of metal liberation (from secondary crushing) could be concentrated via electrostatic separation.

However these observations make electrostatic separation impractical as an industrial technique as production of fractions with such a narrow particle size distribution require extensive crushing and screening. Such processes are energy intensive and time consuming, particularly when other techniques (e.g. eddy current) show more promise at present.

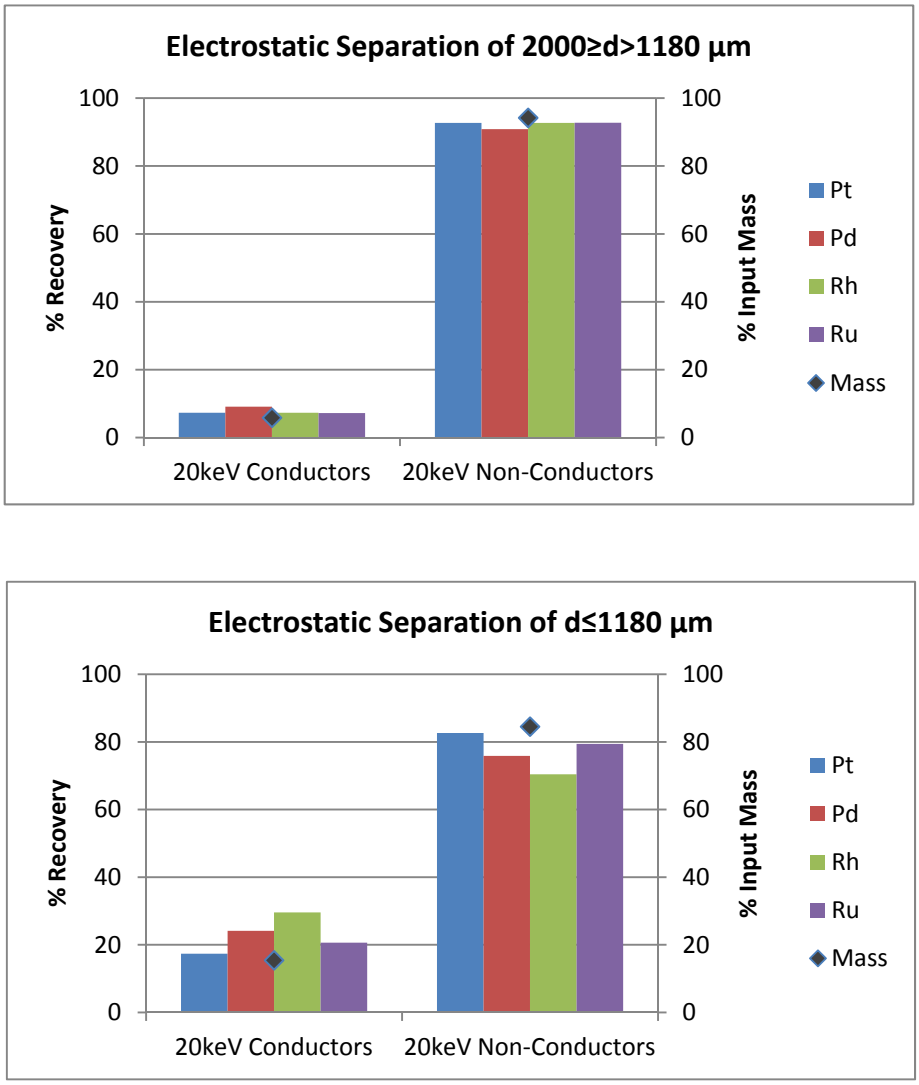

Fig. 4.19 Electrostatic separation of the 2000 ≥ d > 1180 µm and d ≤ 1180 µm size fractions at an operating voltage of 20 keV.

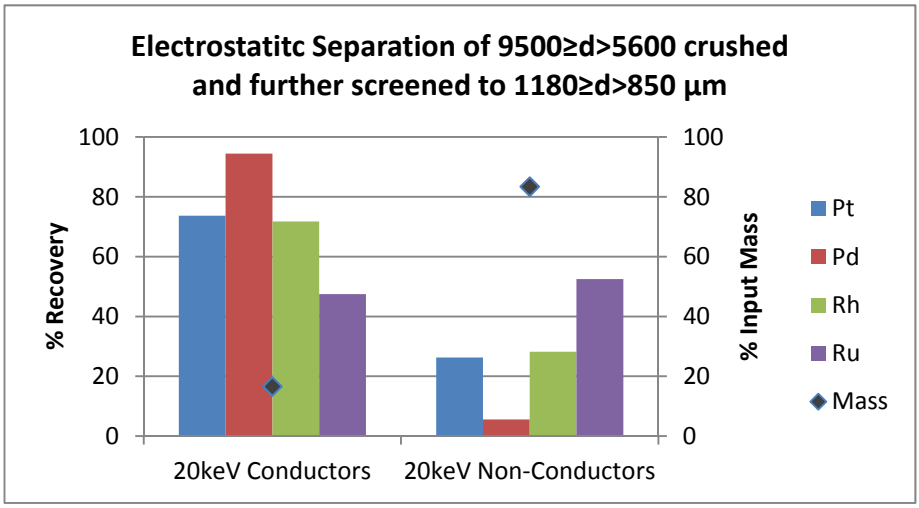

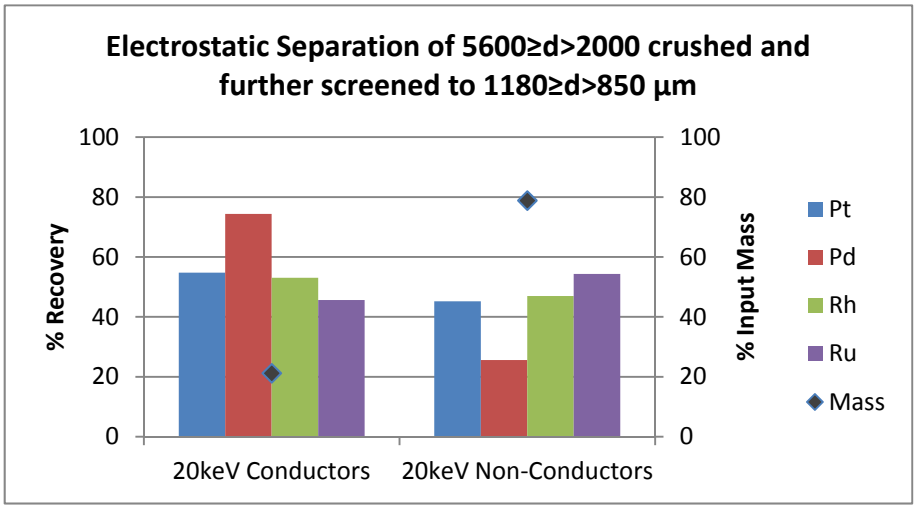

Fig. 4.20 Electrostatic separation of 9500 ≥ d > 5600 µm and 5600 ≥ d > 2000 µm recrushed and further screened to 1180 ≥ d > 850 µm.

4.7.2.5 Induced Roll Magnetic Separation

Due to the aim of avoiding overcrushing and resultant generation of fines several of the size fractions produced were too large for separation on the laboratory induced roll magnetic separator. This was addressed in sample 3 by using industrial scale magnetic drums (capable of separating particles in excess of 16 mm) but during the pilot study magnetic separation

was restricted to particles of 2 mm and smaller on the laboratory scale induced roll. Figure 4.21 shows cumulative metal recovery in the sub-fractions produced during induced roll magnetic separation for 2000 ≥ d > 1180 µm, d ≤ 1180 µm and 850 ≥ d > 212 µm (d ≤ 1180 µm further screened into smaller sub-fractions) and illustrates that separation behaviour is dependent on particle size.

In all cases there appeared to be a difference in behaviour between Pt/Pd and Rh/Ru, with proportionally much more Rh/Ru being extracted in the magnetic fractions and proportionally more Pt/Pd remaining in the non-magnetic fraction. However for d ≤ 1180 µm all of the magnetic fractions were PGM enriched (with respect to mass), whereas for both 2000 ≥ d > 1180 µm and 850 ≥ d > 212 µm Rh and Ru were enriched (with respect to mass) in the magnetic sub-fractions but Pt and Pd were not.

These results indicate that induced roll magnetic separation has the potential to produce a "fast track" PGM concentrate from spent refractory lining but more tests are required as the majority of the PGM reports in the larger size fractions that could not be processed on laboratory scale equipment.

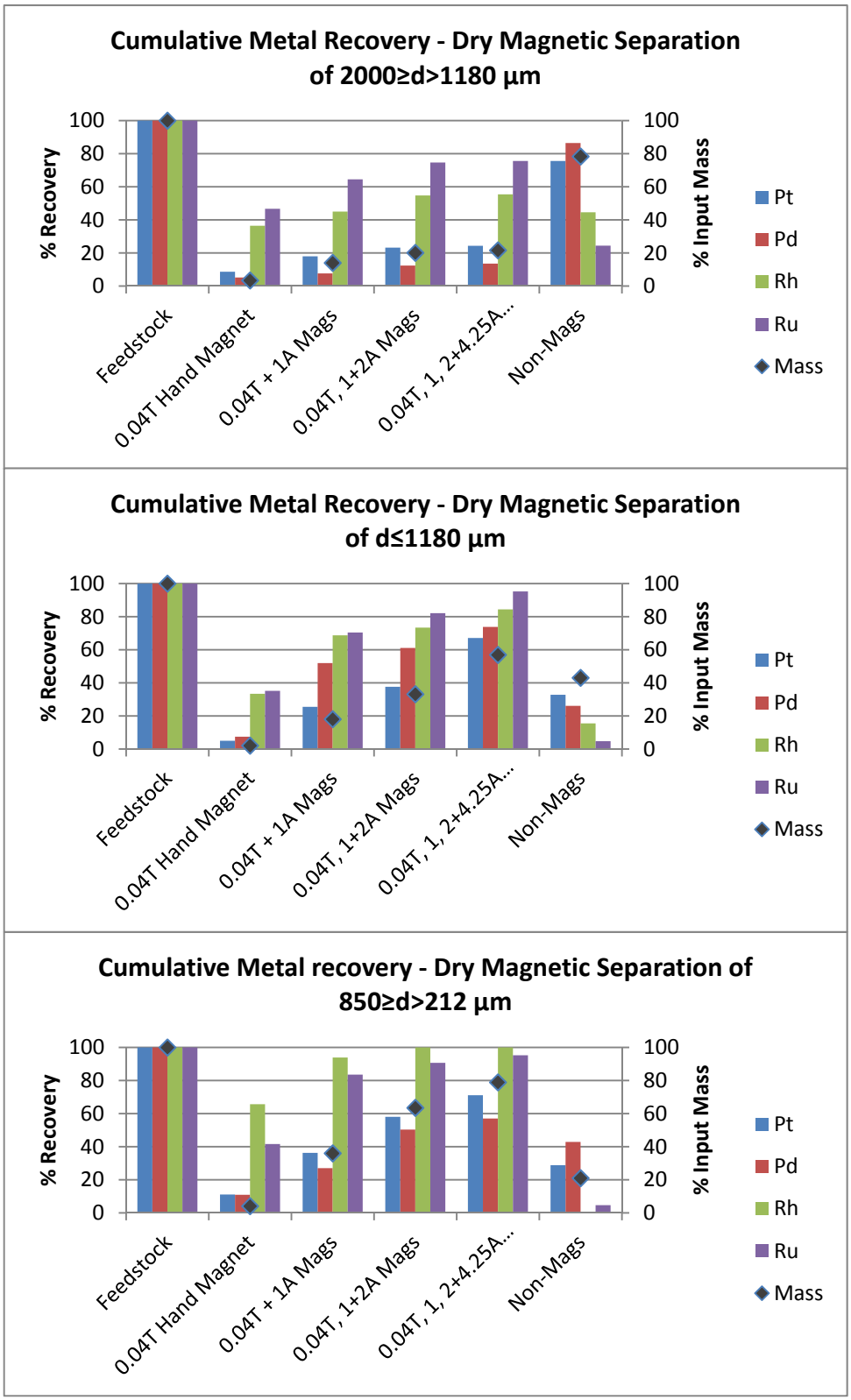

Fig. 4.21 Cumulative PGM recovery during dry magnetic separation at increasing field strengths for 3 size fractions of spent refractory lining.

4.7.2.6 Separation of Brick Types using an Air Table

Despite the restricted applications of air tables in modern separation plants, due to the density differences between the three linings (table 4.1) it was considered to be a potentially inexpensive method of separating different brick types. There was a relatively large difference in density between the outer safety lining and intermediate and hot face layers (0.87 – 1.1 g/cm^3), but the difference between the intermediate and hot face layers was only 0.23 g/cm^3 i.e. less than the minimum 10% density difference recommended by the manufacturer. However these values are for uncontaminated brick and as metal permeation is likely to be greater in the hot face layer than the secondary intermediate safety layer in reality the density difference is likely to be significantly larger.

4.7.2.6.1 Preparation of Test Sample

Figure 4.6 (b) shows that the bulk of the spent lining (after removal from furnace) appeared brown in colour due to dust from the dark bricks coating the lighter ones. This was considered unsuitable as a test material (as visual differences are useful when optimising a separation) and so unused blocks of each refractory type were sourced and crushed to the same size as the spent lining. The three bricks were jaw crushed (Sturtevant 150 mm jaw crusher; 2 passes with a 22 mm gap between the plates) and then screened into the same size fractions as per section 4.7.2.1.

The hot face and intermediate safety layer bricks were similar in colour (brown and dark purple). In order to enhance the colour difference and to simulate metal contamination of the hot face layer a green high density metallic paint was used to coat all of the hot face

particles (three coats) after crushing and before recombination with particles from the other two layers. This made them more visible and also increased their density making the "model" mixture better approximate the "real" spent lining. The 9.5 mm ≥ d > 5.6 mm size fraction was used for testing and the three brick types were recombined in a 1:1:1 ratio by mass. Figure 4.22 shows the test mixture prior to testing. The three brick colours (green; hot face, purple; intermediate safety layer and yellow; outer safety layer) are all clearly visible.

Figures 4.23 and 4.24 show the "heavy" concentrate and the "light" concentrate after separation on the air table. Although this pilot experiment was not quantitative the photographs indicate that the green particles (hot face layer with paint simulating metal contamination) have concentrated in the heavy concentrate. The light concentrate had a higher proportion of yellow safety layer particles present than the initial feed material. In addition there are only 6 misclassified green particles (circled for identification) in this fraction, suggesting that this fraction would have a low PGM content. JM require Pt and Rh levels of <2 ppm before brick can be discharged to landfill and so this separation is unlikely to provide a completely metal free fraction for immediate disposal, but it could potentially provide a fast track concentrate for rapid reprocessing and metal recovery. In addition the spent lining is likely to have larger differences in specific gravity due to metal ingress and so any separation on that material is likely to be more effective than the (worst case) simulated test material. However air tables require skilled operators and constant supervision and so may be too labour intensive for Johnson Matthey. In addition particles larger than 9.5 mm

were too large to be fluidised by the air jets and particles smaller than 5.6 mm were difficult to distinguish by colour on a moving deck.

Fig.4.22 The "model" lining mixture produced from unused refractory bricks. The hot face particles have been painted green in order to make them more visible.

Fig. 4.23 The heavy concentrate produced from separation of crushed and sized refractory bricks on an air table. This fraction contains a higher proportion of green particles than the feed material.

Fig. 4.24 The light concentrate produced from separation of crushed and sized refractory bricks on an air table. This fraction contains a higher proportion of yellow (uncontaminated) outer safety layer particles than the feed material. The six visible misclassified green particles are circled.

4.7.3 Conclusions from Refractory Brick Feasibility Study

During the feasibility study over 160 samples were produced from two different brick samples. A number of physical processes, including screening, wet and dry magnetic separation, electrostatic separation, eddy current separation and air tabling were applied to the material in order to examine the prospects of producing a low volume, PGM enriched fraction for rapid metal recovery. A number of techniques showed promise, in particular magnetic separation and eddy current separation, but the powder XRF analytical technique proved unsuitable for the material and so accuracy of the data was poor and no replicates were analysed.

The ball milled sample gave more accurate XRF results. However it was difficult to process dry as the majority of the material was too fine. Wet processing was not feasible onsite at JM and so work was discontinued in favour of a non-milled sample that could undergo controlled comminution in order to produce particles of the correct size for dry physical processing to underpin a more generic method. This partially crushed brick showed significant concentration in a number of tests but created greater analysis difficulties and inaccuracies due to the large particle sizes involved.

A clean discard fraction was not considered possible as any brick with a concentration of >2 ppm for Pt or Rh must be reprocessed before being allowed to leave site. Although several fractions had significantly reduced PGM levels none of them approached these trace values. Experiments with an air table produced a concentration of the safety lining which could

potentially be set aside and smelted last, after all other fractions had been processed, thereby separating out several grades of brick depending on furnace capacity. This flexibility to select the amount of fast track material dependent on furnace capacity is an attractive future process option.

4.8 Extended Study on Spent Refractory Lining Using Selected Separation Methods

Physical processing of samples 1 and 2 showed that concentration of PGMs in spent lining was achievable, however sampling and analytical issues limited the accuracy and reproducibility of results. As a result the project was extended in order to collect and process a much larger and more representative sample. More accurate analysis techniques would be applied and reproducibility would be studied.

4.8.1 Sampling

Jillavenkatesa *et al.* (2001) stated that for routine plant sampling, where possible two to three times the minimum weight of sample should be taken to allow for the many unknowns. However, oversampling should also be avoided in order to minimise handling and preparation problems. Wills (2008) recommended taking at least 5% of the total weight of material as a primary sample in order to ensure accuracy.

4.8.1.1 Collecting a Representative Sample

Sample 2 (the" lump" brick sample) proved more amenable to physical concentration using dry processing than sample 1 as the particle size was larger. However the bricks had been hand selected from a single container of material at the refinery and so were not necessarily representative of the whole lining. Thus the third sample was collected immediately after a furnace lining was "wrecked."

Figure 4.6 shows that the bricks were extremely heterogeneous and so a large number of samples were considered necessary in order to ensure overall representivity. However sampling constraints were in place at JM (due to the high value of the PGMs in the material) that had to be accommodated, namely:

1) No single assay could be assigned to more than 10 tonnes of scrap.
2) The sample taken could not exceed £70,000 in precious metal value

These constraints affected the sampling regime adopted. Ideally, in order to ensure complete representivity, sampling would have taken place at regular intervals throughout the jaw crushing of the entire 40 tonne lining. However, as an accurate assay of the PGM content of this sample was required as a baseline to assess subsequent concentration efficiency, a maximum of 10 tonnes was available for sampling (i.e. JM would ball mill the remainder of the 10 tonnes and assay it to establish accurate initial PGM values). In addition

normally Gy's sampling theory (Gy, 1979) would have been applied in order to calculate the minimum mass of sample required to ensure representivity, however as the maximum sample value could not exceed £70K it was decided to take the largest sample possible without exceeding this limit.

JM stated that the 200 tonnes of spent lining generated annually contained an average of £23 to £50 million of precious metal (PGMs, gold and silver). Therefore a maximum sample of 250 kg of lining could be collected for further processing. This was only $1/8^{th}$ of the ideal mass recommended by Wills (2008) (as 5% of 40 tonnes would be 2000 kg), but is around ten times larger than the previous samples processed during the feasibility study and so was deemed a good compromise between statistical significance and operational constraints.

Hence, 10 tonnes were separated from the rest of the lining to be crushed, sampled and then assayed for this research. The 10 tonnes were separated from the complete 40 tonne lining by assigning a number to each of the 12 storage containers and then selecting three numbers at random to make-up the sample. These were then processed using a jaw crusher operating at approximately six tonnes per hour. This reduced the size of the bricks from as large as 300 x 200 x 75 mm to pieces of 100 x 100 x 75 mm or smaller.

Figure 4.25 shows the sampling set-up at JM's Enfield Refinery, with the crushed brick being sampled during discharge from a conveyor into a storage bin. 10 tonnes of crushed lining

filled two of these bins. Samples were taken from underneath the jaw crusher conveyor using a long handled scoop every sixty seconds. These scoops were relatively small (2-3 kg capacity) and so successive samples could look very different depending on the brick types being crushed at any given time (figure 4.26).

Fig. 4.25 The sampling point for collection of refractory lining sample 3. One hundred 2-3 kg samples were taken at 60 second intervals.

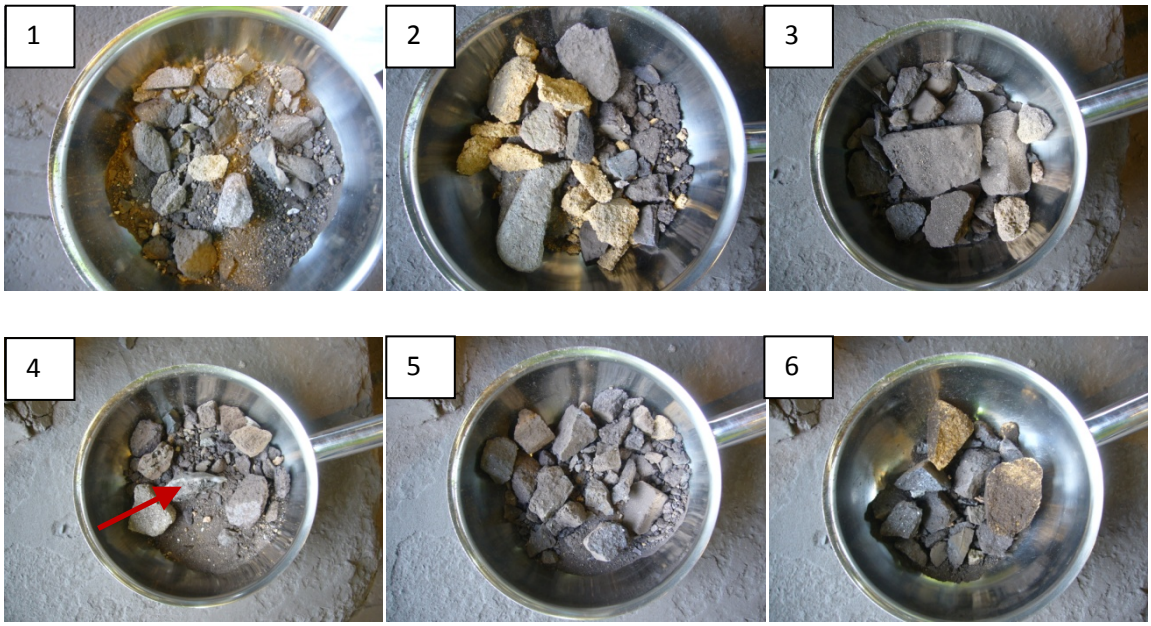

Fig. 4.26 Six successive samples taken during crushing of refractory lining sample 3.

Figure 4.26 illustrates how variable the crushed lining was as the six samples pictured have visibly different compositions. For example sample 1 had more fine material than the others, sample 2 had a lot of the yellow (uncontaminated) alumina outer safety lining visible and sample 4 has a very large piece of metal in the centre of the picture (arrowed). It was therefore crucial to take many small samples to ensure the collected material was representative of the bulk lining.

The onsite crusher operated at 6 tonnes per hour. The 10 tonnes of lining segregated for this study was therefore crushed in 100 minutes, creating 100 sampling points sixty seconds apart for the collection of the 250 kg representative test sample.

4.8.1.2 Primary Processing of Refractory Lining Sample 3

The 250 kg sample was transported to Birmingham and was jaw crushed, coned and quartered, screened and riffled (following the same methodology as for brick sample 2 in section 4.7.2.1) in order to create samples of a suitable size for further test work. The size fractions generated from this work were the same as for lining sample 2 (the pilot lump brick sample). The entirety of each size fraction was then sub-divided into individual samples of between 1 and 5 kg via box riffling. These individual samples were considered large enough to be representative of that particular size fraction and were used "whole" to ensure representivity i.e. there was no further sub-sampling from these bags prior to undergoing various physical separation tests. Thus all practical precautions were taken (within JMs operational limitations) to ensure that not only the bulk 250 kg sample, but also the individual samples of each size fraction which would serve as feed material for selected physical concentration trials, were representative of the bulk furnace lining. This was necessary as a combination of both sampling errors and analytical errors had affected the accuracy of results for the first "lump" brick sample (JM sample 2).

4.8.2 Development of an Accurate Analytical Technique for Determining PGM Concentration in Refractory Lining

Both samples of refractory brick used in the pilot study had shown amenability to concentration via physical separation techniques, however the powder XRF analysis had been found to be inaccurate for this type of material, despite efforts to improve consistency

as the project developed. In order to generate meaningful data a more suitable analytical solution was sought to compliment the improved sampling regime.

Due to high numbers of customer samples in 2007-2008 (when PGM prices were at record levels) and a lack of small scale metal smelting furnaces JM decided to subcontract the analysis to Engelhard (BASF) Ltd. In conjunction with University of Birmingham Engelhard developed a method based upon collection PGMs in copper and production of a homogenised, polished copper disc which was assayed by XRF. To achieve this analysis the entire sample from each processing test was tema milled and blended. The blended material was screened using a 100 mesh screen in order separate metallic particles “mets” from the milled brick “fines.” Both fractions were then riffled in order to generate representative sub-samples for analysis. The sub-samples (mets and fines) were both smelted (with a known mass of copper as the collector metal) and the resultant molten copper from each fraction was first cast into a primary button and then re-melted and cast into a secondary button in a graphite crucible in order to facilitate rapid cooling and limit metal segregation. Each button was then polished and scanned by XRF (9 measurements taken whilst rotating each disc) and after compensating for the copper dilution factors the PGM content of the sub-fraction could be determined. Combining the “mets” (where present) and “fines” results via a weighted average allowed the PGM content of the overall test sample to be calculated. A minimum of two copper buttons were be produced for each sample in order to allow error levels to be investigated.

As analysis was being contracted externally JM cross verified the Engelhard reported PGM content of the primary feed stocks (the screened size fractions) by full *aqua regia* dissolution of each copper disc followed by ICP of the resulting solution. Comparison of Engelhard's XRF method with JM's full acid digest and ICP method established that Engelhard's method was accurate for Rh and Ag at a wide range of concentrations, but was inaccurate for Ir and Ru. The method was accurate for Pt and Pd if the data from the highly metallic (high concentration) fractions was discarded. Accuracy decreases with decreasing concentration as expected. Figures 4.27, 4.28 and 4.29 plot the average Engelhard assay against the average JM assay for Ag, Rh and Ru in order to show the close agreement between methods for Ag and Rh but poor agreement for Ru. The "mets" and "fines" results were compared separately as highly metallic particles are much more challenging to assay accurately.

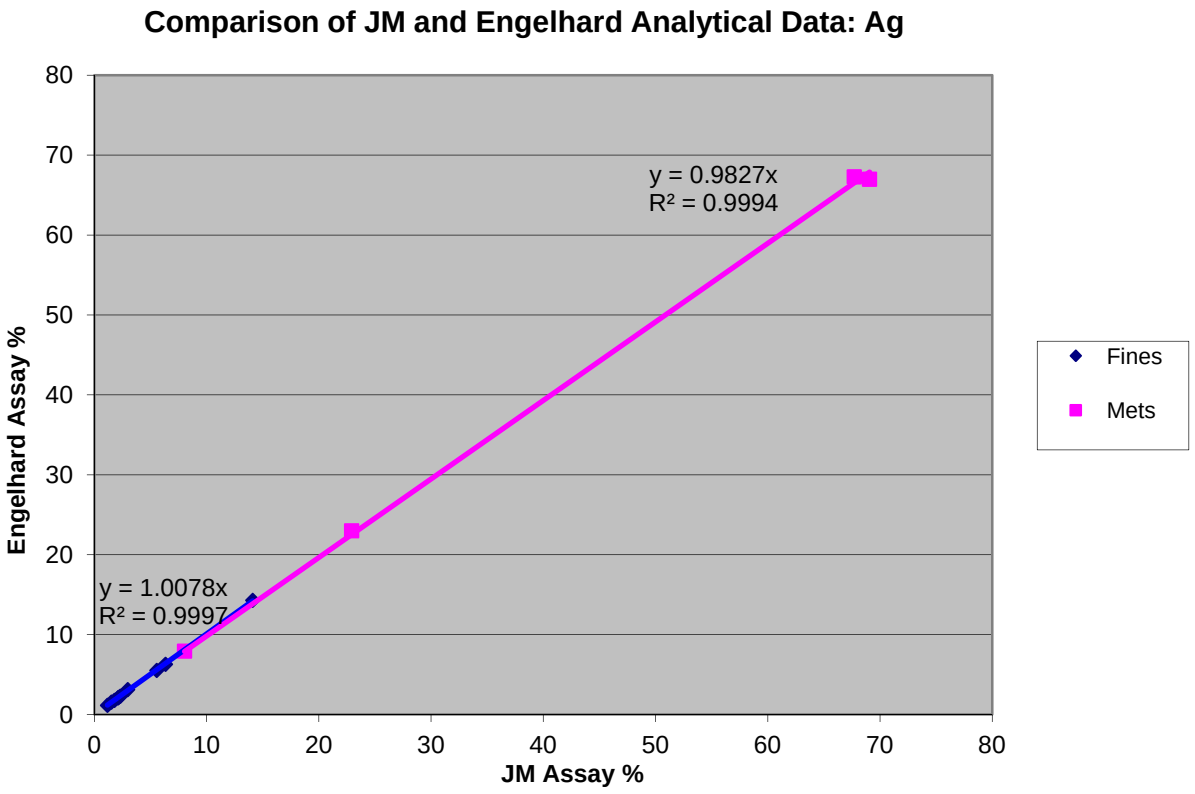

Fig. 4.27 Comparison of Engelhard and JM analyses for silver. Both fines and mets fractions have good agreement with R^2 values in excess of 0.99.

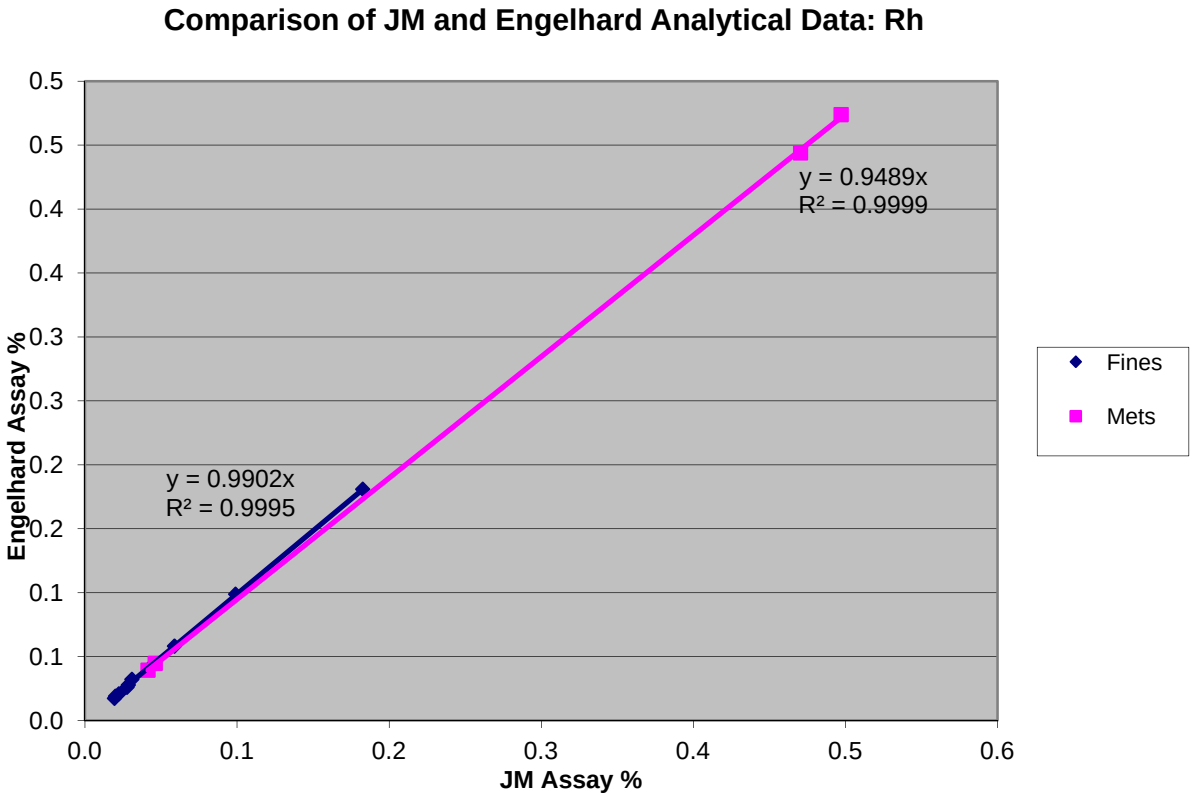

Fig. 4.28 Comparison of Engelhard and JM analyses for rhodium. Both fines and mets fractions have good agreement with R^2 values in excess of 0.99.

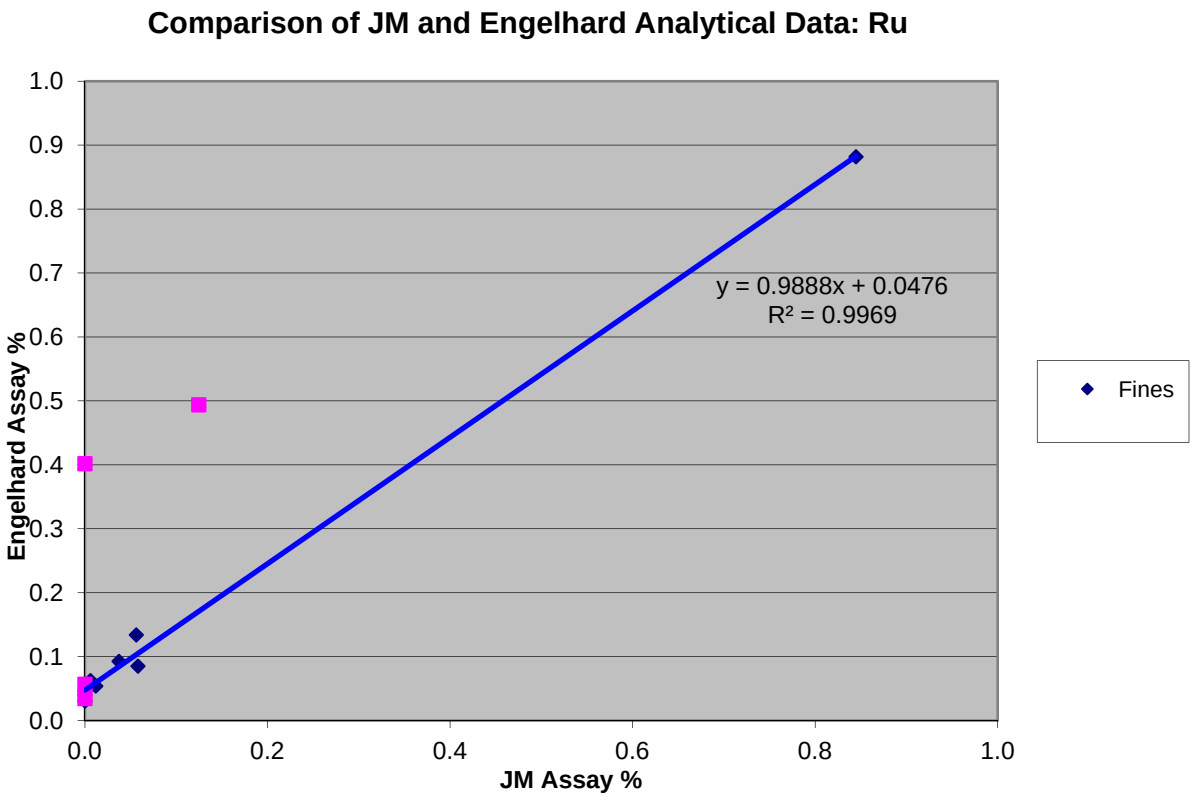

Fig. 4.29 Comparison of Engelhard and JM analyses for ruthenium. Mets agreement (pink) is very poor. Although the agreement for fines looks okay the trend line has been drawn based upon one high concentration value – closer inspection reveals few patterns among the rest of the data points.

It is likely that there is some metal segregation occurring within the Cu discs even with the rapid cooling protocol in place. Different PGMs have varying solubility for Cu and Ir and Ru are known to be particularly challenging to recover (thus the occurrence of "ball-up metallics" of Ir and Ru that have dropped out of solution with copper in the bottom of the rev furnaces, see section 4.6.4). The higher the metal content of the material under test the

more it appears to affect the analysis, thus the reason for the “fines” assay (containing less metal) showing better agreement.

Based upon these graphs it was decided to focus analysis on Ag, Pt, Pd and Rh and to discount Ir and Ru. The most accurate analysis was generated by using a combination of the data from the XRF method for fractions with low metallic content and using JM full digest and ICP analysis for the corresponding highly metallic fraction (after Engelhard had homogenised the material, sampled and produced the copper button). By using this methodology the difference between the XRF analyses and the ICP analyses was reduced to + / - 10% for all samples. Mass balance calculations also showed that for most samples the recombined assay matched the feed assay to within 15%. This was considered to be excellent for such a “difficult” material with highly variable metal content and a complex, multi-stage analysis protocol.

4.8.3 Physical Processing of Refractory Lining Sample 3

4.8.3.1 Particle Size Classification

Five size fractions from d > 9.5 mm to d > 850 µm were considered to be suitable for further processing. These accounted for 76.8% of the lining by mass. The other 23% was fine material generated due to the friable nature of the bricks and was unsuitable for the techniques selected. Table 4.9 lists these fractions and the percentage of the total PGM content of the lining that each one contained.

Table 4.9 The PGM content and mass of the five size fractions selected for further processing

Size Fraction	Pt %	Pd %	Rh %	% Total Mass
16000 ≥ d > 9500	35.9	35.8	29.8	22.5
9500 ≥ d > 5600	19.9	18.7	27.1	13.7
5600 ≥ d > 2000	23.2	23.6	24.1	25.8
2000 ≥ d > 1180	5.1	5.7	5.4	9.2
1180 ≥ d > 850	2.8	3.1	2.3	5.6
TOTAL	**86.8**	**87.0**	**88.7**	**76.8**
Not Used (d ≤ 850)	**13.2**	**13.0**	**11.3**	**23.2**

Table 4.9 indicates that almost 90% of the total PGM content is contained within 75% of the mass of the lining and that the majority of PGM (80%) reports in the three largest size fractions (+9.5 mm, +5.6 mm and +2 mm). These fractions account for just over 60% of the total mass of lining. These three sizes are ideally suited to further physical processing techniques.

4.8.3.2 Magnetic Separation

The five fractions listed in table 4.9 were processed by magnetic separation in order to give two magnetic concentrates and a non-magnetic fraction. The results of the two magnetic separations (at 0.1 T and 0.5 T) were combined in order to show cumulative recovery. Table 4.10 shows the PGM recoveries possible for each particle size.

Using only a combination of particle size classification and magnetic separation it is possible to recover 53% of the platinum, 33% of the palladium and 66% of the rhodium in only 14% of the starting mass.

Table 4.10 The PGM recoveries achieved via cumulative magnetic separation

	Pt Recovery %	Pd Recovery %	Rh Recovery %	% Mass of Lining
>9.5mm 0.1T + 0.5T Magnetics	22.8	13.8	22.1	5.0
>5.6mm 0.1T + 0.5T Magnetics	12.7	8.3	21.9	2.5
>2.0mm 0.1T + 0.5T Magnetics	13.4	7.8	17.0	4.1
>1.18mm 0.1T + 0.5T Magnetics	2.8	1.8	3.3	1.5
>850um 0.1T + 0.5T Magnetics	1.5	0.9	1.6	1.1
TOTAL RECOVERY %	**53.2**	**32.6**	**65.9**	**14.2**

4.8.3.3 Eddy Current Separation

Table 4.11 shows the PGM recovery possible in each of the non-ferrous metallic fractions from eddy current separation. It is possible to recover up to 15% of the platinum, 23% of the palladium and 14% of the rhodium in only 1.6% of the starting mass by fast tracking only the metallic concentrate from the three largest size fractions.

To place this in context if a 30 tonne furnace lining was processed there would be 480kg of metallic material produced. If it was a 40 tonne lining there would be 640kg of metallic material produced. Although it only contains 14 - 23% of the total PGM content this metallic concentrate is “clean” as it contains very little brick. Thus there is the possibility for fast

tracking it through later parts of the smelter circuit thereby avoiding diluting it by returning it to the reverberatory furnaces with other low grade PGM containing material.

Table 4.11 PGM recovery in the non-ferrous metallic fractions produced by eddy current separation

	Pt Recovery %	Pd Recovery %	Rh Recovery %	% Mass of Lining
>9.5mm NF Mets	6.8	8.2	4.5	0.6
>5.6mm NF Mets	4.0	10.2	5.2	0.4
>2.0mm NF Mets	4.1	4.3	3.8	0.6
	14.9	**22.7**	**13.5**	**1.6**
>1.18mm NF Mets	0.4	0.6	0.3	0.8
>850um NF Mets	0.3	0.6	0.2	0.9
TOTAL RECOVERY %	**15.7**	**23.9**	**14.1**	**3.3**

4.8.3.4 Combining Particle Size Classification, Magnetic Separation and Eddy Current Separation

Table 4.12 summarises the most promising combinations of results from laboratory test work. Columns have been added to give an indication of the likely mass for rapid recycling that would be generated by each combination of process techniques, based upon both 30 and 40 tonne linings.

The best recoveries come from a combining the magnetic fractions and the metallic fraction from eddy current separation and "fast-tracking" this material in order to recover the majority of the PGM in a greatly reduced mass fraction.

Depending on furnace capacity as much as 80% of the Rh could be concentrated in 17% of the initial mass or as little as 480kg (1.6% by mass) of highly concentrated metallics could be generated from a whole lining, recovering 15% of the Pt, 23% of the Pd and 14% of the Rh.

Table 4.12 The best combination of process techniques for PGM recovery from spent refractory lining sample 3

Fraction	Pt Recovery %	Pd Recovery %	Rh Recovery %	% Mass of Lining	Kg of Recycle Generated	
					30 tonne Lining	40 tonne Lining
All sizes Magnetics plus Metallics	68.9	56.5	80.0	17.4	**5220**	**6960**
+9.5mm to +2mm Magnetics plus Metallics	63.9	52.6	74.5	13.1	**3930**	**5240**
All sizes Combined Magnetics	53.2	32.6	65.9	14.2	**4260**	**5680**
All Sizes Metallics	15.7	23.9	14.1	3.3	**990**	**1320**
+9.5mm to +2mm Metallics	14.9	22.7	13.5	1.6	**480**	**640**

4.8.3.5 Estimated Cost of Processing Refractory Brick at Pilot Scale

Upon completion of the extended study on lining sample 3 Johnson Matthey decided to conduct some onsite trials at pilot scale based upon to some of the best / most practical concentrations achieved during this study. The aim of the pilot trials was to test realistic,

near market and cost effective options for 'fast track' reprocessing and rapid PGM recovery from spent refractory lining. If successful the plant could potentially provide a rapid PGM recycle in the future for other, similar, waste materials produced onsite (e.g. arc furnace slag, used crucibles etc.). Based upon these guidelines the simple flow sheet for these pilot trials was finalised as per figure 4.30.

As the final part of this study Johnson Matthey requested a summary of costs for purchasing and operating the equipment necessary for the flow sheet outlined in figure 4.30, capable of processing between two and five tonnes of material per hour (tph).

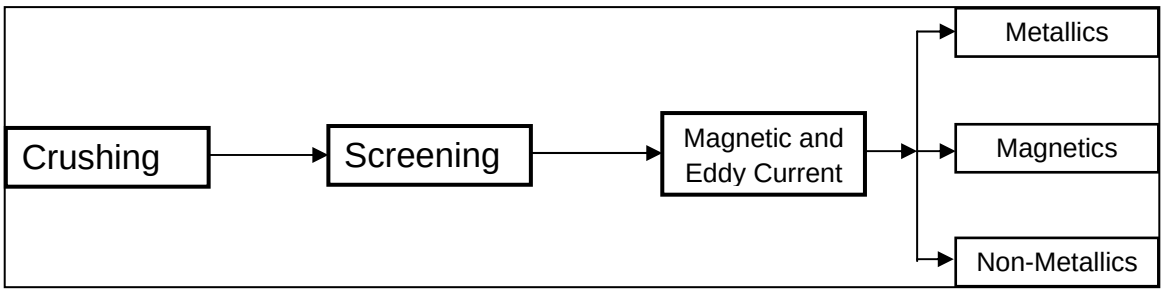

Fig. 4.30 *The simplified flow sheet recommended for initial pilot scale trials.*

The capital equipment costs were compiled from selected UK equipment manufacturers (Russell Finex, Eriez magnetics and Master Magnets) in 2009. Typical used equipment prices were also provided by the same companies. The equipment costs and energy consumption figures are provided in tables 4.13 and 4.14. The cost table includes a provision for materials handling of the separated brick fractions (e.g. hoppers and small vibratory feeders). This is a cost estimated at 10% of the total new capital plant cost in line with IChemE design

guidelines (Hirst *et al.*, 2002). The cost and energy requirements of crushing are not included in these tables as used linings are currently crushed prior to storage and smelting in order to produce a suitably sized feed for the rev furnaces.

As per table 4.13 the cost of the equipment includes two magnetic separation drums. The low intensity ferrite drum (0.1 T) is only capable of removing ferromagnetic particles from feed material. Weakly magnetic / poorly liberated particles will not be separated and will remain in the feed to the eddy current separator unit, potentially reducing the separation efficiency. Adding a second rare earth drum (with a higher field strength of 0.5 T) allows removal of this paramagnetic material in order to further enhance the performance of the eddy current unit and to provide an additional magnetic concentrate which has enhanced PGM levels for rapid processing through the smelter. It is not possible to use the rare earth drum magnet to remove all magnetic phases (paramagnetic and ferromagnetic) in one pass due to discharge problems with the large ferromagnetic particles from the revolving drum. Hence it is recommended that the magnetic drums are used in series to optimise the performance of the eddy current separator downstream. This will give maximum possible PGM concentration and recovery combined with minimum processing problems and operator input.

Overall, the capital costs for the flow sheet containing both the ferrite and rare earth magnetic drum separators is £51,029 for new equipment and £20,939 for used equipment. The energy consumption for this process ranges from 66 kWh to 165 kWh for a 40 tonne furnace lining.

Table 4.13 *Capital costs for new and used PGM concentrating equipment.*

EQUIPMENT	Costs (£)	
	New	Used
Russell Finex Screens	14,000	1,000
Low Intensity Ferrite Drum	2,750	300
High Intensity Rare Earth Drum	7,670	3,000
Eddy Current Separator	19,970	10,000
Spares	2,000	2,000
Materials Handling	4,639	4,639
Total	**51,029**	**20,939**

Table 4.14 *Energy consumption of each element of the flow sheet at two different feed rates. 2 tph is anticipated for development work with the fully operational plant running at 5 tph.*

Equipment	Energy Consumption per Lining kWh	
	2 tph Feed Rate	5 tph Feed Rate
Russell Finex Screens	30	12
Low Intensity Ferrite Drum	5	2
High Intensity Rare Earth Drum	5	2
Eddy Current Separator	125	50
Total	**165**	**66**

In 2009 electricity cost 12.5 pence per kWh on average for large scale commercial users. Therefore if the plant operated at 2 tph it would cost less than £21 per lining to produce two magnetic concentrates and one eddy current concentrate for fast track metal recovery, based on the energy requirements in table 4.14. If the plant operated at its full capacity of 5 tph the cost would decrease to just over £8 per lining. Given that a lining is 40 tonnes these figures equate to an additional cost of £0.21 to £0.52 per tonne (excluding capital equipment

costs). Table 4.12 showed that using this flow sheet (in a laboratory setting) 69% of the Pt, 57% of the Pd and 80% of the Rh in a lining could be concentrated in less than 17% of the initial mass, generating 7 tonnes of material for fast track metal recovery.

Due to the low discard limits in place at the Brimsdown refinery (less than 2 ppm Pt or Rh) it was not possible to produce a clean throwaway fraction that did not require smelting and so all spent lining ultimately has to undergo high temperature pyrometallurgical treatment for PGM recovery. However for a small additional cost (i.e. £0.21 to £0.51 per tonne) it is possible to recover significant amounts of metal, rapidly, in less than a fifth of the starting mass. To set these processing figures in context PGM smelting costs around £125 per tonne (Anglo Platinum, 2011 www.angloplatinum.com/business/operations/smelters.asp) and so the pilot plant processing costs are small by comparison. The annual fast track concentrate produced from 200 tonnes of lining could contain as much as £16 to £35 million of PGM (depending on individual PGM prices) and so the ability to recover this metal and return it to the recycling chain rapidly at minimal cost is an attractive one.

4.8.3.6 Conclusions from Physical Processing of Refractory Lining Sample 3

Just over 75% of the spent refractory lining is suitable for processing via magnetic and eddy current separation. 23% is too fine to be handled without dust issues. This 75% contains almost 90% of the total PGM content. Therefore a relatively inexpensive set of physical processing equipment is suitable for processing the bulk of the lining containing almost all of the PGM.

By using established physical processing techniques it is possible to produce a PGM-rich concentrate thereby reducing the mass for recycling via a traditional smelting route. This will provide significant energy saving and environmental benefits over the current method.

It would be beneficial to conduct a complete magnetic profile for each size fraction in order to establish the necessary field strengths for optimum PGM recovery. The rare earth hand magnet used for these tests had a field strength of 0.5 T, however it is now possible to purchase rare earth permanent magnetic drum separators with field strengths up to 1.2 T. Future work will explore this possibility.

4.9 Additional Test Work Carried Out

In addition to the test work reported here refractory lining sample 3 was also subjected to magnetic profiling via the use of a disc separator for particles below 2 mm and the use of four industrial scale magnetic drum separators (with varying sizes, shapes and strengths of magnetic blocks which in turn affected the magnetic field gradient, field intensity and pole pitch) for particle sizes above 2 mm. Samples of metal contaminated brick were also characterised using EPMA in order to investigate metal associations within individual metallic prills in the brick particles. Colour, infrared and conductivity separations were carried out on a sensor based sorter and a potential route for metal recovery in the finest fraction (which accounted for 23% of the third test sample) via the use of a vertical vibration separator.

5. Characterising and Leaching Two Automotive Catalysts

5.1 History and Function of Catalytic Converters

Catalytic converters ("autocats", "car cats") have been in use since the 1970's and are one of the most effective ways to reduce smog and related pollution due to car exhausts (Ozkaya *et al.*, 2006).

It is necessary for TWCs to convert three main pollutants (unburned hydrocarbons, carbon monoxide and nitrogen oxides) simultaneously. With the implementation of stricter automotive emission regulations (Euro V and VI legislation) (European Union, 2010 http://europa.eu/legislation_summaries/environment/air_pollution/l28186_en.htm), this technology must soon guarantee a conversion level in the range of 96% and even higher for major pollutants over the lifetime of the vehicle (Liwei *et al.*, 2008).

5.2 Structure of Catalytic Converters

There are five major components in vehicle exhaust catalysts: the support (usually a ceramic monolith), the washcoat (usually alumina), stabilisers and promoters (usually rare earth oxides) and platinum group metals (PGMs). Figure 5.1 shows both a schematic diagram and a photograph of a catalytic converter (comprising two monoliths) in an exhaust system.

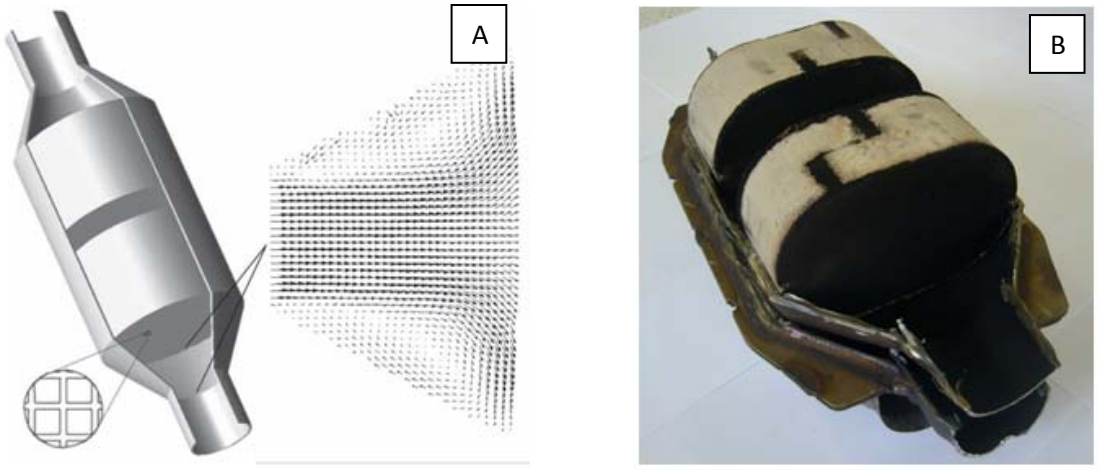

Fig. 5.1 (A) Schematic diagram showing catalyst configuration comprising two monoliths in an exhaust system, catalyst channels and flow separation in a diffuser, compared with (B) a photograph of an autocatalyst (with top casing removed) used for leachate production. (A) is reproduced from Quadri *et al.* (2010).

5.2.1 Supports

The most commonly used support materials are multicellular ceramic monoliths, which have a highly open structure and exert little back pressure in the exhaust system. The design of the substrate should provide a maximum superfacial surface area, as it is upon this surface that the catalytic coating is applied, and on which the pollutant and reactant gases must impinge in order to react (Angelidis and Sklavounos, 1995; Quadri *et al.*, 2010).

A variety of materials can be used to produce substrates; typical examples are alumina, silicon carbide and boron nitride. However monoliths formed from alumina are particularly susceptible to thermal shock problems and readily crack during rapid temperature variations and although silicon carbide and boron nitride both have suitable material properties they are both expensive materials (Twigg and Wilkins, 2006).

As a result the monolith honeycomb structure is generally composed of magnesium cordierite $2MgO.2Al_2O_3.5SiO_2$, and in excess of 90% of catalyst substrates in cars today are made in this way (Twigg and Wilkins, 2006). The channels of the monolith are small, in the order of 1 mm, which allows for a large number of channels, increasing the surface area to volume ratio and conversion rates (Depcik and Assanis, 2005).

In order to further increase the surface area of the monolith, a coating of a highly porous support material is applied to the monolith - this is known as the washcoat. Figure 5.2 shows a small section of the catalyst from figure 5.1 (B) with the gas flow channels clearly visible. It also contains a schematic illustrating the typical distribution of washcoat on the walls of square monolith channels.

Fig. 5.2 (Left) A small section of the car catalyst from figure 5.1 (B) set in resin prior to SEM analysis, showing individual gas flow channels. (Right) Schematic showing a typical distribution of washcoat (B) on the walls (A) of square monolith channels.

5.2.2 The Washcoat

The washcoat usually consists of ɣ-alumina as a substrate for the valuable catalytic metals (platinum group metals; PGMs) and a variety of additives to improve the catalytic action and to stabilise alumina and active metals at exhaust operating conditions (Harrison *et al.*, 1988; Angelidis and Sklavounos, 1995; Papavasiliou *et al.*, 2009). The washcoat typically makes up around 20% of the total monolith weight (Papavasiliou *et al.*, 2009) and is usually 50-200 µm in thickness (Jimenez de Aberasturi *et al.*, 2011).

Washcoats can be applied as either a single layer or multiple layers may be applied on top of each other. This is sometimes done to ensure good physical separation of components that interact together in a negative way (Twigg and Wilkins, 2006).

Washcoat additives are generally rare earth oxides (such as ceria) and / or zirconia. These serve as stabilisers and catalytic activity promoters and significant improvements in TWC performance have been achieved through their inclusion (Muraki and Zhang, 2000; Papavasiliou *et al.*, 2009). Stabilisers are often added to the washcoat to maintain the high surface area at the elevated temperatures which are encountered under operating conditions. Promoters are included to improve the activity or selectivity of the catalyst and can have a strong influence on performance.

5.2.2.1 Ceria

The primary function of ceria (CeO_2) in three way catalysts is to provide oxygen storage capacity in order to allow the catalyst to operate over a wider range of air / fuel ratios (Harrison *et al.*, 1988; Muraki and Zhang, 2000; Papavasiliou *et al.*, 2009). It does this due to its ability to undergo rapid redox cycles, $2CeO_2 \rightarrow Ce_2O_3 + (1/2)O_2$, thus acting as an oxygen buffer by storing / releasing O_2 due to the Ce^{4+} / Ce^{3+} redox couple (Papavasiliou *et al.*, 2009).

The beneficial properties of ceria such as oxygen storage capacity are closely related to its specific surface area and are thus attenuated upon thermal treatment. Sintering of ceria facilitates the sintering of the precious metal supported on it, leading to thermal deactivation of the catalyst (Nagai *et al.*, 2006). Zotin *et al.* (2005) noted that thermal deactivation is related to a number of factors, namely the washcoat sintering process, alloy formation among the compounds, support alterations (mainly phase changes of alumina) and interactions among precious metals and other metals.

Cerium-based oxide is also widely used (in addition to its oxygen storing / releasing performance) for stabilising precious metal dispersion. Diwell *et al.* (1991) reported that formation of a Pt-ceria complex under oxidising conditions could maintain Pt stability against sintering. Murrell *et al.* (1991) showed that the precious metal oxide structure interacts strongly with the ceria surface; however the nature of the Pt-ceria interaction is complicated and not yet well understood.

5.2.2.2 Zirconia

Addition of zirconia (ZrO_2) is considered the most effective way for ceria stabilisation. It has been reported that ceria-zirconia solid solution yields an improvement in the oxygen storage capacity of ceria, redox properties, thermal resistance and catalytic activity at low temperatures (Papavasiliou *et al.*, 2009). Harrison *et al.* (1988) stated that exhaust temperatures can exceed 1000˚C during operation but Twigg and Wilkins (2006) claimed that most present day catalysts commonly operate at 600 to 800˚C. Zotin *et al*. (2005) concurred with this and stated that thermal degradation of catalysts begins at temperatures between 800 and 900˚C, depending on the specific composition. High thermal durability is particularly important as a more thermally durable catalyst can be fitted much closer to the engine, where exhaust temperatures are higher and where it will reach light off (the temperature at which it becomes active and starts converting pollutants) more rapidly. This is critical as the pollutants emitted before the catalyst reaches light off account for the great majority of total emissions (Johnson Matthey, 2003).

Papavasiliou *et al.* (2009) stated that washcoat of a typical modern catalyst contains somewhere in the order of 80% alumina, 9% ceria and 11% zirconia (i.e. a 4:5 ratio of ceria to zirconia), however the two test catalysts are ten years older and so may differ in composition.

5.2.3 PGM Loading

The primary catalytic components of current car exhaust catalysts are platinum group metals (PGMs), which combine the benefits of high activity, particularly at low temperatures, with stability and resistance to poisoning (Harrison *et al.*, 1988; Shelef and McCabe, 2000). Since emissions legislation is set to get tighter and the duty required of the catalyst grows, it seems likely that PGMs will continue to be used for the foreseeable future as base metals are generally not as active or as stable as the PGMs over the life of a vehicle (Twigg and Wilkins, 2006).

The PGMs are located in the surface of the washcoat where they are exposed to exhaust gases. Generally these PGMs are fixed in the washcoat surface by impregnation or coating from a solution of hexachloroplatinic (IV) acid, palladium chloride ($PdCl_2$) and rhodium chloride ($RhCl_3$), before being reduced to their metallic form (Moldovan *et al.*, 1999; Jimenez de Aberasturi *et al.*, 2011).

Patents submitted by Wan *et al*. (1987), Mussman *et al*. (2001) and Wei *et al*. (2009) all suggested an initial PGM loading of between 0.001 wt% and 10wt% but state that more typically between 0.05 wt% and 5 wt% of the washcoat is PGM. This equates to 0.01 to 1 wt% of the entire catalyst being PGM.

Ozkaya *et al.* (2006) stated that the required particle size of PGM particles in Johnson Matthey catalyst washcoat is in the region of 8-10 nm when produced. Twigg and Wilkins

(2006) stated that PGMs are highly dispersed in a washcoat in the form of crystallites of less than 10 nm in order to maximise catalytic performance. Over the operational life of the catalyst agglomeration and sintering can cause the active metal to form larger, less active crystallites, decreasing the active surface area (Nagai *et al.*, 2006). Ozkaya *et al.*, (2006) found (using a FEGSEM with elemental mapping capability) that a range of PGM particle sizes were observed in the alumina washcoat of spent car catalysts, ranging from 8 nm to 100 nm. As the recorded particle sizes at manufacture were 8 to 10 nm, some particle enlargement had clearly taken place over the operational life of the catalyst.

To achieve the best overall performance from the PGMs it is common practice to combine the advantages of platinum, palladium and rhodium in individual catalysts. As technology has improved, enhanced performance, lower cost palladium / rhodium three-way (i.e. platinum free) catalysts have been developed for some applications, especially smaller cars (Twigg and Wilkins, 2006).

5.3 Contaminants

Two of the key catalyst poisons found in petrol until recently were lead and sulphur. Although levels of lead currently found in unleaded fuel (more correctly identified as low-lead fuel as it is not entirely absent) have reduced to the point where they are on the borderline of detection, until the mid-1990s they were significantly higher and could substantially affect catalyst performance.

Prior to 1996 sulphur levels in European petrol and diesel could vary between around 75 and 1000 ppm with a national UK average of around 300 ppm. By 2005 this had been reduced to 50 ppm and by 2009 10 ppm was the maximum permissible level (Twigg and Wilkins, 2006). Thus catalysts that were produced ten to fifteen years ago and have recently completed their operational cycle may have significant levels of these "legacy" contaminants.

Angelidis and Sklavounos (1995) carried out a comparison between new and spent car catalysts and found other contaminants, namely phosphorus, calcium, zinc, lead and nickel. Twigg and Wilkins (2006) also noted these contaminants and deduced they came from engine additives, detergents and lubricating oil consumption. A widely employed engine oil additive which was discussed in depth was zinc dialkyldithiophosphate (ZDDP). This organothiol was particularly singled-out for its potential negative effect on catalyst durability and was in fact phased out during 2006 for this reason. However, once again spent catalysts that were in use before 2006 could potentially have zinc and phosphorus contamination.

5.4 Conventional Pyrometallurgical Processing of Autocatalysts

Due to the scarcity, non-renewability and high value of PGMs there is already a well developed recycling route for autocatalysts (Angelidis and Skouraki, 1996; Nowottny *et al.*, 1997; Baghalha *et al.*, 2009). Pyrometallurgical processes have the potential for high recovery rates as well as coping with the impurities found in catalysts (Benson *et al.*, 2000).

Johnson Matthey developed and operates a well-documented recovery process which is now common in the recycling industry. Autocatalysts are decanned and crushed, before being mixed with flux materials and melted in a crucible containing a molten collector metal such as iron or copper, using a plasma torch (Benson *et al.*, 2000). The resulting molten slag is allowed to equilibriate for a period of time while the PGM is recovered into the collector metal at the base of the crucible. The collector metal is then tapped off and the PGM recovered from this by conventional refining techniques. Overall recovery rates of >95% are achieved from a charge with a very low concentration of PGM (<0.1%) (Benson *et al.*, 2000). This process is illustrated in figure 5.3.

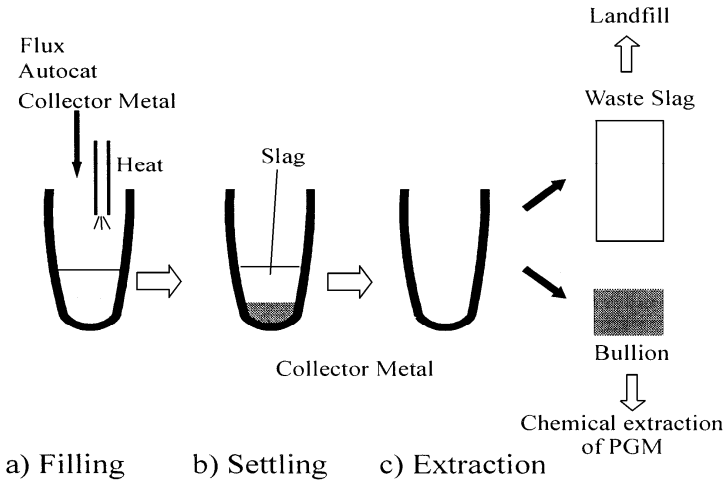

Fig. 5.3 Schematic outline of the JM pyrometallurgical process (from Benson *et al.*, 2000).

5.5 Hydrometallurgical Processing of Autocatalysts

As detailed in section 5.4, commercial recycling of autocatalysts is generally done via a pyrometallurgical route; however this is energy-expensive and carries a heavy CO_2 burden. A number of researchers have published work on alternative hydrometallurgical extraction

(e.g. Taylor, 1993; Gaita and Al-Bazi, 1995; Angelidis and Skouraki, 1996; Balcerzak, 2002; Jafarifar *et al.*, 2005; Jimenez de Aberasturi *et al.*, 2011).

The applied hydrometallurgical processes are based on the selective dissolution of the washcoat where the PGMs are dispersed (Angelidis, 2001). One problem is that precious metals are very resistant to dissolution in ordinary acids because of their chemical inertness. Therefore a large amount of strong acid with strong oxidant is required for the dissolution (Jimenez de Aberasturi *et al.*, 2011). Historically these hydrometallurgical processes were very slow and could take several hours, however microwave-assisted leaching has been shown to improve the yield of extracted metal and reduce process time (Taylor, 1993; Jafarifar *et al.*, 2005).

PGMs in general are very resistant to acid dissolutions. For solubilisation of platinum, palladium and rhodium metals from catalysts in aqueous chloride media forming corresponding complexes ($PtCl_6^{2-}$, $PdCl_4^{2-}$, $RhCl_6^{3-}$) the standard electrode potentials for the half reactions are (from Jimenez de Aberasturi *et al.*, 2011):

$$PtCl_6^{2-} + 4e^- \leftrightarrow Pt + 6Cl^- \quad [E^\circ = 0.74V] \qquad (1)$$

$$PdCl_4^{2-} + 2e^- \leftrightarrow Pd + 4Cl^- \quad [E^\circ = 0.62V] \qquad (2)$$

$$RhCl_6^{3-} + 3e^- \leftrightarrow Rh + 6Cl^- \quad [E^\circ = 0.44V] \qquad (3)$$

Equations (1) to (3) show that for a mixture of Pt, Pd and Rh in aqueous chloride media, the standard potentials for the formation of the platinum, palladium and rhodium chloro-complexes require an oxidising agent with a reduction potential >0.74V.

In the case of PGM dissolution with *aqua regia*, the formed nascent chlorine (Cl_2) and nitrosyl chloride (NOCl) provide high oxidation potential and the high chloride ion concentration acts as the complexing agent. HNO_3 and HCl in *aqua regia* undergo the following reactions (4) and (5) (Massucci *et al.*, 1999).

$$HNO_3 + 3HCl \leftrightarrow NOCl + Cl_2 + 2H_2O \quad (4)$$

$$NOCl + H_2O \leftrightarrow HNO_2 + HCl \quad (5)$$

Platinum and palladium can be completely dissolved in *aqua regia*, however rhodium is only partially dissolved. The dissolution of these metals is a redox reaction, described in equations (6), (7) and (8) (Jimenez de Aberasturi *et al.*, 2011).

$$3Pt(s) + 18HCl(aq) + 4HNO_3(aq) \leftrightarrow 3[PtCl_6]^{2-}(aq) + 6H^+(aq) + 4NO(g) + 8H_2O \quad (6)$$

$$3Pd(s) + 12HCl(aq) + 2HNO_3(aq) \leftrightarrow 3[PdCl_4]^{2-}(aq) + 6H^+(aq) + 2NO(g) + 4H_2O \quad (7)$$

$$2Rh(s) + 12HCl(aq) + 2HNO_3(aq) \leftrightarrow 2[RhCl_6]^{3-}(aq) + 6H^+(aq) + 2NO(g) + 4H_2O \quad (8)$$

Research shows monolithic type catalysts can be processed by partial dissolution (Hoffman, 1988). The total dissolution approach is not applicable due to the insoluble cordierite substrate and would in any case be wasteful due to the presence of PGMs in the washcoat

layer only. Hoffman (1988) found that the use of *aqua regia* is advantageous because it produces nascent chlorine which is a more aggressive oxidant than gaseous chlorine. The ɣ-alumina washcoat and PGMs can be dissolved, leaving the cordierite substrate as a leach residue. However problems can be encountered as nitric acid is expensive, the decomposition of *aqua regia* is spontaneous and any residual nitric acid can hamper PGM recovery (Hoffman, 1988). Taylor (1993) showed that PGM extractions of over 95% were possible from monolithic catalysts using *aqua regia*.

5.5.1 Previous Relevant Leaching Studies

Previous work at University of Birmingham (Yong *et al.*, 2003) investigated the hydrometallurgical leaching of autocatalysts using both conventional and microwave assisted leaching. Little detail was given regarding specific methodology but the following was noted as a starting position to develop the leaching protocol used in this work:

- Liquid to solid ratio of 10:1
- Analysis of solids by sieving showed PSD to be 0.04-0.7 mm but no detailed data given
- Conventional leaching = 2 hours, 80˚C, glass impeller
- Microwave assisted leaching = 15 minutes, 120˚C, 92 psi

Yong *et al*. (2003) stated that conventional leaching with 50% *aqua regia* was not effective for PGM solubilisation and that although concentrated (100%) *aqua regia* performed better the long leaching times involved meant that microwave assisted leaching was considered a

more effective method. Using microwave leaching (in a MARS 5 reactor) a temperature of 120˚C for 15 minutes at 92 psi gave approximately 80% PGM recovery in a 50% diluted *aqua regia* solution. Significantly the study did not give the specific proportions of Pt, Pd and Rh recovered during these tests.

It should also be noted that this work appeared to use an unconventional *aqua regia* composition. Normally the formula is 3 parts HCl to 1 part HNO_3 but this work used 3:2 HCl to HNO_3. No reason for this choice was provided by Yong *et al.* but Hoffman (1988) stated that problems during leaching can occur due to residual nitric acid hampering PGM recovery. Thus it would be interesting to compare Yong's values with the data obtained from leaching catalyst 2 (defined in section 5.7) using a conventional *aqua regia* ratio.

Jafarifar *et al.*, (2005) investigated microwave assisted leaching for the recovery of platinum from spent industrial catalyst. Although this is a different substrate to autocatalyst it is a comparable low grade PGM containing material. They investigated the effectiveness of *aqua regia* at a range of different times, temperatures and liquid to solid ratios. Using microwave assisted leaching (Teflon container with microwave heating) they reported a maximum recovery of 98% after 5 minutes at 109˚C with a liquid to solid ratio of 5:1 (i.e. acid to catalyst). As a comparison they conducted the same experiment with conventional leaching technology (heated glass balloon flask with a return-flow cooler) and only reported a maximum recovery of 95.5% after 2.5 hours. Thus as can be seen microwave assisted leaching is substantially faster and gives a slightly higher overall recovery.

5.6 The Choice of Autocatalyst for the Preparation of PGM Leachate

The majority of previous PGM biorecovery research focused on either using model solutions or "real" leachates from mixed metal wastes e.g. spent furnace lining that contained many different metals in addition to the desired PGMs (Murray *et al*. 2007). Model solutions are considered too simple (and therefore non-representative of real world wastes) as they contain only the metals of interest. Conversely complex "real" leachates are difficult to study due to interference effects and the difficulty and expense of accurate mixed metal analysis.

The leaching of autocatalysts provides a good intermediate step between model solutions and complex waste leachates as the cordierite honeycomb is insoluble and hence the leachate is composed of the alumina washcoat and the solubilised PGMs i.e. it is relatively simple with respect to the number of components.

5.7 Characterisation of Car Catalyst

Two spent car catalysts were used in this research. Catalyst 1 was an OEM catalyst from a 2000 Nissan Primera (chassis number SJNTEAP11U0371159, engine number 002572). This catalyst was removed (by Humphries Garage, Oxford) from a known vehicle when it failed to meet emissions standards. The total mileage (130,000) as well as the proportion of urban (8%), A-road (22%) and motorway (70%) mileage from new is well documented for this catalyst. Catalyst 2 was a Peugeot 106 aftermarket (replacement) catalyst that was removed

(by Humphries Garage, Bearwood, Birmingham) after failing to meet emissions standards during an MOT test, however the operational lifecycle of this catalyst is unknown.

5.7.1 Scanning Electron Microscopy (SEM)

Both catalysts were characterised by scanning electron microscopy (Philips XL-30 Environmental SEM with Oxford Inca EDS) prior to undergoing predetermined crushing and leaching protocols. Small pieces (around 1 cm^3) were removed from the monolith for characterisation purposes. These were either mounted directly onto a stub using conductive cement or were set in resin in order to avoid potentially causing stress fractures within the washcoat during polishing and to allow EDS to be carried out on the sample.

Both secondary electron (SE) and backscattered electron (BSE) analysis was used to evaluate the samples. In backscattered mode (BSE) heavy elements (high atomic number) backscatter electrons more strongly than light elements (low atomic number), and thus appear brighter in the image i.e. BSE mode is used to detect contrast between areas with different chemical compositions. For autocatalysts the cordierite support and the alumina in the washcoat should appear darker (lower atomic number) than the ceria, zirconia and PGMs in the washcoat.

5.7.1.1 SEM of Catalyst 1

Figure 5.4 depicts catalyst 1 (the case history catalyst) and clearly shows areas where the washcoat has become detached from the support and lost from the autocatalyst. There are also fairly extensive areas of cracking along the surface of the washcoat.

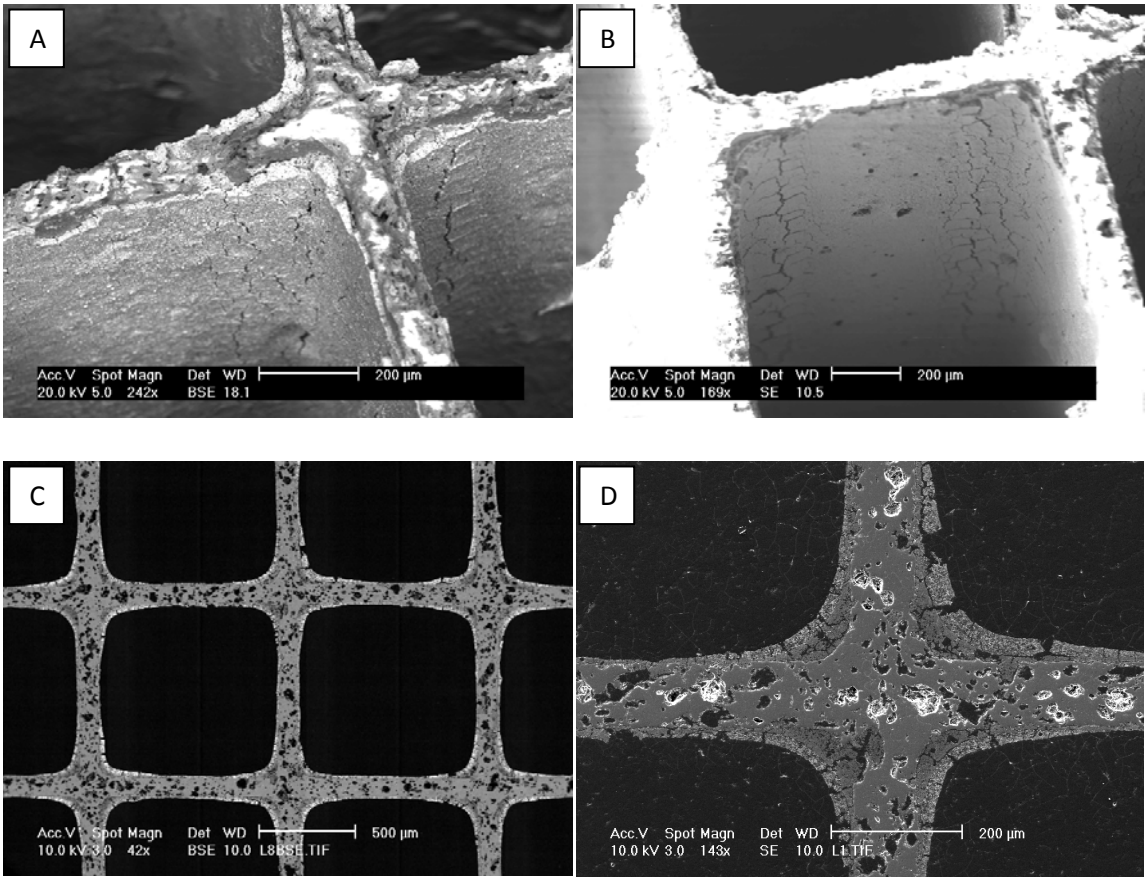

Fig. 5.4 SEM imaging of catalyst 1. (A), (B) and (C) are BSE images and (D) is an SE image.

Figures 5.4 (A) and (B) show catalyst that has not been set in resin. Stage tilting was used so that the internal walls of the catalyst were visible. (A) is was taken from the centre of the catalyst and so fine grinding (by hand with wet fine sanding discs) was employed to ensure the cross section was relatively flat for imaging purposes. (B) was taken from the outside

face of the catalyst and so did not require grinding. Both show extensive cracking across the surface of the washcoat and (B) also shows darker patches where areas of washcoat have been completely detached.

To avoid potential criticism that the sample preparation may have caused / contributed to the cracks observed in the surface pieces of catalyst were also set in resin and then polished (to a depth of approximately 1 mm into the sample) in order to examine them in cross-section. Tilted images are not possible once samples have been set in resin and so figures 5.4 (C) and (D) show the catalyst in cross-section from directly above. (C) shows both the washcoat and the cordierite support of several cells. As expected the cordierite appears darker than the washcoat (visible as lighter material in the corners of each channel). (D) shows that even when no force was applied to the catalyst during sample preparation (encapsulated in resin) there were still numerous cracks and holes in the washcoat i.e. these are not a function of sample preparation.

Figure 5.5 also shows catalyst 1. The magnification has been increased and it can now be observed that this catalyst has been coated with two separate washcoats. The outer coating appears as much lighter than the inner coating and suggests that the (heavy atomic number) precious metals occur in the outer layer only. The inner coating appears to have been applied to reduce “dead space” in the corner regions in order to thrift PGMs by applying them only where they will be effective. (H) shows that there is very little of the PGM containing outer washcoat remaining in the middle of the channels and suggests that a

reduction of reaction surface for PGM – exhaust gas interaction or a reduction in overall PGM content may be reasons for failure of this catalyst.

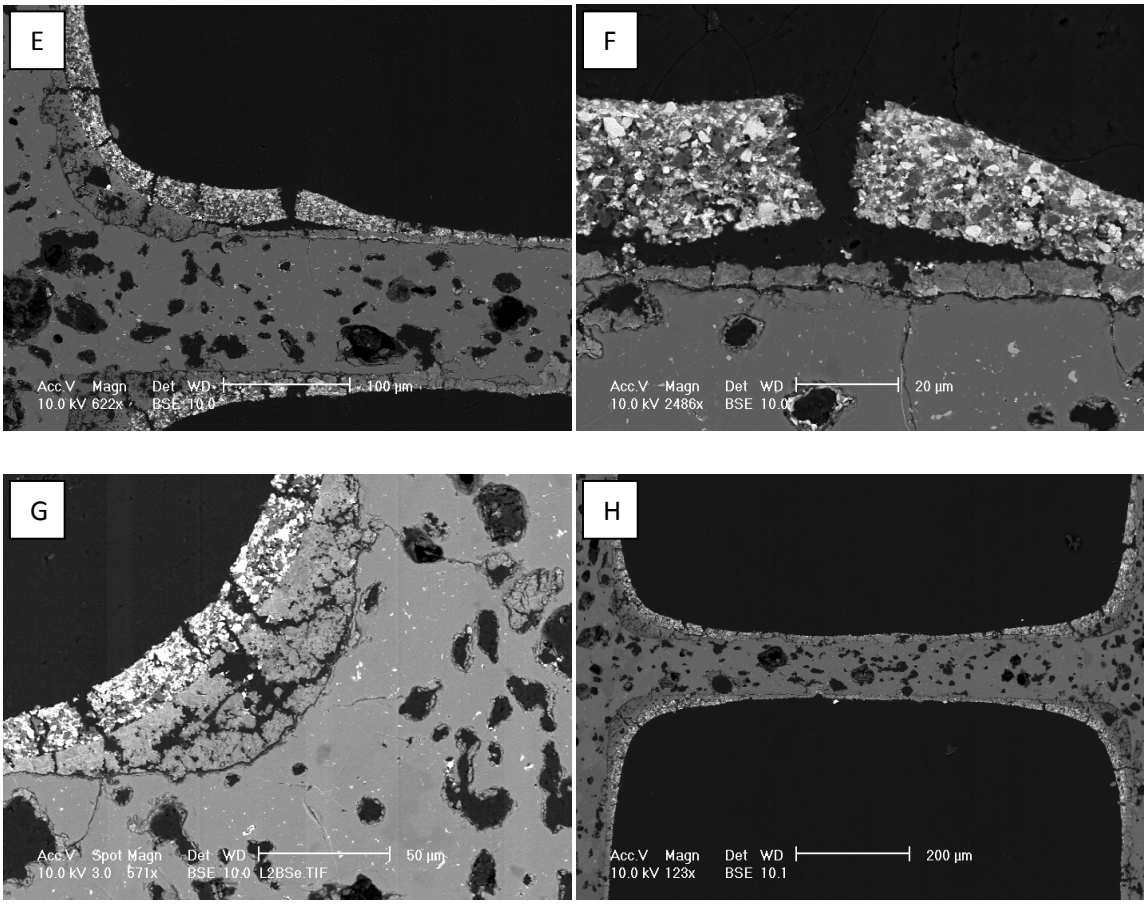

Fig. 5.5 Higher magnification backscattered electron images of samples of catalyst 1. Two distinct washcoat layers are clearly visible in (E), (F) and (G). (H) shows that there is very little of the outer PGM containing washcoat remaining in the middle of the channels.

Figure 5.6 shows measurements of washcoat layer thickness in the corner sections where four channels intersect i.e. the place where the washcoat is thickest. This measurement micrograph was typical of the larger catalyst sample. The total washcoat thickness varied

from 48 to 58µm, with the inner layer being 27 to 41 µm and the outer PGM containing layer being only 17 to 22 µm in thickness.

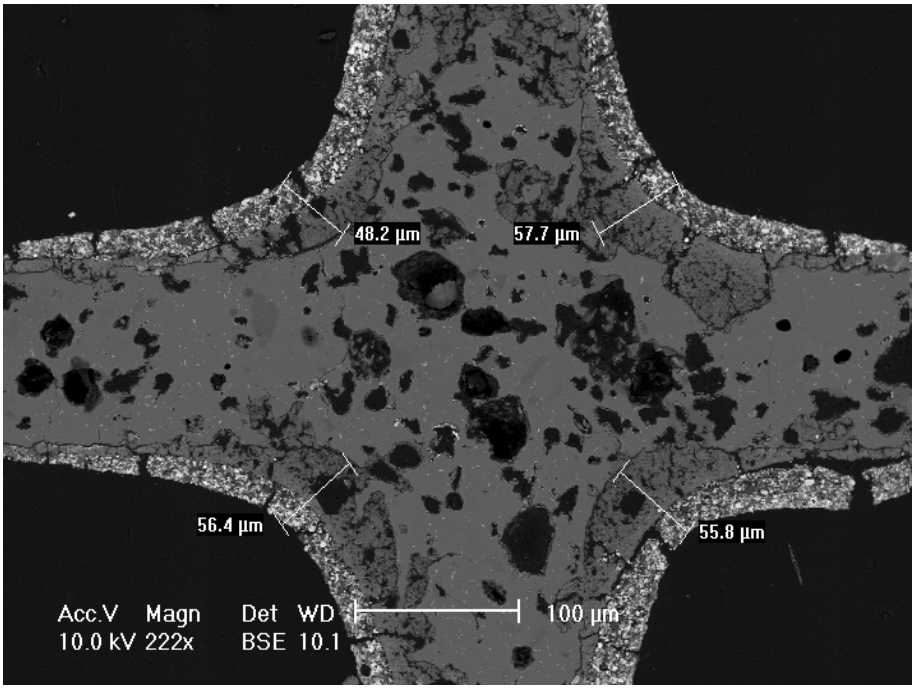

Fig. 5.6 The total thickness of washcoat in the corner sections of four adjacent monolith channels in catalyst 1.

5.7.1.2 SEM of Catalyst 2

Figure 5.7 shows SEM characterisation of catalyst 2. This differs from catalyst 1 (the original manufacturers catalyst) as it only has a single layer of washcoat (visible in (C) and (D)) and appears to have less surface cracking. However as can be seen in (B) the extrusion of the support in this catalyst seems to be poorer than the case history catalyst as the cells are deformed. Although there appears to be less surface degradation overall (D) shows that pieces have still been lost from the washcoat during operation. The particle size of heavy atomic number elements (brighter particles) in the washcoat of this catalyst appear to be

larger than catalyst 1, however there are more dark areas in the washcoat suggesting that fewer heavy elements are present overall.

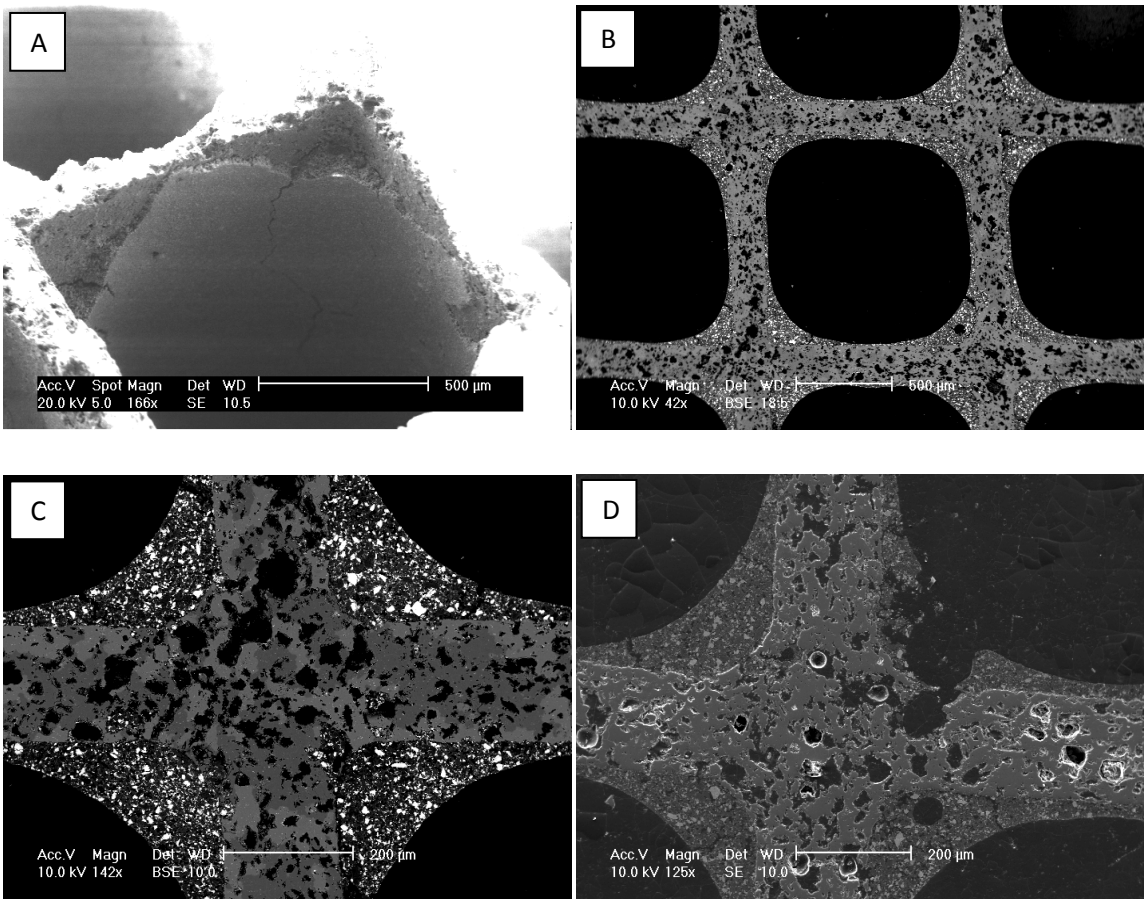

Fig. 5.7 SEM imaging of catalyst 2. (B) and (C) are BSE images and (A) and (D) are SE images. As per catalyst 1 areas of cracking (A) and missing washcoat (D) are visible, however they seem less extensive in this example than in the case history catalyst sample.

Figure 5.8 shows measurements of washcoat layer thickness in the corner sections where four channels intersect (for comparison with catalyst 1). This catalyst had a single layer of washcoat which varied in thickness from 120 to 140 µm. Cracks and small areas of missing washcoat are visible in this picture, but to a lesser extent than that observed with catalyst 1.

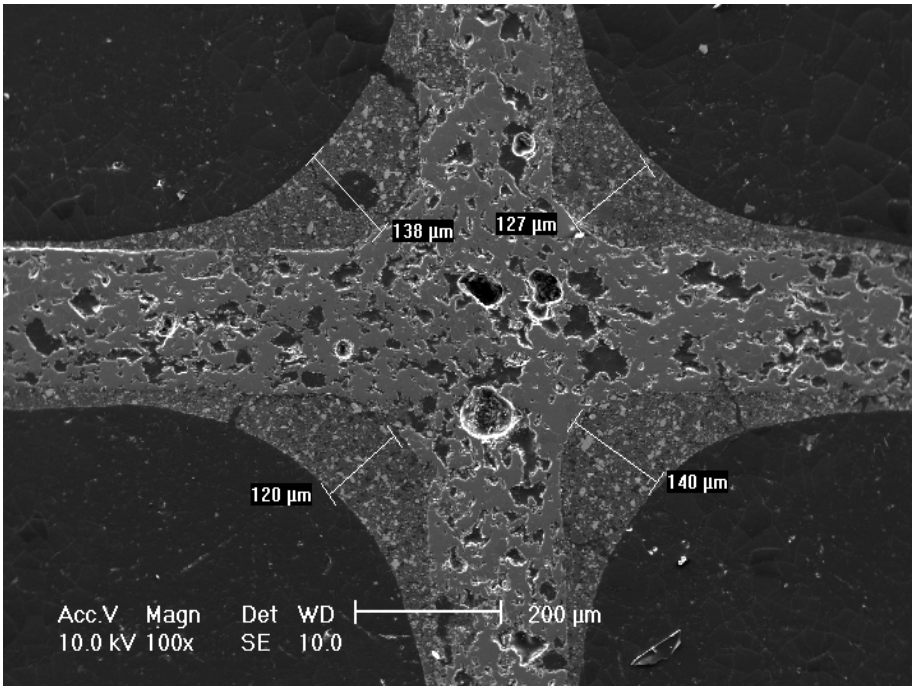

Fig. 5.8 The total thickness of washcoat in the corner sections of four adjacent monolith channels in catalyst 2.

5.7.2 Energy Dispersive X-Ray Spectroscopy (EDS)

5.7.2.1 EDS of Catalyst 1

The SEM was equipped with an INCA EDS system for elemental analysis. Both catalysts were examined using this technique. The EDS results for catalyst 1 are shown in figure 5.9. As expected analysis of the cordierite support (A) showed the presence of Al, Mg, Si and O. The inner washcoat appears to be alumina (Al_2O_3), with small amounts of Ce and Zr. The outer washcoat is also alumina but has significantly more Ce and Zr present. This is expected as these metals (in the form of oxides) will stabilise the outer layer at the high temperatures encountered during operation.

No PGMs were recorded in any of the component layers but this is unsurprising due to two main difficulties with SEM / EDS analysis. Firstly the low concentration of precious metals in automotive catalysts is often below the detection limit of EDS detectors. The relative detection limits of the INCA EDS system is in the range of 0.1 to 0.3% and a worn catalyst is likely to have PGM levels significantly below this. Secondly interferences by other elements present a significant difficulty for identification. For used catalysts the main interferences are the Pt-M line, P-K line and Zr-L line. P comes from oil additives and Zr is a component of the washcoat (Palacios *et al*., 2000). Table 5.1 lists the X-ray peaks for selected PGMs and elements that overlap (and therefore interfere) at these energies.

Table 5.1 X-ray peaks for selected PGMs and list of elements that have overlap with these peaks (and can therefore produce interference on EDS spectra). Data from Microanalyst "MA-Table" software.

Element	X-Ray Peaks (keV)	Elements with Peak Overlap
Pd Lα1	2.838	**Cl**-Kβ1, **Rh**-Lβ1
Pd Lβ1	2.990	**Ce**-Lα1
Pd Lβ2	3.172	
Pd Lɣ1	3.328	**K**-Kα1
Pt (Mα1, Mα2, Mβ)	2.0-2.1	**P**-Kα1, **S**-Kα, **Y**-Lβ1, **Zr**-Lβ1
Pt Lα1	9.442	ZnKβ1
Rh Lα1	2.697	**Cl**-Kα1
RhLβ1	2.834	**Pd**-Lα1
RhLβ2	3.001	**Ce**-Lα1
RhLɣ1	3.144	**Cd**-Lα1, **Ce**-Lα1

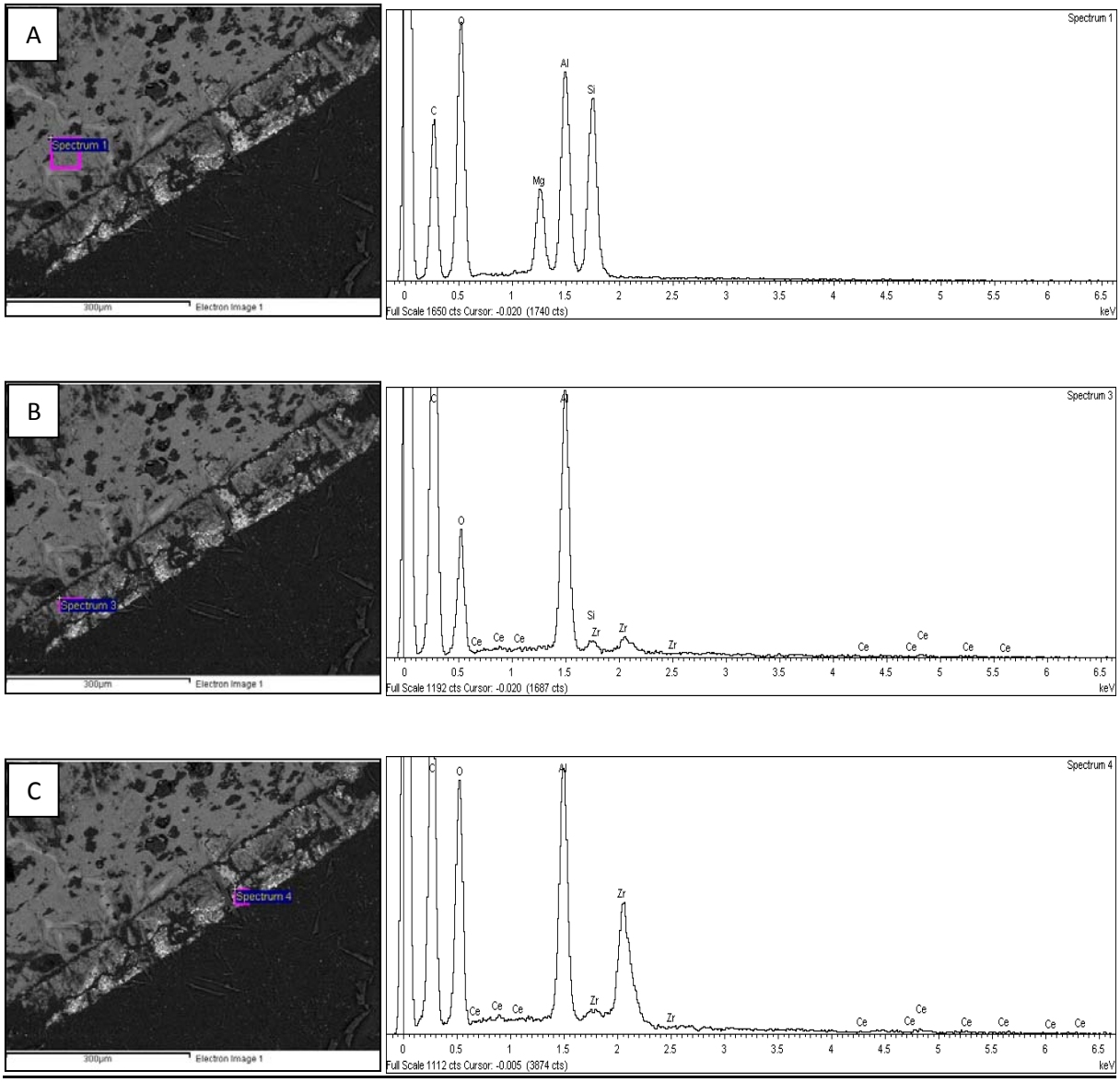

Fig. 5.9 EDS spectra for each layer of catalyst 1. (A) shows the monolith support, (B) shows the inner washcoat layer and (C) shows the outer washcoat layer. Each spectrum was acquired a minimum of three times to ensure accuracy; representative data are shown.

5.7.2.2 EDS of Catalyst 2

Catalyst 2 was also analysed using the INCA EDS system and the results are shown in figure 5.10. The washcoat (B) has a very similar spectrum to the outer washcoat layer of the case

history catalyst 1 with Al, O, Ce and Zr being present. The support (A) has all the elements present in cordierite (Al, Mg, Si and O).

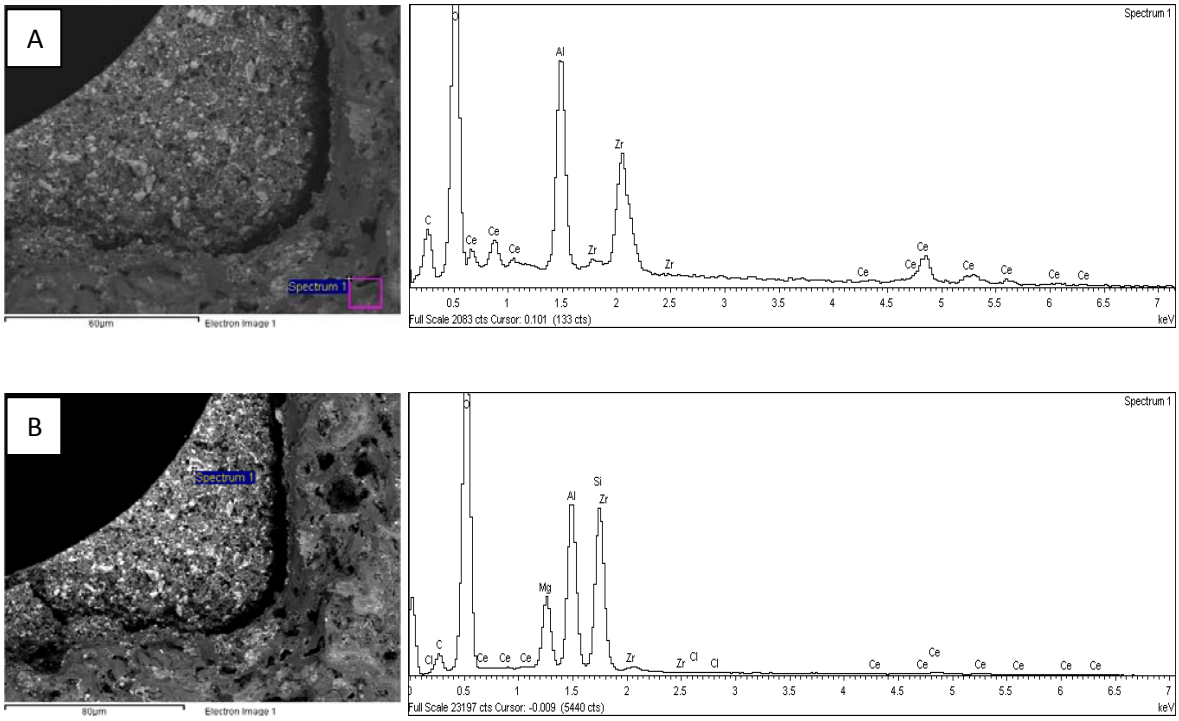

Fig. 5.10 EDS spectra for each layer of catalyst 2. (A) shows the monolith support and (B) shows the washcoat layer.

5.7.3 X-Ray Powder Diffraction (XRD) of Catalysts 1 and 2

The XRD pattern for a representative sample of catalysts 1 and 2 can be seen in figure 5.11. The pattern for both catalysts shows the distinct spinel structure associated with cordierite ceramics. Interpretation of the peaks confirms the presence of cordierite and also indicates the possible presence of cobalt phosphate hydrate in catalyst 1. There is a high probability that this is a misidentification due to the number of peaks associated with multi-phase

systems. It is not listed in the literature as a component of autocatalysts and the EDS analysis did not indicate the presence of Co.

The presence of ɣ-alumina, ceria or Ce-Zr-O_2 solid solution were not found due to the strong intensity of the spinel structure of cordierite. The absence of alumina in the XRD traces of car catalysts has previously been investigated by Liwei *et al.*, (2008), however the presence of alumina is clearly confirmed by the EDS data.

Spinel minerals crystallise in the cubic crystal system, with the oxide anions arranged in a cubic close-packed lattice (Liwei *et al.*, 2008). The intense peaks from this closely packed lattice structure can mask the peaks generated by ɣ-alumina. In addition ɣ-alumina can have broad peaks if it is not well crystallised due to low firing from boehmite and this can exacerbate the problem of masking. XRD is generally only capable of identifying phases that occur in concentrations of 5 wt% or greater. Although there can be as much as 20 wt% ɣ-alumina in a freshly produced autocats, end of life catalysts will have significantly less and may be approaching the detection limits of the equipment. This low concentration in combination with the intense peaks from the cordierite may explain why ɣ-alumina was not detected. There are some small peaks in both patterns that correspond with peaks on "model" XRD patterns for ɣ-alumina but they are weak and do not confirm its presence.

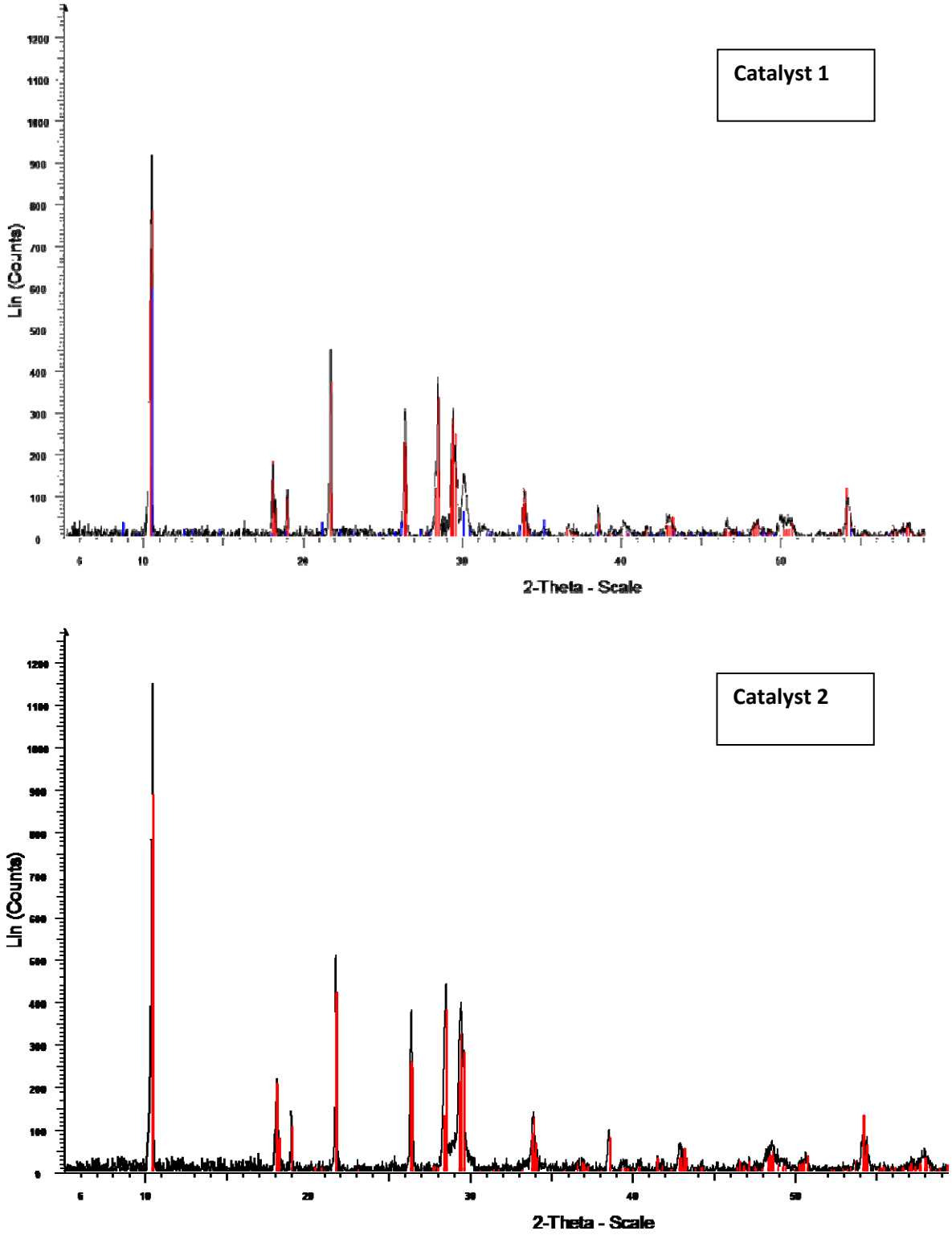

Fig. 5.11 XRD patterns of samples of crushed case history catalyst 1 (top), showing the presence of characteristic cordierite peaks $Mg_2(AL_4Si_5O_{18})$ (red) and cobalt phosphate hydrate $Co_3(PO_4)2.4H_2O$ (blue) and crushed catalyst 2 (bottom), showing the presence of cordierite $Mg_2(AL_4Si_5O_{18})$ (red).

5.7.4 Energy Dispersive X-Ray Spectroscopy (EDS) Elemental Mapping

Based upon initial visual characterisation it was hypothesized that catalyst 2 was likely contain more platinum group metals than catalyst 1 as the former had only a single washcoat layer (i.e. it did not have the lighter atomic number inner layer to thrift metal) and also had a residual washcoat layer that was approximately twice as thick as that on catalyst 1 at the end of its life. Elemental XRF analysis had to be contracted externally and thus was not available during initial material characterisation. As a result the decision was taken to conduct EDS elemental mapping of catalyst 2 in order to attempt to map the location of the PGM particles, while awaiting longer term XRF confirmation.

The INCA EDS software features elemental "mapping" capability, where the composition of the elements on the surface of a specimen can be analysed to produce spatial maps of distribution. The sample is divided into a series of pixels and then the electron beam dwells on each of these pixels to collect X-ray counts via the detector. The number of counts per pixel directly relates to intensity and so the brighter a feature within a map the more of that element is present.

Figure 5.12 shows the elemental map produced from a section of catalyst 2. This map confirms a number of features discussed in section 5.2. Firstly the maps show that silicon and magnesium only occur in the support – this is consistent with it being composed of cordierite ($2MgO.2Al_2O_3.5SiO_2$). Aluminium and oxygen are shown to occur throughout the sample which is also expected due to alumina being a key constituent of both the support

and the washcoat and both Ce and Zr occurring in the form of oxides. Zirconium and cerium only occur in the washcoat layer which again corresponds with the fact that they are used to stabilise the catalytic metals in the washcoat.

Both platinum and palladium are shown to occur in significantly lower concentrations than other elements. However both were shown to occur throughout the sample, with slightly more platinum in the washcoat than the support and palladium evenly distributed throughout. This conflicts with the literature as it is universally stated that PGMs are added to the washcoat layer only in order to minimise metal usage and therefore cost. EDS maps are affected by spectral interferences in the same way as point sample EDS spectra and so it was deduced that this was causing the spurious mapping (see table 5.1).

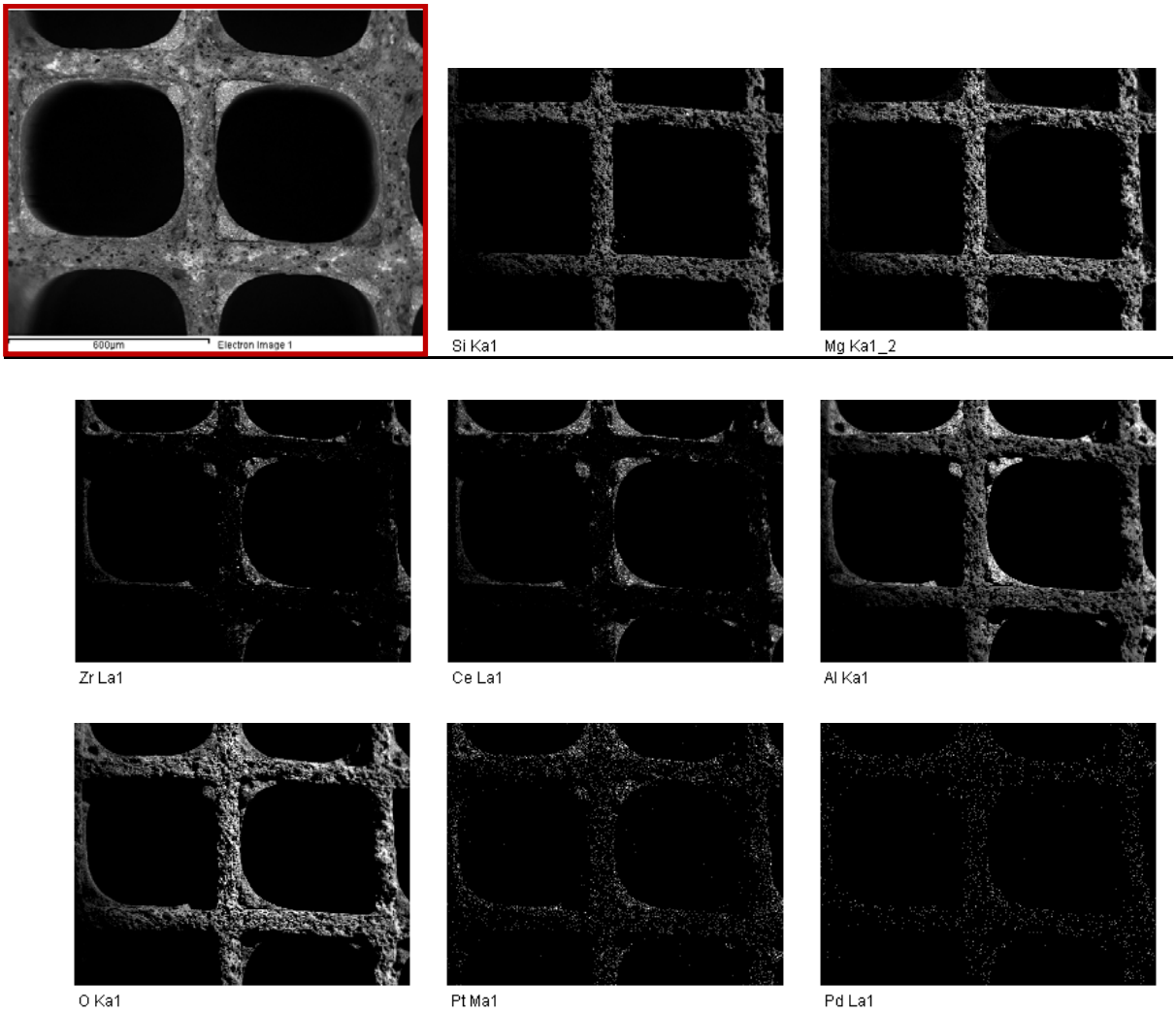

Fig. 5.12 INCA EDS elemental mapping of a section of catalyst 2. The SEM image is highlighted in red with each subsequent map labelled by element.

5.7.5 Wavelength Dispersive X-Ray Spectroscopy (WDS) Elemental Mapping

EDS mapping is rapid and widely available, however its main limitations are relatively poor spectral resolution, high detection limits and element mis-identification due to spectral interferences (Andrews, 2007). WDS mapping operates in a similar way to EDS but its detector classifies and counts the x-rays in terms of characteristic wavelength (instead of

energy level) and so has a much higher resolution, preventing many of the peak overlap errors frequently encountered in EDS analysis.

The combination of better resolution and the ability to deal with higher count rates allows WDS to detect elements at typically an order of magnitude lower concentration than EDS. Its disadvantages include longer scanning times and high cost.

This technique is particularly suitable in the case of a sample where some elements are present in bulk quantities and others in trace amounts and hence a sample of the catalyst 1 was examined by this method to see if information could be gained about PGM location and dispersion. A WDS map was constructed for platinum, palladium and rhodium. The instrument used was a Jeol 7000F with Oxford Inca EDS and Wave WDS located at the University of Birmingham. The INCA Wave WDS software automatically corrects for background counts. For cost reasons only one sample was examined. Figure 5.13 shows the WDS map generated from (case history) catalyst 1.

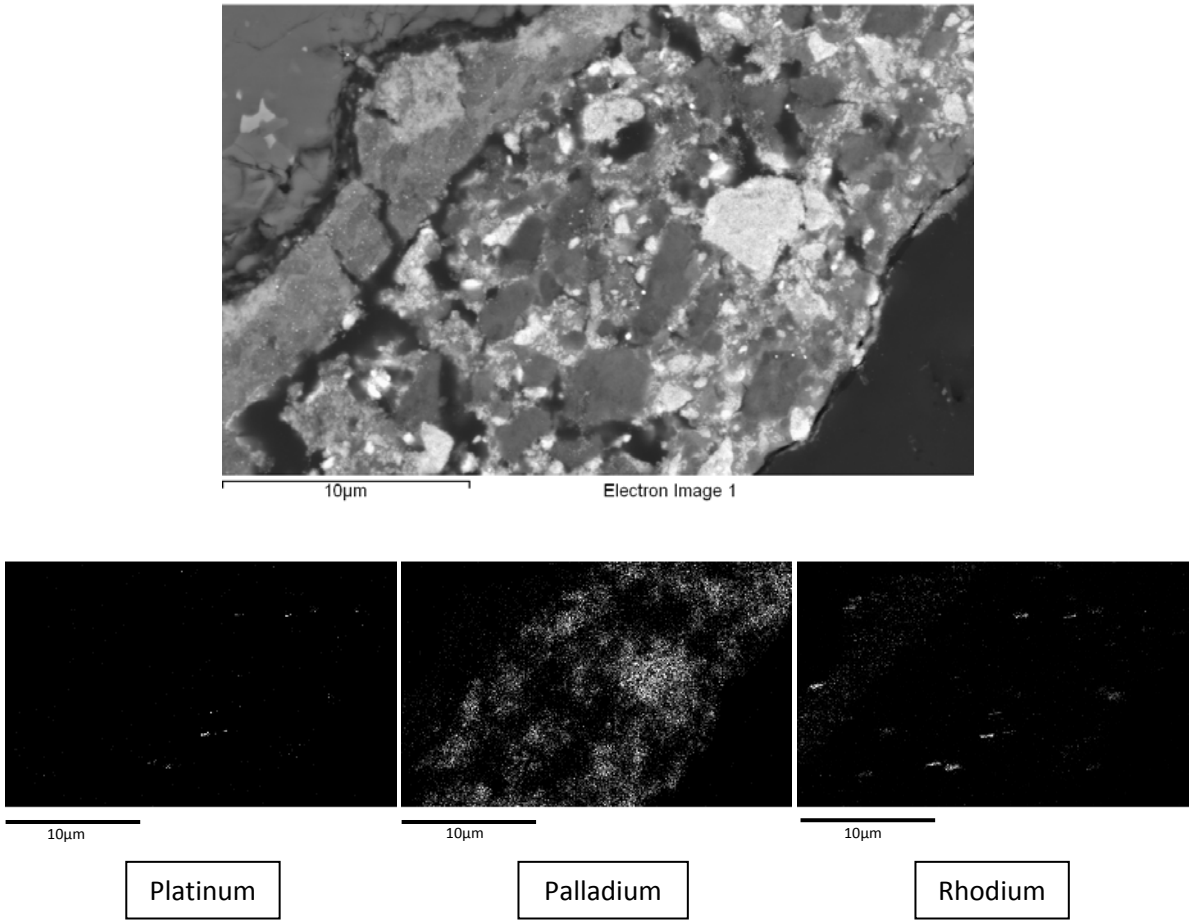

Fig. 5.13 WDS maps of a small area of catalyst 1. The SEM image is shown at the top with the maps for platinum, palladium and rhodium displayed below.

Figure 5.13 indicates that the majority of the PGM in the sample is palladium and that it occurs predominantly in the outer washcoat layer, as expected. There is only a faint trace of platinum visible suggesting very low quantities of this metal are present. The rhodium map indicates that there is more rhodium present than platinum but still far less than palladium. However the rhodium map indicates that much of it is occurring in the inner washcoat layer which is unlikely as rhodium is the most expensive of the three metals and needs to be in contact with exhaust gases in order to be effective. A possible explanation was given in Andrews (2007) describing electron microbeam techniques. He stated that peak overlaps

can occur even in WDX spectra when dealing with the platinum group elements or the rare earth elements, particularly when one of the elements is present in minor to trace quantities. Both of these conditions occur here due to presence of the rare earth element cerium and the very low concentrations of PGMs. Another explanation may be that some of the washcoat has been "smeared" during sample preparation, thereby transporting some of the PGM particles onto the surface of the inner washcoat.

Figure 5.14 shows the PGM positions superimposed onto the SEM image. Colours are used to differentiate the PGMs with palladium being red, rhodium being green and platinum being blue.

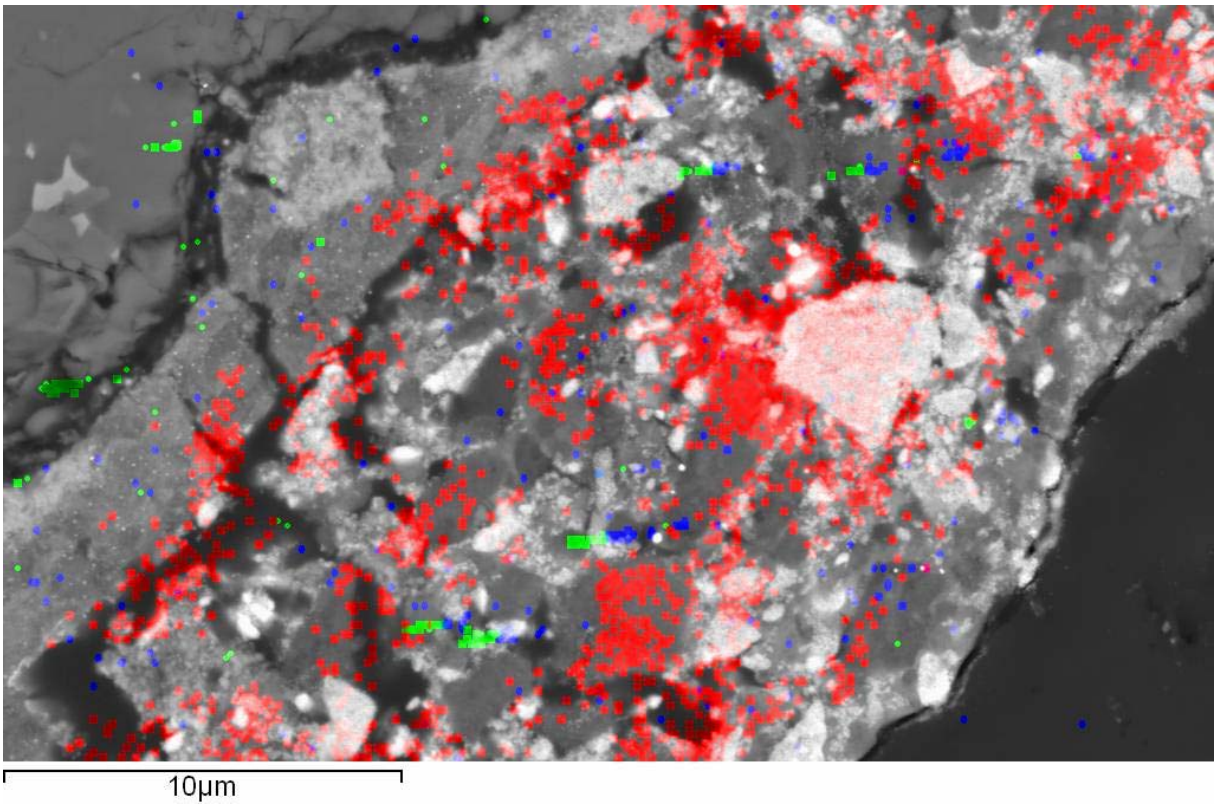

Fig. 5.14 WDS maps superimposed onto their positions on the surface of catalyst 1. Red = palladium, green = rhodium and blue = platinum.

5.7.6 X-Ray Fluorescence (XRF) of Crushed Catalyst

Table 5.2 shows the PGM content of representative samples of both crushed catalysts, verified by XRF by two independent analysis companies. Engelhard analysed two subsamples from the material supplied by copper collection and then XRF of the copper buttons. JM analysed the powder by XRF after fine milling as a check of Engelhard's analysis. Engelhard stated that their XRF method for these samples loses accuracy below 50 ppm (0.005%) due to 6x dilution of sample with copper to form the analysis button.

Table 5.2 The PGM concentration (as % of total mass) of catalysts 1 and 2 after representative sampling (crushing and riffling).

CATALYST 1	Pt%	Pd%	Rh%
Engelhard A	0.000	0.409	0.031
Engelhard B	0.000	0.416	0.030
JM Cross Check	<0.001	0.408	0.036

CATALYST 2	Pt %	Pd %	Rh %
Engelhard A	0.000	0.043	0.007
Engelhard B	0.000	0.040	0.006
JM Cross Check	<0.001	0.046	0.007

The XRF analysis in table 5.2 indicates that both of the used autocatalysts contained less than the detectable limit of platinum. This corresponds with the literature (section 5.2.3) which states that different PGM combinations are used depending on metal price and availability. Engelhard's senior analyst confirmed that Pt free catalysts are now becoming

much more common in the recycling chain (personal communication with Ben Hillary, senior analytical chemist at Engelhard, June 2009). This is due to the fact that palladium has been significantly cheaper than platinum since 2002 and so catalyst manufacturers use palladium in their formulations when possible to control costs.

The XRF data also shows that Pd and Rh were 10 x and 6 x respectively higher in catalyst 1 (the original manufacturers case history catalyst) than the catalyst 2 (the aftermarket test catalyst). Catalyst 1 had over 300 ppm Rh in the crushed solids but catalyst 2 had less than 70.

Based upon initial visual characterisation, in section 5.7.4 it was hypothesised that catalyst 2 (the test catalyst without history) was likely to contain more PGM than catalyst 1 (the case history catalyst) as the former had only a single washcoat layer (i.e. it did not have the lighter atomic number inner layer with the purpose to thrift metal) and also had a residual washcoat layer that was approximately twice as thick as that on catalyst 1 at the end of its life. As the commercial XRF results were subject to delays of approximately three months the decision was taken to leach catalyst 2. However as the XRF data shows in fact catalyst 1 contained significantly more PGM than catalyst 2.

5.7.7 Comparison of Catalysts 1 and 2 with Typical Scrap Car Catalyst PGM Values

Although information on the amount and ratio of PGMs applied to an autocatalyst during production is widely available (and is discussed in section 2.10.3.1) data on the specific composition of catalysts when they are returned for recycling are generally kept confidential by PGM refiners as it has a direct impact on revenue. However Dr. Ben Hillary (senior analytical chemist at Engelhard International Metals, personal communication, 2009) provided some information in order to set the results of this study in context. A large consignment of assorted vehicle catalysts (typically 1000+ catalysts) generally has an overall assay value of approximately 1000 ppm Pt, 800 ppm Pd and 200-300 ppm Rh. However he stated that both catalyst 1 and 2 were well within the normal concentration values for individual catalysts and also provided 100 typical assays so that this could be verified (Hillary, 2009). Catalyst 2 (harvested at 130 000 miles) is particularly valuable since its precise history under load is known. A duplicate (catalyst 3) from a similar vehicle under identical load will become available in 2013 (projected 130,000 mile harvest).

The majority of Pt entering the autocatalyst recycling chain in 2009 came from diesel particulate filters (Johnson Matthey, 2009) and so this may explain why there was no Pt detected in either of the 2 petrol engine catalysts studied, as these more commonly use a palladium-rhodium formulation.

The question of car catalyst variability is such an issue that PRL (Platinum Recoveries Ltd.), currently the largest specialist autocatalyst recycler in the UK, pay customers based upon an extensive catalogue of catalyst types. PRL purchase spent catalytic converters from various sources including fleet management companies, vehicle maintainers, vehicle breakers, collectors, waste companies and approved treatment facilities and then use the production number of each catalyst in order to locate it in their catalogue, thereby determining the likely PGM content and amount to be paid for that particular catalyst (Deagan, 2009). Although this sounds laborious catalysts can be worth as little as £5 or as much as £125 depending on composition (i.e. assuming average wear and attrition) and so a brief check of the production number prior to decanning and crushing can have a significant impact on profits.

5.7.8 Comminution, Sieving and Sampling of Autocatalysts used in this Study

The outer steel casing was removed and the catalyst monolith was stage crushed to d < 3.5 mm using a jaw crusher (Sturtevant 150 mm Jaw Crusher), followed by secondary comminution in a roll crusher (Sturtevant 150 mm Roll Crusher). All material was then passed through a 1 mm screen. Any oversize material was reground in the Roll crusher so that all test material was of diameter d ≤ 1 mm. The automotive catalysts used for leachate production had 600 channels per square inch, thus each channel was 1.04 mm wide.

Conventional leaching protocol states that higher extraction efficiencies are obtained with finely milled powders due to increasing surface area with decreasing particle size. However

autocatalysts are a potential exception to this due to partial dissolution being desirable i.e. dissolution of the external alumina washcoat layer from the insoluble cordierite support. Hence the crushing regime was designed in order to ensure all material was below 1 mm (the width of an individual channel), whilst avoiding overproduction of very fine material. Table 5.3 and figure 5.15 show the particle size distribution achieved for both catalysts 1 and 2 (in a √2 sieve series) and demonstrate that the crushing regime has prevented over generation of fines, with less than 8% of either catalyst being classified as having a diameter of ≤ 45 µm.

After verification of the particle size distribution by sieving all size fractions were recombined and then riffled to ensure representative samples of the bulk material for leaching tests.

Table 5.3 Mass reporting to each size fraction in a √2 sieve series for catalysts 1 and 2

Particle Size (µm)	Catalyst 1		Catalyst 2	
	% Total Mass	Cumulative Mass (%)	% Total Mass	Cumulative Mass (%)
1000 ≥ d > 710	12.2	12.2	18.4	18.4
710 ≥ d > 500	17.0	29.2	18.0	36.4
500 ≥ d > 355	14.1	43.3	14.2	50.6
355 ≥ d > 250	14.4	57.7	14.6	65.2
250 ≥ d > 180	8.9	66.6	7.8	73.0
180 ≥ d > 125	10.8	77.4	5.2	78.2
125 ≥ d > 90	7.2	84.7	5.5	83.7
90 ≥ d > 63	4.5	89.1	5.3	88.9
63 ≥ d > 45	3.7	92.9	3.2	92.2
d ≤ 45	7.1	100.0	7.8	100.0

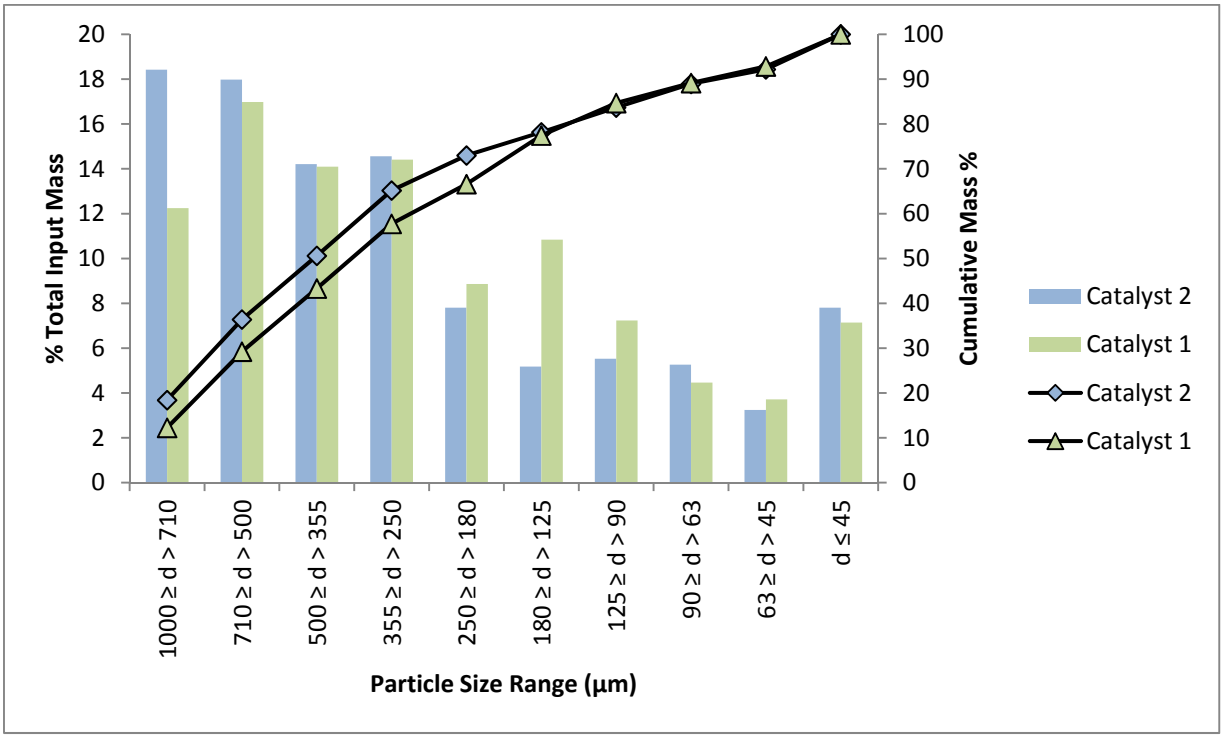

Fig. 5.15 The mass (as a percentage of total input mass) reporting to each size fraction in a √2 sieve series for both autocatalysts

5.8 Microwave Assisted Leaching of Spent Autocatalysts

5.8.1 Aqua Regia

In this work 100% *aqua regia* refers to this standard 3:1 hydrochloric to nitric ratio. 50% *aqua regia* refers to this solution when diluted with an equal volume of distilled water. 100% *aqua regia* has a boiling point of 109˚C.

Ideally, rather than recombining the size fractions described in 5.7.8, it would have been preferable to have analysed and leached each one separately under several sets of leaching conditions (temperature, acid concentration etc.). However due to analysis constraints it was only possible to analyse 5 liquid and 7 solid samples in total and so experimental

conditions had to be prioritised based on relevant literature and previous experimental work.

5.8.2 Pilot PGM Leaching Experiments Using Spent Furnace Lining

Autocatalyst material was limited hence in order to develop the leaching protocol use was made of a readily available material; Johnson Matthey spent furnace refractory lining (detailed in chapter 4). This had the additional benefit of a higher content of precious metals, including Pt. A ball milled sample of used lining was leached under a series of time and temperature combinations (all with 100% *aqua regia* and a liquid to solid ratio of 5:1 as per the maximum extraction efficiencies achieved by Jafarifar *et al.*, (2005)) in order to assess optimal leaching conditions. The sample was ball milled and then sieved and the largest size fraction (1400 ≥ d > 212 μm), which was shown to have elevated PGM levels compared to the feed material, was used for leaching tests. Each leaching test was repeated three times and the resulting leachates were combined in order to produce a single sample (with minimal experimental error) for analysis. One of the leachates produced from this test work was retained and used for the production of biocatalysts in chapter 6. Due to loss of solid samples prior to analysis by XRF it was not possible to determine total metal recovery from the spent lining.

Table 5.4 shows the Pt, Pd and Rh concentrations measured in the leachates produced from each set of experimental conditions. All leachates were analysed via ICP-MS by JM and they reported that each result was the average of three analyses agreeing to within 3%.

Figure 5.16 shows that for each of the three leaching temperatures (90˚C, 109˚C and 150˚C) the 5 minute leach was the least efficient. For both the 90˚C and the 109˚C leaches leaching for longer than 10 minutes produced little additional Pt or Pd extraction but it did produce additional Rh extraction. This could not be verified for the 150˚C leach as leaching times in excess of 10 minutes could not be carried out due to pressure build-up (and resultant leakage) in the MARS 5 reactor. At 109˚C there was less of a difference between the final Pt and Pd concentrations than there was at 90˚C.

Thus in general the higher the leaching temperature or the longer the leaching time the higher the final PGM concentrations. However increasing the temperature to 150˚C significantly increases energy usage and the risk of acid leakage from the reactor vessels. Thus it was concluded that the optimum temperature for PGM leaching from powdered PGM containing waste was 109˚C. 15 minutes was selected as the optimal leaching time at 109˚C as no further Pt and Pd extraction was observes after 20 minutes. Although Rh recovery increased by approximately 4% if leaching time was extended by 33% (from 15 to 20 minutes) this was deemed uneconomic due to the extra energy consumption during a 20 minute leach period. Thus leaching conditions of 109˚C for 15 minutes were concluded to be the best combination for maximum recovery and minimal energy usage. This is significantly longer than the times reported by Jafarifar *et al.*, (2005) who achieved a maximum recovery of 98% after 5 minutes but their material did not contain any Rh (Pt only) and was in a much simpler matrix than the JM lining material.

Table 5.4 Leaching conditions applied to ball milled JM refractory lining and the Pt, Pd and Rh concentrations reported in the resulting leachates. ICP-MS analysis was carried out by JM and each result is the reported average of three analyses agreeing to within 3%.

Description	Pt (ppm)	Pd (ppm)	Rh (ppm)
90˚C t=5	566	478	148
90˚C t=10	628	572	167
90˚C t=15	607	546	167
90˚C t=20	639	576	176
109˚C t=5	564	501	144
109˚C t=10	656	638	165
109˚C t=15	681	637	176
109˚C t=20	685	647	183
150˚C t=5	696	664	182
150˚C t=10	788	710	197

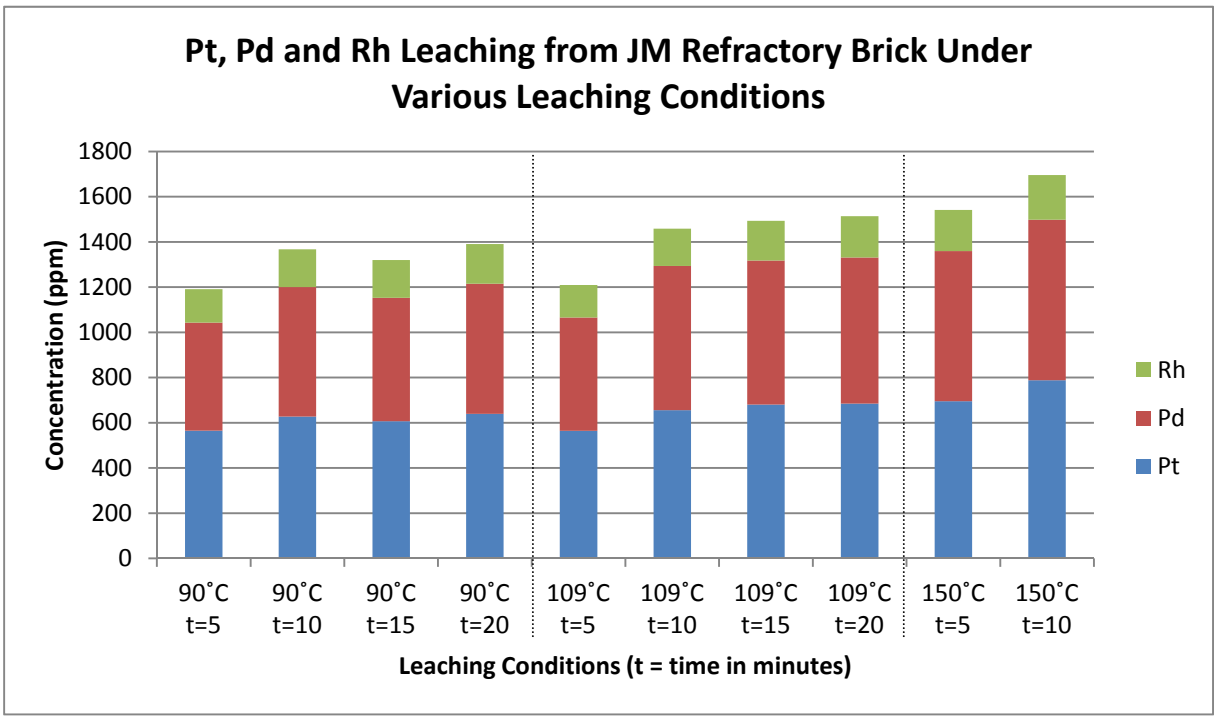

Fig. 5.16 Pt, Pd and Rh content in leachates produced under a variety of leaching conditions (ranging from 90˚C to 150˚C and leaching times of 5 to 20 minutes). All tests used 100% *aqua regia* and a liquid to solid ratio of 5:1

5.8.3 Selection of Key Leaching Conditions for Autocatalysts

Having defined optimal leaching conditions using refractory brick (above) autocatalyst was examined. Two solid samples were analysed in section 5.7.6 in order to determine the initial content of both crushed catalysts; hence there were 5 solid and 5 liquid sample analyses remaining for the leaching test work. Since Yong *et al.*, (2003) had reported relatively high PGM recoveries (>80% of maximum) using 50% *aqua regia* tests were conducted using both 50% and 100% *aqua regia*. Table 5.5 lists the five different leaching schemes employed on catalyst 2 (the test catalyst). As per the optimal conditions established with the furnace lining leaching in section 5.8.2 all leaches were carried out at 109˚C for 15 minutes.

Table 5.5 The five different leaching schemes employed on catalyst 2.

Leaching Scheme	*Aqua Regia* Concentration	Liquid to Solid Ratio (ml/g)	Coarse or Fine material
A	50%	5:1	Coarse
B	50%	10:1	Coarse
C	100%	5:1	Coarse
D	100%	10:1	Coarse
E	50%	5:1	Fine

In order to test the hypothesis that fine milling produces no additional benefit in the extraction of PGMs from autocatalysts by leaching it was decided to replicate the 50% *aqua regia*, 5:1 liquid to solid ratio experiment (A in table 5.5) with catalyst that had been subjected to milling (tema mill) for 30 seconds in order to reduce the particle size so that all particles were d ≤ 38µm (E in table 5.5). This particular set of experimental conditions (50%

AR, 5:1 L/S ratio) was chosen for comparison as available literature indicated that 100% *aqua regia* may facilitate complete extraction in both coarsely and finely ground samples, thereby masking any differences that may occur at lower acid concentrations, or any advantage of using finely milled samples. The use of 50% *aqua regia* should allow any potential extraction differences due to the effect of particle size to be quantified.

Due to the differing liquid to solid ratios used in individual tests the level of dilution caused by wash water (when removing samples from tubes and cleaning samples) was different for each sample. Thus for all results the effect of dilution has been corrected and the data normalised. Other researchers have countered this effect by evaporating the leachate back to the original volume after washing but as *aqua regia* is considered too aggressive for subsequent biorecovery experiments this concentration step was circumvented in this case.

5.8.4 PGM Content of Leachates produced from Catalyst 2

Leaching was conducted as per table 5.5. ICP-MS analysis was carried out on each of the leachates by Engelhard (BASF) Ltd. The stated ICP limit of detection was 0.1 ppm for PGMs with an error of less than 3%. Subsequent analysis of the leach residue solids was carried out by copper collection and XRF of copper button, as per section 5.7.6 (analysis of reference samples of both crushed catalysts). XRF analysis becomes inaccurate below 50 ppm due to sample dilution in the copper matrix. Figure 5.17 shows the concentration of Pd and Rh (no platinum was detected) in each of the five leachates. The results for both metals are stacked in order to show total PGM concentration, as well as using colours to show the contribution each metal makes. Rhodium concentration in the leachate was 3-10 ppm and palladium

concentration was 35-80 ppm. However as different liquid to solid (L/S) ratios were used in the experiment they are not directly comparable in this form. For example if the catalyst solid had been diluted with twice as much acid then the concentration per ml is likely to be lower, even if overall extraction from the solid is higher. In order to calculate total extraction (and therefore make them comparable with the pre-leach solids) the acid dilution factor must be taken into account. Thus the PGM values in each leachate were multiplied by the L/S ratio for that particular set of leaching conditions. Figure 5.18 shows the extraction of Pd and Rh under each set of leaching conditions i.e. after the L/S ratio had been taken into account.

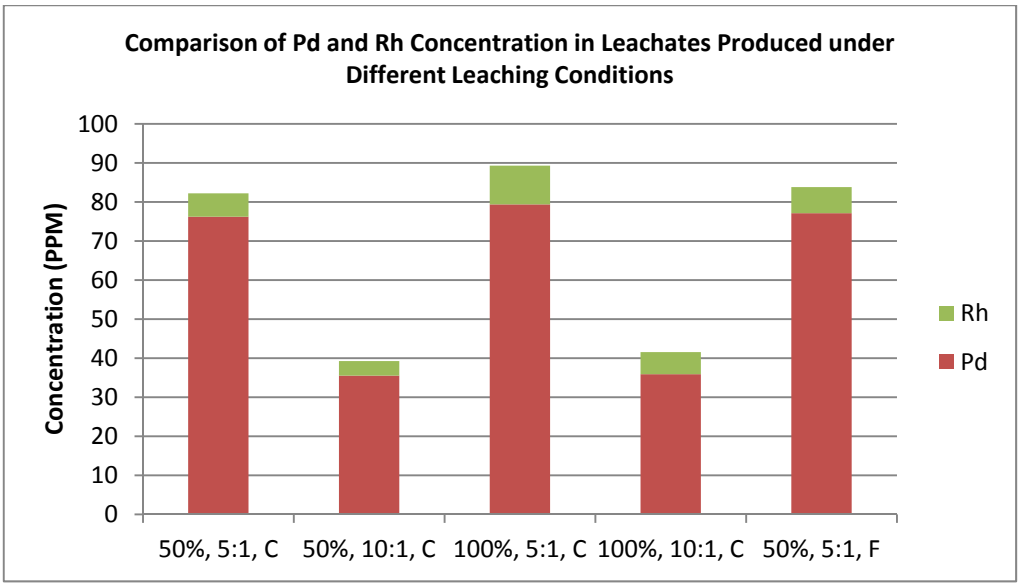

Fig. 5.17 Pd and Rh concentrations for each leachate (as produced). C = coarse sample; F = fine sample; % is *aqua regia* concentration; ratio is liquid to solid ratio.

Figure 5.18 (A) shows that using 100% *aqua regia*, with a L/S ratio of 5:1 produced the highest overall PGM extraction from catalyst 2. However 5.18 (B) shows that these conditions are not quite optimal for Rh extraction, as they only produced the second highest Rh extraction of all the tests. 100% *aqua regia* with a L/S ratio of 10:1 are the best for Rh

recovery, however extraction only increased by 11% (+/-3%) between these two sets of conditions and so from an economic point of view the L/S ratio of 5:1 is more attractive as doubling acid usage for an 11% increase in Rh recovery and a 9% decrease in Pd recovery is not advantageous. 5.18 (B) and (C) confirm that fine grinding to small size does not increase leaching efficiency for either Pd or Rh. The y-axis scale differs in (B) and (C) in order to allow detailed comparison of the lower Rh concentration.

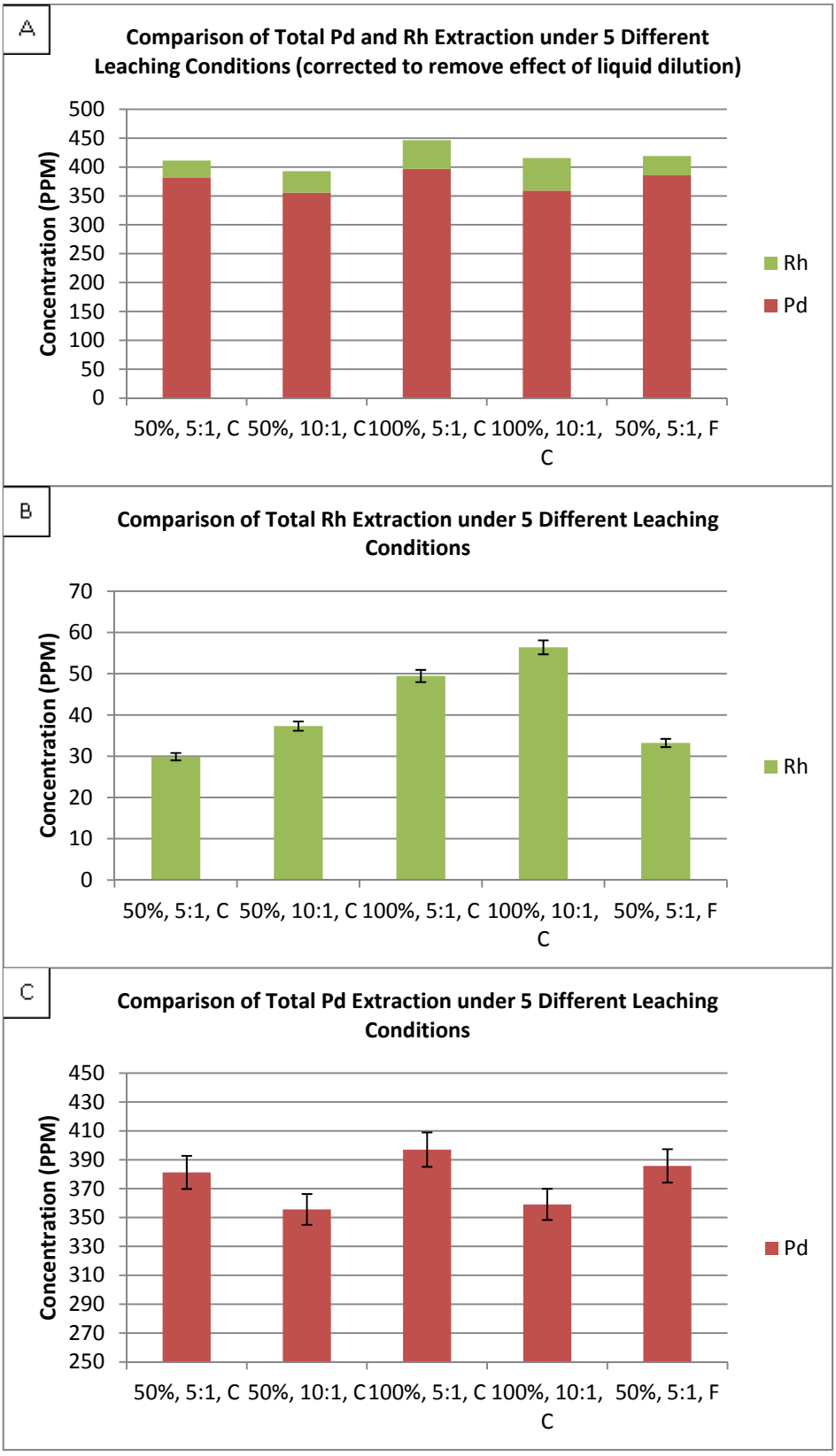

Fig. 5.18 Total Pd and Rh extraction from catalyst 2. Graphs are corrected to remove the effect of the L:S ratio used during leaching. The error bars are +/- 3% (no. of replicates = 3) as quoted by the commercial analyst.

Table 5.2 shows the two XRF analyses provided by Engelhard for catalyst 2. Table 5.6 shows these analyses in ppm instead of % (wt/wt) and also reports the percentage difference (and therefore the error) between the two analyses.

Table 5.6 Commercial XRF analysis of the PGM content of Catalyst 2.

Catalyst 2	Pd (ppm)	Rh (ppm)
Engelhard A	430	70
Engelhard B	400	60
Average Value	**415**	**65**
% Difference	**7.2%**	**15.4%**

Engelhard stated that the accuracy of the XRF assay decreased with decreasing concentration and became markedly more inaccurate below 50 ppm. Table 5.6 illustrates this as the low Rh concentration in this catalyst has caused a much larger difference between analyses. Engelhard stated that the liquid ICP analyses had a higher degree of accuracy overall and were more suitable for low level detection; the stated limit of detection was 0.1 ppm. The average of three results were provided (but not the accompanying raw data) with an error of <3%.

In contrast to the liquid samples the crushed catalyst XRF data has an error of +/- 3.6% for Pd and +/- 7.7% for Rh, which is greater than the 3% quoted for the liquid leachate samples. This creates a problem when calculating overall the extraction efficiency of each leach, as the data for both the solids and the liquids have to be used and therefore the cumulative error is much larger.

Comparing leachate concentration (as in figure 5.18) allows a lower error level (of 3%) to be applied when directly comparing liquid samples – these liquid analyses lose some statistical significance when used in conjunction with the solids analysis to produce overall extraction efficiencies for each set of leaching conditions due to the larger error associated with XRF (7 to 15%). This is demonstrated in figure 5.19 where leachate PGM content (from figure 5.18) is converted into percentage extraction from the crushed catalyst solids, using the average XRF value from the solids and applying error bars based on the % difference between the 2 solid XRF analyses.

Despite the large error bars some conclusions can be drawn from figure 5.19. Firstly all leaching efficiencies are less than 100% and hence (despite the larger than ideal error bars and relatively small differences between certain leaching conditions), the analysis looks realistic with regards to mass balance. Overall extraction efficiencies of 86 – 93% Pd (+/- 3.6%) and 46 – 87% Rh (+/- 7.7%) were observed, dependent on leaching conditions.

Due to the large error bars figure 5.19 cannot definitively demonstrate what the best Pd and Rh leach conditions are, however it does give an indication of suitable conditions, as the error level is constant for each metal and the results are internally consistent (i.e. analysed in the same batch). 50% *aqua regia* at both L/S ratios (5:1 and 10:1) can be discounted for Rh extraction as these conditions are 30-40% less efficient than equivalent conditions with 100% *aqua regia*. Pd extraction is always higher using a L/S ratio of 5:1. The concentration of *aqua regia* appears to be less important for Pd extraction as differences between 50% and 100% concentration are smaller than the analytical error bars.

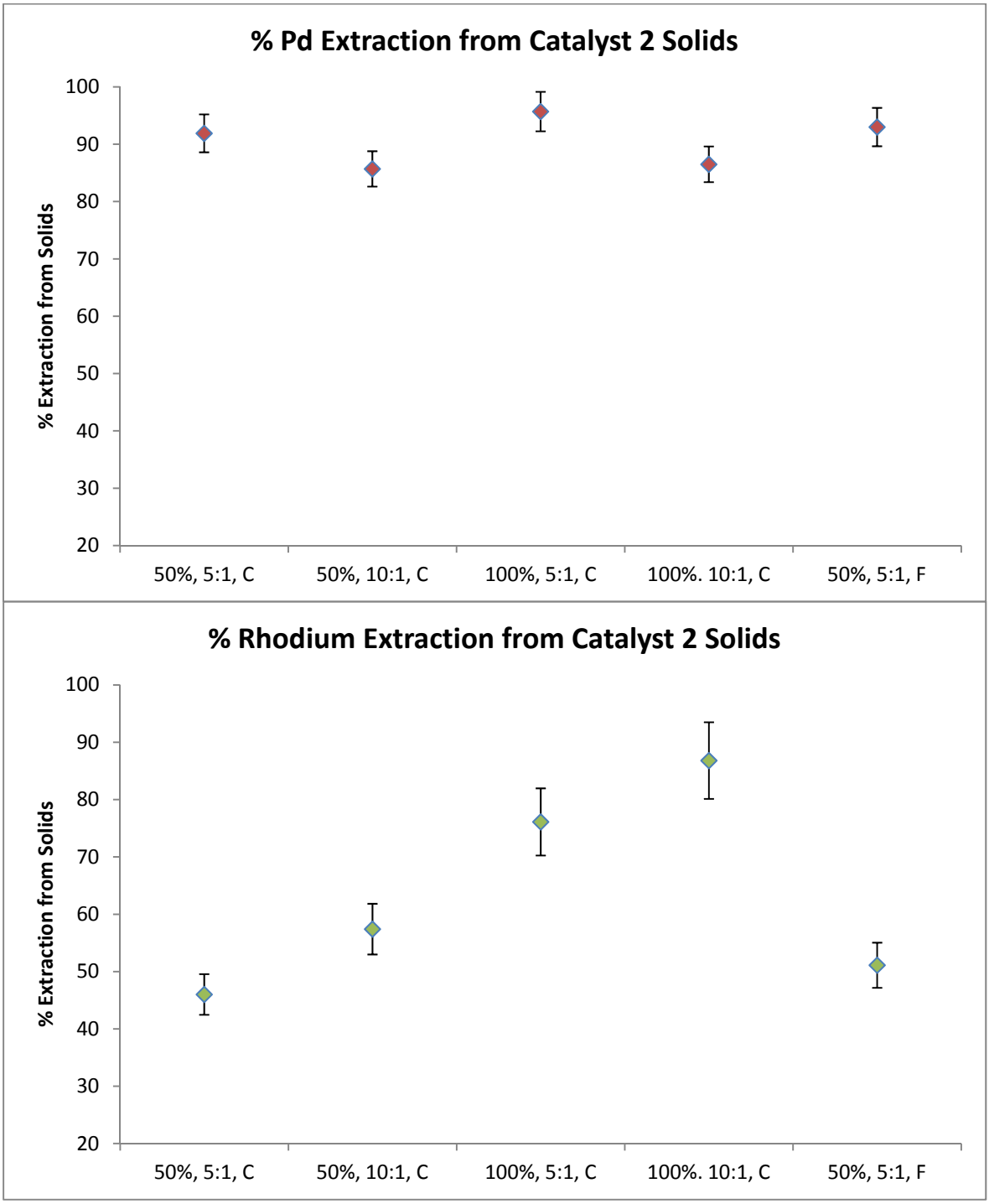

Fig. 5.19 Pd and Rh extraction efficiencies for each set of leaching conditions. The error bars are +/- 3.6% for Pd and +/- 7.7% for Rh (as per the analytical error calculated in table 5.6).

When figure 5.19 is used in conjunction with the liquid analysis in figure 5.18 additional conclusions can be drawn (as the error level is <3% for this figure). This shows that the best set of leaching conditions overall is 100% *aqua regia* with a L/S ratio of 5:1 at 109˚C. It is not necessary to grind the catalyst finely before leaching as it does not affect recovery and hence these leaching conditions were adopted for the remainder of the study.

Yong *et al.*, (2003) used a L/S ratio of 10:1 and reported 80% PGM extraction in 50*% aqua regia* (microwave leached at 120˚C for 15 minutes) but did not give the specific proportions of Pt, Pd and Rh recovered. This study found a 5:1 L/S ratio to be better for overall extraction and established the requirement for 100% *aqua regia* in order to maximise Rh recovery. Up to 93% of the Pd and 87% of the Rh was extracted at the lower temperature of 109˚C using the same microwave type of reactor by adjusting the *aqua regia* concentration and L/S ratio.

The "case history" catalyst 1 was then treated according to conditions A and C in table 5.5. This catalyst had a much higher Rh concentration (approximately 6x higher than the "test" catalyst 2) and so it will be interesting to see if there are differences in extraction with 50% and 100% *aqua regia* with this higher initial Rh loading. The leachate samples are currently undergoing commercial analysis for Pd and Rh.

5.8.5 Mass of Catalyst 2 Before and After Leaching

All experiments used 12 g of solid sample (with the amount of *aqua regia* adjusted depending on the L/S ratio). Table 5.7 lists the absolute masses after leaching and also the

percentage mass lost for each set of conditions. It is not possible to conclude any difference between samples on the basis of one measurement but overall there was a 12.5-17% mass loss during leaching.

Table 5.7 Change in mass of crushed samples of catalyst 2 as a result of acid leaching under a variety of experimental conditions (A-E).

Leaching Scheme	Initial Mass (g)	Mass after Leaching (g)	Change in Mass (%)
A	12.0	10.5	12.5
B	12.0	10.0	16.7
C	12.0	10.5	12.5
D	12.0	10.2	15.0
E	12.0	10.1	15.8

As described in section 5.2.2.2 car catalysts contain approximately 20% washcoat by mass, of which around 16% is alumina, 1.8% is ceria and 2.2% is zirconia. Although leaching efficiencies of up to 93% Pd and 87% Rh were achieved it was likely there was still some washcoat remaining in the post leach solids as less than 20% mass loss has occurred. This assumption was confirmed by SEM imaging, shown in figure 5.20. Although there were far fewer light areas than in BSE mode than in the pre-leach micrographs, there are still small areas of lighter washcoat visible.

ɣ-alumina is transformed into α-alumina at 1250˚C and α-alumina is insoluble in leach liquors. Although Twigg and Wilkins (2006) claimed that most present day catalysts commonly operate at 600 to 800˚C, Zotin *et al.*, (2005) stated that thermal degradation of catalysts begins at temperatures between 800 and 900˚C and Harrison *et al.* (1988) stated that exhaust temperatures can exceed 1000˚C during operation. It is possible that if exhaust gases were elevated at some point during catalyst operation then some of the ɣ-alumina could have been transformed to α-alumina, resulting in the insoluble alumina remaining in the sample after leaching. Alternatively a longer leaching time may result in full dissolution of the washcoat layer, which would indicate that no α-alumina had formed.

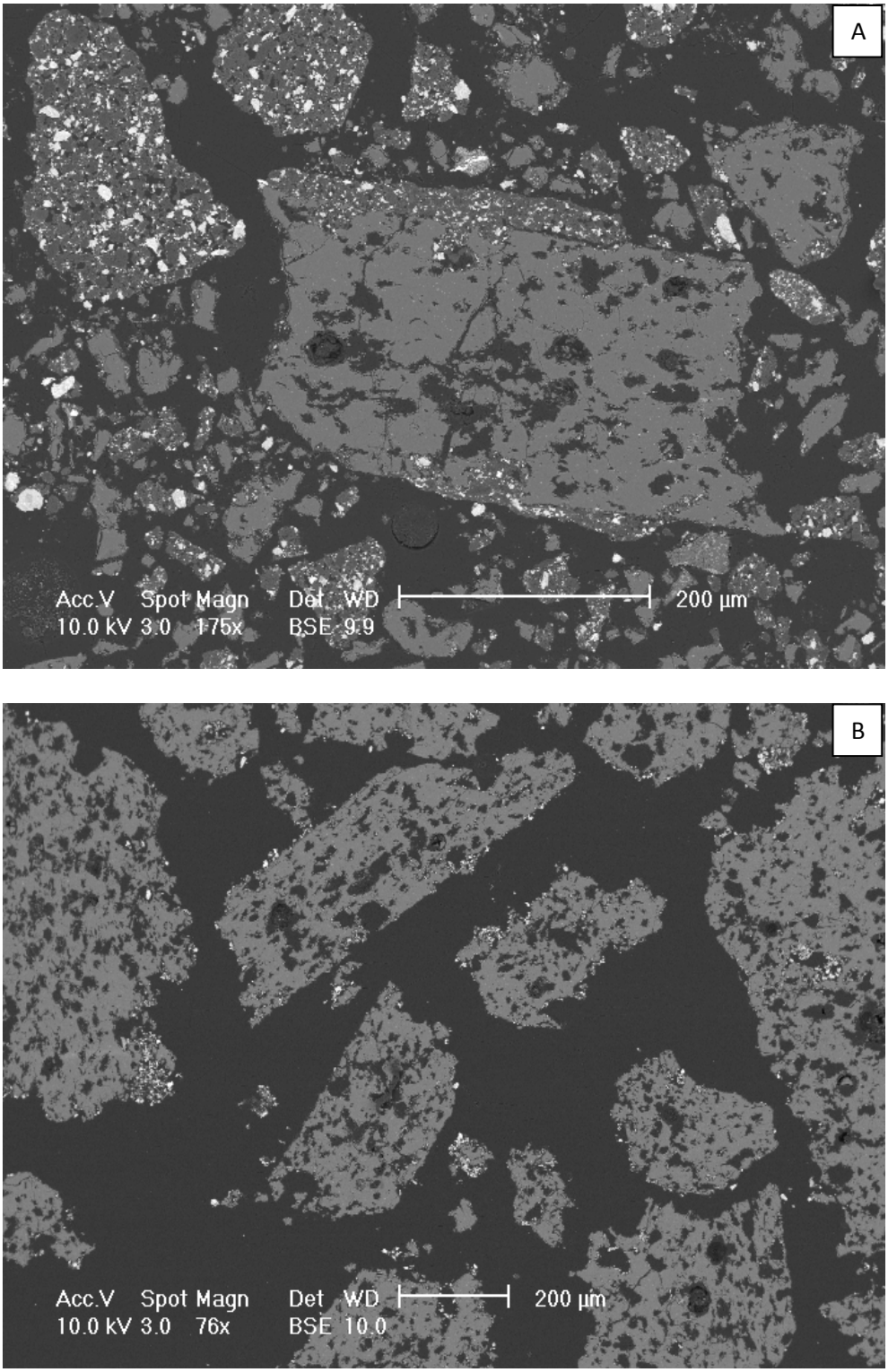

Fig. 5.20 BSE images of crushed samples of catalyst 2 (the test catalyst) (A) prior to undergoing leaching and (B) after leaching. Both samples were set in epoxy resin and polished as per previous characterisation samples.

5.9 Conclusions

Two autocatalysts were characterised by SEM imaging, EDS, XRD and elemental mapping. This characterisation revealed differences in structure and PGM content, with catalyst 1 (the case history catalyst) having two washcoat layers and 10-fold more Pd and 6-fold more Rh than catalyst 2. Both catalysts had failed emissions testing but appear to have different failure mechanisms; Catalyst 1 had a lack of reactive surface (only the corner sections of the outer washcoat were visible under SEM) despite XRF analysis confirming significant PGM remained in this layer. Catalyst 2 (the test catalyst) appeared to have ample washcoat remaining (the majority of each channel was still covered, even though there were areas of cracking and fragments were missing) but much less metal was contained within this washcoat. BSE imaging suggested less heavy (metallic) elements as there were more dark areas than catalyst one and this was backed-up by XRF analysis of PGM content. Catalyst 2 was very sooty and so the few remaining PGM sites may have been physically covered and thus rendered unavailable for catalysis. The SEM study shows that end of life catalysts have shed significant amounts of washcoat and provides evidence of the mechanism by which PGMs are found in road dust.

Catalyst 2 (the test catalyst) was leached with *aqua regia* under a variety of conditions. Fine grinding was not found to improve leaching efficiency. The optimal conditions were found to be 100% *aqua regia* with a L/S ratio of 5:1 at 109˚C for 15 minutes in a microwave reactor. Overall extraction efficiencies of 86 – 93% Pd (+/- 3.6%) and 46 – 87% Rh (+/- 7.7%) were observed, dependent on leaching conditions. Spectral interferences made PGM analysis

complex and low concentration XRF had relatively high error levels, making data interpretation difficult and preventing direct comparison of extraction efficiencies for all samples.

6. Biorecovery of Pt, Pd and Rh from Model Solutions and Refractory Lining and Autocatalyst Leachates

6.1 Bioreduction

Bioreduction is a system involving enzymatically-assisted metal precipitation from a high valence to a zerovalent state. The identification of the enzymatic step responsible for metal reduction may permit metal deposition in a growth-decoupled mode (Yong *et al.*, 2002). Enzymatic systems may promote metal reduction under favourable conditions, independently of cell metabolism. In some cases, metal reduction to lower valence states is directly involved *via* electron transport reactions giving crystals of metal oxide or base metal coated on the cell surface (Deplanche *et al.*, 2011).

6.1.1 Bioreduction and Biocatalysis

The ability of *Escherichia coli* (*E. coli*) and many other bacteria to reduce various metals including PGMs onto their surface through hydrogenase enzyme activity is well documented (e.g. Lloyd *et al*., 1998; Deplanche *et al*., 2010; 2011). The deposited metals are nanoparticulate and this ability has been exploited to create “bionanocatalysts” comprising bacterial cells coated with a well distributed layer of metallic nanoparticles (NPs) (see Deplanche *et al*., 2011 for review). Studies have illustrated the use of metals biorecovered from wastes to produce these catalysts, derived from bacteria, and their biomass supported metal clusters (biocatalysts) (Mabbett *et al.*, 2006; Murray *et al*., 2007; Macaskie *et al*., 2010); some, for reasons as yet still unknown, can produce catalysts in this way with

superior activity to their monometallic counterparts (Yong *et al*., 2010; Macaskie *et al.,* 2010). For applications in fine chemicals synthesis an undefined 'dirty' catalyst may be unattractive but for applications such as decontamination of pesticides (Mertens *et al*., 2007), removal of chlorinated organic compounds from groundwater (Deplanche *et al.*, 2008) or decontamination of toxic metals (Mabbett *et al.*, 2006) this approach pioneers a new area of environmental nanotechnology where the potential hazards of NP migration are mitigated by the retention of multiple catalytic NPs onto micron-sized 'carrier' bacterial cells that are structurally robust and can be immobilised as bacterial biofilm for continuous use (Beauregard *et al*., 2010; Macaskie *et al*., 2012).

6.1.2 Mechanism of Bioreduction

Early studies (e.g. e.g. Lloyd *et al*., 1998; Yong et al., 2002; Baxter-Plant *et al.*, 2003) helped to define the role of microbial cells and enzymatic mechanisms in Pd reduction and inspired a large number of subsequent studies in this area. Three key roles for cells were identified:

1. act as an enzyme catalyst for formate dehydrogenase (formate as electron donor) and hydrogenase(s) (hydrogen as electron donor) by providing an initial pool of electrons to reduce Pd(II)
2. provide foci of metal deposition for subsequent growth of Pd(0) crystals
3. act as a scaffold for Pd(0), the primary crystals ("seeds") which then autocatalyse further reduction, leading to stable Pd(0)-nanocluster growth (Deplanche, *et al.*, 2011).

Research by Mikheenko *et al.* (2003) indicated that the choice of an organism possessing a high number of active hydrogenases was necessary to improve Pd recovery yields. Consequently much early work focused on *Desulfovibrio* spp. as organisms of choice for Pd(II) precipitation as they have several active hydrogenases (Deplanche *et al.*, 2011). By distributing the nucleation sites around multiple enzymatic foci a large number of small metallic NPs as opposed to fewer larger ones will be obtained per unit mass of metal, giving a high surface area for catalysis (Macaskie *et al.*, 2012). Attempts to move away from *Desulfovibrio* spp. reflect the fact that, to be used at industrial scale, the ideal organism should be non-pathogenic, easily culturable and fast-growing, in addition to having strong hydrogenase activity (Deplanche *et al.*, 2011). As a result *E. coli* MC4100 was used in this study. It produces three [Ni-Fe] hydrogenases (Hyd-1, Hyd-2 and Hyd-3) and, furthermore, waste *E. coli* left over from another 'primary' fermentation can be used ('second life') as Pd-nanocatalyst (Orozco *et al.*, 2010; Yong *et al.*, 2010).

Previous work at Birmingham (Baxter-Plant *et al.*, 2003; Creamer *et al.*, 2007, Deplanche *et al.*, 2007) demonstrated catalytically active bacterially based catalysts from single metal model solutions produced using analytical grade salts. The use of "real" waste leachate adds complexity as many different metals (e.g. Cu, Fe, Al, Cr etc.) are present in the same solution in addition to more than one PGM. For this reason mixed metal model PGM solutions were also tested for biomineralisation in order to provide an intermediate step between single metal model solutions and biomass behaviour in "real" leachate. The bioreduction process is sensitive enough to recover metal at parts per million (ppm) concentrations, which is often below the economic threshold of traditional recovery methods (Deplanche *et al.*, 2010).

6.2 Bioreduction from Model Solutions Using Fresh and Pre-platinised Cells

The methodology for production of 'model' PGM solutions from analytical grade salts is described in section 3.12.3. Before commencing reduction of precious metal from real leachates preliminary experiments utilised cells challenged with Pd(II), Pt(IV) and Rh(III) solutions and mixtures of these (referred to as "model" solutions) to provide a comparison with the recoveries achieved from leachate. Individual metal concentration for Bio-PGM preparation in all cases was 2 mM. Freshly harvested cells and 5% pre-platinised cells were used in each test. The use of pre-platinised cells was necessitated by the pH of the *aqua regia* based leachate. Here, the cells were allowed to deposit Pt at permissive pH (2.2) at which pH hydrogenase activity is retained for sufficiently long for metal nucleation to occur (Mikheenko, 2004). This follows an early study (Creamer *et al.*, 2006) that showed pre-palladisation of cells allowed subsequent target metal removal from an acidic leachate since the second, autocatalytic stage of metal removal, is a chemical, not a biochemical, process.

After complete reduction the metallised bacteria produced from the single and mixed metal model solutions were recovered by centrifugation and dried and ground in an agate mortar in preparation for catalytic activity measurement in the Cr(VI) reduction test (described in section 3.12.7). Table 6.1 lists the biocatalysts produced and assigns a number to each sample in order to allow easier identification on the results graphs in section 6.3. Note for convenience the metals are assigned as Pd^{2+}, Pt^{4+} and Rh^{3+}. However in practice the free cations barely exist in solution, the PGMs forming extensively the chloride complexes and

they present to the cells as (e.g.) $PdCl_2$, $RhCl_3$. It is normal practice to show them as Pd(II), Pt(IV), Rh(III) etc.

Table 6.1 Sample codes and metals deposited on biocatalysts produced from model solutions.

Sample Number		Metal Mixture Reduced from Solution
Freshly Harvested Cells	**Pre-Platinised Cells (5%)**	
1	8	Pd^{2+}
2	9	Pt^{4+}
3	10	Rh^{3+}
4	11	$Pt^{4+} + Pd^{2+}$
5	12	$Pt^{4+} + Rh^{3+}$
6	13	$Pd^{2+} + Rh^{3+}$
7	14	$Pd^{2+} + Pt^{4+} + Rh^{3+}$

6.3 Catalytic Activity of E. Coli Bio-PGMs in the Reduction of Cr(VI)

Complete metal removal from test solution was confirmed by $SnCl_2$ assay. The catalytic activity of preparations obtained using fresh and pre-platinised cells from model solutions was compared by the Cr(VI) reduction test (figure 6.1). Bacteria not exposed to PGM reduced negligible Cr(VI) (not shown). The catalytic activity for freshly harvested cells-PGM is shown in figure 6.1 (A). Bio-Pd from the model solution (i.e. not pre-platinised) exhibited a similar catalytic activity to the commercial Pd catalyst, with over 90% Cr (VI) reduction within two hours in both cases. Bio-(Pt/Pd) showed around 50% reduction in the same time period (at equal loadings of Pd and Pt). Bio-Rh exhibited some (low) catalytic activity. Bio-Pt, Bio-(Pd/Rh), Bio-(Pd/Rh) and Bio-(Pd/Pt/Rh) showed 7 to 11% Cr (VI) reduction.

Corresponding data for pre-platinised cells (figure 6.1 (B)) showed that the control was almost twice as active as any of the Bio-PGMs; none showed more than 40% Cr reduction over 3h but overall, and in contrast to the beneficial effect of pre-palladisation reported earlier in the recovery of PGMs from electronic scrap leachates (Creamer *et al.*, 2006) the effect of pre-platinisation was to give very poor catalytic activity against the model solution; pre-platinised preparations are less active catalytically than the equivalent fresh cell preparations.

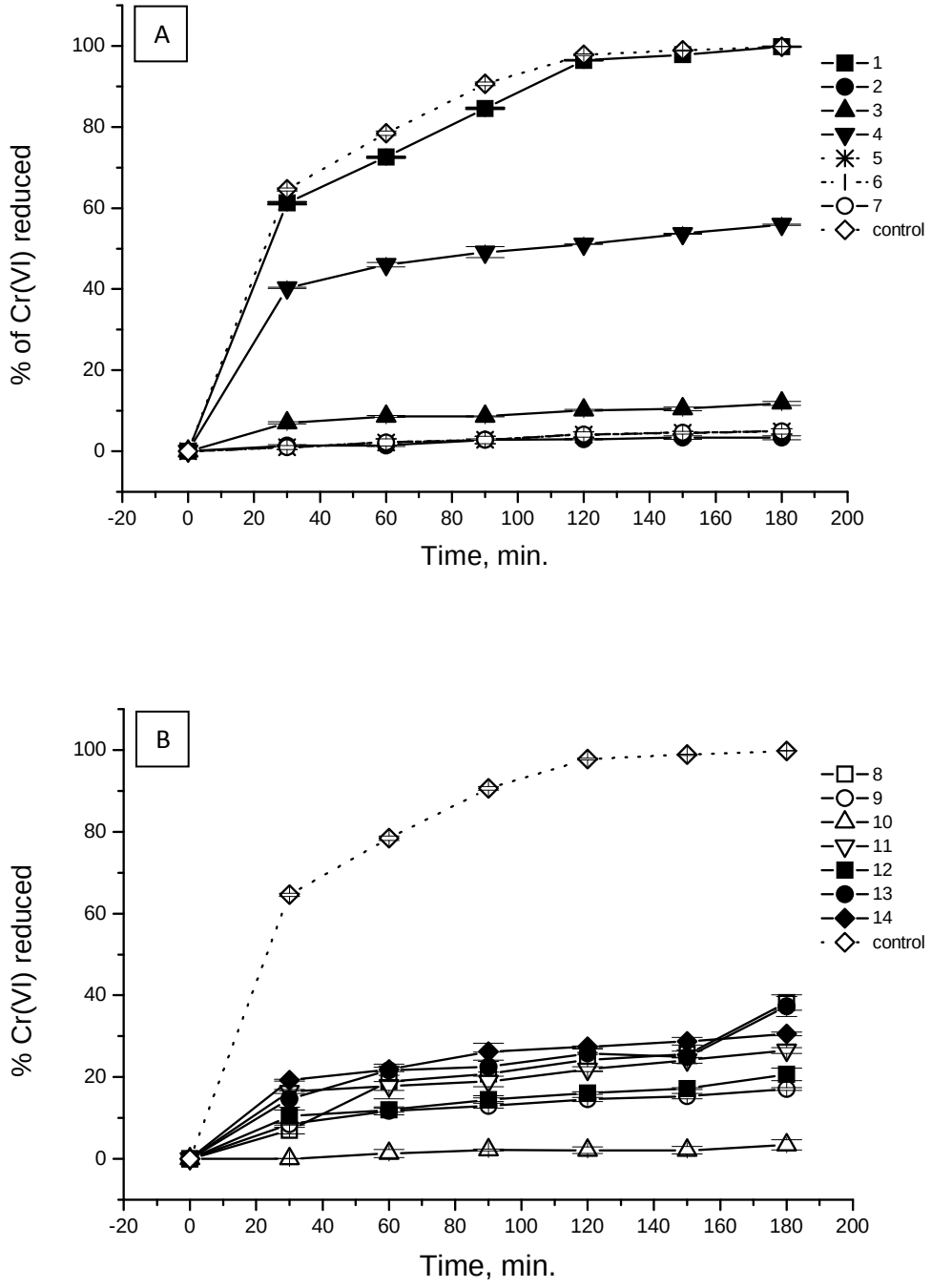

Fig. 6.1 Catalytic activity of *E. coli* Bio-PGMs made from model solutions expressed as % of reduced Cr(VI) per mg of PGM. 1-7: freshly harvested cells; 8-14: pre-platinised cells (5% Bio-Pt). Control: 5% Pd/C. Data are means ± SEM from 3 experiments.

6.4 Bioreduction from Spent Refractory Lining Leachate Using Pre-platinised Cells

The method for production of leachate from spent refractory lining is detailed in section 3.12.4. The use of pre-metallised cells was necessitated by pH of the leachate and the presence of other cations. Partial neutralisation of the leachate was impractical; preliminary studies showed this caused co-precipitation of PGMs with other metals. Diluted leachate (pH 1.6) is sub-optimal for bacterial hydrogenase (the enzyme involved in metal reduction). At pH ~2 hydrogenases remain active for only a few hours (Mikheenko, 2004). Enzyme activity was not assured below this pH thus the metal reducing potential of fresh cells at pH 1.6 was unknown.

After successful reduction of model solutions, the technique was applied to diluted leachate using freshly prepared and pre-platinised cells. Addition of fresh cells gave negligible reduction, possibly attributable to the low pH, or to inhibitory effects of other metals present in the leachate. Further work showed that additional dilution increased metal reduction but PGM levels then became very low. Pre-platinised cells showed significantly higher metal reduction (65%) compared with fresh cells in diluted leachate. The PGM from leachate was not fully reduced as the $SnCl_2$ reading never reached zero; 35% (±5%) of the PGM persisted in solution but the selectivity of metal removal was not investigated.

6.5 Catalytic activity of preparations made from Refractory Lining Leachate in the Reduction of Cr(VI)

The results of figure 6.1 have implications for studies using real leachates. Pre-metallisation prior to leachate exposure is necessary due to the inhibitory effect of the low pH or of other metals present in the solution but this step reduces the catalytic activity of some metal combinations. Figure 6.2 shows that he preparations produced from diluted leachate (reduced onto pre-platinised cells) all exhibited catalytic activity (approx 20% reduction of Cr(VI) or below), i.e. comparable to that shown in Fig 6.1 (B). This once again confirms that catalysts produced using pre-platinised cells have low catalytic activity in the Cr(VI) reduction reaction.

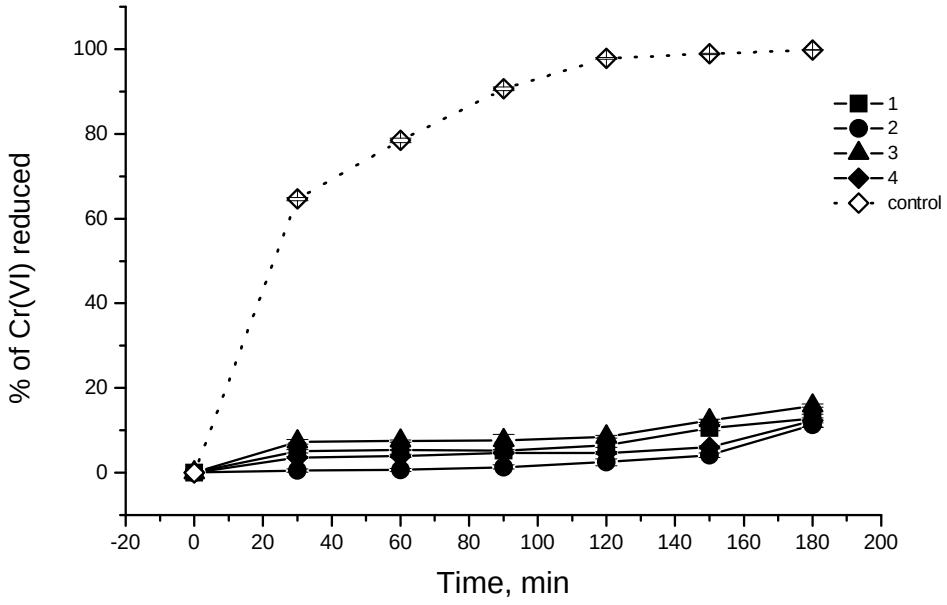

Fig. 6.2 Catalytic activity of *E. coli* Bio-PGMs made from spent refractory lining leachate expressed as % of reduced Cr(VI) per mg of PGM. Control: 5% Pd/C. Numbers 1-4 indicate 4 replicate experiments.

In these tests Cr(VI) reduction was chosen as a simple test because this is easy to quantify by loss of Cr(VI) from solution (Humphries *et al.*, 2006). However figure 6.1 shows that only Bio-Pd and Bio-Pd/Pt have good activity against Cr(VI) reduction. Other studies have shown that palladised cells are catalytically active in the hydrogenolysis (reductive dehalogenation) of chlorinated aromatic molecules (Baxter-Plant *et al.*, 2003) and in reactions involving hydrogen such as H_2 release from hypophosphite, in hydrogenation of unsaturated compounds (Creamer *et al.*, 2007) as well as in fuel cell electrodes (Yong *et al.*, 2007). Hence a wider study might embrace additional catalytic tests. The results of figure 6.1 (B) and the comparable results using real leachates (figure 6.2) justify a wider examination, which is ongoing.

6.6 Conclusions from Bioreduction of PGM from Model Solutions and Industrial Leachate

Bio-reduction of PGM from industrial leachate and subsequent production of a bionanocatalyst has been demonstrated. The low pH of leachate necessitates use of pre-platinised cells. The presence of additional metals reduces the catalytic effect attributable to the Pd(0) component but in some tests pre-platinised cells were more active than fresh biomass after metallisation with the test mixtures. Pre-removal of interfering/inhibitory metals should be investigated in order to be able to increase the working pH and hence the efficiency of reduction by freshly harvested cells. Different metal loadings should also be investigated during initial production of pre-platinised cells in order to determine if this can enhance their catalytic activity. However the results clearly indicate that, in addition to the likelihood of interfering components in the complex leachate from the refractory material, palladium is a better choice of pre-metallisation

metal. Hence the focus switched to the use of this, and a simpler waste source material (autocatalysts).

6.7 TEM of Biocats Produced from Model Solutions

The localisation of precious metal deposition onto biomass was established via a TEM study of cells challenged with model solutions. Figure 6.3 is an ESEM image of *E. coli* cells metallised with palladium in order to demonstrate the appearance of metallised biomass (Mikheenkho, 2011). TEM imaging showed that Pd(0), (in this case 25% of the cell dry weight, since cells loaded at 5% were difficult to visualise) deposits on *E. coli* (using fresh and pre-platinised cells) were localised in the periplasm and at the outermost cell surface. The example shown in figure 6.4 was typical of all micrographs. Figure 6.4 (A) shows a single bacterial cell with Pd nanoclusters visible on the cell surface. Figure 6.4 (B) is high magnification image showing Pd crystals forming in the periplasm between the inner and outer membranes (arrowed). Figure 6.4 (A) shows, notably, two populations: small Pd nanoparticles and larger, extracellular deposits which have a 'bunch of grapes' appearance (arrowed). Residual cellular material is also visible around the extruded nanoparticles (arrowed). This residuum was conjectured by Redwood *et al.* (2008) to act as a 'bridge' to enable access of the Pd(0) into a nonpolar solvent phase and the substrate therein and was subsequently proved by Attard *et al.* (2012) who applied progressive cleaning in conc. NaOH to remove the residual biolayers, visualising the emerging naked metal surface via cyclic voltammetry.

Full recovery of the metals from model solutions by bacteria was confirmed by $SnCl_2$ assay. Freshly prepared cells (i.e. non pre-metallised) took about three times longer to achieve full reduction than pre-metallised cells, attributable to the fact that pre-platinised cells are suggested already to have platinum nanoclusters to act as autocatalytic deposition sites. However in contrast to the Pd deposits (see figure 6.4) and in accordance with the observation that pre-platinised cells are not very useful in subsequent metal removal or in catalysis the Pt deposits were observed as fewer, but larger, deposits which suggests different mechanisms of pre-palladisation and pre-platinisation (see later). In other studies Mikheenko (unpublished) substituted the Pd-amine salt and neutral pH for metal loading, in this way producing the same pattern of 'disabled' metal deposition as shown in figure 6.5.

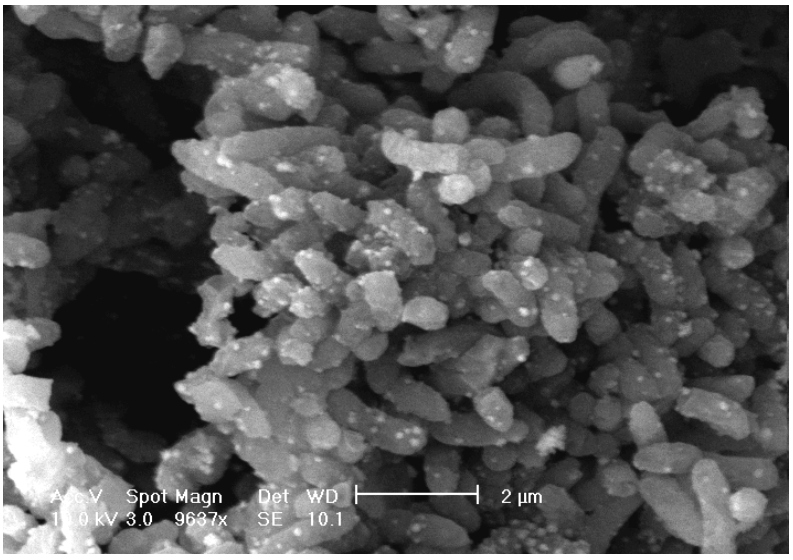

Fig. 6.3 Metallised cells of *E. coli* MC4100 after bioreduction. Palladium clusters are visible on the surface of the cells (image from Mikheenko, personal communication, June 2011).

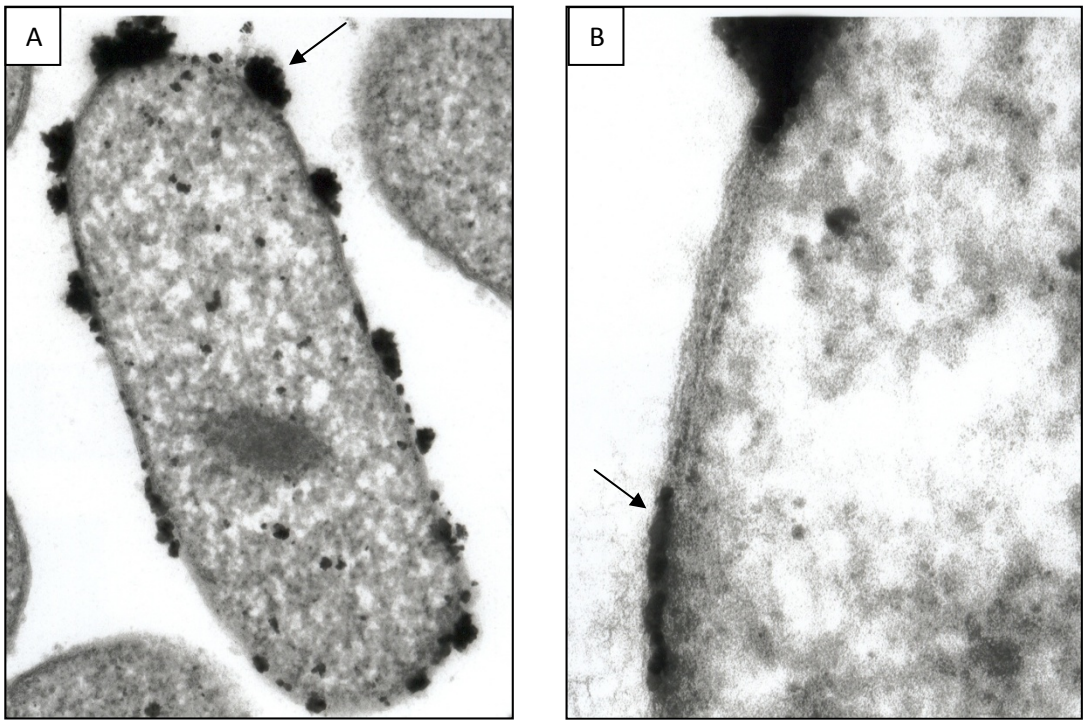

Fig. 6.4 (A) TEM of a palladised *E. coli* cell showing the formation of black Pd clusters on the cell surface. (B) High magnification image of crystal formation in the periplasm. The metal loading was 25% by mass.

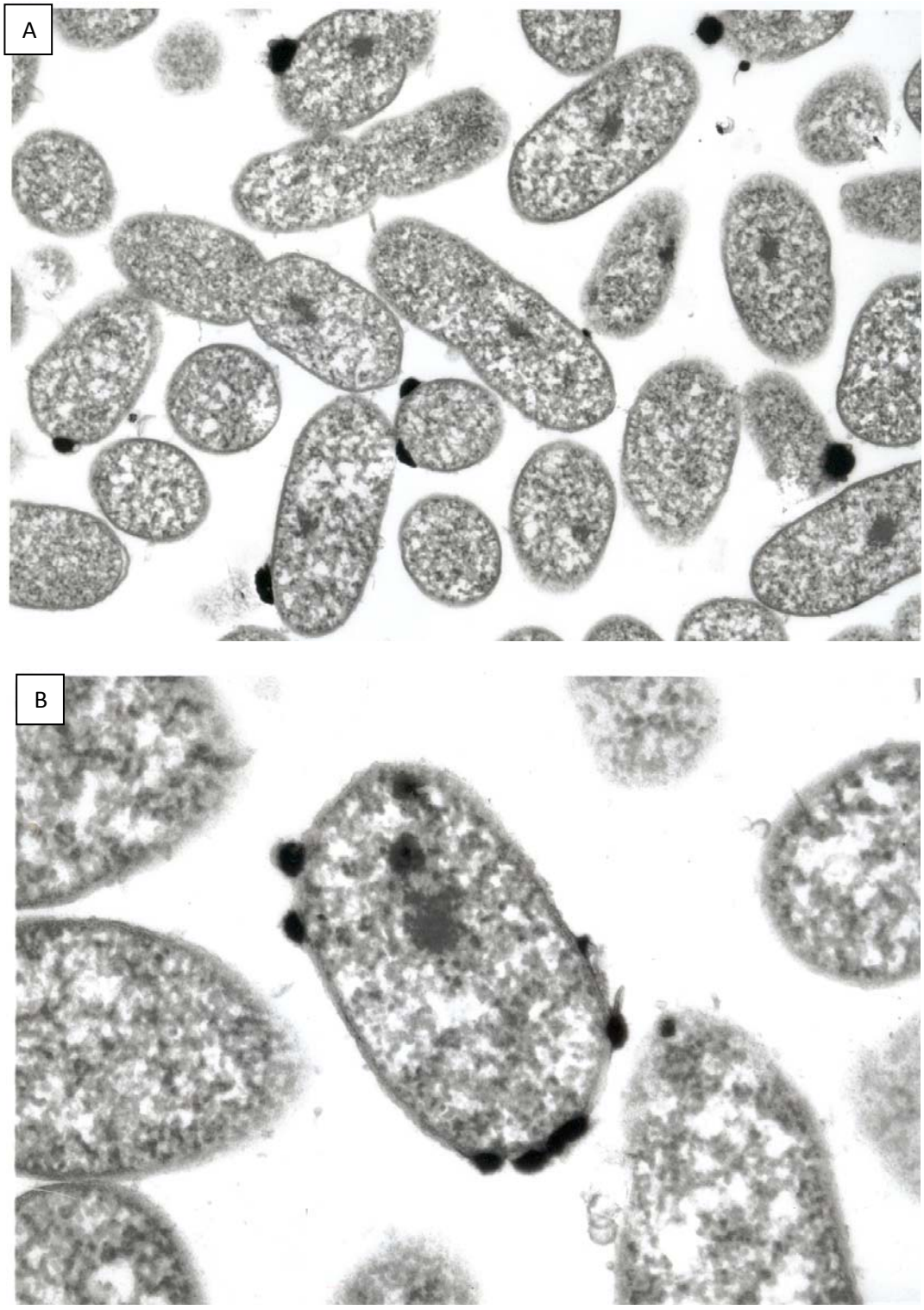

Fig. 6.5 (A) TEM of a platinised *E. coli* cell showing the formation of black Pd clusters on the cell surface. Note that many cells do not show Pt deposits and, where these occur, they are few and large but the surrounding layer of residual biomaterial is still apparent. (B) Higher magnification image of Pt crystal locations. The metal loading was 25% by mass.

6.8 Bioreduction and Metal Recovery from Autocatalyst Leachate

Autocatalysts were leached using *aqua regia* as described in section 5.8.3. The leachate used for metallisation tests was produced under set of conditions D in table 5.5. A 'model' autocatalyst leachate was also produced in the laboratory (a mixed solution of 0.34 mM Pt(IV) and 0.42 mM Pd(II) in HNO_3). This was chosen as an approximation to a real catalyst leachate, but it had a less acidic background matrix and did not contain any significant metals other than PGMs; this can be deduced since the composition of automotive catalysts, although variable with respect to the actual PGMs in each, is well known in comparison to refractory brick which varies on a 'per sample' basis.

In contrast to refractory lining leachate 100% of the PGM in the model leachate was recovered by 5% pre-palladised cells within 60 minutes. Recovery of PGMs from the autocatalyst leachate is shown in figure 6.6. Note that whereas PGM recovery from model solutions was complete within a few minutes (not shown) the reaction took ~ 60 h to proceed to completion in a real waste (figure 6.6). The slow PGM reduction from the catalyst leachate by the pre-palladised *E. coli* cells proceeded in three distinct phases (figure 6.6). An initially rapid rate of metal removal (0-10 h) was followed by a ~ halving of the rate between 10-35 h; selectivity of metal removal was not tested. Removal of the final ~20% of the metals was very slow over the final 20h. Full disappearance of PGM species in solution was achieved after ~60 hours of contact.

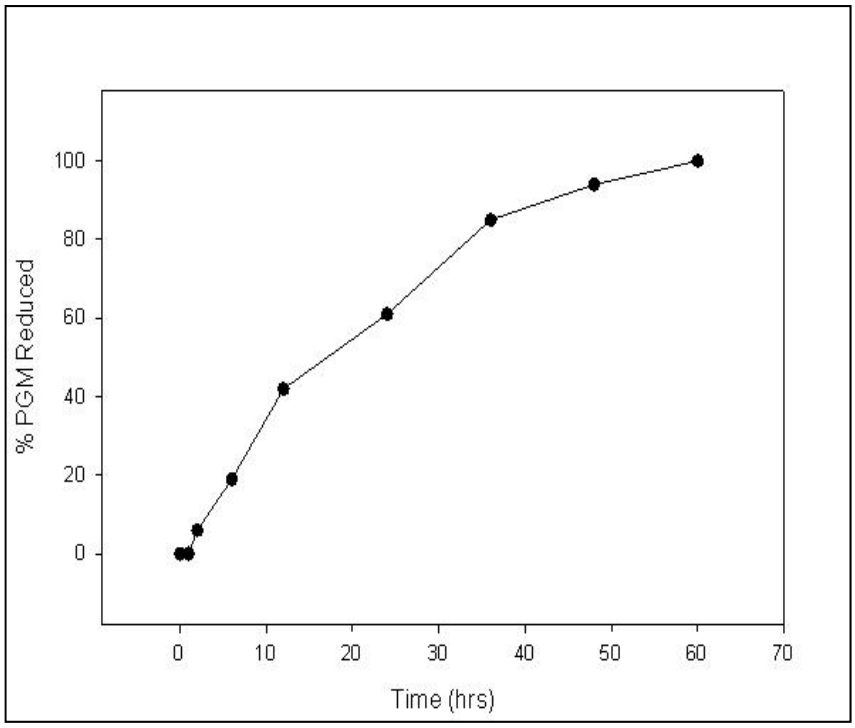

Fig. 6.6 PGM Recovery from autocatalyst leachate using 5% pre-palladised cells. 100% metal reduction took 60 hours.

6.9 Catalytic activity of preparations Recovered from Autocatalyst Leachate in the Reduction of Cr(VI)

Cells pre-palladised with 5% Pd(0) were used in the reduction and removal of Pd and Pt from the model solution and from the catalyst leachates prepared as described above. In contrast to the activity given by pre-platinised, refractory-derived catalyst (see section 6.4) both catalysts were active in Cr(VI) reduction (figure 6.7), with similar initial reaction rates. Near-complete Cr(VI) reduction was obtained with the catalyst made from model leachate after 120 min whereas the catalyst obtained from real leachate showed an ~ 2-fold slower rate after 30 min, probably attributable to the presence of non-PGM contaminants (possibly Si

and Al) which could partially poison catalytic PGM nanoparticles. Nevertheless, more than 90% of the Cr(VI) was reduced after 180 min by the biorecovered material.

In order to implicate the agent responsible for the inhibition of PGM reduction a simple test was carried out. Model leachates were prepared using fresh *aqua regia* and aliquots were spiked with Pd(II) and neutralised and diluted as before. The pH was adjusted to 2.0. Aliquots of the model leachates were spiked with silica (SiO_2 (to 173 ppm) and Al_2O_3 (to 173 ppm) final concentrations) and a mixture of both. The 5% Pd- 'seeded' bioinorganic catalyst was added to each reactor and the rates of PGM reduction were followed as before. Addition of either Al or Si promoted a significant decrease of the rate of PGM reduction; Pd(II)/Pt(IV) disappearance from the supplemented model solution was observed after 6 and 14 hours of contact with the bioinorganic catalyst with SiO_2 or Al_2O_3 respectively (c.f. a few minutes in the 'non-spiked' mixtures). Complete PGM removal was not observed from the solution supplemented with both Si and Al even after 48 h exposure, whereas metal was removed from the unsupplemented control (leachate + distilled water) within 5 mins as seen with the model solutions. These results suggest that the presence of Al and Si inhibit PGM recovery and are responsible for a more than 30-fold increase in reduction time as observed with the spent car catalyst leachate. Nevertheless, the 'catalytic quality' of the bioproduct was largely unaffected (Fig. 6.7).

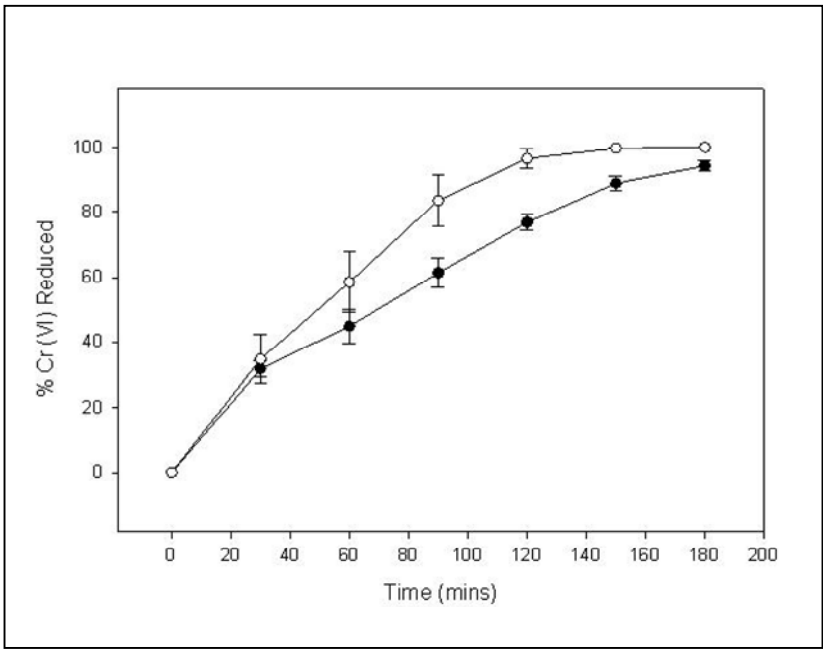

Fig. 6.7 Catalytic activity of biorecovered catalyst using 5% pre-palladised cells. Open circles: catalyst made from a model autocatalyst leachate. Closed circles: catalyst made from real waste leachate. Data are means ± SEM from three experiments.

6.10 Costs of leaching and biorecovery vs. Smelting for Spent Autocatalysts

Platinum Recoveries Ltd. (PRL), the UKs largest specialist autocatalyst smelting company use a proprietary waste concentration calculator to determine the minimum PGM content necessary for economic metal recovery for a given set of economic conditions (i.e. PGM prices, cost of electricity, cost of labour, current price paid by refiners for the PGM concentrate generated etc.). In 2009 PRL provided confidential access to this calculator (Deagan, personal communication, 2009) to enhance the understanding at Birmingham of the likely cost considerations / barriers to implementing new PGM recovery technologies. The figures showed that in June 2008 it cost £1.23 per kg of waste catalyst to smelt and

recover the precious metals. The value of the metal contained per kg allowed them a 10% profit margin from PGM recovery.

It should be noted however that this figure is based upon large batch (several tonnes at a time) PGM recovery and that an emerging laboratory scale technique will be made significantly cheaper upon scale-up (e.g. buying acid commercially and not from a scientific laboratory supply company etc.). Paterson-Beedle 2007 (unpublished report for the Royal Society) found that the production of biocatalysts from wastes is currently uneconomic due to the cost of growing the biomass. However a current project focuses on using 'end of life' biomass from other process to overcome this cost barrier.

In addition there are several PGM containing wastes (e.g. road dust and incinerator ash) that are currently not recycled (and indeed have a landfill cost associated with them) and the economics of recovery from these are likely to be far more attractive than an established waste (autocatalyst) with a very developed and cost optimised recycling process. Autocat is merely a relatively simple 'waste' leachate for investigation and understanding of the bioreduction process.

A cost analysis for recovery of PGMs from road dust was conducted by Professor Jonathan Levie (head of the Hunter Centre for Entrepreneurship at Strathclyde University) for a (successful) grant submission in 2011. He concluded that the economics for biocatalyst

production from road dust were favourable if a suitable source of waste biomass could be identified (Levie, personal communication, 2011).

In additional the price of a catalyst (e.g. from a catalyst manufacturer such as Johnson Matthey) is usually around ten to twenty times the value of the PGM contained within it. Thus the production of a functionalised end product (as opposed to just a PGM concentrate) is potentially very attractive due to the rapidly fluctuating PGM prices experienced over the last ten years.

6.11 Conclusions

This study showed that biocatalysts produced from two different PGM containing waste leachates (refractory lining and spent autocatalysts) exhibited activity in Cr(VI) reduction. However the aggressive nature of the *aqua regia* (necessary to solubilise the PGMs in the solid waste) meant that cells required a 'pre-seeding' step with either 5% Pt or Pd. Ideally both pre-seeding metals would have been tried on one leachate, but due to iterative method development pre-platinised cells were used on the refractory lining leachate and pre-palladised cells were used on the autocatalyst leachate. Pre-seeding with Pt produced material which exhibited poor catalytic activity in the Cr(VI) reduction test, whereas pre-seeding with Pd produced a much more active biocatalyst. The pre-platinised cells also failed to reduce all the available PGM from the leachate (~35% remained in solution).

A recent paper by Deplanche *et al.*, (2012, for submission) may help to explain both why reduction of PGMs was incomplete with pre-platinised cells and also why the resulting mixed-PGM biocatalysts performed poorly in comparison with those that used pre-palladised cells. In anaerobically-grown *E. coli* the bulk of the Pd(II) reducing activity was attributable to inner membrane bound hydrogenases, requiring Pd(II) to traverse the periplasmic space to the site of these enzymes (Deplanche *et al.*, 2010). Hydrogenases are one of the few enzymes that require nickel (they have a Ni-Fe centre). Hence Deplanche *et al.*, (2012) propose that a microbial Ni trafficking mechanism is expected within cells, to ensure adequate Ni supply. Waldron and Robinson (2009) suggested that Ni supply via the NikA-E importer is hardwired to hydrogenase. As Pd and Ni are in the same group of the periodic table and Pd(II) and Ni(II) have chemical similarities (e.g. in their binding to diagnostic agents (see Deplanche *et al.*, 2012)) the Ni transport/trafficking mechanism may be implicated in Pd(II) trafficking and, if so, this would explain how Pd(II) is delivered to the site of hydrogenase assembly (Deplanche *et al.*, 2012). Assuming this is the case this mechanism would provide an explanation as to why pre-seeding with Pd produces many small dispersed nanoparticulate clusters at the sites of hydrogenase, whereas pre-seeding with Pt produces a much smaller number of larger clusters (if the Ni transport mechanism only has affinity for Pd; effectively the metal would not get 'collected' from the cell surface and remain there to grow large particles via chemical reduction). Catalysts require a large surface area in order to be effective and so having many small PGM clusters (as seen with bio-Pd pre-seeding) is likely to produce a more effective catalyst than having few large clusters (as seen with bio-Pt pre-seeding).

In addition the refractory lining contained a large amount of nickel, which may have competed with Pt uptake using fresh cells (it was presumed their ineffectiveness was attributable solely to pH). Future work in this area will focus on dosing model PGM solutions with nickel and assessing what effect this has on biorecovery and the effectiveness of the biocatalysts produced. Pre-palladised cells will provide the focus of future work.

7. Conclusions and Further Work

7.1 Conclusions

7.1.1 Processing of Spent Furnace Refractory Lining

Three samples of spent furnace refractory lining were characterised using established physical processing techniques, namely comminution, wet and dry magnetic separation, electrostatic separation, eddy current separation and gravity separation. The first sample had been ball milled before delivery and was therefore not representative of the usual form of the 'wrecked' lining. The other two samples were 'lump' brick (coarsely crushed to pieces of approximately 10 x 10 cm) and were typical of the material produced at Johnson Matthey. Accurate PGM analysis is complex and expensive and a trade-off was evident in the data generated during this study; a ball milled sample gave relatively accurate low cost XRF results for PGM concentration, however it was difficult to process ball milled brick as the majority of the material was too fine for dry concentration techniques. Wet processing of fine material was not feasible onsite at JM and so work was discontinued in favour of a non-milled sample that could undergo controlled comminution in order to produce particles of the correct size for dry physical processing to underpin a more generic method. 'Lump' brick samples proved more suitable for physical concentration (with 77% of the lightly crushed material containing 90% of the total PGM content being suitable for processing and only 23% being too fine), however low cost XRF analysis was completely unsuitable for this material and so significant effort was made to develop an analysis system that had cross validation by two separate laboratories. However this copper collection and full digest method was extremely expensive and thus limited the number of samples that could be assayed.

By using established physical processing techniques it was possible to produce a PGM-rich concentrate thereby reducing the mass for recycling via a traditional smelting route. A highly flexible system was developed that could separate out several grades of brick; this flexibility to select the amount of fast track material dependent on furnace capacity is an attractive future process option and will provide significant energy saving and environmental benefits over the current method of reprocessing.

7.1.2 Autocatalyst Characterisation and Leaching

Two separate autocatalysts were characterised by SEM imaging, EDS, XRD and elemental mapping. This characterisation revealed differences in structure and PGM content, with catalyst 1 (the case history catalyst) having two washcoat layers and 10-fold more Pd and 6-fold more Rh than catalyst 2 (an aftermarket replacement catalyst). The characterisation study indicated that end of life catalysts have shed significant amounts of washcoat by the time they are recycled and provides evidence of the mechanism by which PGMs are found in road dust. Catalyst 1 only had washcoat remaining in the corners of each channel and therefore likely failed due to a lack of reactive surface, despite still having significant amounts of PGM remaining. Catalyst 2 was very sooty and so the few remaining PGM sites may have been physically covered and thus rendered unavailable for catalysis, suggesting failure due to poor engine combustion.

Catalyst 2 was leached with *aqua regia* under a variety of conditions in order to investigate optimal leaching conditions in terms of energy, reagent usage and PGM recovery. Microwave leaching in a MARS 5 reactor with sealed pressure vessels was chosen for PGM

solubilisation as previous studies had shown that this was more effective than conventional ambient pressure leaching. The optimal conditions were found to be 100% *aqua regia* with a L/S ratio of 5:1 at 109˚C for 15 minutes. Overall extraction efficiencies of 86 – 93% Pd (+/- 3.6%) and 46 – 87% Rh (+/- 7.7%) were observed, dependent on specific leaching conditions. Catalyst 1 has also undergone leaching and the results are being prepared for a journal publication. Another (duplicate) case history catalyst (from a similar vehicle, with the same driver as catalyst 1 and the same mileage) is due to be removed from the vehicle and will allow replication and validation of the results for catalyst 1.

7.1.3 Biorecovery of PGMs

Samples of spent furnace lining and used autocatalyst were leached and then subjected to biorecovery in order to convert the waste PGMs into new bacterially derived catalysts (nanoscale PGM clusters tethered on micron sized carrier particles; bio-PGMs). These 'waste' derived catalysts were tested against single and multimetal bio-PGMs produced from analytical grade model solutions.

Full recovery of PGMs was achieved from model solutions and autocatalyst leachate but not from furnace lining leachate, attributable to potentially inhibitory base metal cations present in this material (e.g. Cu, Fe, Al etc.). In the Cr(VI) reduction test the bio-PGMs from spent autocatalyst reduced 0.5 mM CrO_4^{2-} at half the rate of the 'model' material. The poorer quality of the automotive leachate-derived catalyst was attributed to the Si and Al components in the source material. In all cases the catalytic activity was lower than a commercially available palladium catalyst used for comparison. Pre-depositing Pd on the

cells before exposing them to leachate produced superior catalysts than pre-depositing Pt, discussed in terms of the possible ability of the cells to 'recognise' and 'traffic' Pd(II) as an analogue of Ni(II), an essential metal.

7.2 Further Work

This study on the recovery of PGMs from waste sources had a broad scope and so a lack of depth in some areas presents several opportunities for further work. The potential exists to apply this technology to a number of other abundant waste sources (road dust, incinerator ash etc.).

A follow-on PhD project (co-supervised by Murray) is currently investigating ways in which the activity of waste derived biocatalysts can be improved by controlling the ratio of metals present and the final loading of bacterial cells. This project also aims to improve understanding of another secondary waste (road dust) with no current recycling route by designing and creating a 'model' road dust in the laboratory. This 'model' road dust is being created by fabricating car catalyst washcoat, loading it with a single PGM, instead of the three that are normally present, and then adding it to silica sand to create a free flowing powder with similar particle size distribution and metal content to samples of road dust collected in busy urban areas in the UK.

The analytical difficulties and expense of trace level PGM detection hampered work with 'real' road dusts. Although concentration was observed using several physical processing

techniques only a small number of samples could be sent for accurate analysis. The 'model' road dust being developed contains only one PGM and so is not affected by the severe, non-linear interference effects observed when several PGMs are analysed together. Use of this simplified material should allow PGM segregation and concentration to be fully characterised for a range of physical separation processes, using an inexpensive, simple and quick XRF assay. This work will help to underpin a patent application filed by the University based on preliminary road dust results.

A second car catalyst (identical car and model) of known mileage and road use (motorway / A-road / in town) is due to become available. Another study is planned in order to further assess how leaching efficiency varies under different experimental conditions. The previous case history catalyst contained no platinum and so it is hoped that this one (produced at ~ the same time but harvested approximately five years later than the previous one) will contain all three PGMs so that the minimum energy and acid requirements for leaching of all three metals can be verified. Experiments will also be undertaken on the scope for acid reuse in order to reduce the costs and environmental impacts associated with *aqua regia* leaching.

REFERENCES

Acres, G.J.K. (1987) Platinum group metal catalysis at the end of this century. **Materials & Design**, 8: 258-262

Amatayakul, W. and Ramnas, O. (2001) Life cycle assessment of a catalytic converter for passenger cars. **Journal of Cleaner Production,** 9: 395-403

Andrews, L. (2007) The use of electron microbeam techniques in metallurgical analysis. **Journal of the South African Institute of Mining and Metallurgy**, 107: 79-82

Angelidis, T.N. and Sklavounos, S.A. (1995) A SEM-EDS study of new and used automotive catalysts. **Applied Catalysis A: General,** 133: 121-132

Angelidis, T.N. and Skouraki, E. (1996) Preliminary studies of platinum dissolution from a spent industrial catalyst. **Applied Catalysis A: General,** 142: 387-395

Angelidis, T.N. (2001) Development of laboratory scale hydrometallurgical procedure for the recovery of Pt and Rh from spent automotive catylists. **Topics in Catalysis,** 16-17: 419-423

Anglo Platinum **Smelter Operating Costs 2011** [online]. Available from: http://www.angloplatinum.com/business/operations/smelters.asp [Accessed May 2012]

Aplan, F.F. (2003) "Gravity Concentration." In Fuerstenau, M. C. (ed.) and Han, K.N. (ed.) **Principles of Mineral Processing.** Littleton: Society for Mining, Metallurgy and Exploration Inc. pp. 214-220

Artelt, S., Kock, H., Konig, H.P., Levsen, K. and Rosner, G. (1999) Engine dynamometer experiments: platinum emissions from differently aged three-way catalytic converters. **Atmospheric Environment,** 33: 3559-3567

Artelt, S., Levsen, K., Konig, H.P. and Rosner, G. (2000) "Engine test bench experiments to determine platinum emissions from three-way catalytic converters." In Zereini, F. (ed.) and Alt, F. (ed.) **Anthropogenic Platinum Group Element Emissions: Their Impact on Man and Environment**. Berlin: Springer. pp. 33-44

Attard, G., Casadesus, M., Macaskie, L.E. and Deplanche, K. (2012) Biosynthesis of platinum nanoparticles by *Escherichia coli* MC4100: Can such nanoparticles exhibit intrinsic surface enantioselectivity? **Langmuir** 28: 5267-5274

Automobile Association, UK. (2010) **General Advice** [online] Available from: http://www.theaa.com/motoring_advice/general-advice/car-servicing-and-repair-faqs.html#section12 [Accessed March 2011]

Baghalha, M., Khosravian, H. and Mortaheb, H.R. (2009) Kinetics of platinum extraction from spent reforming catalysts in *aqua regia* solutions. **Hydrometallurgy,** 95: 247-253

Balcerzak, M. (2002) Sample digestion methods for the determination of traces of precious metals by spectrometric techniques. **Analytical Sciences,** 18: 737-750

Ballhaus, C. and Sylvester, P. (2000) Noble metal enrichment processes in the Merensky Reef, Bushveld Complex. **Journal of Petrology,** 41: 545-561

Barefoot, R.R. (1997) Determination of platinum at trace levels in environmental and biological materials. **Environmental Science & Technology,** 31: 309-314

Barnes, J.E. and Edwards, J.D. (1982) Solvent extraction at Inco's Acton Precious Metals Refinery. **Chemistry and Industry,** 5: 151-155

Baxter-Plant, V.S., Mikheenko, I.P. and Macaskie, L.E. (2003) Sulphate-reducing bacteria, palladium and the reductive dehalogenation of chlorinated aromatic compounds. **Biodegradation,** 14: 83-90

Beauregard, D.A., Yong, P., Maccaskie, L.E. and Johns, M.L. (2010) Using non-invasive magnetic resonance imaging (MRI) to assess the reduction of Cr(VI) using a biofilm-palladium catalyst. **Biotechnology and Bioengineering**, 107: 11-20

Benson, M., Bennett, C.R., Harry, J.E., Patel, M.K. and Cross, M. (2000) The recovery mechanism of platinum group metals from catalytic converters in spent automotive exhaust systems. **Resources, Conservation and Recycling,** 31: 1-7

Bernardis, F.L., Grant, R.A. and Sherrington, D.C. (2005) A review of methods of separation of the platinum-group metals through their chloro-complexes. **Reactive and Functional Polymers,** 65: 205-217

Bloxham, L. (2009) The impact of CO_2 legislation on PGM demand in autocatalysts. **Platinum Metals Review,** 53: 179-180

Boch, K. and Schuster, M. (2006) "Determination of palladium in road dust and sewage sludge ashes." In Zereini, F. (ed.) and Alt, F. (ed.) **Palladium Emissions in the Environment: Analytical Methods, Environmental Assessment and Health Effects**. Berlin: Springer. pp. 191-201

British Standards Institution (1989) **Test Sieving – Part 1: Methods using Test Sieves of Woven Wire Cloth and Perforated Metal Plate.** London: BS 1796-1: 1989

Brumby, A., Verhelst, M. and Cheret, D. (2005) Recycling GTL catalysts – a new challenge. **Catalysis Today,** 106: 166-169

Brynard, H.J., de Villiers, J.P.R. and Viljoen, E.A. (1976) A mineralogical investigation of the Merensky reef at the Western Platinum Mine, near Mirikana, South Africa. **Economic Geology,** 71: 1299-1307

Buckley, M.R. (2008) **Dry Processing of Industrial Minerals.** PhD Thesis, University of Birmingham

Bulatovic, S. (2003) Evaluation of alternative reagent schemes for the flotation of platinum group minerals from various ores. **Minerals Engineering,** 16: 931-939

Callister, W.D. (2006) **Materials Science and Engineering: An Introduction**. 7th Ed. New York: Wiley

Cawthorn, R.G. (1999) The platinum and palladium resources of the Bushveld Complex. **South African Journal of Science,** 95: 481-489

CEM (1999) **MARS 5 Operation Manual by CEM Ltd.** [online]. Available from: www.ietltd.com/PDF_datasheets/MARS [Accessed October 2011]

Charlot, G. (1978) **Dosages Absorptiometriques Des Elements Mineraux**. 2nd Ed. Paris: Masson

Clipsham, J. and Claes, P. (2010) **Biocatalysts.** Confidential Market Study for Birmingham University by Catalytic Technology Management (CTML) Ltd.

Cole, S., and Ferron, C.J. (2002) “A view of the beneficiation and extractive metallurgy of the platinum group elements, highlighting recent process innovations.” In Cabri, L. J. (ed) **The Geology, Geochemistry, Mineralogy and Mineral Beneficiation of Platinum-Group Elements, The Canadian Institute of Mining, Metallurgy and Petroleum,** Special volume 54: pp. 811-818

Coombes, J.S. (1992) Platinum 1992, Platinum supply and demand reached record levels. **Platinum Metals Review**, 36: 150

Creamer, N.J., Baxter-Plant, V.S., Henderson, J., Potter, M. and Macaskie, L.E. (2006) Palladium and gold removal and recovery from precious metal solutions and electronic scrap leachates by *Desulfovibrio desulfuricans*. **Biotechnology Letters**, 28: 1475-1484

Creamer, N.J., Mikheenko, I.P., Yong, P., Deplanche, K., Sanyahumbi, D., Wood, J., Pollmann, K., Merroun, M., Selenska-Pobell, S. and Macaskie, L.E. (2007) Novel supported Pd hydrogenation bionanocatalyst for hybrid homogeneous / heterogeneous catalysis. **Catalysis Today,** 128: 80-87

Deagen, D. (2009) **Personal Communication with the Processing Manager for Platinum Recoveries Ltd.** Swindon, England

Department for Transport (2006) **Platinum and Hydrogen for Fuel Cell Vehicles** [online]. Available from: www2.dft.gov.uk/pgr/roads/environment/research/cqvcf/platinumandhydrogenforfuelce3838.html [accessed March 2011]

Depcik, C. and Assanis, D. (2005) One-dimensional automotive catalyst modelling. **Progress in Energy and Combustion Science**, 31: 308-369

Deplanche, K., Attard, G.A. and Macaskie, L.E. (2007) Biorecovery of gold from jewellery wastes by *Escherichia coli* and biomanufacture of active au-nanomaterial. **Advanced Materials Research,** 20-21: 647-650

Deplanche, K. and Macaskie, L.E. (2008) Biorecovery of gold by Escherichia coli and *Desulfovibrio desulfuricans*. **Biotechnology and Bioengineering**, 99: 1055-1064

Deplanche, K., Mikheenko, I.P., Bennett, J.A., Merroun, M., Mounzer, H., Wood, J. and Macaskie, L.E. (2010) Selective oxidation of benzyl-alcohol over biomass-supported Au/Pd bioinorganic catalysts. **Topics in Catalysis**, 54: 1110–1114

Deplanche, K., Murray, A.J., Mennan, C., Taylor, S. and Macaskie, L.E. (2011) "Biorecycling of precious metals and rare earth elements." In Rahman, M. (ed.) **Nanomaterials**. 1st Ed. Intech

Deplanche, K., Bennett, J.A., Mikheenko, I.P., Omajali, J., Wells, A., Meadows, R., Wood, J. and Macaskie L.E. (2012) Catalytic activity of biomass-supported Pd nanoparticles: influence of the biological component in catalytic efficacy and potential application in 'green' synthesis of platform chemicals. **Journal of Applied Catalysis B: Environmental**, Awaiting submission

Diwell, A.F., Rajaram, R.R., Shaw, H.A. and Truex, T.J. (1991) The role of ceria in three-way catalysts. **Studies in Surface Science and Catalysis,** 71: 139-152

Earthworks (2004) **Dirty Metals: Mining, Communities and the Environment.**

Edwards, R.I., te Riele, W.A M. and Bernfield, G.J. (1986) "Review on the recovery of the platinum group metals." In Acres, G.J.K. (ed.) and Swars, K. (ed.) **Gmelin Handbook of Inorganic Chemistry, Platinum Supplement, Platinum Group Metals Technology**. Berlin: Springer-Verlag. pp. 1-23

Ek, K.H., Morrison, G.M. and Rauch, S. (2004) Environmental routes for platinum group elements to biological materials - a review. **Science of the Total Environment,** 334-335: 21-38

European Commission (2009).[online]. Available from: www.ec.europa.eu/environmentair/transport/co2).[Accessed March 2010]

European Union. Summaries of EU Legislation (2010) **Euro V and Euro VI standards: reduction of pollutant emissions from light vehicles** [online]. Available from: http://europa.eu/legislation_summaries/environment/air_pollution/l28186_en.htm [Accessed 30th September 2011]

Farago, M.E., Kavanagh, P., Blanks, R., Kelly, J., Kazantzis, G., Thornton, I., Simpson, P.R., Cook, J.M., Parry, S. and Hall, G.E.M. (1996) Platinum metal concentrations in urban road dust and soil in the United Kingdom. **Fresenius' Journal of Analytical Chemistry,** 354: 660-663

Fears, P. (2008) **Personal Communication.** Interview with Managing Director of Eriez Europe Ltd. Cardiff, Wales

Furr, A.K., Lawrence, A.W., Tong, S.S.C., Grandolfo, M.C., Hofstader, R.A., Bache, C.A., Gutenmann, W.H. and Lisk, D.J. (1976) Multielement and chlorinated hydrocarbon analysis of municipal sewage sludges of American cities. **Environmental Science and Technology,** 10: 683-687

Gaita, R. and Al-Bazi, S.J. (1995) An ion-exchange method for selective separation of palladium, platinum and rhodium from solutions obtained by leaching automotive catalytic converters. **Talanta,** 42: 249-255

Gerlach, R.W., Dobb, D.E., Raab, G.A. and Nocerino, J.M. (2002) Gy sampling theory in environmental studies: Assessing soil splitting protocols. **Journal of Chemometrics,** 16: 321-328

Goldberg, E.D., Hodge, V., Kay, P., Stallard, M. and Koide, M. (1986) Some comparative marine chemistries of platinum and iridium. **Applied Geochemistry,** 1: 227-232

Goodquarry (2011) **Crushing Plant Technology Tutorial** [online] Available from: www.goodquarry.com/images/productiontechnology/PPT_photo8_large.gif [Accessed October 2011]

Gordon, R.B., Bertram, M. and Graedel, T.E. (2006) Metal stocks and sustainability. **Proceedings of the National Academy of Sciences,** 103: 1209-1214

Greenwood, N.N. and Earnshaw, A. (1989) **Chemistry of the Elements.** Oxford: Pergamon Press. pp. 1242-1363

Gruenewaldt, V.G. (1977) The mineral resources of the Bushveld Complex. **Minerals Science and Engineering**, 9:83-95

Gy, P. (1979) **Sampling of Particulate Materials, Theory and Practice.** New York: Elsevier Scientific Publishing Company.

Hagelukan, C., Buchert, M and Ryan, P. (2006) "Materials flow of platinum group metals in Germany". **In 13 CIRP International Conference on Life Cycle Engineering**. Leuven, May 31st to June 2nd 2006 (Proceedings of LCE 2006 pp.487-482)

Harrison, B., Diwell, A.F. and Hallett, C. (1988) Promoting platinum metals by ceria. **Platinum Metals Review,** 32: 73-83

Hillary, B. (2009) **Personal Communication**. Interview with senior analytical chemist at Engelhard International Metals Ltd. Cinderford, UK

Hirst, N., Brocklebank, M. and Ryder, M. (2002) **Containment Systems – A Design Guide**. Rugby: IChemE

Hodge, V.F. and Stallard, M.O. (1986) Platinum and palladium in roadside dust. **Environmental Science and Technology,** 20: 1058-1060

Hoffman, J.E. (1988) Recovery of platinum group metals from automobile catalysts. **Precious and Rare Metal Technologies, Proceedings of Symposium on Precious and Rare Metals**, Albquerque NM, USA, 6^{th}-8^{th} April 1988

Humphries, A.C., Mikheenko, I.P. and Macaskie, L.E. (2006) Chromate reduction by immobilized palladized sulfate-reducing bacteria. **Biotechnology and Bioengineering**, 94: 81-90

Inculet, I.I. (1984) **Electrostatic Mineral Separation.** Letchworth: John Wiley & Sons

International Centre for Science and High Technology (2002) **Cleaner Technologies for Sustainable Chemistry,** Triest: ICS-UNIDO

International Energy Agency (2007) **CO_2 Emissions from Fuel Combustion 1971-2005,** Paris: OECD Publishing

Jafarifar, D., Daryanavard, M.R. and Shiebani, S. (2005) Ultra fast microwave-assisted leaching for recovery of platinum from spent catalyst. **Hydrometallurgy,** 78: 166-171

Jarman, W. (1941) **Meeting of the American institute of Mining, Metallurgical and Petroleum Engineers,** February 1941

Jarvis, K.E., Parry, S.J. and Piper J.M. (2001) Temporal and spatial studies of autocatalyst-derived platinum, rhodium, and palladium and selected vehicle-derived trace elements in the environment. **Environmental Science and Technology,** 35: 1031-1036

Jillavenkatesa, A., Dapkunas, S.J. and Lum, L.S.H. (2001) Particle size characterization. **National Institute of Standards and Technology, Special Publication 960-1,** Washington: US Government Printing office

Jimenez de Aberasturi, D., Pinedo, R., Ruiz de Larramendi, I., Ruiz de Larramendi, J.I. and Rojo, T. (2011) Recovery by hydrometallurgical extraction of the platinum-group metals from car catalytic converters. **Minerals Engineering,** 24: 505-513

Johnson Matthey (2001) The outlook for PGM supplies: new mines and expansions in North America and Zimbabwe. **Platinum 2001 Special Report,** pp. 19-21

Johnson Matthey (2003) Autocatalyst development and the use of PGM. **Platinum 2003 Special Report,** pp. 25-27

Johnson Matthey (2004) PGM mining in Russia. **Platinum 2004 Special Report,** pp. 16-21

Johnson Matthey **Platinum Today, South Africa** [online]. Available from: http://www.platinum.matthey.com/production/africa.html). [Accessed March 2010]

Johnson Matthey **Platinum Today, Platinum Charts** [online]. Available from: http://www.platinum.matthey.com/market_data/1147696813.html [Accessed March 2010]

Johnson Matthey **Platinum Today, Price Charts** [online]. Available from: http://www.platinum.matthey.com/prices/price_charts.html [Accessed March 2010]

Johnson Matthey (2009) **Personal Communication: Interviews with the Director of Refining, the Chief Analytical Chemist and a Process Engineer at Johnson Matthey.** Enfield Refinery, England**.**

Johnson Matthey (2009**) Platinum 2009**, Royston: Johnson Matthey Precious Metals Marketing

Kelly, E.G. and Spottiswood, D.J. (1982) **Introduction to Mineral Processing.** New York: John Wiley and Sons

Kim, C., Kohler, A., Mulvaney, K. and Wagner, L. (1992) Chrome in refractories. **Ceramic Industry,** 142: 57-61

Konig, H.P., Hertel, R.F., Koch, W. and Rosner, G. (1992) Determination of platinum emissions from a three-way catalyst-equipped gasoline engine. **Atmospheric Environment. General Topics,** 26 (A): 741-745

Lesniewska, B.A., Godlewska-Zylkiewicz, B., Bocca, B., Caimi, S., Caroli, S. and Hulanicki, A. (2004) Platinum, palladium and rhodium content in road dust, tunnel dust and common grass in Bialystok area (Poland): a pilot study. **Science of the Total Environment,** 321: 93-104

Levie, J. (2011) **Personal Communication with the Head of the Hunter Centre for Entrepreneurship**. University of Strathclyde, Scotland

Liwei, J., Meiqing, S., Jun, W. and Jaiming, W. (2008) Durability of three-way and close-coupled catalysts for Euro IV regulation. **Journal of Rare Earths**, 26: 827-830

Lloyd, J.R., Yong, P. and Macaskie L.E. (1998) Enzymatic recovery of elemental palladium by using sulfate-reducing bacteria. **Applied and Environmental Microbiology,** 64: 4607-4609

Lottermoser, B.G. (1994) Gold and platinoids in sewage sludges. **International Journal of Environmental Studies,** 46: 167-171

Lui, Y.K. and Dettling J.C. (1993) "Evolution of Pd/Rh TWC catalyst technology." In **International Congress and Exposition. Detroit, March 1993.** Society of Automotive Engineers paper number 930249.

Mabbett, A.N., Yong, P., Farr, J.P. and Macaskie, L.E. (2004) Reduction of Cr(VI) by "palladised" biomass of *Desulfovibrio desulfuricans* ATCC 29577. **Biotechnology and Bioengineering**, 87: 104–109

Mabbett, A.N., Sanyahumbi, D., Yong, P. and Macaskie, L.E. (2006) Biorecovered precious metals from industrial wastes: single step conversion of a mixed metal liquid waste to a bioinorganic catalyst with environmental application. **Environmental Science and Technology,** 40: 1015-1021

Macaskie, L.E., Mikheenko, I.P., Yong, P., Deplanche, K., Murray, A.J., Paterson-Beedle, M., Coker, V.S., Pearce, C.I., Cutting, R., Pattrick, R.A.D., Vaughan, D., Van der Laan, G.and Lloyd, J.R. (2010) "Today's wastes, tomorrow's materials for environmental protection." In Moo-Young, M. (ed.) **Comprehensive Biotechnology.** 2nd Ed. Vol 6. Oxford: Elsevier pp. 719-725

Macaskie, L.E., Humphries, A.C., Mikheenko, I.P., Baxter-Plant, V.S., Deplanche, K., Redwood, M.D., Bennett, J. A. and Wood, J. (2012) Use of *Desulfovibrio* and *Escherichia coli* Pd-nanocatalysts in reduction of Cr(VI) and hydrogenolytic dehalogenation of polychlorinated biphenyls and used transformer oil. **Journal of Chemical Technology & Biotechnology**, ISSN 0268-2575 (In Press)

Mason, B. (1958) **Principles of Geochemistry.** 2nd ed. New York: Wiley

Massucci, M., Clegg, S.L. and Brimblecombe, P. (1999) Equilibrium partial pressures, thermodynamic properties of aqueous and solid phases, and Cl_2 production from aqueous HCl and HNO_3 and their mixtures. **Journal of Physical Chemistry A,** 103: 4209-4226

Mertens, B., Blothe, C., Windey, K., De Windt, W. and Verstraete, W. (2007) Biocatalytic dechlorination of lindane by nano-scale particles of Pd(0) deposited on *Shewanella oneidensis*. **Chemosphere**, 66: 99-105

Microanalyst Line Energy Table "MA-Table" Software. **Interactive atomic data for energy dispersive X-ray Spectroscopy (EDX)**. Available for download from http://microanalyst.mikroanalytik.de/manual.html [Accessed 27th September 2011]

Mikheenko, I.P., Baxter-Plant, V.S., Rousset, M., Dementin, S., Adryanczyk-Perrier, G. and Macaskie, L.E. (2003) Reduction of Pd(II) with *Desulfovibrio fructosovorans*, its [Fe]-only hydrogenase negative mutant and the activity of the obtained hybrid bioinorganic catalysts. **Proceedings of the International Biohydrometallurgy Symposium**, Athens, Greece, 14th-19th September 2003

Mikheenko, I.P. (2004) **Nanoscale palladium recovery**. PhD thesis, University of Birmingham

Mikhennko, I.P. (2011) **Personal Communication with Research Fellow**. University of Birmingham, England

Mine-Engineer (2011) **Roll Crusher Tutorial** [online]. Available from: www.mine-engineer.com/mining/rollcrush.htm [Accessed October 2011]

Mine-Engineer (2011) **Air Table Diagram** [online] Available from: www.mine-engineer.com/mining/minproc/air-table2.htm [Accessed October 2011]

Mohabuth, N. and Miles, N. (2005) The recovery of recyclable materials from waste electrical and electronic equipment (WEEE) by using vibration separation. **Resources, Conservation and Recycling,** 45: 60-69

Moldovan, M., Gomez, M.M. and Palacios, M.A. (1999) Determination of platinum, rhodium and palladium in car exhaust fumes. **Journal of Analytical Atomic Spectrometry,** 14: 1163-1169

Mouza, A.A., Peolides, C.A. and Paras, S.V. (1995) Utilization of used auto-catalytic converters in small countries: the Greek paradigm. **Resources, Conservation and Recycling,** 15: 95-110

Muraki, H. and Zhang, G. (2000) Design of advanced automotive exhaust catalysts. **Catalysis Today,** 63: 337-345

Murray, A.J., Mikheenko, I.P., Goralska, E., Rowson, N.A. and Macaskie, L.E. (2007) Biorecovery of platinum group metals from secondary sources. **Advanced Materials Research**, 20-21: 651-654

Murrell, L.L., Tauster, S.J. and Anderson, D.R. (1991) Laser raman characterization of surface phase precious metal oxide formed on CeO_2. **Studies in Surface Science and Catalysis,** 71: 275-289

Mussmann, L., Lindner, D., Votsmeier, M., Lox, E. and Kreuzer, T. (2001) **Single layer high performance catalyst**, US Patent 20010046941

Nagai, Y., Hirabayashi, T., Dohmae, K. Takagi, N., Minami, T., Shinjoh, H. and Matsumoto, S. (2006) Sintering inhibition mechanism of platinum supported on ceria-based oxide and Pt-oxide-support interaction. **Journal of Catalysis**, 242: 103-109

Nowottny, C., Halwachs, W. and Schugerl, K. (1997) Recovery of platinum, palladium and rhodium from industrial process leaching solutions by reactive extraction. **Separation and Purification Technology,** 12: 135-144

Orozco, R.L., Redwood, M.D., Yong, P., Caldelari, I., Sargent, F. and Macaskie, L.E. (2010) Towards an integrated system for bio-energy: Hydrogen production by *Escherichia coli* and use of palladium-coated waste cells for electricity generation in a fuel cell. **Biotechnology Letters,** 32: 1837-1845

Ozkaya, D., Mathews, M., Spratt, S., Goodlet, G., Ash, P. and Boyd, D. (2006) Site-specific characterisation of an auto catalyst using EPMA, FIB and TEM/STEM. **Journal of Physics: Conference Series**, 26: 323-326

Palacios, M.A., Moldovan, M. and Gomez, M.M. (2000) "The automobile catalyst as an important source of PGE in the environment." In Zereini, F. (ed.) and Alt, F. (ed.) **Anthropogenic platinum group element emissions: their impact on man and environment.** Berlin: Springer. pp. 3-14

Palacios, M.A., Gomez, M.M., Moldovan, M., Morrison, G., Rauch, S., McLeod, C., Ma, R., Laserna, J., Lucena, P., Caroli, S., Alimonti, A., Petrucci, F., Bocca, B., Schramel, P., Lustig, S., Zischka, M., Wass, U., Stenbom, B., Luna, M., Saenz, J.C., Santamaria, J. and Torrens, J.M. (2000a) Platinum-group elements: quantification in collected exhaust fumes and studies of catalyst surfaces. **Science of the Total Environment**, 257: 1-15

Papavasiliou, A., Tsetsekou, A., Matsouka, V., Konsolakis, M., Yentekakis, I.V. and Boukos, N. (2009) Development of a Ce-Zr-La modified Pt / γ-Al_2O_3 TWCs' washcoat: Effect of synthesis procedure on catalytic behaviour and thermal durability. **Applied Catalysis B: Environmental**, 90: 162-174

Pincock (2008) The processing of platinum group metals (PGM) - Part 1. **Pincock Perspectives,** Issue 89: 1-4

Pryor, E.J. (1965) **Mineral Processing.** 3rd ed. London: Elsevier

Quadri, S.S., Benjamin, S.F. and Roberts, C.A. (2010) Flow measurements across an automotive catalyst monolith situated downstream of a planar wide-angled diffuser. **Proceedings of the Institute of Mechanical Engineers, Part C: Journal of Mechanical Engineering Science,** 224: 321-328

Rao, R.S. (2006) **Resource Recovery and Recycling from Metallurgical Wastes, Waste Management Series, Volume 7.** Oxford: Elsevier

Rauch, S., Motelica-Heino, M., Morrison, J.M. and Donard, O.F.X. (2000) Critical assessment of platinum group element determinations in road and urban river sediments using ultrasonic nebulisation and high resolution ICP-MS. **Journal of Analytical Atomic Spectrometry,** 15: 329-334

Redwood, M.D., Deplanche, K., Baxter-Plant, V.S. and Macaskie, L.E. (2008) Biomass-supported palladium catalysts on *Desulfovibrio desulfuricans* and *Rhodobacter sphaeroides*. **Biotechnology and Bioengineering**, 99: 1045-54

Resource Efficiency KTN (2008) **Material Security Ensuring Resource Availability for the UK Economy.** Cheshire: Environment Agency

Rowson, N.A. (2006) **Personal Communication with Senior lecturer.** University of Birmingham, England

Saurat, M. (2006) **Material flow analysis and environmental impact assessment related to current and future use of PGM in Europe.** MPhil thesis, Chalmers University of Technology

Shelef, M. and McCabe, R.W. (2000) Twenty-five years after introduction of automotive catalysis: what next? **Catalysis Today,** 62: 35-50

Sibley, S. F., Butterman, W.C. and Staff, (1995) Metals recycling in the United States. **Resources, Conservation and Recycling,** 15: 259-267

Star Trace (2011) Eddy Current Separator [online]. Available from: http://www.magneticseparator.in/eddy_current_separator.php [Accessed October 2011]

Stillwater Palladium (2008) **Pricing history of Palladium** [online]. Available from: http://www.stillwaterpalladium.com/priceJM.html [Accessed March 2010]

Stokes, J. (1987) Platinum in the glass industry, ZGS materials supplement on conventional alloys. **Platinum Metal Review,** 31: 54-62

Stuben, D. and Kupper, T. (2006) "Anthropogenic emission of Pd and traffic-related PGEs – Results based on monitoring with sewage sludge." In Zereini, F. (ed.) and Alt, F. (ed.) **Palladium Emissions in the Environment: Analytical Methods, Environmental Assessment and Health Effects**. Berlin: Springer. pp. 325-341

Taggart, A.F. (1954) **Handbook of Mineral Dressing.** New York: John Wiley & Sons.

Taylor, A.A. (1993) **The application of mineral processing techniques prior to the hydrometallurgical leaching of autocatalysts**. MPhil thesis, University of Birmingham

Taylor, S. R. and McLennan, S.M. (1985) **The Continental Crust: it's Composition and Evolution,** Palo Alto**:** Blackwell Scientific Publications

Tollefson, J. (2007) Worth its weight in platinum. **Nature,** 450: 334-335

Twigg, M.V. and Wilkins, J.J. (2006) “Autocatalysts: Past, Present and Future.” In Cybulski, A. (ed.) and Moulijn, J.A. (ed.) **Structured Catalysts and Reactors**. 2nd Edition. Florida: CRC Press. pp. 109-146

Veit, H.M., Diehl, T.R., Salami, A.P., Rodrigues, J.S., Bernardes, A.M. and Tenorio, J.A.S. (2005) Utilization of magnetic and electrostatic separation in the recycling of printed circuit boards scrap. **Waste Management,** 25: 67-74

Velez, M. (2000) **Chromium in Refractories** [online]. Available from: http://www.icdachromium.com/pdf/publications/thcrfl1.htm [Accessed March 2011]

Vermaak, C. F. (1995) **The Platinum Group Metals – A Global Perspective.** Randburg: Mintek

Waldron, K.J. and Robinson, N.J. (2009) How do bacterial cells ensure that metalloproteins get the correct metal? **Nature Reviews Microbiology**, 7: 25-35

Wan, C., Dettling, J. and Jagel, K. (1987) **Three Way Catalyst for Lean Exhaust Systems**, US Patent 4678770

Wei, J., Wassermann, K. and Li, Y. (2009) **Gasoline Engine Emission Systems Having Particulate Traps**, US Patent 20090193796

Wells, I. (2007) **Personal Communication with Dr Iain Wells, Consultant Minerals Engineer for Eriez Magnetic Europe Ltd.**

Wells, I. (2009) **Disc Separator Information,** Courtesy of Dr Iain Wells, Consultant Minerals Engineer

Whiteley, J.D. and Murray, F. (2003) Anthropogenic platinum group element (Pt, Pd and Rh) concentrations in road dust and roadside soils from Perth, Western Australia. **Science of the Total Environment,** 317: 121-135

Wiese, J., Harris, P. and Bradshaw, D. (2006) The role of reagent suite in optimizing pentandlite recoveries from the Merensky Reef. **Minerals Engineering,** 19: 1290-1300

Wills, B.A. (2008) **Mineral Processing Technology.** 7th Ed. London: Elsevier

Wiseman, C.L.S. and Zereini, F. (2009) Airborne particulate matter, platinum group elements and human health: A review of recent evidence. **Science of the Total Environment,** 407: 2493-2500

Wright, M. J. (2008). **Personal Communication with Head of Smelting Operations at Johnson Matthey.** Enfield Refinery, England.

Wright, M. J. (2009). **Personal Communication with Head of Smelting Operations at Johnson Matthey.** Enfield Refinery, England.

Xiao, Z. and Laplante, A.R. (2004) Characterising and recovering the platinum group minerals - a review. **Minerals engineering,** 17: 961-979

Xiao, Z., Laplante, A.R. and Finch, J A. (2009) Quantifying the contents of gravity recoverable platinum group minerals in ore samples. **Minerals Engineering**, 22: 304-310

Yang, C.J. (2009) An impending platinum crisis and its implications for the future of the automobile. **Energy Policy,** 37: 1805-1808

Yong, P.,Rowson, N.A., Farr, J.P., Harris, I.R. and Macaskie, L.E. (2002) Bioreduction and biocrystallization of palladium by *Desulfovibrio desulfuricans* NCIMB 8307. **Biotechnology and Bioengineering**, 80: 369-379

Yong, P., Rowson, N.A., Farr, J.P.G., Harris, I.R. and Macaskie, L.E. (2003) A novel electrobiotechnology for the recovery of precious metals from spent automotive catalysts. **Environmental Technology,** 24: 289-297

Yong, P., Paterson-Beedle, M., Mikheenko, I.P. and Macaskie, L.E. (2007) From bio-mineralisation to fuel cells: biomanufacture of Pt and Pd nanocrystals for fuel cell electrode catalyst. **Biotechnology Letters**, 29: 539-544

Yong, P., Mikheenko, I.P., Deplanche, K., Redwood, M.D. and Macaskie, L.E. (2010) Biorefining of precious metals from wastes: an answer to manufacturing of cheap nanocatalysts for fuel cells and power generation via an integrated biorefinery? **Biotechnology Letters**, 32: 1821-1828

Zereini, F., Skerstupp, B., Alt, F., Helmers, E., and Urban, H. (1997) Geochemical behavior of platinum group elements (PGE) in particulate emission by automobile exhaust catalysts: experimental results and environmental investigations. **Science of the Total Environment,** 206: 137-146

Zereini, F., Dirksen, F., Skerstupp, B. and Urban, H. (1998) Sources of anthropogenic platinum-group elements (PGE): automotive catalysts verses PGE-processing industries. **Environmental Science and Pollution Research,** 5 (4): 223-230

Zereini, F., Skerstupp, B., Rankenburg, K., Dirksen, F., Beyer, J.M., Claus, T. and Urban, H. (2000) “Anthropogenic emission of platinum group elements (Pt, Pd and Rh) into the environment: concentration, distribution and geochemical behavior in soils.” In Zereini, F. (ed.) and Alt, F. (ed.) **Anthropogenic Platinum Group Element Emissions: Their Impact on Man and Environment**. Berlin: Springer pp. 73-83

Zotin, F.M.Z., Da Fonseca Martins Gomes, O., De Oliveira, C.H., Neto, A.A. and Cardoso, M.J.B. (2005) Automotive catalyst deactivation: case studies. **Catalysis Today,** 107-108: 157-167